

CRANFIELD UNIVERSITY

Pierre-Alexandre BOURBON

DESIGN OF A SUB 115 Kg MICROLIGHT AIRCRAFT  
FOR DEREGULATED REGIME

-  
HLM07 COLAB

SCHOOL OF ENGINEERING

MSc THESIS

CRANFIELD UNIVERSITY  
SCHOOL OF ENGINEERING

MSc THESIS  
Academic Year 2006-2007

Pierre-Alexandre BOURBON

DESIGN OF A SUB 115 Kg MICROLIGHT AIRCRAFT  
FOR DEREGULATED REGIME

-  
HLM07 COLAB

Supervisor: Mr. Jason BROWN

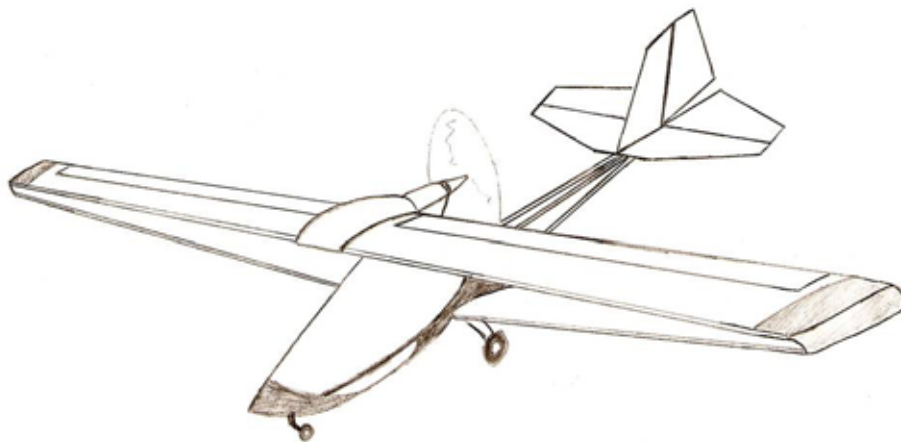
September 2007

This thesis is submitted in partial fulfilment of the requirements for the degree of  
Master of Science

© Cranfield University 2007. All rights reserved. No parts of this publication may be  
reproduced without the written permission of the copyright owner.

# ABSTRACT

- ➔ Flying has always been one of the greatest dreams of Man. For about one hundred years now, aeronautic science has kept progressing and now, flying is not a dangerous adventure anymore. Large civil airliners have become the most used means of transport of passengers for long distances, and private aviation enables each individual to learn how to fly on some of the 1000's of different light aircraft designs available all around the world. However, for an individual flying is becoming a very complex and expensive experience...
- ➔ The British Civil Aviation Authority (CAA) has established a new regime for sub 115kg aircraft. This regime is deregulated and therefore would enable more freedom for the personal aircraft builders and pilots. The aircraft has to comply with the following requirements:
  - Single seat aircraft
  - Empty mass without pilot and fuel less than 115kg
  - Wing loading with empty mass less than 10kg/m<sup>2</sup>
  - Comply with the microlight noise emission requirementThese rules impose the designer tough conditions but still allow large margins of manoeuvre for imagination.
- ➔ The purpose of this thesis is to come up with a design which meets this requirement without sacrificing the performance of the aircraft. This aircraft is intended to be a competitor to win the world's microlight competition.
- ➔ It is also intended to build a 1/3 scale flying test model to validate the stability and manoeuvrability performance of the aircraft.



# ACKNOWLEDGEMENTS

I would like to thanks Mr Jason Brown for his help and the time he gave me during this project.

I would also like to thanks the Colab team, and especially Mr Lucien Cabrol, for his hospitality and all the information provided concerning the Colab wing concept.

I would like to thank Mr Broom from Broom Engineering for his useful advices and his constant support all along the project.

Finally, thank you to Mr Gibbins for building the 1/3 scale flying test model, which is the first step of the concretisation of the project.

# TABLE OF CONTENT

|   |               |
|---|---------------|
| <b>ABSTRACT</b>   | <b>III</b>    |
| <b>ACKNOWLEDGEMENTS</b>                                       | <b>IV</b>     |
| <b>LIST OF NOTATIONS</b>                                      | <b>XIV</b>    |
| GENERAL AERODYNAMIC NOTATIONS                                 | XIV           |
| GENERAL FLIGHT MECHANICS NOTATIONS                            | XV            |
| UNITS SYSTEM  | XV            |
| <b>1. INTRODUCTION</b>  | <b>- 1 -</b>  |
| 1.1. REGULATION OUTLINES                                      | - 1 -         |
| 1.1.1. <i>Standard microlights airworthiness requirements</i> | - 1 -         |
| 1.1.2. <i>New deregulated regime requirement</i>              | - 1 -         |
| 1.2. DESIGN OVERVIEW AND OBJECTIVES                           | - 2 -         |
| 1.2.1. <i>An amazing experience</i>                           | - 2 -         |
| 1.2.2. <i>Objectives</i>                                      | - 2 -         |
| 1.3. AIRCRAFT DESIGN PROCESS                                  | - 3 -         |
| 1.4. AIRCRAFT SPECIFICATIONS                                  | - 4 -         |
| 1.4.1. <i>General geometry</i>                                | - 4 -         |
| 1.4.2. <i>Mass summary</i>                                    | - 4 -         |
| 1.4.3. <i>Performance summary</i>                             | - 4 -         |
| 1.5. 3 VIEWS SKETCHES   | - 5 -         |
| 1.5.1. <i>Side view</i>                                       | - 5 -         |
| 1.5.2. <i>Front view</i>                                      | - 5 -         |
| 1.5.3. <i>Top view</i>  | - 6 -         |
| 1.5.4. <i>Isometric view</i>                                  | - 6 -         |
| <b>2. SURVEY OF ULTRALIGHT MARKET</b>                         | <b>- 7 -</b>  |
| 2.1. MICROLIGHTS DESIGNS LIST                                 | - 7 -         |
| 2.1.1. <i>Top wing pusher propeller configurations</i>        | - 7 -         |
| 2.1.2. <i>Top wing puller propeller configurations</i>        | - 14 -        |
| 2.1.3. <i>Conventional low wing 3 axis layout</i>             | - 17 -        |
| 2.1.4. <i>Less than 55kg microlight</i>                       | - 19 -        |
| 2.1.5. <i>Non common designs</i>                              | - 21 -        |
| 2.2. AIRCRAFT SPECIFICATIONS SUMMARY                          | - 32 -        |
| 2.3. PERFORMANCE STUDY  | - 33 -        |
| 2.3.1. <i>Engine power – wing loading diagram</i>             | - 33 -        |
| 2.3.2. <i>Engine power –cruise speed diagram</i>              | - 35 -        |
| 2.3.3. <i>Engine power –Climb rate diagram</i>                | - 36 -        |
| 2.3.4. <i>Aspect Ratio – Glide ratio diagram</i>              | - 37 -        |
| <b>3. AIRCRAFT DESIGN OPTIONS</b>                             | <b>- 39 -</b> |
| 3.1. STUDIES OF THE AIRCRAFT CONFIGURATIONS                   | - 39 -        |
| 3.1.1. <i>Wing arrangements</i>                               | - 39 -        |
| 3.1.2. <i>Engine arrangements</i>                             | - 47 -        |
| 3.1.3. <i>Tail arrangements</i>                               | - 50 -        |
| 3.1.4. <i>Undercarriage arrangement</i>                       | - 52 -        |
| 3.2. MATERIALS  | - 53 -        |
| 3.2.1. <i>Wood and fabric</i>                                 | - 53 -        |
| 3.2.2. <i>Metallic structures</i>                             | - 54 -        |

|           |   |               |
|-----------|---|---------------|
| 3.2.3.    | <i>Composite materials</i>                    | - 55 -        |
| 3.3.      | AIRCRAFT DESIGN CHOICE                        | - 56 -        |
| 3.3.1.    | <i>General configuration</i>                  | - 56 -        |
| 3.3.2.    | <i>Materials</i>                              | - 56 -        |
| <b>4.</b> | <b>THE COLAB DESIGN</b>                       | <b>- 57 -</b> |
| 4.1.      | PRESENTATION OF THE CONCEPT                   | - 57 -        |
| 4.1.1.    | <i>Introduction</i>                           | - 57 -        |
| 4.1.2.    | <i>Design overview</i>                        | - 57 -        |
| 4.1.3.    | <i>Why can we trust this design?</i>          | - 58 -        |
| 4.2.      | ADVANTAGES OF THE CONCEPT                     | - 60 -        |
| 4.2.1.    | <i>Structural advantages</i>                  | - 60 -        |
| 4.2.2.    | <i>Conception advantages</i>                  | - 61 -        |
| 4.2.3.    | <i>Aerodynamics and performance advantage</i> | - 61 -        |
| 4.3.      | UNDERSTANDING OF THE CONCEPT                  | - 63 -        |
| 4.3.1.    | <i>Basics of aerodynamics</i>                 | - 63 -        |
| 4.3.2.    | <i>The Nenadovitch effect</i>                 | - 63 -        |
| 4.3.3.    | <i>The closing coefficient</i>                | - 64 -        |
| 4.3.4.    | <i>Conceptual explanations</i>                | - 64 -        |
| 4.3.5.    | <i>Large range of velocities</i>              | - 67 -        |
| 4.3.6.    | <i>Smart fuselage design</i>                  | - 68 -        |
| 4.4.      | MEETING WITH THE COLAB INVENTOR               | - 69 -        |
| 4.4.1.    | <i>Purpose of this visit</i>                  | - 69 -        |
| 4.4.2.    | <i>Results of the visit</i>                   | - 69 -        |
| 4.4.3.    | <i>Terms of the collaboration</i>             | - 69 -        |
| <b>5.</b> | <b>PARAMETRIC ANALYSIS</b>                    | <b>- 70 -</b> |
| 5.1.      | NOTATIONS AND UNITS RELATIVE TO THIS PART     | - 70 -        |
| 5.1.1.    | <i>General notice</i>                         | - 70 -        |
| 5.1.2.    | <i>Notations and units</i>                    | - 70 -        |
| 5.1.3.    | <i>Notations for the graphs</i>               | - 70 -        |
| 5.2.      | AIRCRAFT SPEED PREDICTION                     | - 71 -        |
| 5.2.1.    | <i>Equations</i>                              | - 71 -        |
| 5.2.2.    | <i>Graph</i>                                  | - 71 -        |
| 5.2.3.    | <i>Conclusion</i>                             | - 72 -        |
| 5.3.      | AIRCRAFT STALLING SPEED PREDICTION            | - 72 -        |
| 5.3.1.    | <i>Equations</i>                              | - 72 -        |
| 5.3.2.    | <i>Graph</i>                                  | - 73 -        |
| 5.3.3.    | <i>Conclusion</i>                             | - 73 -        |
| 5.4.      | TAKE OFF GROUND RUN PERFORMANCE               | - 74 -        |
| 5.4.1.    | <i>Equations</i>                              | - 74 -        |
| 5.4.2.    | <i>Graph</i>                                  | - 74 -        |
| 5.4.3.    | <i>Conclusions</i>                            | - 75 -        |
| 5.5.      | CLIMB PERFORMANCE                             | - 75 -        |
| 5.5.1.    | <i>Equations</i>                              | - 75 -        |
| 5.5.2.    | <i>Graph</i>                                  | - 76 -        |
| 5.5.3.    | <i>Conclusions</i>                            | - 77 -        |
| 5.6.      | MATCHING DIAGRAM                              | - 77 -        |
| 5.6.1.    | <i>Introduction</i>                           | - 77 -        |
| 5.6.2.    | <i>Parametric equations</i>                   | - 77 -        |
| 5.6.3.    | <i>Graph</i>                                  | - 79 -        |
| 5.7.      | WEIGHT ESTIMATION                             | - 79 -        |
| 5.7.1.    | <i>Equations</i>                              | - 79 -        |

|           |  |                |
|-----------|--|----------------|
| 5.7.2.    | Graph  | - 80 -         |
| 5.7.3.    | Conclusion   | - 81 -         |
| 5.8.      | CROSS CHECKING OF THE RESULTS                              | - 81 -         |
| 5.8.1.    | $C_{lt}$ equation  | - 81 -         |
| 5.8.2.    | Engine power drag equation                                 | - 82 -         |
| 5.9.      | PARAMETRIC ANALYSIS EXAMPLES                               | - 82 -         |
| 5.10.     | CONCLUSIONS  | - 82 -         |
| 5.10.1.   | Validity of the model                                      | - 82 -         |
| 5.10.2.   | Utility of the analysis                                    | - 83 -         |
| 5.11.     | TABLE OF RESULTS   | - 84 -         |
| <b>6.</b> | <b>AIRCRAFT GENERAL LAYOUT</b>                             | <b>- 85 -</b>  |
| 6.1.      | PARAMETRIC ANALYSIS  | - 85 -         |
| 6.1.1.    | Input data   | - 85 -         |
| 6.1.2.    | Matching diagram   | - 85 -         |
| 6.1.3.    | Parametric analysis results                                | - 86 -         |
| 6.2.      | WING LAYOUT  | - 87 -         |
| 6.2.1.    | Wing airfoil and gross area                                | - 87 -         |
| 6.2.2.    | Colab wing parameters                                      | - 88 -         |
| 6.2.3.    | Wing layout  | - 90 -         |
| 6.3.      | CONTROL SURFACES AND TAIL                                  | - 91 -         |
| 6.3.1.    | Ailerons   | - 91 -         |
| 6.3.2.    | Tail design  | - 91 -         |
| 6.3.3.    | Variable camber flaps                                      | - 92 -         |
| 6.3.4.    | Drawings   | - 92 -         |
| 6.4.      | ENGINE SELECTION   | - 94 -         |
| 6.4.1.    | Engine selection list                                      | - 94 -         |
| 6.4.2.    | Engine choice  | - 94 -         |
| 6.4.3.    | Propeller choice   | - 95 -         |
| <b>7.</b> | <b>MASS BALANCE AND STABILITY</b>                          | <b>- 96 -</b>  |
| 7.1.      | LONGITUDINAL STATIC STABILITY                              | - 96 -         |
| 7.1.1.    | Main wing aerodynamic centre position                      | - 96 -         |
| 7.1.2.    | Main wing lift curve slope and pitching moment             | - 97 -         |
| 7.1.3.    | Lift curve slope of the tailplane                          | - 99 -         |
| 7.1.4.    | Lift curve slope of the tailplane with elevator deflection | - 100 -        |
| 7.1.5.    | Average downwash at the tailplane                          | - 101 -        |
| 7.1.6.    | Stick fixed stability                                      | - 102 -        |
| 7.1.7.    | Maximum CG range   | - 102 -        |
| 7.2.      | MASS BREAKDOWN   | - 103 -        |
| 7.3.      | CG CALCULATION   | - 104 -        |
| <b>8.</b> | <b>LOADING ACTIONS AND AIRWORTHINESS</b>                   | <b>- 105 -</b> |
| 8.1.      | N-V DIAGRAM  | - 105 -        |
| 8.1.1.    | Design air speeds  | - 105 -        |
| 8.1.2.    | Gusts cases  | - 106 -        |
| 8.1.3.    | n-V diagram  | - 107 -        |
| 8.2.      | WING LOADS   | - 108 -        |
| 8.2.1.    | Wing load cases  | - 108 -        |
| 8.2.2.    | Low wing shear force diagram                               | - 109 -        |
| 8.2.3.    | Low wing bending moment diagram                            | - 110 -        |
| 8.2.4.    | Maximum loads in the low wings                             | - 111 -        |
| 8.2.5.    | Top wing shear force diagram                               | - 112 -        |

|            |  |                |
|------------|--|----------------|
| 8.2.6.     | Low wing bending moment diagram                                  | - 113 -        |
| 8.2.7.     | Maximum loads in the top wings                                   | - 113 -        |
| 8.3.       | CONTROL SURFACES LOADS   | - 114 -        |
| 8.3.1.     | Ailerons and flaps loads   | - 114 -        |
| 8.3.2.     | Horizontal tail surfaces symmetrical loads                       | - 116 -        |
| 8.3.3.     | Horizontal tail surfaces unsymmetrical loads                     | - 122 -        |
| 8.3.4.     | Vertical tail surfaces loads                                     | - 122 -        |
| 8.3.5.     | Rudder and elevator loading                                      | - 125 -        |
| <b>9.</b>  | <b>DETAILED WING DESIGN</b>                                      | <b>- 126 -</b> |
| 9.1.       | WING LAYOUT  | - 126 -        |
| 9.1.1.     | Spars layout   | - 126 -        |
| 9.1.2.     | Ribs position  | - 127 -        |
| 9.2.       | SIZING OF THE SKIN   | - 128 -        |
| 9.2.1.     | Shear centre and torque diagram                                  | - 128 -        |
| 9.2.2.     | Torsional shear skin thickness                                   | - 130 -        |
| 9.2.3.     | Torsional stiffness skin thickness                               | - 131 -        |
| 9.2.4.     | Wing skin buckling   | - 132 -        |
| 9.2.5.     | Wing skin strength   | - 133 -        |
| 9.3.       | SPARS SIZING   | - 134 -        |
| 9.3.1.     | Shear force repartition between the front spar and the rear spar | - 134 -        |
| 9.3.2.     | Preliminary thickness calculation                                | - 134 -        |
| 9.3.3.     | Spars shear buckling   | - 135 -        |
| 9.3.4.     | Spar strength checking   | - 136 -        |
| 9.4.       | BOOM SIZING, WING STIFFNESS                                      | - 137 -        |
| 9.4.1.     | Minimum boom area calculation                                    | - 137 -        |
| 9.4.2.     | Wing stiffness criterion   | - 137 -        |
| 9.4.3.     | Booms layout   | - 139 -        |
| 9.4.4.     | Boom strength  | - 140 -        |
| 9.5.       | RIBS SIZING  | - 140 -        |
| 9.5.1.     | Wing rib air load  | - 140 -        |
| 9.5.2.     | Shear flow distribution:   | - 141 -        |
| 9.5.3.     | Shear Force and Bending Moment diagrams                          | - 143 -        |
| 9.5.4.     | Strength of the rib:   | - 144 -        |
| 9.6.       | BUCKLING OF THE TOP WING   | - 145 -        |
| 9.6.1.     | Presentation of the problem                                      | - 145 -        |
| 9.6.2.     | Section properties   | - 145 -        |
| 9.6.3.     | Calculation of the Euler buckling                                | - 146 -        |
| 9.7.       | ATTACHMENT DETAILS   | - 146 -        |
| 9.7.1.     | Rear wing attachments  | - 146 -        |
| 9.7.2.     | Top wing root attachment   | - 147 -        |
| 9.7.3.     | Wing tips attachments  | - 149 -        |
| <b>10.</b> | <b>TAIL AND CONTROL SURFACES DESIGN</b>                          | <b>- 150 -</b> |
| 10.1.      | TAILPLANE DESIGN   | - 150 -        |
| 10.1.1.    | Tailplane layout   | - 150 -        |
| 10.1.2.    | Tailplane preliminary design                                     | - 150 -        |
| 10.2.      | ELEVATOR DESIGN  | - 152 -        |
| 10.2.1.    | Elevator layout  | - 152 -        |
| 10.2.2.    | Elevator preliminary design                                      | - 152 -        |
| 10.2.3.    | Elevator hinge design  | - 153 -        |
| 10.3.      | FIN AND RUDDER DESIGN  | - 154 -        |
| 10.3.1.    | Fin and rudder layout  | - 154 -        |



|            |   |                |
|------------|---|----------------|
| 10.3.2.    | <i>Fin initial design</i>                   | - 154 -        |
| 10.3.3.    | <i>Rudder initial design</i>                | - 155 -        |
| 10.3.4.    | <i>Rudder hinge design</i>                  | - 155 -        |
| 10.4.      | TAIL STRUCTURE DESIGN                       | - 156 -        |
| 10.4.1.    | <i>Tail general layout</i>                  | - 156 -        |
| 10.4.2.    | <i>Details of the tail beam attachments</i> | - 158 -        |
| 10.4.3.    | <i>Tail beam initial stress calculation</i> | - 160 -        |
| 10.5.      | FLAPS AND AILERONS DESIGN                   | - 162 -        |
| 10.5.1.    | <i>Ailerons and flaps general layout</i>    | - 162 -        |
| 10.5.2.    | <i>Ailerons and flaps materials</i>         | - 163 -        |
| 10.5.3.    | <i>Ailerons and flaps design</i>            | - 164 -        |
| <b>11.</b> | <b>FUSELAGE AND UNDERCARRIAGE</b>           | <b>- 166 -</b> |
| 11.1.      | FUSELAGE GENERAL LAYOUT                     | - 166 -        |
| 11.2.      | MAIN COMPONENTS DESIGN                      | - 166 -        |
| 11.2.1.    | <i>Front cantilever beam design</i>         | - 166 -        |
| A.1.1.     | <i>Top wing beams</i>                       | - 167 -        |
| 11.3.      | ENGINE MOUNTING                             | - 169 -        |
| 11.3.1.    | <i>Engine mounting general layout</i>       | - 169 -        |
| 11.3.2.    | <i>Engine mounting design</i>               | - 169 -        |
| 11.4.      | UNDERCARRIAGE                               | - 170 -        |
| 11.4.1.    | <i>Dynaero MCR-01 undercarriage</i>         | - 170 -        |
| 11.4.2.    | <i>Key ideas for the design</i>             | - 171 -        |
| <b>12.</b> | <b>FINITE ELEMENT ANALYSIS</b>              | <b>- 172 -</b> |
| 12.1.      | GLOBAL OVERVIEW OF THE MODEL                | - 172 -        |
| 12.2.      | GEOMETRY AND MESH                           | - 174 -        |
| 12.2.1.    | <i>Wing</i>                                 | - 174 -        |
| 12.2.2.    | <i>Tail</i>                                 | - 174 -        |
| 12.2.3.    | <i>Fuselage</i>                             | - 175 -        |
| 12.3.      | ELEMENT PROPERTIES                          | - 176 -        |
| 12.3.1.    | <i>Wing</i>                                 | - 176 -        |
| 12.3.2.    | <i>Fuselage</i>                             | - 176 -        |
| 12.3.3.    | <i>Tail</i>                                 | - 177 -        |
| 12.4.      | LOADS AND BOUNDARIES CONDITIONS             | - 177 -        |
| 12.4.1.    | <i>Wing loads</i>                           | - 177 -        |
| 12.4.2.    | <i>Tail loads</i>                           | - 179 -        |
| 12.4.3.    | <i>Fuselage loads</i>                       | - 179 -        |
| 12.5.      | STRENGTH RESULTS (ULTIMATE LOAD)            | - 180 -        |
| 12.5.1.    | <i>Wing structure</i>                       | - 180 -        |
| 12.5.2.    | <i>Tail</i>                                 | - 185 -        |
| 12.5.3.    | <i>Fuselage</i>                             | - 186 -        |
| 12.6.      | DEFORMATIONS (LIMIT LOAD)                   | - 187 -        |
| 12.6.1.    | <i>Wing</i>                                 | - 187 -        |
| 12.6.2.    | <i>Tail</i>                                 | - 187 -        |
| 12.6.3.    | <i>Fuselage</i>                             | - 188 -        |
| 12.7.      | DYNAMIC ANALYSIS                            | - 189 -        |
| <b>13.</b> | <b>1/3 SCALE MODEL</b>                      | <b>- 190 -</b> |
| 13.1.      | PURPOSE OF THE MODEL                        | - 190 -        |
| 13.2.      | MANUFACTURING OF THE WINGS                  | - 190 -        |
| 13.3.      | GLOBAL WING ASSEMBLY                        | - 191 -        |
|            | <b>CONCLUSIONS AND IMPRESSIONS</b>          | <b>- 192 -</b> |

|   |                |
|---|----------------|
| <b>REFERENCES</b>   | <b>- 193 -</b> |
| <b>APPENDICES</b>   | <b>- 194 -</b> |
| <b>A. BMAA TECHNICAL LEAFLET</b>  | <b>- 195 -</b> |
| A.1. INTRODUCTION   | - 195 -        |
| A.2. THE DEFINITION   | - 195 -        |
| A.3. WHAT THE CHANGE IN RULES MEANS                                     | - 196 -        |
| A.4. WHAT THE CHANGE IN RULES DOES NOT MEAN                             | - 196 -        |
| A.4.1. Pilot licensing  | - 197 -        |
| A.4.2. What types are there?  | - 197 -        |
| A.5. HOW SHOULD I DECIDE WHICH TO BUY?                                  | - 197 -        |
| A.5.1. I've got a microlight on a permit and want use the new rules     | - 198 -        |
| A.5.2. I've got a new microlight that I want to fly under the new rules | - 198 -        |
| A.6. THE BMAA'S INVOLVEMENT   | - 198 -        |
| A.7. MODIFICATIONS AND NOISE CERTIFICATES                               | - 199 -        |
| A.8. ADVICE ON DEREGULATED MICROLIGHTS                                  | - 199 -        |
| A.8.1. Maintenance  | - 200 -        |
| A.8.2. Designing your own aircraft, modification or repair              | - 200 -        |
| <b>B. PARAMETRIC ANALYSIS EXAMPLES</b>                                  | <b>- 202 -</b> |
| B.1. SLOW HIGH ASPECT RATIO AIRCRAFT                                    | - 202 -        |
| B.1.1. Matching diagram   | - 202 -        |
| B.1.2. Input parameters   | - 203 -        |
| B.1.3. Output results   | - 203 -        |
| B.1.4. Interpretation   | - 203 -        |
| B.2. FAST AIRCRAFT  | - 204 -        |
| B.2.1. Matching diagram   | - 204 -        |
| B.2.2. Input parameters   | - 204 -        |
| B.2.3. Output results   | - 205 -        |
| B.2.4. Interpretation   | - 205 -        |

## LIST OF FIGURES

|   |        |
|---|--------|
| <i>HLM-07 COLAB side view</i>                             | - 5 -  |
| <i>HLM-07 COLAB front view</i>                            | - 5 -  |
| <i>HLM-07 COLAB top view</i>                              | - 6 -  |
| <i>HLM-07 COLAB isometric view</i>                        | - 6 -  |
| <i>Kolb Firestar</i>                                      | - 7 -  |
| <i>Golden Circle T Bird</i>                               | - 8 -  |
| <i>Seahawk Condor</i>                                     | - 8 -  |
| <i>Gull 2000</i>  | - 9 -  |
| <i>Rans S-17 Stinger</i>                                  | - 9 -  |
| <i>Interplane Griffon 103</i>                             | - 10 - |
| <i>Aerolite 103</i>                                       | - 10 - |
| <i>Aviasud Sirocco</i>                                    | - 11 - |
| <i>CFM shadow C &amp; D</i>                               | - 11 - |
| <i>Avanced aviation Carrera 150</i>                       | - 12 - |
| <i>Quicksilver MX sprint</i>                              | - 12 - |
| <i>Maxair Drifter DR532 Rocket</i>                        | - 13 - |
| <i>Weedhopper</i>   | - 14 - |
| <i>Flying K sky raider</i>                                | - 15 - |
| <i>AeroLites Bearcat</i>                                  | - 15 - |
| <i>Flightstar Spyder</i>                                  | - 16 - |
| <i>MB 02 Souricette</i>                                   | - 17 - |
| <i>Fisher Avenger</i>                                     | - 18 - |
| <i>Hovey Whing Ding II</i>                                | - 19 - |
| <i>E-12n</i>  | - 20 - |
| <i>MC-12 Cricket</i>                                      | - 21 - |
| <i>Lazair</i>   | - 22 - |
| <i>Pou du ciel</i>  | - 23 - |
| <i>Pouchel</i>  | - 24 - |
| <i>Piel Onyx CP 150</i>                                   | - 25 - |
| <i>Nike aeronautica PUL 9</i>                             | - 26 - |
| <i>Zenair Zipper</i>                                      | - 27 - |
| <i>Sorell SNS-8 Hiperlight</i>                            | - 28 - |
| <i>Prototype of microlight fitted with a © Colab wing</i> | - 29 - |
| <i>Micro-B World champion microlight</i>                  | - 30 - |
| <i>Alatus ultralight motor sailplane</i>                  | - 31 - |
| <i>Engine power – wing loading diagram</i>                | - 33 - |
| <i>Engine power-cruise speed diagram</i>                  | - 35 - |

|   |        |
|---|--------|
| <i>Engine power-climb rate diagram</i>  | - 36 - |
| <i>Aspect Ratio – Glide Ratio Diagram</i>   | - 37 - |
| <i>High wing microlight (Popham Meeting, May 2007, author property)</i>                                   | - 39 - |
| <i>Antonov 225</i>  | - 40 - |
| <i>Robin DR-400 (left) and Cessna 172 (Right)</i>   | - 40 - |
| <i>Samba, low wing microlight</i>   | - 41 - |
| <i>De Havilland Mosquito</i>  | - 42 - |
| <i>Pitts</i>  | - 43 - |
| <i>Piaggio P180 Avanti II</i>   | - 44 - |
| <i>(<a href="http://www.piaggioaero.com/">http://www.piaggioaero.com/</a>, 22<sup>nd</sup> June 2007)</i> | - 44 - |
| <i>Northrop Grumman B-2 Spirit</i>  | - 45 - |
| <i>Colab microlight prototype</i>   | - 46 - |
| <i>Rutan Long-EZ home-built aircraft</i>  | - 48 - |
| <i>Cessna 337 Skymaster</i>   | - 49 - |
| <i>Piper Pa 28</i>  | - 50 - |
| <i>Duo Discus</i>   | - 50 - |
| <i>Beechcraft Bonanza</i>   | - 51 - |
| <i>De Havilland dH-110 Sea Vixen D3,</i>  | - 51 - |
| <i>Piper Cub</i>  | - 52 - |
| <i>Lockheed Super Constellation</i>   | - 52 - |
| <i>Fournier RF6-B wood and Fabric Aircraft</i>  | - 53 - |
| <i>Zenith</i>   | - 54 - |
| <i>Scaled Composites Global Flyer</i>   | - 55 - |
| <i>Colab technology demonstrator digital model</i>  | - 57 - |
| <i>Colab technology demonstrator digital model 3 views</i>  | - 58 - |
| <i>2 seater Colab microlight</i>  | - 59 - |
| <i>Edelweiss Colab (6m span)</i>  | - 59 - |
| <i>Jean Michel Bouquet with the prize for its Edelweiss Colab glider</i>                                  | - 59 - |
| <i>Colab wing structure</i>   | - 60 - |
| <i>Nenadovitch geometry</i>   | - 63 - |
| <i>Closing coefficient and equivalent wing</i>  | - 64 - |
| <i>Compression of the extrados boundary layer on the low wing</i>   | - 65 - |
| <i>Suction of the extrados boundary layer on the top wing</i>   | - 65 - |
| <i>Pictures of the wing tip of a Colab wing</i>   | - 66 - |
| <i>Colab wing with flaps deflected</i>  | - 66 - |
| <i>Theoretical Colab drag polar</i>   | - 67 - |
| <i>Colab fuselage interferences reduction</i>   | - 68 - |
| <i>HLM Colab fuselage propeller efficiency optimisation</i>   | - 68 - |
| <i>Pictures taken during the visit to see Lucien CABROL</i>   | - 69 - |
| <i>Graph: Variation of speed with power index</i>   | - 71 - |

|   |         |
|---|---------|
| <i>Graph: Variation of stalling speed with wing loading parameter</i> | - 73 -  |
| <i>Graph: Variation of Take-off distance with take-off parameter</i>  | - 74 -  |
| <i>Graph: Variation of climb rate with climb parameter</i>            | - 76 -  |
| <i>Parametric analysis matching chart</i>                             | - 79 -  |
| <i>Graph: Variation of Useful load fraction with power loading</i>    | - 80 -  |
| <i>HLM-Colab-Cranfield Matching diagram</i>                           | - 85 -  |
| <i>FX 62K-153/20 Airfoil shape</i>                                    | - 87 -  |
| <i>Colab wing dihedral limits</i>                                     | - 88 -  |
| <i>Colab wing sweepback limits</i>                                    | - 88 -  |
| <i>Colab wing tip geometrical limits</i>                              | - 89 -  |
| <i>Colab wing root geometrical limits</i>                             | - 89 -  |
| <i>Wing layout</i>  | - 90 -  |
| <i>Microlights ailerons surfaces data</i>                             | - 91 -  |
| <i>Microlights tail surfaces data</i>                                 | - 92 -  |
| <i>Aircraft aerodynamic surfaces layout and dimensions</i>            | - 93 -  |
| <i>Mini 3 engine</i>  | - 94 -  |
| <i>Corsair M25Y engine</i>  | - 94 -  |
| <i>Carbon propeller</i>   | - 95 -  |
| <i>Colab wing shape and CG position</i>                               | - 96 -  |
| <i>Airfoil lift coefficient polar</i>                                 | - 97 -  |
| <i>Airfoil pitching moment coefficient polar</i>                      | - 98 -  |
| <i>Tail geometry: Real tail model (left), ESDU notations (right)</i>  | - 99 -  |
| <i>Aircraft main CGs positions</i>                                    | - 104 - |
| <i>HLM-07 n-V diagram</i>   | - 107 - |
| <i>Wing load cases diagram</i>  | - 109 - |
| <i>Low wing beam model</i>  | - 109 - |
| <i>Bottom right wing shear force diagram</i>                          | - 110 - |
| <i>Bottom right wing bending moment diagram</i>                       | - 111 - |
| <i>Top wing beam model</i>  | - 112 - |
| <i>top right wing shear force diagram</i>                             | - 112 - |
| <i>Bottom right wing bending moment diagram</i>                       | - 113 - |
| <i>Velocity profile on a flat plate mounted on a surface</i>          | - 114 - |
| <i>Ailerons limit loads cases</i>                                     | - 115 - |
| <i>Manoeuvring load distribution (CS-VLA Figure B7)</i>               | - 117 - |
| <i>Gust load distribution (CS-VLA Figure B8)</i>                      | - 118 - |
| <i>Downward lift cases diagram</i>                                    | - 119 - |
| <i>Downward Shear Force diagram</i>                                   | - 119 - |
| <i>Downward Bending moment diagram</i>                                | - 120 - |
| <i>Upward lift cases diagram</i>                                      | - 120 - |
| <i>Upward shear force diagram</i>                                     | - 121 - |

|   |         |
|---|---------|
| <i>Upward bending moment diagram</i>  | - 121 - |
| <i>Case (2) distribution (Figure B6)</i>  | - 123 - |
| <i>Case (1) distribution (Figure B7)</i>  | - 123 - |
| <i>Case (3) distribution (Figure B8)</i>  | - 123 - |
| <i>Gust cases distribution (Figure B8)</i>  | - 123 - |
| <i>Lift on the fin diagram</i>  | - 124 - |
| <i>Shear force on the fin diagram</i>   | - 124 - |
| <i>Bending moment on the fin diagram</i>  | - 125 - |
| <i>Wing spar positions</i>  | - 126 - |
| <i>Wing layout</i>  | - 127 - |
| <i>Aerodynamic and shear centres</i>  | - 128 - |
| <i>Torque diagram of the top right wing (case 4)</i>                                | - 129 - |
| <i>Torque diagram of the bottom right wing (case 4)</i>                             | - 129 - |
| <i>Shear buckling of the wing skin</i>  | - 132 - |
| <i>Shear flows in the spars</i>   | - 134 - |
| <i>Wing maximum deflection beam model</i>   | - 137 - |
| <i>Mass booms layout</i>  | - 139 - |
| <i>Rib loading</i>  | - 140 - |
| <i>Rib airload distribution chordwise</i>   | - 141 - |
| <i>Shear flow in a rib submitted to airload</i>                                     | - 141 - |
| <i>Rib under airload shear force diagram</i>  | - 143 - |
| <i>Rib under airload bending moment diagram</i>                                     | - 143 - |
| <i>Wing axes of inertia for buckling</i>  | - 145 - |
| <i>Buckling of a simply restrained beam</i>   | - 145 - |
| <i>Rear wing attachments beams</i>  | - 146 - |
| <i>Detailed rear wing assembly</i>  | - 147 - |
| <i>Top wing attachment beams</i>  | - 147 - |
| <i>Top view of the top wing attachments</i>   | - 148 - |
| <i>Wing tips attachments</i>  | - 149 - |
| <i>Tailplane general layout</i>   | - 150 - |
| <i>Elevator layout</i>  | - 152 - |
| <i>Elevator hinge configuration</i>   | - 153 - |
| <i>Fin and rudder layout</i>  | - 154 - |
| <i>Rudder hinge configuration</i>   | - 156 - |
| <i>Tail general layout</i>  | - 156 - |
| <i>Tail beam assembly layout, fuselage (left) &amp; tailplane (right) junctions</i> | - 157 - |
| <i>Tail beam layout</i>   | - 157 - |
| <i>Patran tail beam Finite Element model.</i>                                       | - 158 - |
| <i>Tailplane / fin brackets attachments</i>   | - 159 - |
| <i>Tail bracket assembly detail</i>   | - 159 - |

|  |         |
|--|---------|
| <i>Force on the tail beam</i>  | - 160 - |
| <i>Tail beam second moment of area</i>                                     | - 160 - |
| <i>Aileron general layout: side view</i>                                   | - 162 - |
| <i>Aileron general layout: top view</i>                                    | - 162 - |
| <i>Aileron and flaps hinges position</i>                                   | - 163 - |
| <i>Aileron spar deflection under limit load (mm)</i>                       | - 164 - |
| <i>Aileron spar maximum combined stress under ultimate load (MPa)</i>      | - 165 - |
| <i>Fuselage general layout</i>   | - 166 - |
| <i>Engine mounting layout</i>  | - 169 - |
| <i>Dynaero MCR aircraft</i>  | - 170 - |
| <i>Dynaero MCR front view</i>  | - 171 - |
| <i>Finite element model side view</i>                                      | - 172 - |
| <i>Finite element model top view</i>                                       | - 172 - |
| <i>Finite element model front view</i>                                     | - 173 - |
| <i>Finite element model iso view</i>                                       | - 173 - |
| <i>Right wings tips spar and ribs mesh</i>                                 | - 174 - |
| <i>Tail mesh</i>   | - 175 - |
| <i>Fuselage mesh</i>   | - 175 - |
| <i>Wing properties</i>   | - 176 - |
| <i>Fuselage properties</i>   | - 176 - |
| <i>Tail properties</i>   | - 177 - |
| <i>Wing box equivalent loading</i>   | - 178 - |
| <i>Pressure load on the bottom and top skin (rear view, spars removed)</i> | - 178 - |
| <i>Tail loads</i>  | - 179 - |
| <i>Fuselage loads and boundary conditions</i>                              | - 179 - |
| <i>Spar Tsai-Wu criterion result (No units)</i>                            | - 180 - |
| <i>Spar maximum strain results (no units)</i>                              | - 180 - |
| <i>Skin Minimum Principal 2D stress results (MPa)</i>                      | - 181 - |
| <i>Skin maximum strain results (No units)</i>                              | - 182 - |
| <i>Ribs Von Mises stress results (MPa)</i>                                 | - 182 - |
| <i>Booms bar maximum combined stress (MPa)</i>                             | - 183 - |
| <i>Booms bar maximum combined strain (No Units)</i>                        | - 183 - |
| <i>Wing tip bar maximum combined stress (MPa)</i>                          | - 184 - |
| <i>Aerodynamic surfaces Tsai Wu stress criterion (No units)</i>            | - 185 - |
| <i>Tail beam bar maximum combined stress (MPa)</i>                         | - 185 - |
| <i>Fuselage bar maximum combined stress results (MPa)</i>                  | - 186 - |
| <i>Wing deflection under limit load (mm), magnified</i>                    | - 187 - |
| <i>Tail deformations under limit load (mm), magnified</i>                  | - 187 - |
| <i>Fuselage deformations under limit load (mm), magnified</i>              | - 188 - |
| <i>Vibration mode 1 (No units)</i>   | - 189 - |

|   |         |
|---|---------|
| <i>Vibration Mode2 (No units)</i>                       | - 189 - |
| <i>1/3 scale model wings</i>                            | - 190 - |
| <i>Global wing assembly and wing tips details</i>       | - 191 - |
| <i>Parametric analysis matching chart slow aircraft</i> | - 202 - |
| <i>Parametric analysis matching chart fast aircraft</i> | - 204 - |



|   |
|---|
| <h2 style="text-align: center;">LIST OF TABLES</h2> |
|---|

|  |         |
|--|---------|
| <i>Aircraft specifications table</i> _____                           | - 32 -  |
| <i>Parametric analysis results table</i> _____                       | - 84 -  |
| <i>HLM-Colab-Cranfield parametric analysis input data</i> _____      | - 85 -  |
| <i>HLM-Colab-Cranfield parametric analysis results</i> _____         | - 86 -  |
| <i>Mass breakdown table</i> _____                                    | - 103 - |
| <i>Wing load cases summary</i> _____                                 | - 108 - |
| <i>Ailerons load results table</i> _____                             | - 115 - |
| <i>Tailplane loads summary table</i> _____                           | - 118 - |
| <i>Fin load cases summary</i> _____                                  | - 122 - |
| <i>Skin buckling results table and laminate D matrix</i> _____       | - 133 - |
| <i>Front spar buckling results table and laminate D matrix</i> _____ | - 135 - |
| <i>Rear spar buckling results table and laminate D matrix</i> _____  | - 135 - |
| <i>Spars strength analysis results</i> _____                         | - 136 - |
| <i>Booms strength results</i> _____                                  | - 140 - |
| <i>Tailplane laminate result table</i> _____                         | - 151 - |
| <i>Fin laminate result table</i> _____                               | - 155 - |
| <i>Low speed aircraft input parameters table</i> _____               | - 203 - |
| <i>Low speed aircraft output results table</i> _____                 | - 203 - |
| <i>Fast aircraft input parameters table</i> _____                    | - 204 - |
| <i>Fast aircraft output results table</i> _____                      | - 205 - |

# LIST OF NOTATIONS

## GENERAL AERODYNAMIC NOTATIONS

|                 |   |
|-----------------|---|
| $A$             | Wing aspect ratio                             |
| $a$             | Wing lift curve slope                         |
| $a_l$           | Tailplane lift curve slope                    |
| $b$             | Wing span                                     |
| $\beta$         | Compressibility parameter                     |
| $C_D$           | Aircraft drag coefficient with flaps deployed |
| $C_L$           | Wing lift coefficient with flaps deployed     |
| $C_M$           | Wing pitching moment                          |
| $C_{D0}$        | Zero lift drag coefficient for basic wing     |
| $C_{L0}$        | Wing lift coefficient at zero angle of attack |
| $C_{M0}$        | Wing pitching moment at zero angle of attack  |
| $c$             | Wing geometric mean chord                     |
| $\bar{c}$       | Wing aerodynamic mean chord                   |
| $M$             | Mach number                                   |
| $\lambda$       | Wing taper ration                             |
| $\Lambda_{0.5}$ | Wing mid chord sweep angle                    |
| $Re$            | Reynolds number                               |
| $t$             | Airfoil maximum thickness                     |
| $\nu$           | Air kinematic viscosity                       |
| $T^\circ$       | Air temperature                               |
| $\rho$          | Air density                                   |
| $V$             | Velocity                                      |
| $\bar{V}$       | Tail volume coefficient                       |

|             |   |
|-------------|---|
| $W$         | Aircraft gross weight   |
| $x_{um}$    | Chordwise location of maximum upper surface aerofoil ordinate |
| $Z_{u1.25}$ | Upper surface ordinate at $x=0.0125c$ for basic aerofoil      |

## GENERAL FLIGHT MECHANICS NOTATIONS

|          |  |
|----------|--|
| $V_{NE}$ | Velocity Never Exceed                                |
| $V_{SO}$ | Stall velocity with flaps and undercarriage deployed |
| $V_C$    | Cruise velocity                                      |
| $E$      | Young modulus  |
| $G$      | Shear modulus  |
| $\nu$    | Poisson Coefficient                                  |

## UNITS SYSTEM

All the calculations in this thesis are made using the International System Units (ISU) when possible. (Mass=kg, length=m, time=s, temperature=K). However, in the American literature especially, the Imperial Units (IU) are very common. That is why they will be used sometimes. When no units are mentioned the figure is non dimensional.

# 1. INTRODUCTION

## 1.1. REGULATION OUTLINES

The BMAA (British Microlight Aircraft Association) has campaigned for a long time to obtain an airworthiness requirement simplification for the single seat lightweight microlights. In April 2007 the CAA (Civil Aviation Authority) published the rules for this new regime. The basic outline of this new regulation is explained in this chapter.

### 1.1.1. *Standard microlights airworthiness requirements*

The official airworthiness requirement document for the design of microlights is the Section S of the CAP 482, British Civil Airworthiness Requirements. This is edited by the CAA.

This document is mostly based on the JAR22 or CS-VLA, edited by the EASA (**European Aviation Safety Agency**). The main difference between the section S of the CAP 482 and the CS-VLA is that the section S of the CAP 482 is less detailed and does not provide as many calculation methods to help with the airworthiness requirements.

It is possible to work with both of the regulations since the numbers of the chapters are consistent between the two documents. However, extra precautions need to be taken to make sure that the aircraft is compliant with at least one of the two documents.

The main outline of the JAR 22 for the microlight category is explained below:

- **MTWA Less than 300/450 kg, single/doubled seat**
- **Wing loading at MTWA < 25kg/m<sup>2</sup> OR stall speed < 65 km/h**

(MTWA=Maximum Take-off Weight Authorized)

### 1.1.2. *New deregulated regime requirement*

The new deregulated regime creates a subcategory in the standard microlight category. The criteria are:

- **Single seat.**
- **Empty weight less than 115kg.**
- **Wing loading without pilot and without fuel less than 10kg/m<sup>2</sup>.**

This new deregulated regime makes the regulations much more flexible and easier for the pilots, but still gives large margins of manoeuvre for the design. This regulation works for Great Britain ONLY. It is not approved by the EASA.

This new regulation allows the aircraft to fly without a permit to fly. However, the rest of the legislation remains applicable:

- The pilot must have a valid license.
- The aircraft must have a noise certification.
- The aircraft must be registered at the CAA and have insurance.
- The aircraft obeys the rules of the air.

➔ More information can be found on the detailed technical information leaflet concerning the deregulated regime published by the BMAA in **APPENDIX A** (BMAA Deregulated single seat microlights handbook).

## 1.2. DESIGN OVERVIEW AND OBJECTIVES

### 1.2.1. *An amazing experience*

Designing an aircraft is a long and challenging process, but there is always the motivation of imagining that, eventually, the design will be flying. This is the purpose of this thesis.

The design was submitted the 31<sup>st</sup> of July to take part in the Popular Flying Association design competition for the sub 115 kg deregulated aircraft.

### 1.2.2. *Objectives*

The objectives of this thesis are the following:

- Perform an aircraft survey and determine the best design
- Determine the general specifications
- Determine the layout of the main structural components

These objectives are aimed at making possible:

- To get an aircraft design with outstanding performance to win the world's microlight championship.
- To begin the manufacturing process

## 1.3. AIRCRAFT DESIGN PROCESS

### ➔ SURVEY OF EXISTING AIRCRAFT IN THIS CLASS

This part allows us to collect data and get a good idea of the existing microlight market in the category less or around 115 kg empty weight. The data collected will be used for the parametric analysis. Then we do quick comparisons to evaluate the relative aircraft performances.

### ➔ GENERAL STUDY OF AIRCRAFT DESIGN OPTION

In this chapter we are going to study the designs options: wing arrangement, tail arrangement, undercarriage, materials, etc. At the end of the chapter we will have selected a layout for the aircraft.

### ➔ STUDY OF THE COLAB AIRCRAFT DESIGN

The Colab design is based on a revolutionary wing. This is the design that has been selected from the study in the previous chapter, and the aim of this new chapter is to list and explain all the advantages of the Colab design and why it has been chosen.

### ➔ PARAMETRIC ANALYSIS

The parametric analysis allows us produce a tool to choose and predict the aircraft general performance. Basically, we use all the data collected in the aircraft survey, and thanks to a method established by Loftin in a NASA Paper [Ref. 9], we establish correlations between the aircraft properties and then generate a diagram which allows us to predict the aircraft performance. The strength of this method is that it is based on existing aircraft that we have selected, which are in the same category as our design. This gives much more consistent data than the generic formulae found in the books.

### ➔ AIRCRAFT GENERAL LAYOUT

In this part we determine the geometric properties of the aircraft, the global performance based on the parametric analysis and on the survey done in the previous chapters.

### ➔ AIRCRAFT MASS AND STABILITY

The aim of this part is to check the stability and CG position of the aircraft.

### ➔ AIRWORTHINESS AND LOADING ACTIONS

In this part we study the Section S of the CAP 482 and the CS-VLA to establish the loading actions on the aircraft, the n-V diagram and verify that our aircraft is safe.

### ➔ DETAILED DESIGN

In this part we design the various components of the aircraft, choose the materials, stress them, and check the reserve factors.

### ➔ FINITE ELEMENT ANALYSIS

In this part we check that the overall structure is safe, using Patran / Nastran. Then we do an iterative process to optimise the structure properties and make sure that the aircraft has the minimum weight.

## 1.4. AIRCRAFT SPECIFICATIONS

### 1.4.1. *General geometry*

|                |                     |
|----------------|---------------------|
| Wing span      | 7.6m                |
| Overall length | 6.3m                |
| Overall height | 2.1m                |
| Wing chord     | 0.76m               |
| Wing area      | 11.5 m <sup>2</sup> |
| Tailplane area | 1.23 m <sup>2</sup> |
| Elevator area  | 1.3 m <sup>2</sup>  |
| Fin area       | 0.69 m <sup>2</sup> |
| Rudder area    | 0.57 m <sup>2</sup> |

### 1.4.2. *Mass summary*

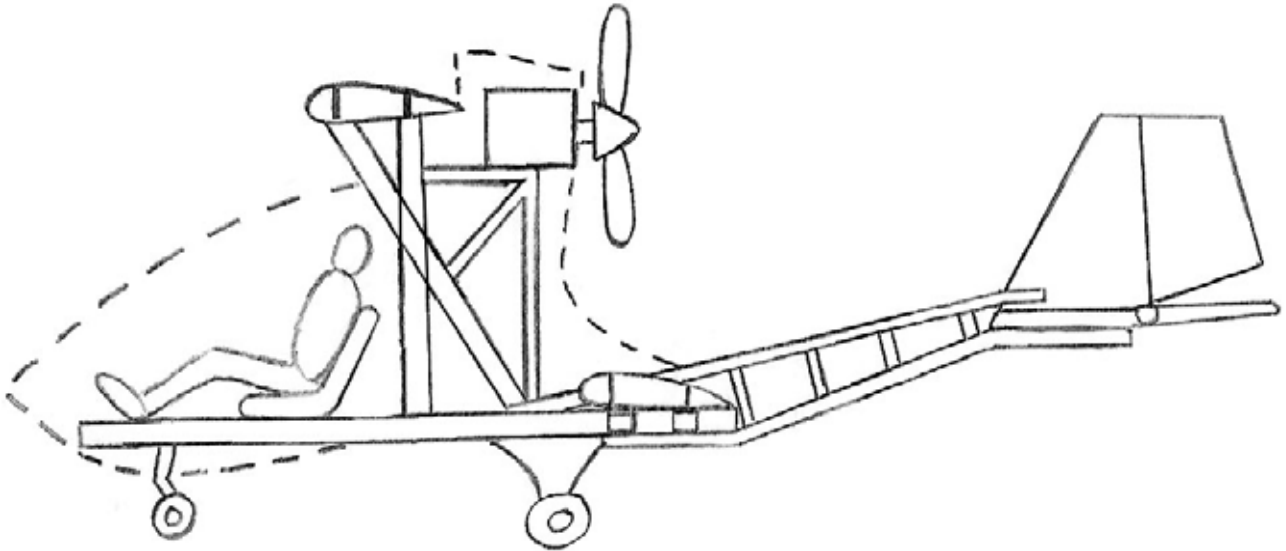
|                  |            |
|------------------|------------|
| Empty weight     | 110-115 kg |
| Max pilot weight | 100 kg     |
| Max fuel weight  | 25 kg      |
| MTOW             | 240 kg     |

### 1.4.3. *Performance summary*

|                              |          |        |
|------------------------------|----------|--------|
| Engine power                 | 17.65 kW | 31 hp  |
| VNE                          | 70 m/s   | 135 kt |
| Vcruise max                  | 50 m/s   | 97 kt  |
| V <sub>F</sub>               | 22 m/s   | 43 kt  |
| V <sub>S</sub> with flaps    | 5 m/s    | 11 kt  |
| V <sub>S</sub> without flaps | 15 m/s   | 32 kt  |
| Take-off run                 | 50 m     |        |
| Landing run                  | 50 m     |        |

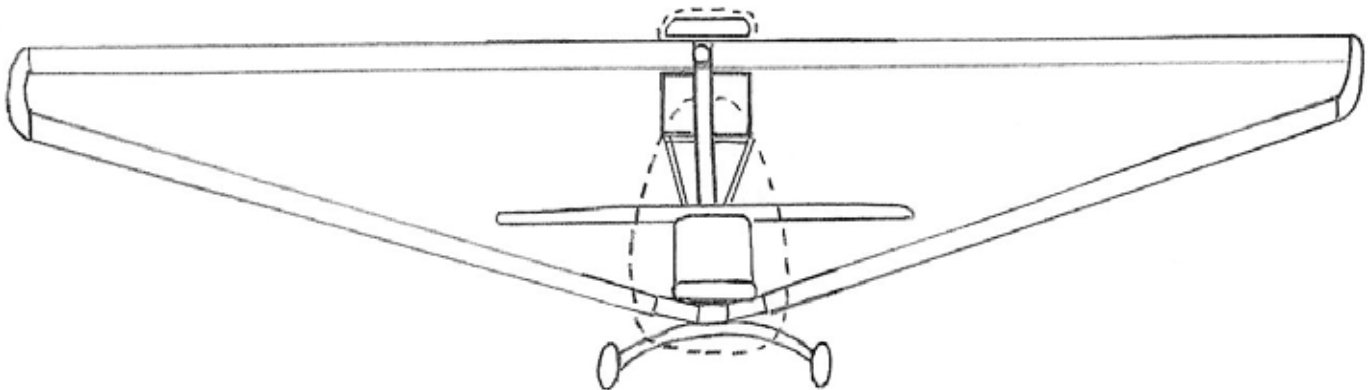
## 1.5. 3 VIEWS SKETCHES

### 1.5.1. Side view



HLM-07 COLAB side view

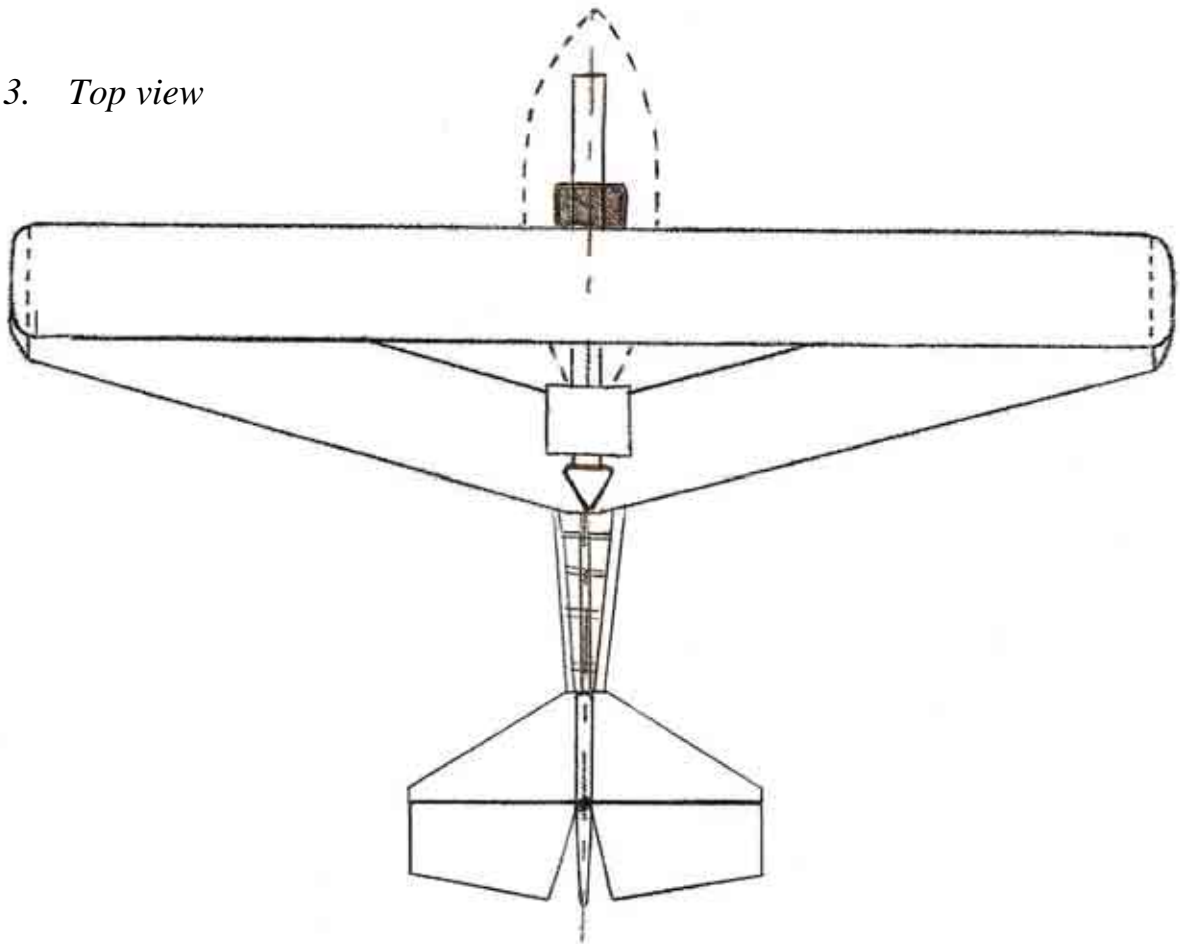
### 1.5.2. Front view



HLM-07 COLAB front view

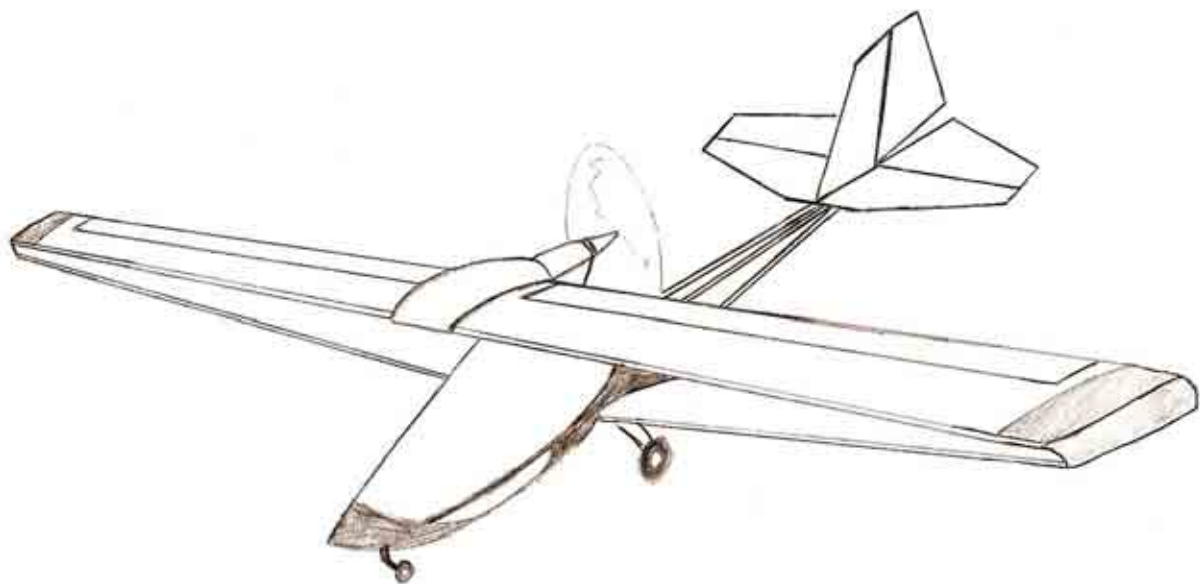


1.5.3. *Top view*



HLM-07 COLAB top view

1.5.4. *Isometric view*



HLM-07 COLAB isometric view

## 2. SURVEY OF ULTRALIGHT MARKET

In this part we are going to study different existing designs which have roughly the same characteristics as our design. This study will allow us to get an idea of the existing designs and also the data collected will be used for the parametric analysis.

### 2.1. MICROLIGHTS DESIGNS LIST

#### 2.1.1. *Top wing pusher propeller configurations*

The top wing configuration with the pusher propeller is the most common configuration in this category of microlight. We will discuss later the advantages and inconveniences of this configuration.



Kolb Firestar

(<http://www.pilotmix.com>, 22<sup>nd</sup> May 2007)

|                             |       |                    |                          |
|-----------------------------|-------|--------------------|--------------------------|
| Empty weight (Kg)           | 115   | Take-off run (m)   | 46                       |
| Gross weight (Kg)           | 226   | Landing run (m)    | 46                       |
| Engine power (hp)           | 40    | Climb rate (m/min) | 305                      |
| Wing span (m)               | 6.71  | Range (km)         | -                        |
| Wing area (m <sup>2</sup> ) | 10.87 | Flying control     | Full-span flaperons      |
| Overall length (m)          | 5.94  | Number of seats    | 1                        |
| Overall height (m)          | 1.75  | Cockpit            | Open                     |
| Cruise speed (kt)           | 55    | Undercarriage      | Tailwheel type           |
| Stalling speed (kt)         | 24    | Material           | Steel, aluminium, fabric |
| Fuel capacity (L)           | 18.9  | Country            | USA                      |



Golden Circle T Bird  
(<http://www.pilotmix.com>, 23<sup>rd</sup> May 2007)

|                             |      |                    |                            |
|-----------------------------|------|--------------------|----------------------------|
| Empty weight (Kg)           | 122  | Take-off run (m)   | 49                         |
| Gross weight (Kg)           | 272  | Landing run (m)    | 46                         |
| Engine power (hp)           | 40   | Climb rate (m/min) | 240                        |
| Wing span (m)               | 9.5  | Range (km)         | -                          |
| Wing area (m <sup>2</sup> ) | 14.3 | Flying control     | 3 axis                     |
| Overall length (m)          | -    | Number of seats    | 1                          |
| Overall height (m)          | 53   | Cockpit            | Open cabin                 |
| Cruise speed (kt)           | 22   | Undercarriage      | tricycle type or tailwheel |
| Stalling speed (kt)         | -    | Material           | Steel, aluminium, fabric   |
| Fuel capacity (L)           | -    | Country            | USA                        |



Seahawk Condor  
(<http://www.pilotmix.com>, 23<sup>rd</sup> May 2007)

|                             |      |                    |                          |
|-----------------------------|------|--------------------|--------------------------|
| Empty weight (Kg)           | 106  | Take-off run (m)   | 76                       |
| Gross weight (Kg)           | 215  | Landing run (m)    | 91                       |
| Engine power (hp)           | 43   | Climb rate (m/min) | 160                      |
| Wing span (m)               | 9.8  | Range (km)         | -                        |
| Wing area (m <sup>2</sup> ) | 14.5 | Flying control     | 2 axis + spoilerons      |
| Overall length (m)          | -    | Number of seats    | 1                        |
| Overall height (m)          | -    | Cockpit            | Open cabin               |
| Cruise speed (kt)           | 30   | Undercarriage      | Tailwheel type           |
| Stalling speed (kt)         | 22   | Material           | Steel, aluminium, fabric |
| Fuel capacity (L)           | -    | Country            | USA                      |



Gull 2000

(<http://www.pilotmix.com>, 23<sup>rd</sup> May 2007)

|                             |     |                    |                        |
|-----------------------------|-----|--------------------|------------------------|
| Empty weight (Kg)           | 113 | Take-off run (m)   | 38                     |
| Gross weight (Kg)           | 250 | Landing run (m)    | 23                     |
| Engine power (hp)           | 28  | Climb rate (m/min) | 213                    |
| Wing span (m)               | 6.1 | Range (km)         | -                      |
| Wing area (m <sup>2</sup> ) | 8.8 | Flying control     | 3 axis                 |
| Overall length (m)          | 5.6 | Number of seats    | 1                      |
| Overall height (m)          | 1.6 | Cockpit            | Sided open cabin       |
| Cruise speed (kt)           | 55  | Undercarriage      | Tricycle               |
| Stalling speed (kt)         | 23  | Material           | Glass fibre, aluminium |
| Fuel capacity (L)           | 19  | Country            | USA                    |



Rans S-17 Stinger

(<http://www.pilotmix.com>, 24<sup>th</sup> May 2007)

|                             |      |                    |                           |
|-----------------------------|------|--------------------|---------------------------|
| Empty weight (Kg)           | 114  | Take-off run (m)   | 30                        |
| Gross weight (Kg)           | 239  | Landing run (m)    | 30                        |
| Engine power (hp)           | 40   | Climb rate (m/min) | 274                       |
| Wing span (m)               | 8.99 | Range (km)         | 114                       |
| Wing area (m <sup>2</sup> ) | 11.8 | Flying control     | 3 axis + flaps            |
| Overall length (m)          | 5.3  | Number of seats    | 1                         |
| Overall height (m)          | 2.13 | Cockpit            | Side open cabin           |
| Cruise speed (kt)           | 48   | Undercarriage      | Tailwheel                 |
| Stalling speed (kt)         | 25   | Material           | Aluminium tube and fabric |
| Fuel capacity (L)           | 19   | Country            | USA                       |



Interplane Griffon 103

(<http://www.pilotmix.com>, 24<sup>th</sup> May 2007)

|                             |       |                    |                           |
|-----------------------------|-------|--------------------|---------------------------|
| Empty weight (Kg)           | 115   | Take-off run (m)   | -                         |
| Gross weight (Kg)           | 235   | Landing run (m)    | -                         |
| Engine power (hp)           | 41.6  | Climb rate (m/min) | 210                       |
| Wing span (m)               | 9     | Range (km)         | -                         |
| Wing area (m <sup>2</sup> ) | 13.98 | Flying control     | 3 axis                    |
| Overall length (m)          | 5.73  | Number of seats    | 1                         |
| Overall height (m)          | 2.2   | Cockpit            | Side open cabin           |
| Cruise speed (kt)           | 49    | Undercarriage      | Tricycle                  |
| Stalling speed (kt)         | 25    | Material           | Aluminium tube and fabric |
| Fuel capacity (L)           | 18.9  | Country            | Czech Republic            |



Aerolite 103

(<http://www.pilotmix.com>, 24<sup>th</sup> May 2007)

|                             |      |                    |                           |
|-----------------------------|------|--------------------|---------------------------|
| Empty weight (Kg)           | 114  | Take-off run (m)   | 31                        |
| Gross weight (Kg)           | 204  | Landing run (m)    | 31                        |
| Engine power (hp)           | 28   | Climb rate (m/min) | 244                       |
| Wing span (m)               | 8.18 | Range (km)         | 148                       |
| Wing area (m <sup>2</sup> ) | 11.5 | Flying control     | 3 axis                    |
| Overall length (m)          | -    | Number of seats    | 1                         |
| Overall height (m)          | -    | Cockpit            | open cabin                |
| Cruise speed (kt)           | 39   | Undercarriage      | Tricycle                  |
| Stalling speed (kt)         | 23   | Material           | Aluminium tube and fabric |
| Fuel capacity (L)           | 18.9 | Country            | USA                       |





Aviasud Sirocco

(<http://www.pilotmix.com>, 28<sup>th</sup> May 2007)

|                             |       |                    |                                |
|-----------------------------|-------|--------------------|--------------------------------|
| Empty weight (Kg)           | 115   | Take-off run (m)   | -                              |
| Gross weight (Kg)           | 250   | Landing run (m)    | -                              |
| Engine power (hp)           | 30 hp | Climb rate (m/min) | 300                            |
| Wing span (m)               | 10.12 | Range (km)         | -                              |
| Wing area (m <sup>2</sup> ) | 13.80 | Flying control     | 3 axis                         |
| Overall length (m)          | 5.85  | Number of seats    | 1                              |
| Overall height (m)          | 2.80  | Cockpit            | closed cabin                   |
| Cruise speed (kt)           | 43    | Undercarriage      | Tricycle                       |
| Stalling speed (kt)         | 21    | Material           | Aluminium, fabric, glass fibre |
| Fuel capacity (L)           | 20    | Country            | France                         |



CFM shadow C & D

(<http://www.pilotmix.com>, 28<sup>th</sup> May 2007)

|                             |       |                    |                           |
|-----------------------------|-------|--------------------|---------------------------|
| Empty weight (Kg)           | 158   | Take-off run (m)   | 91                        |
| Gross weight (Kg)           | 382   | Landing run (m)    | 137                       |
| Engine power (hp)           | 64 hp | Climb rate (m/min) | 128                       |
| Wing span (m)               | 13.41 | Range (km)         | 370                       |
| Wing area (m <sup>2</sup> ) | 17.56 | Flying control     | 3 axis                    |
| Overall length (m)          | 7.01  | Number of seats    | 2                         |
| Overall height (m)          | 1.52  | Cockpit            | closed cabin              |
| Cruise speed (kt)           | 75    | Undercarriage      | Tricycle                  |
| Stalling speed (kt)         | 34    | Material           | Aluminium tube and fabric |
| Fuel capacity (L)           | 20    | Country            | Great Britain             |



Avanced aviation Carrera 150  
(Jane's, all the world's aircraft)

|                             |       |                    |                           |
|-----------------------------|-------|--------------------|---------------------------|
| Empty weight (Kg)           | 118   | Take-off run (m)   | -                         |
| Gross weight (Kg)           | 249   | Landing run (m)    | -                         |
| Engine power (hp)           | 40 hp | Climb rate (m/min) | 305                       |
| Wing span (m)               | 8.43  | Range (km)         | -                         |
| Wing area (m <sup>2</sup> ) | 12.45 | Flying control     | 3 axis                    |
| Overall length (m)          | 6.22  | Number of seats    | 1                         |
| Overall height (m)          | 1.68  | Cockpit            | Side opened cabin         |
| Cruise speed (kt)           | 52    | Undercarriage      | Tailwheel                 |
| Stalling speed (kt)         | 23    | Material           | Aluminium tube and fabric |
| Fuel capacity (L)           | 19    | Country            | Italy                     |



Quicksilver MX sprint  
(<http://www.pilotmix.com>, 28<sup>th</sup> May 2007)

|                             |       |                    |                           |
|-----------------------------|-------|--------------------|---------------------------|
| Empty weight (Kg)           | 112   | Take-off run (m)   | 70                        |
| Gross weight (Kg)           | 236   | Landing run (m)    | 30                        |
| Engine power (hp)           | 40 hp | Climb rate (m/min) | 128                       |
| Wing span (m)               | 8.52  | Range (km)         | 370                       |
| Wing area (m <sup>2</sup> ) | 14.42 | Flying control     | 3 axis                    |
| Overall length (m)          | 5.49  | Number of seats    | 1                         |
| Overall height (m)          | 2.68  | Cockpit            | Open cabin                |
| Cruise speed (kt)           | 46    | Undercarriage      | Tricycle                  |
| Stalling speed (kt)         | 21    | Material           | Aluminium tube and fabric |
| Fuel capacity (L)           | 19    | Country            | USA                       |



Maxair Drifter DR532 Rocket  
(<http://www.pilotmix.com>, 21<sup>st</sup> May 2007)

|                             |       |                    |                           |
|-----------------------------|-------|--------------------|---------------------------|
| Empty weight (Kg)           | 109   | Take-off run (m)   | -                         |
| Gross weight (Kg)           | 227   | Landing run (m)    | -                         |
| Engine power (hp)           | 46 hp | Climb rate (m/min) | 244                       |
| Wing span (m)               | 9.14  | Range (km)         | 193                       |
| Wing area (m <sup>2</sup> ) | 14.12 | Flying control     | 3 axis                    |
| Overall length (m)          | 5.79  | Number of seats    | 1                         |
| Overall height (m)          | 2.67  | Cockpit            | Open                      |
| Cruise speed (kt)           | 48    | Undercarriage      | Tricycle                  |
| Stalling speed (kt)         | 23    | Material           | Aluminium tube and fabric |
| Fuel capacity (L)           | 19    | Country            | USA                       |



### 2.1.2. *Top wing puller propeller configurations*

The configuration with the top wing and the puller propeller is the second most common configuration in this category of microlight. We will compare later this configuration with the pushing propeller configuration.



Weedhopper

(<http://www.pilotmix.com>, 21<sup>st</sup> May 2007)

|                             |      |                    |                           |
|-----------------------------|------|--------------------|---------------------------|
| Empty weight (Kg)           | 113  | Take-off run (m)   | 31                        |
| Gross weight (Kg)           | 250  | Landing run (m)    | 31                        |
| Engine power (hp)           | 40   | Climb rate (m/min) | 305                       |
| Wing span (m)               | 8.5  | Range (km)         | -                         |
| Wing area (m <sup>2</sup> ) | 15.6 | Flying control     | 2 axis                    |
| Overall length (m)          | 8.3  | Number of seats    | 1                         |
| Overall height (m)          | 2.9  | Cockpit            | open cabin                |
| Cruise speed (kt)           | 48   | Undercarriage      | Tricycle                  |
| Stalling speed (kt)         | 17.5 | Material           | Aluminium tube and fabric |
| Fuel capacity (L)           | 19   | Country            | USA                       |



Flying K sky raider  
(<http://www.pilotmix.com>, 21<sup>st</sup> May 2007)

|                             |       |                    |                           |
|-----------------------------|-------|--------------------|---------------------------|
| Empty weight (Kg)           | 113   | Take-off run (m)   | 23                        |
| Gross weight (Kg)           | 249   | Landing run (m)    | 23                        |
| Engine power (hp)           | 41.6  | Climb rate (m/min) | 183                       |
| Wing span (m)               | 7.99  | Range (km)         | 222                       |
| Wing area (m <sup>2</sup> ) | 10.22 | Flying control     | 3 axis                    |
| Overall length (m)          | 5.18  | Number of seats    | 1                         |
| Overall height (m)          | 1.59  | Cockpit            | Side open                 |
| Cruise speed (kt)           | 56    | Undercarriage      | Tailwheel                 |
| Stalling speed (kt)         | 20    | Material           | Aluminium tube and fabric |
| Fuel capacity (L)           | 18.9  | Country            | USA                       |



AeroLites Bearcat  
(<http://www.pilotmix.com>, 21<sup>st</sup> May 2007)

|                             |         |                    |                           |
|-----------------------------|---------|--------------------|---------------------------|
| Empty weight (Kg)           | 130     | Take-off run (m)   | 61                        |
| Gross weight (Kg)           | 317     | Landing run (m)    | -                         |
| Engine power (hp)           | 41.6 hp | Climb rate (m/min) | 228                       |
| Wing span (m)               | 9.14    | Range (km)         | 231                       |
| Wing area (m <sup>2</sup> ) | 13.94   | Flying control     | 3 axis                    |
| Overall length (m)          | 5.33    | Number of seats    | 1                         |
| Overall height (m)          | 1.96    | Cockpit            | Side open                 |
| Cruise speed (kt)           | 56      | Undercarriage      | Tailwheel                 |
| Stalling speed (kt)         | 24      | Material           | Aluminium tube and fabric |
| Fuel capacity (L)           | 19      | Country            | USA                       |



Flightstar Spyder  
(<http://www.pilotmix.com>, 21<sup>st</sup> May 2007)

|                             |       |                    |                           |
|-----------------------------|-------|--------------------|---------------------------|
| Empty weight (Kg)           | 126   | Take-off run (m)   | 31                        |
| Gross weight (Kg)           | 292   | Landing run (m)    | 31                        |
| Engine power (hp)           | 42    | Climb rate (m/min) | 201                       |
| Wing span (m)               | 9.12  | Range (km)         | 177                       |
| Wing area (m <sup>2</sup> ) | 13.31 | Flying control     | 3 axis                    |
| Overall length (m)          | -     | Number of seats    | 1                         |
| Overall height (m)          | -     | Cockpit            | Open                      |
| Cruise speed (kt)           | 56    | Undercarriage      | Tricycle                  |
| Stalling speed (kt)         | 32    | Material           | Aluminium tube and fabric |
| Fuel capacity (L)           | 18.9  | Country            | USA                       |

### 2.1.3. Conventional low wing 3 axis layout

This configuration is the most common for light aircraft. However, it is not the most prevalent in the microlight category. We will explain later why.



MB 02 Souricette  
(<http://air.souris.set.free.fr>, June 3<sup>rd</sup>)

|                             |     |                    |                 |
|-----------------------------|-----|--------------------|-----------------|
| Empty weight (Kg)           | 95  | Take-off run (m)   | 150             |
| Gross weight (Kg)           | 200 | Landing run (m)    | 100             |
| Engine power (hp)           | 12  | Climb rate (m/min) | 132             |
| Wing span (m)               | 9   | Range (km)         | -               |
| Wing area (m <sup>2</sup> ) | 10  | Flying control     | 3 axis          |
| Overall length (m)          | 5.7 | Number of seats    | 1               |
| Overall height (m)          | -   | Cockpit            | Closed          |
| Cruise speed (kt)           | 54  | Undercarriage      | Tailwheel       |
| Stalling speed (kt)         | 24  | Material           | Wood and fabric |
| Fuel capacity (L)           | 19  | Country            | France          |



Fisher Avenger

(<http://www.pilotmix.com>, 30<sup>th</sup> May 2007)

|                             |       |                    |                 |
|-----------------------------|-------|--------------------|-----------------|
| Empty weight (Kg)           | 113   | Take-off run (m)   | 61              |
| Gross weight (Kg)           | 270   | Landing run (m)    | -               |
| Engine power (hp)           | 35 hp | Climb rate (m/min) | 120             |
| Wing span (m)               | 8.2   | Range (km)         | -               |
| Wing area (m <sup>2</sup> ) | 11.26 | Flying control     | 3 axis          |
| Overall length (m)          | -     | Number of seats    | 1               |
| Overall height (m)          | -     | Cockpit            | Open            |
| Cruise speed (kt)           | 52    | Undercarriage      | Tailwheel       |
| Stalling speed (kt)         | 25    | Material           | Wood and fabric |
| Fuel capacity (L)           | 19    | Country            | USA             |

#### 2.1.4. *Less than 55kg microlight*

This category contains the lightest 3 axis microlight with rigid structures.



Hovey Whing Ding II  
(Jane's, all the world's aircraft)

|                             |       |                    |                 |
|-----------------------------|-------|--------------------|-----------------|
| Empty weight (Kg)           | 55.5  | Take-off run (m)   | 76              |
| Gross weight (Kg)           | 140   | Landing run (m)    | 40              |
| Engine power (hp)           | 14 hp | Climb rate (m/min) | 60              |
| Wing span (m)               | 5.69  | Range (km)         | 32              |
| Wing area (m <sup>2</sup> ) | 9.85  | Flying control     | 3 axis          |
| Overall length (m)          | 4.27  | Number of seats    | 1               |
| Overall height (m)          | 1.68  | Cockpit            | Open            |
| Cruise speed (kt)           | 35    | Undercarriage      | Tailwheel       |
| Stalling speed (kt)         | 23    | Material           | Wood and fabric |
| Fuel capacity (L)           | 2     | Country            | France          |



E-12n

(<http://www.pilotmix.com>, 4th June 2007)

|                             |      |                    |                            |
|-----------------------------|------|--------------------|----------------------------|
| Empty weight (Kg)           | 48   | Take-off run (m)   | 60                         |
| Gross weight (Kg)           | 160  | Landing run (m)    | 90                         |
| Engine power (hp)           | 14.2 | Climb rate (m/min) | 192                        |
| Wing span (m)               | 6.5  | Range (km)         | 130                        |
| Wing area (m <sup>2</sup> ) | 5.38 | Flying control     | 3 axis                     |
| Overall length (m)          | 4.45 | Number of seats    | 1                          |
| Overall height (m)          | -    | Cockpit            | Open                       |
| Cruise speed (kt)           | 43   | Undercarriage      | Tricycle                   |
| Stalling speed (kt)         | 32   | Material           | Aluminium tubes and fabric |
| Fuel capacity (L)           | 6    | Country            | Czech Republic             |



### 2.1.5. *Non common designs*

In this category some of the most incredible microlight designs are presented. These designs present all specific features which make them unique.



MC-12 Cricket

(<http://www.pilotmix.com>, 28th May 2007)

|                             |        |                    |                      |
|-----------------------------|--------|--------------------|----------------------|
| Empty weight (Kg)           | 75     | Take-off run (m)   | 120                  |
| Gross weight (Kg)           | 170    | Landing run (m)    | -                    |
| Engine power (hp)           | 2 x 15 | Climb rate (m/min) | 360                  |
| Wing span (m)               | 4.9    | Range (km)         | 500                  |
| Wing area (m <sup>2</sup> ) | 3.1    | Flying control     | 3 axis               |
| Overall length (m)          | 3.9    | Number of seats    | 1                    |
| Overall height (m)          | 0.97   | Cockpit            | Closed               |
| Cruise speed (kt)           | 102    | Undercarriage      | Tricycle             |
| Stalling speed (kt)         | 42     | Material           | Metal and composites |
| Fuel capacity (L)           | 23     | Country            | France               |

This aircraft is one of the most effective aircraft in the world in this weight category. The prototype flew for the first time in 1973. The “Cricri” is actually the smallest 2 engine aircraft in the world. Its empty weight is only 75kg but the VNE is 220 km/h. The Cricri is also certified for aerobatic manoeuvres in positive G.





Lazair

(<http://www.pilotmix.com>, 5th June 2007)

|                             |                      |                    |                        |
|-----------------------------|----------------------|--------------------|------------------------|
| Empty weight (Kg)           | 95                   | Take-off run (m)   | 50                     |
| Gross weight (Kg)           | 240                  | Landing run (m)    | 50                     |
| Engine power (hp)           | 2 x 9.5              | Climb rate (m/min) | 120                    |
| Wing span (m)               | 11.1 (D-cell design) | Range (km)         | -                      |
| Wing area (m <sup>2</sup> ) | 13.7                 | Flying control     | 3 axis                 |
| Overall length (m)          | -                    | Number of seats    | 1                      |
| Overall height (m)          | -                    | Cockpit            | open                   |
| Cruise speed (kt)           | 35                   | Undercarriage      | 2 tailwheels on V-tail |
| Stalling speed (kt)         | 22                   | Material           | Metal and fabric       |
| Fuel capacity (L)           | 19                   | Country            | Canada                 |

The Lazair was one of the first microlights and, as a pioneer, it helped to define the microlight category. This aircraft first flew in 1978. The design has been optimised and we can especially notice the inverted V tail with the wheels at the tips. Furthermore, this aircraft is fitted with 2 engines.



Pou du ciel

(<http://www.pilotmix.com>, 29th May 2007)

|                             |     |                    |                 |
|-----------------------------|-----|--------------------|-----------------|
| Empty weight (Kg)           | 115 | Take-off run (m)   | 61              |
| Gross weight (Kg)           | 225 | Landing run (m)    | -               |
| Engine power (hp)           | 40  | Climb rate (m/min) | 150             |
| Wing span (m)               | 6   | Range (km)         | -               |
| Wing area (m <sup>2</sup> ) | 13  | Flying control     | 2 axis          |
| Overall length (m)          | -   | Number of seats    | 1               |
| Overall height (m)          | -   | Cockpit            | Closed          |
| Cruise speed (kt)           | 60  | Undercarriage      | Tricycle        |
| Stalling speed (kt)         | 30  | Material           | Wood and fabric |
| Fuel capacity (L)           | 19  | Country            | France          |

The Pou du Ciel is a plane designed in 1936. The initial design has evolved, but the original spirit is still the same: tiny, two wings with different incidence, wood and fabric. More than 10 derived designs of the Pou du Ciel are currently flying all around the world.



Pouchel

(<http://www.pilotmix.com>, 27th May 2007)

|                             |          |                    |                           |
|-----------------------------|----------|--------------------|---------------------------|
| Empty weight (Kg)           | 80       | Take-off run (m)   | -                         |
| Gross weight (Kg)           | 170      | Landing run (m)    | -                         |
| Engine power (hp)           | 25       | Climb rate (m/min) | -                         |
| Wing span (m)               | 5.44 & 4 | Range (km)         | -                         |
| Wing area (m <sup>2</sup> ) | 11.40    | Flying control     | 2 axis                    |
| Overall length (m)          | -        | Number of seats    | 1                         |
| Overall height (m)          | -        | Cockpit            | Open                      |
| Cruise speed (kt)           | 54       | Undercarriage      | Tailwheel                 |
| Stalling speed (kt)         | 26       | Material           | Aluminium ladder + fabric |
| Fuel capacity (L)           | -        | Country            | France                    |

The Pouchel is a very recent design, making its first flight in 2002. The inventor of this aircraft wanted to fight against the cost and the time that building an aircraft requires. He noticed how cheap the aluminium ladders are and that they have the properties suitable for an aircraft design: stiff and light. The idea of the Pouchel was born: make aircraft using aluminium ladder structure. (The French translation for “ladder” is “échelle”. The Pouchel is actually a mix between the “pou du ciel” and an “échelle”).



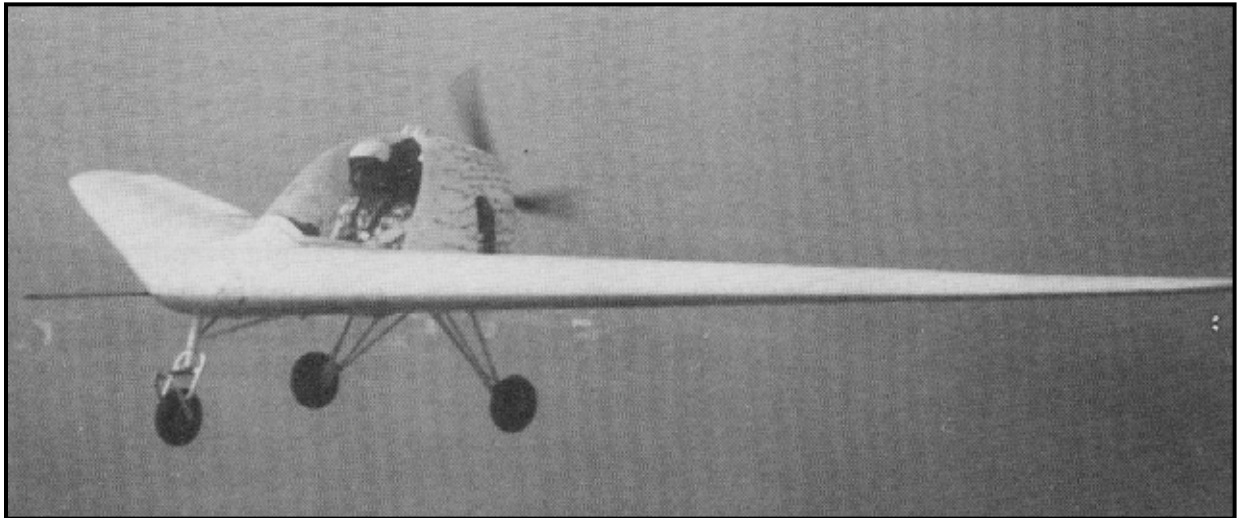
Piel Onyx CP 150

(<http://www.pilotmix.com>, 26th May 2007)

|                             |             |                    |                                  |
|-----------------------------|-------------|--------------------|----------------------------------|
| Empty weight (Kg)           | 70          | Take-off run (m)   | 50                               |
| Gross weight (Kg)           | 180         | Landing run (m)    | 30                               |
| Engine power (hp)           | 18          | Climb rate (m/min) | 137                              |
| Wing span (m)               | 7.30        | Range (km)         | -                                |
| Wing area (m <sup>2</sup> ) | 9.10 / 3.70 | Flying control     | Canard configuration             |
| Overall length (m)          | 3.53        | Number of seats    | 1                                |
| Overall height (m)          | -           | Cockpit            | Closed                           |
| Cruise speed (kt)           | 52          | Undercarriage      | Tricycle                         |
| Stalling speed (kt)         | 22          | Material           | Glass fiber, Kevlar fabric, wood |
| Fuel capacity (L)           | 19          | Country            | France                           |

The Onyx CP 150 is one of the few designs less than 100kg with a canard configuration. This aircraft has outstanding performance compared to other aircraft with the same engine power.





Nike aeronautica PUL 9  
(Jane's, all the world's aircraft)

|                             |       |                    |                        |
|-----------------------------|-------|--------------------|------------------------|
| Empty weight (Kg)           | 150   | Take-off run (m)   | -                      |
| Gross weight (Kg)           | 300   | Landing run (m)    | -                      |
| Engine power (hp)           | 42    | Climb rate (m/min) | 305                    |
| Wing span (m)               | 9.00  | Range (km)         | -                      |
| Wing area (m <sup>2</sup> ) | 11.60 | Flying control     | Flying wing            |
| Overall length (m)          | 3.90  | Number of seats    | 1                      |
| Overall height (m)          | 1.60  | Cockpit            | Closed                 |
| Cruise speed (kt)           | 92    | Undercarriage      | Tricycle               |
| Stalling speed (kt)         | 30    | Material           | Glass fiber, aluminium |
| Fuel capacity (L)           | 20    | Country            | Italy                  |

The concept of the flying wing is well known in aerospace. It is by definition more efficient than a wing + fuselage design since all the structure is used as lifting surface. However, this concept is still rarely used, especially in the microlight area.



Zenair Zipper

(<http://www.pilotmix.com>, 3rd June 2007)

|                             |        |                    |                    |
|-----------------------------|--------|--------------------|--------------------|
| Empty weight (Kg)           | 100    | Take-off run (m)   | 30                 |
| Gross weight (Kg)           | 200    | Landing run (m)    | 24                 |
| Engine power (hp)           | 2 x 26 | Climb rate (m/min) | 122                |
| Wing span (m)               | 8.53   | Range (km)         | 161                |
| Wing area (m <sup>2</sup> ) | 13.29  | Flying control     | 3 axis             |
| Overall length (m)          | 4.42   | Number of seats    | 1                  |
| Overall height (m)          | 1.68   | Cockpit            | Open               |
| Cruise speed (kt)           | 30     | Undercarriage      | Tricycle           |
| Stalling speed (kt)         | 16     | Material           | Aluminium + fabric |
| Fuel capacity (L)           | 19     | Country            | USA                |

The Zenair Zipper presents very interesting characteristics. The performance are quite low, but we can notice interesting features: first of all the Zipper is fitted with 2 engines. Then we can notice that the wing is not made with a conventional rib + fabric structure, but with only a layer of fabric attached at the leading and trailing edges. This gives bad performance but very low price.



Sorell SNS-8 Hiperlight  
(<http://www.pilotmix.com>, 4th June 2007)

|                             |       |                    |                 |
|-----------------------------|-------|--------------------|-----------------|
| Empty weight (Kg)           | 112   | Take-off run (m)   | 92              |
| Gross weight (Kg)           | 227   | Landing run (m)    | 92              |
| Engine power (hp)           | 27    | Climb rate (m/min) | 183             |
| Wing span (m)               | 6.71  | Range (km)         | 410             |
| Wing area (m <sup>2</sup> ) | 13.01 | Flying control     | 3 axis          |
| Overall length (m)          | 4.72  | Number of seats    | 1               |
| Overall height (m)          | 1.60  | Cockpit            | Closed          |
| Cruise speed (kt)           | 70    | Undercarriage      | Tailwheel       |
| Stalling speed (kt)         | 34    | Material           | Wood and fabric |
| Fuel capacity (L)           | 19    | Country            | USA             |

This aircraft uses the design of the first world war aircraft. Despite the age of this design its performance are good compared with other aircraft with the same engine power.



Prototype of microlight fitted with a © Colab wing  
(Colab system property)

|                             |      |                    |                               |
|-----------------------------|------|--------------------|-------------------------------|
| Empty weight (Kg)           | #250 | Take-off run (m)   | -                             |
| Gross weight (Kg)           | #450 | Landing run (m)    | -                             |
| Engine power (hp)           | 40   | Climb rate (m/min) | -                             |
| Wing span (m)               | 7    | Range (km)         | -                             |
| Wing area (m <sup>2</sup> ) | 11.2 | Flying control     | 3 axis                        |
| Overall length (m)          | -    | Number of seats    | 2                             |
| Overall height (m)          | -    | Cockpit            | Closed                        |
| Cruise speed (kt)           | 120  | Undercarriage      | Tricycle                      |
| Stalling speed (kt)         | 20   | Material           | Metal tube, fabric, composite |
| Fuel capacity (L)           | -    | Country            | France                        |

This microlight is fitted with a patented wing designed by the Colab association. This wing allows completely outstanding aerodynamic performance and in the same time simplifies the design by having much better structural properties than a conventional cantilever wing.

**☑ Note: The “#” mean that the values are approximate**





Micro-B World champion microlight  
(<http://www.pilotmix.com>, 16th June 2007)

|                             |       |                    |                               |
|-----------------------------|-------|--------------------|-------------------------------|
| Empty weight (Kg)           | 115   | Take-off run (m)   | 40                            |
| Gross weight (Kg)           | # 250 | Landing run (m)    | -                             |
| Engine power (hp)           | 30    | Climb rate (m/min) | 155                           |
| Wing span (m)               | # 7   | Range (km)         | -                             |
| Wing area (m <sup>2</sup> ) | # 10  | Flying control     | 3 axis                        |
| Overall length (m)          | -     | Number of seats    | 1                             |
| Overall height (m)          | -     | Cockpit            | Closed                        |
| Cruise speed (kt)           | 85    | Undercarriage      | Tricycle                      |
| Stalling speed (kt)         | 22    | Material           | Metal tube, fabric, composite |
| Fuel capacity (L)           | -     | Country            | France                        |

This is the aircraft which took first place in the world's championship. This microlight has a lot of world records in microlight competitions:

- Straight line 15/25km velocity record: 168.55 km/h
- Closed circuit 50 km without landing: 157.44 km/h
- Closed circuit 100 km without landing: 163.61 km/h

This aircraft was designed by Alain Petit, it is actually a prototype, only 2 aircraft are known to have been built. We can notice on this aircraft that a lot of attention has been paid to the aerodynamics. The fuselage is really slick, the engine has a complete fairing and the undercarriage has an efficient shape. This shows that the aerodynamic efficiency has a huge impact on the overall performance of the aircraft.

This airplane uses aluminium boom tube, the fuselage is composite, the wing has an aluminium spar, and the covering is in Dacron. The undercarriage is in composite materials.

The aim of this thesis is to make a design more efficient than this one.



Alatus ultralight motor sailplane  
(<http://www.flylight.co.uk>, 22<sup>nd</sup> June 2007)

|                             |      |                    |                               |
|-----------------------------|------|--------------------|-------------------------------|
| Empty weight (Kg)           | 110  | Take-off run (m)   | -                             |
| Gross weight (Kg)           | 235  | Landing run (m)    | -                             |
| Engine power (hp)           | 18   | Climb rate (m/min) | -                             |
| Wing span (m)               | 13.3 | Range (km)         | -                             |
| Wing area (m <sup>2</sup> ) | 13   | Flying control     | 3 axis                        |
| Overall length (m)          | -    | Number of seats    | 1                             |
| Overall height (m)          | -    | Cockpit            | Closed                        |
| Cruise speed (kt)           | #45  | Undercarriage      | Monocycle                     |
| Stalling speed (kt)         | 20   | Material           | Metal tube, fabric, composite |
| Fuel capacity (L)           | 3.8  | Country            | Ukraine                       |

This aircraft is a challenger: it meets the deregulated regime and it has incredible low speed performance. The highest glide ratio is 27 at 60km/h. This aircraft, fitted with a small engine can take-off and taxi by itself. It is fitted with flaps which decrease the glide ratio to 8, making the landing very easy.

This aircraft uses a lot of composite carbon fibre materials which explains its very light weight.

It has been designed to withstand +4g / -2g which makes it very safe.

A 195cm 100kg person can fit in the glider which is a noticeable performance for a microlight in this category.

However, this aircraft is efficient at very low velocities only. Its VNE is 140km/h.

To conclude we can say that this aircraft shows that it is possible to get very efficient designs even in the deregulated regime. This aircraft is a good example, the design is very modern, optimised, and uses a lot of carbon fibre composite materials.

## 2.2. AIRCRAFT SPECIFICATIONS SUMMARY

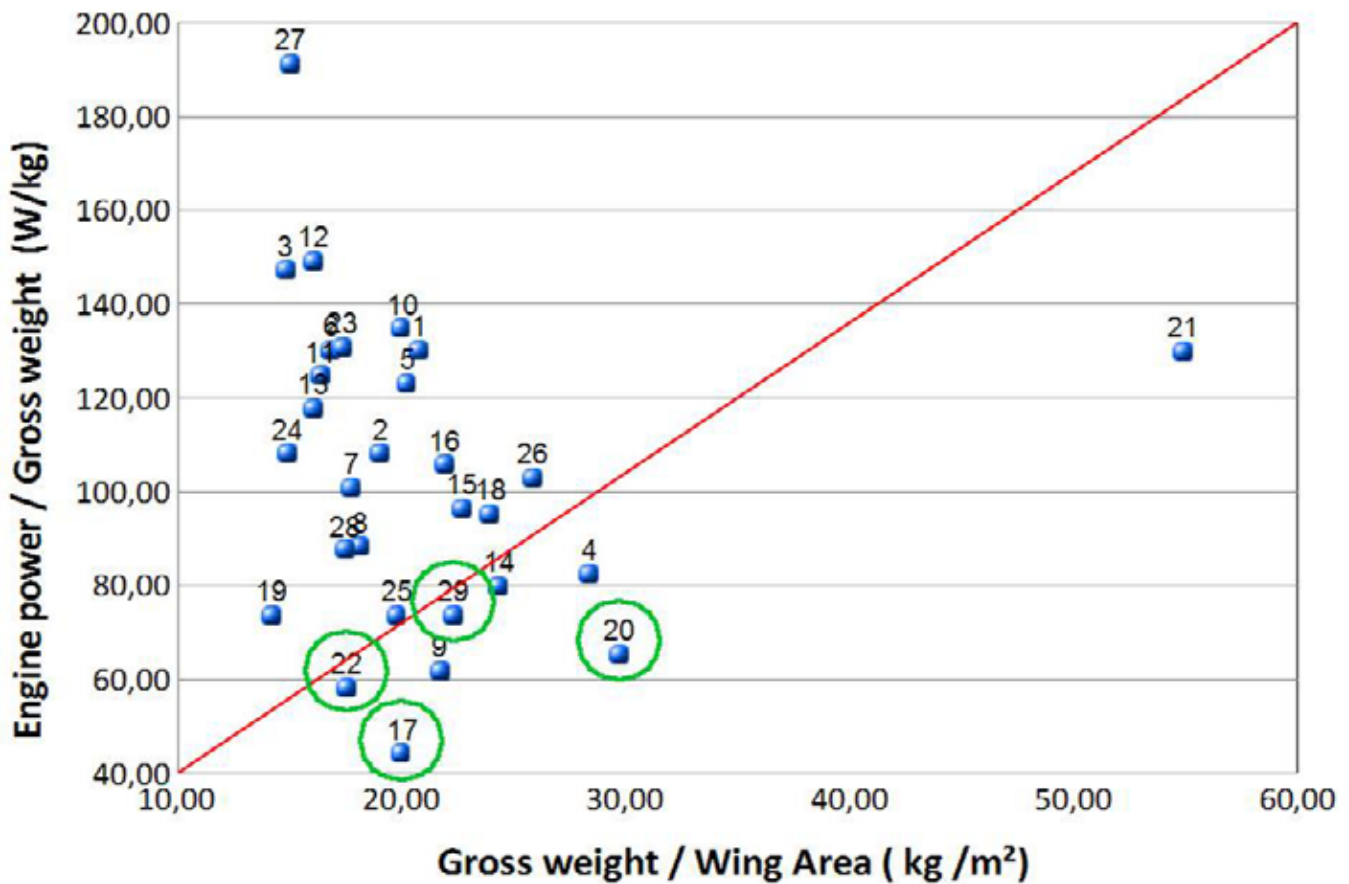
|                               | N° | Type of aircraft       | Empty weight (kg) | Gross Weight (kg) | Engine power (hp) | Engine power (kW) | Wing span (m) | Wing area S (m²) | Aspect Ratio | W/T min      | Max W/S      | Empty W/S   | Stall speed (kt) | Cruise speed (kt) | Max speed (kt) | Vne (kt)  | Climb rate (m/min) | Take-off run (m) | Landing run (m) | Glide Ratio | Structural efficiency | Metal or wood |
|-------------------------------|----|------------------------|-------------------|-------------------|-------------------|-------------------|---------------|------------------|--------------|--------------|--------------|-------------|------------------|-------------------|----------------|-----------|--------------------|------------------|-----------------|-------------|-----------------------|---------------|
| Top wing propulsive propeller | 1  | Kolb firestar          | 115               | 226               | 40,00             | 29,42             | 6,71          | 10,87            | 4,1          | 5,65         | 20,79        | 10,58       | 24               | 55                | 60             | 70        | 305                | 46               | 46              | -           | 2,0                   | M             |
|                               | 2  | Golden Circle T Bird   | 122               | 272               | 40,00             | 29,42             | 9,50          | 14,30            | 6,31         | 6,80         | 19,0         | 8,53        | 22               | 53                | 54             | 96        | 240                | 49               | 46              | 7           | 2                     | M             |
|                               | 3  | Seahawk Condor         | 106               | 215               | 43,00             | 31,63             | 9,80          | 14,50            | 6,6          | 5,00         | 14,83        | 7,31        | 22               | 30                | 38             | 56        | 160                | 76               | 91              | -           | 2,0                   | M             |
|                               | 4  | Gull 2000              | 113               | 250               | 28,00             | 20,59             | 6,10          | 8,80             | 4,2          | 8,93         | 28,41        | 12,84       | 23               | 55                | 55             | 55        | 213                | 38               | 23              | 12,0        | 2,2                   | M             |
|                               | 5  | Rans S-17 Stinger      | 114               | 239               | 40,00             | 29,42             | 8,99          | 11,80            | 6,8          | 5,98         | 20,25        | 9,66        | 25               | 48                | 54             | 82        | 225                | 31               | 54              | -           | 2,1                   | M             |
|                               | 6  | Interplane Griffon 103 | 115               | 235               | 41,60             | 30,60             | 9,00          | 13,96            | 5,8          | 5,65         | 16,83        | 8,24        | 25               | 49                | 55             | 90        | 210                | 50               | 35              | -           | 2,0                   | M             |
|                               | 7  | Aerolite Bearcat       | 114               | 204               | 28,00             | 20,59             | 8,18          | 11,50            | 5,8          | 7,29         | 17,74        | 9,91        | 23               | 39                | 61             | 87        | 213                | 31               | 31              | 9,0         | 1,8                   | M             |
|                               | 8  | Sirocco                | 115               | 250               | 30,00             | 22,06             | 10,12         | 13,80            | 7,4          | 8,33         | 18,12        | 8,33        | 21               | 43                | 62             | -         | 300                | 35               | 40              | 10,0        | 2,2                   | M             |
|                               | 9  | Shadow                 | 158               | 386               | 64,00             | 47,07             | 10,00         | 15,00            | 6,7          | 6,03         | 25,73        | 10,53       | 34               | 75                | 98             | 108       | 213                | 80               | -               | -           | 2,4                   | M             |
|                               | 10 | Carrera 150            | 118,00            | 249               | 40,00             | 29,42             | 8,43          | 12,45            | 5,7          | 6,23         | 20,00        | 9,48        | 23               | 52                | 65             | -         | 350                | 46               | 46              | -           | 2,1                   | M             |
|                               | 11 | Quicksilver            | 112               | 236               | 40,00             | 29,42             | 8,52          | 14,42            | 5,0          | 5,90         | 16,37        | 7,77        | 21               | 46                | 46             | 64        | 128                | 30               | 30              | 4,5         | 2,1                   | M             |
|                               | 12 | Drifter Rocket         | 109               | 227               | 46,00             | 33,83             | 9,14          | 14,12            | 5,9          | 4,93         | 16,08        | 7,72        | 23               | 48                | 61             | 74        | 244                | 60               | -               | -           | 2,1                   | M             |
|                               |    | <b>AVERAGE</b>         | <b>118</b>        | <b>249</b>        | <b>40,05</b>      | <b>29,46</b>      | <b>8,71</b>   | <b>12,96</b>     | <b>5,9</b>   | <b>6,2</b>   | <b>19,51</b> | <b>9,07</b> | <b>24</b>        | <b>49</b>         | <b>59</b>      | <b>78</b> | <b>233</b>         | <b>48</b>        | <b>44</b>       | <b>X</b>    | <b>2,1</b>            | <b>X</b>      |
| Top wing pushing propeller    | 13 | Weedhopper             | 113               | 250               | 40,00             | 29,42             | 8,50          | 15,60            | 4,63         | 6,25         | 16,03        | 7,24        | 18               | 48                | 56             | 57        | 305                | 31               | 31              | -           | 2,2                   | M             |
|                               | 14 | Flying K sky raider    | 113               | 249               | 41,60             | 30,60             | 7,99          | 10,22            | 6,25         | 5,99         | 24,36        | 11,06       | 20               | 56                | 70             | 86        | 320                | 23               | 23              | -           | 2,2                   | M             |
|                               | 15 | Aerolites Bearcat      | 130               | 317               | 41,60             | 30,60             | 9,14          | 13,94            | 5,99         | 7,62         | 22,74        | 9,33        | 24               | 59                | 65             | 95        | 228                | 46               | 46              | -           | 2,4                   | W             |
|                               | 16 | Flightstar Spyder      | 126               | 292               | 42,00             | 30,89             | 9,12          | 13,31            | 6,25         | 6,95         | 21,94        | 9,47        | 32               | 56                | 74             | 83        | 213                | 61               | 91              | 8,0         | 2,3                   | M             |
|                               |    | <b>AVERAGE</b>         | <b>121</b>        | <b>277</b>        | <b>41,30</b>      | <b>30,38</b>      | <b>8,69</b>   | <b>13,27</b>     | <b>5,78</b>  | <b>6,7</b>   | <b>21,27</b> | <b>9,08</b> | <b>23</b>        | <b>55</b>         | <b>66</b>      | <b>80</b> | <b>267</b>         | <b>40</b>        | <b>48</b>       | <b>X</b>    | <b>2,3</b>            | <b>X</b>      |
| 3 axis low wing               | 17 | MB02 Souricette        | 95                | 200               | 12,00             | 8,83              | 9,00          | 10,00            | 8,10         | 16,67        | 20,00        | 9,50        | 24               | 54                | 65             | 0         | 90                 | 61               | -               | 14,0        | 2,1                   | W             |
|                               | 18 | Avenger                | 113               | 270               | 35,00             | 25,74             | 8,20          | 11,26            | 5,97         | 7,71         | 23,98        | 10,04       | 25               | 52                | 82             | 0         | 274                | 30               | 61              | -           | 2,4                   | W             |
|                               |    | <b>AVERAGE</b>         | <b>104</b>        | <b>235</b>        | <b>23,50</b>      | <b>17,28</b>      | <b>8,60</b>   | <b>10,63</b>     | <b>7,04</b>  | <b>10,00</b> | <b>21,99</b> | <b>9,78</b> | <b>25</b>        | <b>53</b>         | <b>74</b>      | <b>0</b>  | <b>182</b>         | <b>46</b>        | <b>61</b>       | <b>X</b>    | <b>2,3</b>            | <b>X</b>      |
| Less than 55 kg               | 19 | Whing Ding II          | 56                | 140               | 14,00             | 10,30             | 5,69          | 9,85             | 3,29         | 10,00        | 14,21        | 5,63        | 23               | 35                | 43             | -         | 60                 | 76               | 40              | -           | 2,5                   | M             |
|                               | 20 | E-12n                  | 48                | 160               | 14,20             | 10,44             | 6,50          | 5,38             | 7,85         | 11,27        | 29,74        | 8,92        | 32               | 43                | 54             | 76        | 192                | 60               | -               | 7,0         | 3,3                   | M             |
|                               |    | <b>AVERAGE</b>         | <b>52</b>         | <b>150</b>        | <b>14,10</b>      | <b>10,37</b>      | <b>6,10</b>   | <b>7,62</b>      | <b>5,57</b>  | <b>10,6</b>  | <b>21,98</b> | <b>6,80</b> | <b>28</b>        | <b>39</b>         | <b>49</b>      | <b>76</b> | <b>126</b>         | <b>68</b>        | <b>40</b>       | <b>X</b>    | <b>2,9</b>            | <b>X</b>      |
| Non conventional designs      | 21 | MC-12 Cricket          | 75                | 170               | 30,00             | 22,06             | 4,90          | 3,10             | 7,75         | 5,67         | 54,84        | 24,19       | 42               | 97                | 135            | 141       | 360                | 120              | -               | 13,0        | 2,3                   | M             |
|                               | 22 | Lazair                 | 95                | 240               | 19,00             | 13,97             | 11,10         | 13,70            | 8,99         | 12,63        | 17,52        | 6,93        | 22               | 35                | 53             | 55        | 120                | 50               | 50              | 12,0        | 2,5                   | M             |
|                               | 23 | Pou du ciel            | 115               | 225               | 40,00             | 29,42             | 6,00          | 13,00            | 2,77         | 5,63         | 17,31        | 8,85        | 30               | 60                | 65             | 97        | 150                | 61               | -               | 9,0         | 2,0                   | W             |
|                               | 24 | Pouchel                | 80                | 170               | 25,00             | 18,39             | 5,44          | 11,40            | 2,60         | 6,80         | 14,91        | 7,02        | 26               | 54                | 54             | 65        | -                  | -                | -               | -           | 2,1                   | M             |
|                               | 25 | Onyx CP 150            | 70                | 180               | 18,00             | 13,24             | 7,30          | 9,10             | 5,86         | 10,00        | 19,78        | 7,69        | 22               | 52                | 61             | 74        | 137                | 46               | 31              | -           | 2,6                   | W             |
|                               | 26 | PUL 9                  | 150               | 300               | 42,00             | 30,89             | 9,00          | 11,60            | 6,98         | 7,14         | 25,86        | 12,93       | 30               | 92                | 121            | -         | 305                | 150              | -               | -           | 2,0                   | M             |
|                               | 27 | Zipper                 | 100               | 200               | 52,00             | 38,25             | 8,53          | 13,29            | 5,47         | 3,85         | 15,05        | 7,52        | 16               | 30                | 39             | 50        | 161                | 30               | 24              | -           | 2,0                   | M             |
|                               | 28 | Hiperlight             | 112               | 227               | 27,00             | 19,86             | 6,71          | 13,01            | 3,46         | 8,41         | 17,45        | 8,61        | 34               | 52                | 55             | 85        | 213                | 53               | 53              | 12,0        | 2,0                   | W             |
|                               | 29 | Colab concept          | 250               | 450               | 40,00             | 29,42             | 7,00          | 11,20            | 4,38         | 11,25        | 40,18        | 22,32       | 20               | 100               | 120            | 150       | -                  | -                | -               | -           | 1,8                   | M             |
|                               | 30 | Micro-B                | 115               | 250               | 30,00             | 22,06             | 7,00          | 10,00            | 4,90         | 8,33         | 25,00        | 11,50       | 22               | 85                | -              | -         | -                  | -                | -               | -           | 2,2                   | M             |
|                               | 31 | Alatus                 | 110               | 235               | 18,00             | 13,24             | 13,30         | 13,00            | 13,61        | 13,06        | 18,08        | 8,46        | 20               | 45                | -              | 76        | -                  | -                | -               | -           | 2,1                   | M             |

Aircrafts matching the deregulated regime

Aircraft specifications table

## 2.3. PERFORMANCE STUDY

### 2.3.1. Engine power – wing loading diagram



Engine power – wing loading diagram  
(See Table page 32 for aircraft numbers)

This diagram allows us to have a general overview of the microlights performance by comparing them with relative figures. The first figure is the maximum wing loading allowable and the second the power of the engine over the maximum weight allowable.

The aircraft under the red line are the most efficient whereas the one with the higher engine power over gross weight ratio are the less efficient. The aircraft circled in green are those which meet the deregulated regime requirements.

The first thing that we can notice is that the microlight performance are mostly grouped in a common zone. Then we can notice aircraft with especially good or bad performance.

The number 27 (Zenair Zipper) has the highest Engine power over gross weight. However, it does not support higher wing loading than aircraft with much less engine power. This aircraft is actually one of the least efficient microlights because of its wing design: A fabric attached between the leading edge and the trailing edge (cf. A.1.5). Furthermore, this aircraft is fitted with two engines. This gives practical advantages (in case of engine failure), but in terms of performance it is less efficient. On the other hand, this aircraft is cheap and reliable.

We can see that the number 21 (MC-12 Cri cri) has outstanding performance. This comes from its ultra small size. Its empty weight is 75kg, it has minimized wing area and fuselage structure and therefore has much better performance than other aircraft with the same engine power but with much larger structures.

The number 22 (Lazaire) meets the deregulated regime requirements and, furthermore, has very interesting performance. This aircraft has a very smart geometry (inverted V tail empennage) which allows a decrease in the aerodynamic area and so a decrease of drag. Then this aircraft has a large aspect ratio of 9, which is more than the average. This aircraft is also fitted with two engines mounted on the leading edge. We already discussed the trade-offs of this configuration, but we should also mention that this configuration allows to have a pulling propeller design (more efficient than a propulsive propeller design) and in the same time this design allows to keep the pilot's view free. We will discuss the advantages and downsides of these configurations later in the thesis.

The number 17 (MB 02 Souricette) is also a design which meets the requirements and shows interesting performance. The Souricette's design is a conventional 3 axis wood and fabric aircraft design. This aircraft has the smallest engine power of all the microlights studied in this thesis and probably one of the smallest engine powers of the world's microlights. With only 12hp this aircraft has a cruise speed almost two times higher than the Zenair zipper with 52hp! How is this possible? The Souricette has been designed in wood and fabric, using a conventional configuration. This design allows for a long and thin fuselage, which means a small cross section, and so better aerodynamics performance. Furthermore, the wing has a large aspect ratio 8, which reduces the induced drag. Finally, the empty weight of this aircraft is only 95 kg.

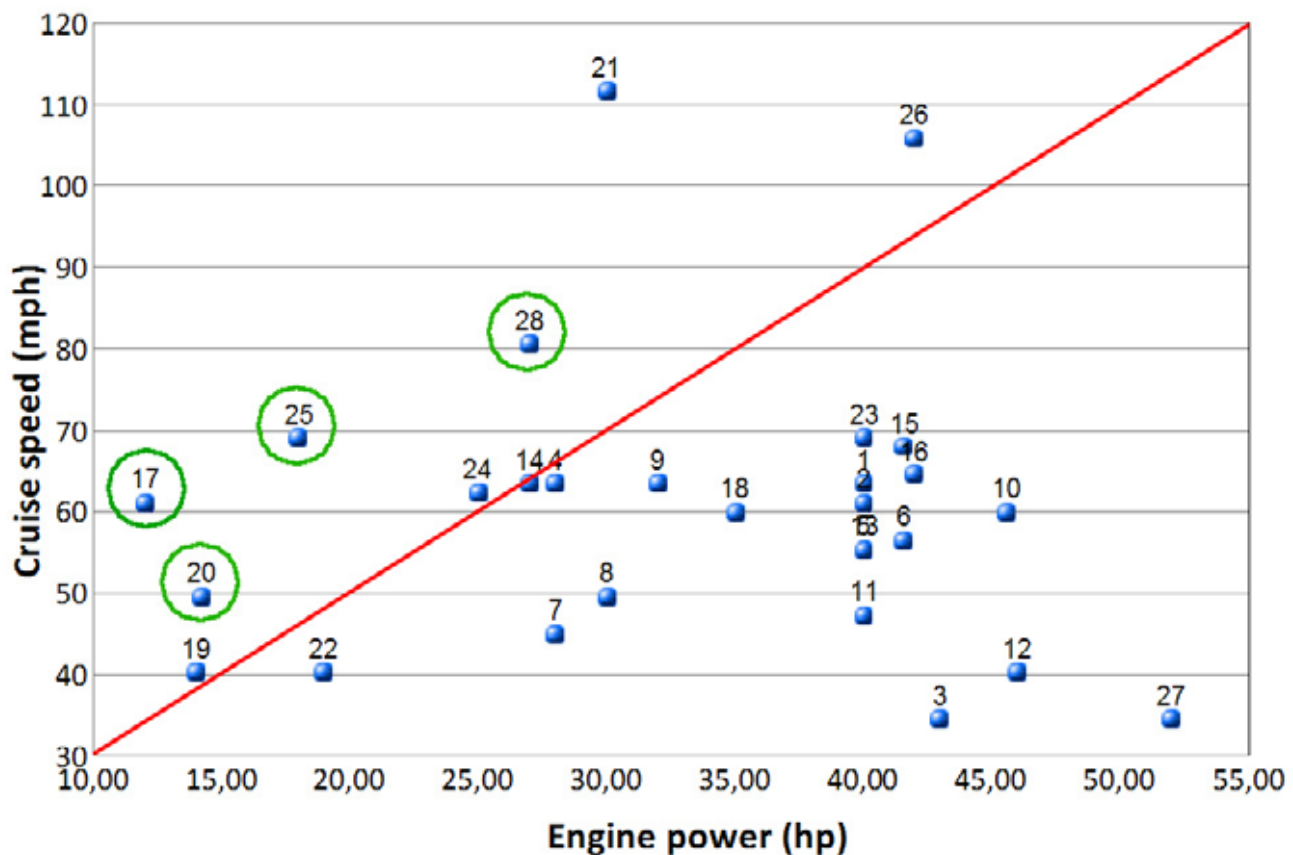
The last aircraft which meets the requirements is the number 20, the E-12n. This aircraft has a classic microlight top wing configuration, but its particularity is its very low weight: 48kg. It is the lightest microlight shown in this study. This low weight allows the E-12n to have very good performance. We can also notice that the E-12n has a pulling propeller, which is more efficient than a propulsive configuration. Finally, the aspect ratio is about 7.9, which is above the average.

The number 29 is a prototype fitted with a revolutionary wing. Although this aircraft does not seem exceptional on this diagram it has incredible aerodynamic properties, thanks to this revolutionary wing.

## CONCLUSIONS

- ➔ Less than 115kg does not imply poor performance.
- ➔ The key of the success is a SMALL design.
- ➔ The aerodynamic properties have a huge influence on the performance (A.R.)
- ➔ A high wing loading gives better performance.

### 2.3.2. Engine power –cruise speed diagram



Engine power-cruise speed diagram  
(See Table page 32 for aircraft numbers)

This diagram shows the aircraft efficiency in terms of speed. The most efficient aircraft are those which can fly fast with a small engine. These are the ones above the red line.

As we noticed in the previous part, we can see that the number 21 (MC-12 Cri cri) has outstanding performance. It has a cruise speed of 97kt with a 30hp engine. The main explanation of this high speed is the high wing loading ( $54.8\text{kg/m}^2$  at gross weight). The other factor is its small dimensions, as we mentioned in the previous part.

We can also notice the number 26 (PUL 9) which is a special concept since it is a flying wing. The flying wing has great aerodynamic performance since all the structure acts as lifting surface. What's more, in this case the wing loading is above the average of the microlights studied:  $25.9\text{kg/m}^2$ .

As we noticed in the previous part, and for the same reasons, the Zenair Zipper has awful performance since it has the lowest cruise speed with the most powerful engine.

We can notice that, as on the previous diagram, the number 17 (Souricette) and the number 20 (E-12n) have very good performance and meet the deregulated regime requirements.



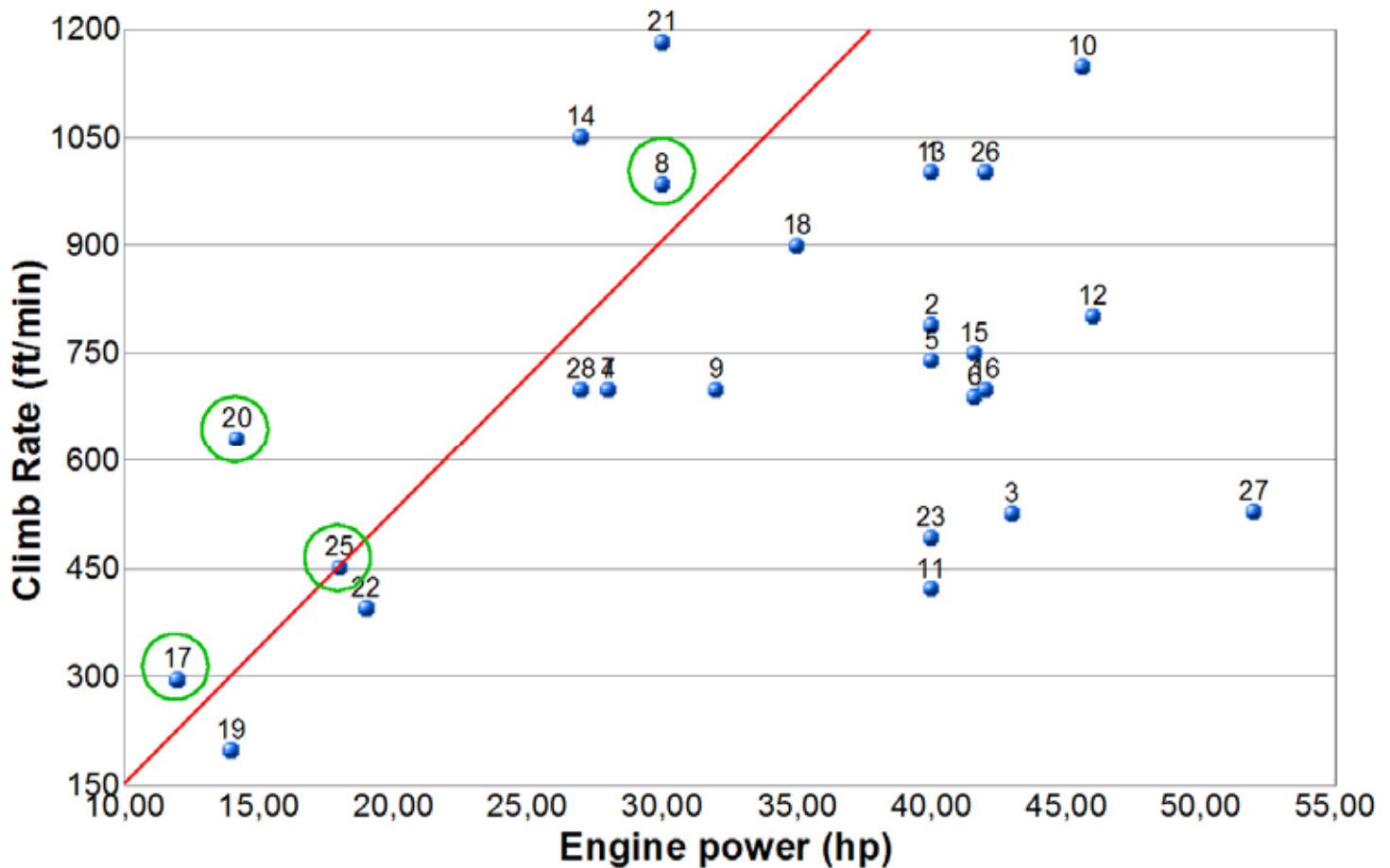
We can see that the number 25, onyx, has good performance too. The onyx is a very aerodynamically efficient design, in glass fibre and it uses a canard configuration. Furthermore, its empty weight of 70kg is an important asset.

Finally, the number 28, Hiperlight, is a biplane aircraft with a conventional configuration. This configuration is more aerodynamically efficient than the usual top wing microlight configuration.

## CONCLUSIONS

- ➔ A high wing loading allows high velocities.
- ➔ A classic configuration with small cross section and fairings is more efficient.
- ➔ A light configuration is more efficient.

### 2.3.3. Engine power –Climb rate diagram



Engine power-climb rate diagram  
(See Table page 32 for aircraft numbers)

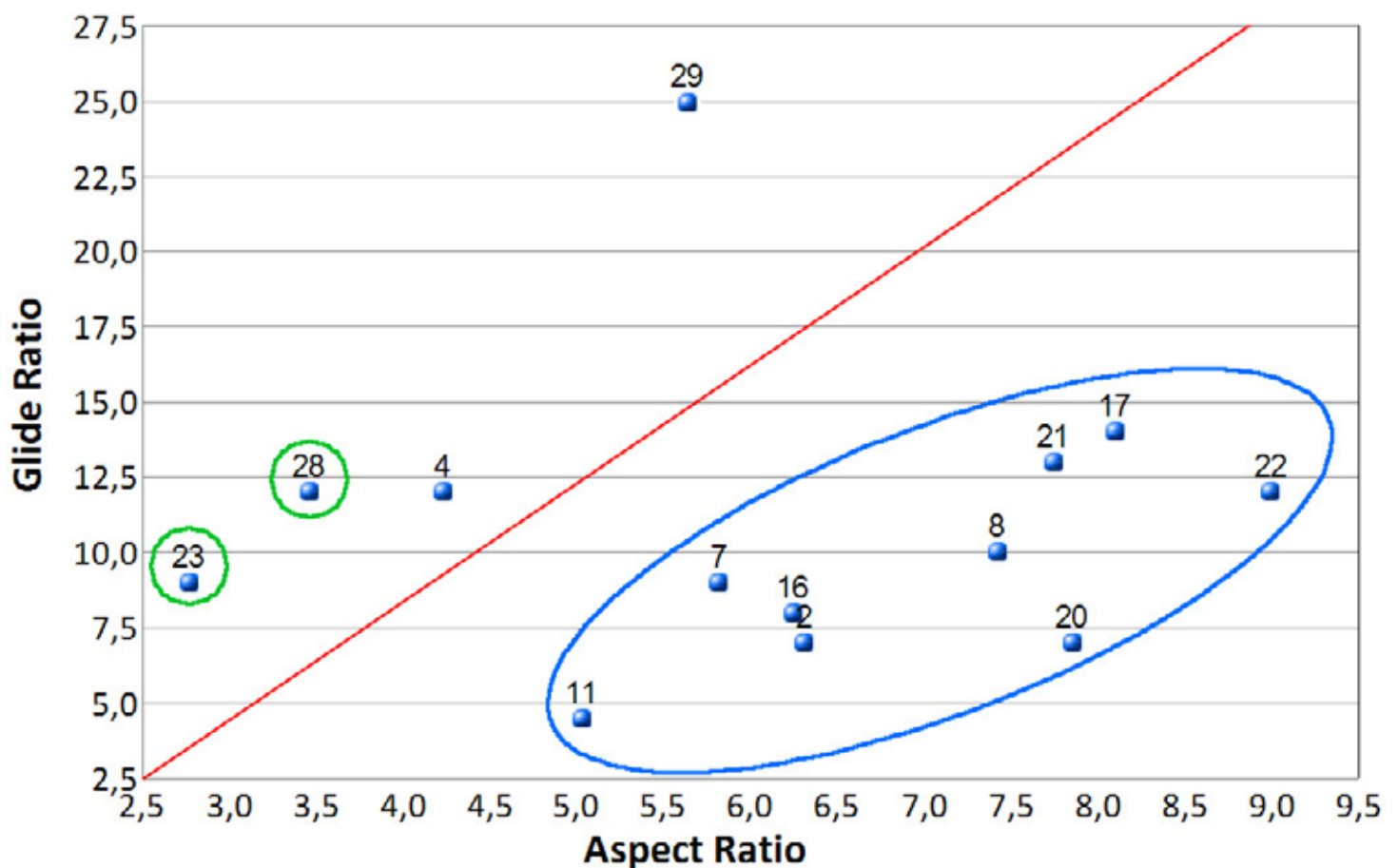
As in the previous diagrams we can see that the Cri cri (number 21) has the best performance. We can also see that the number 20 (E-12n), the number 17 (Souricette) and the number 25 (Onyx) are still in the most efficient airplanes.

The number 8 (Sirocco) has good climbing performance. The Sirocco has the particularity to be a very aerodynamically efficient aircraft. It has fairings all around the fuselage and we can notice that the wing is mounted on a pylon. This feature significantly reduces the interferences induced by the fuselage on the wing and so gives the wing a better efficiency.

## CONCLUSIONS

- ➔ The pylon mounted wing is an idea to keep.
- ➔ The lighter designs have the best climb rates.

### 2.3.4. Aspect Ratio – Glide ratio diagram



Aspect Ratio – Glide Ratio Diagram  
(See Table page 32 for aircraft numbers)

The first thing that we can notice on this diagram is that the Glide ratio increases when the aspect ratio increases. This is a normal trend; the high aspect ratios have better aerodynamic properties than the small aspect ratios.



Then we can notice that the number 29 (Colab wing prototype) has a very high glide ratio, by far the best of all its competitors despite its small aspect ratio. Actually this wing has a design which is extremely efficient and reduces the drag greatly. The actual glide ratio value on this diagram is 25, but this is the value given by the designer for an optimised microlight. This wing is fitted with variable camber flaps, which means that we can optimise the glide ratio for a large interval of velocities.

Then we can notice that the number 4 (Gull 2000) has interesting performance. This is worth paying attention to because it has a design very similar to 11 (Quicksilver), with high wing, 3 axis and propulsive propeller, and the same empty weight, but the glide ratio of the Gull 2000 is much better. The difference between these 2 designs is that the Gull 2000 has fairings all around the fuselage and no rods to sustain the wings. This shows how important the fairings are. The downside is the weight. However, with very light carbon fibre fairings, we can achieve very light weight and very good aerodynamic performance.

Finally, we can note that the numbers 23 (Pou du ciel) and 28 (Hiperlight) have both good glide ratios with regards to their aspect ratios. Furthermore, these aircraft meet the deregulated regime requirements. Actually, the explanation is that these aircraft are both biplane aircraft. They have a small aspect ratio but still a large wing area.

## CONCLUSIONS

- ➔ The aerodynamic fairings are really important for the performance.
- ➔ The Colab design is by far the most efficient.

## 3. AIRCRAFT DESIGN OPTIONS

### 3.1. STUDIES OF THE AIRCRAFT CONFIGURATIONS

In this part we will show the advantages and downsides of the different aircraft configurations.

#### 3.1.1. *Wing arrangements*

There are several wing configurations. In this thesis we will focus on the designs which are the most relevant for the microlights. For example we will not discuss delta wings or inverted seagull shaped wing.

##### ➔ **3 axis high wing configuration**



High wing microlight (Popham Meeting, May 2007, author property)

This configuration is by far the most common in the microlight category. It has a lot of advantages:

##### - *Simple structure:*

The high wing allows a straight design with eventually struts to reinforce the structure. Actually, in most of the cases the lightest design is obtained with the struts, since despite the extra weight they add, they significantly reduce the bending moment in the wing and so the spar thickness, and so the weight. Furthermore, a straight structure is always easier to design; in most of the cases the low wing designs have a positive dihedral for stability reasons. This is not the case for high wings, which are naturally stable in roll.

##### - *Good aerodynamic properties*

Usually it is admitted that roughly 66% of the lift comes from the extrados depression on the wing and 34% from the intrados overpressure. This shows that extrados of the wings has 2 times more impact on the lift than the intrados. The top wing configuration allows having a perfectly flat wing extrados which does not deteriorate the flow.

***- Natural stability of the aircraft.***

The centre of lift is higher than the CG of the aircraft. This gives natural roll stability to the aircraft that the low wing does not have. Sometimes on large aircraft, to increase the manoeuvrability, the wing has a negative dihedral (Antonov 225, cf illustration below). However, this is never the case on microlights.



Antonov 225

(<http://www.airliners.net/>, 22<sup>nd</sup> June 2007)

***- More room for the engines for wing mounted engines***

For wing mounted engines (two engines or more), especially in the case of propeller engines, the high wing gives much more room for the propeller blades. In general the further the propeller is from the ground the better it is. It avoids getting gravel or other things caught in the propeller which could damage the propeller itself and the airplane.

***- Good pilot's view of the ground in steady flight***

In steady flight the pilot has a very good view of the ground. In the low wing configuration a big part of the ground is hidden by the wing. For light aircraft we can mention that the top wing allows easy access to the cabin, compared to low wing: you can find below an illustration of a Cessna 172 and a robin DR-400 with the 2 different wings configurations:



Robin DR-400 (left) and Cessna 172 (Right)

(<http://www.airliners.net/>, 24<sup>th</sup> June 2007)

However this configuration also presents downsides:

- ***Bad pilot's view while turning and to the sky***

In this configuration, a large sky area is hidden by the wings. Furthermore, while turning the wing hides potential other aircraft that could be in the way.

- ***Less manoeuvrability***

This aircraft configuration is more stable and so less manoeuvrable. This is a trade-off.

### ➔ **3 axis low wing configuration**



Samba, low wing microlight  
(<http://www.vlasportaviation.com/>, 24<sup>th</sup> June 2007)

This configuration is very common in the private aircraft category. It presents a lot of advantages that the high wing does not have and, of course, the advantages of the high wing are often the weaknesses of the configuration.

- ***Good manoeuvrability***

We discussed earlier about the stability advantages of the high wings. On the other hands, the low wing gives better manoeuvrability, which is appreciable for more efficient aircraft and aerobatic aircraft.

- ***Good overall pilot's visibility***

The glass « bubble » gives the pilot a very good overall view. This characteristic with the good manoeuvrability explains why the World War Two fighters had this configuration.

***- Lighter undercarriage structure***

For tailwheel as for tricycle undercarriages, when the 2 main wheels are attached to the wings, the low wings design allows shorter and so lighter undercarriage structures. However, on the twin engines aircraft this is solved by putting the undercarriage in the engines compartments, as on the mosquito (cf. below).



De Havilland Mosquito

(<http://www.airliners.net/>, 22<sup>nd</sup> June 2007)

***- Better reaction to cross wind***

The low wing configuration is easier to handle while landing or taking off with cross wind. Basically, the high wing configuration offers more resistance to cross wind than the low wing configuration.

**➔ 3 axis Biplane**

A lot of the first aircraft (World War One period) were biplanes. This can be explained because this configuration has interesting properties:

***- Simple structure***

To achieve the same wing area a biplane needs much shorter wings than the monoplane. This means that the loads (bending moment, torque, shear) are much lower in this configuration. Furthermore, the biplanes are often reinforced with extra beams and cables which make the structure much stiffer.



**- *Good manoeuvrability***

On a biplane, we can have ailerons on both the top and the low wing. This gives the biplanes a very large area of control surface. Furthermore, with a shorter span the moment of inertia along the roll axis is lower than with a long span. These two parameters allow the biplanes to have high roll rate, as illustrated on the aerobatic airplane (Pitts) below:



Pitts

(<http://www.johnjohn.co.uk>, 1<sup>st</sup> July 2007)

However, this configuration has been abandoned because it is by far less aerodynamically efficient than a single wing configuration. There is a large drag penalty which increases significantly with the speed.

**➔ Canard configuration**

The canard configuration is not frequently used, especially in the area of the microlights. However, this is a really interesting configuration which presents a lot of advantages:

**- *Better aerodynamic configuration***

On a conventional classic 3 axis airplane the tailplane has a negative lift. On the contrary, on a canard configuration the canard surface has a positive lift which adds to the wing lift. This gives, by definition better performance to the aircraft.

**- *A good conception avoid the stall***

When the canard configuration is well designed, the aircraft cannot stall. Actually, at high incidences, the canards stall before the wing and so the main wing never stalls. This increases considerably the safety of this kind of design.

**- *Reduction of the wetted surface***

With a canard configuration the moment arm for the tail is not required anymore and so the aircraft structure can be much shorter and there is a reduction of the wetted surface and so a reduction of drag. This configuration also reduces the maximum cross section.

**- Greater CG position variation**

If well designed, the canard configuration allows a bigger variation of the CG position. This can be really useful when for instance, it allows to get rid of special devices such as trim tanks, etc. Below you can find an illustration of one of the unique civil aircraft with canard configuration; the business jet Piaggio Avanti.



Piaggio P180 Avanti II  
(<http://www.piaggioaero.com/>, 22<sup>nd</sup> June 2007)

However, there is a trade off, this configuration also presents downsides:

**- Low wing loading**

The longitudinal stability obliges to have a high loading on the canards compared to the main wing. Thus, the main wing remains loaded under its optimal wing loading.

**- Non homogeneous flow on the wing**

The canards induce a downwash of the flow. This disturbance has an impact on the main wing. Thus, we get a non homogeneous flow spanwise on the wing, which makes it hard to optimise.

**- Low efficiency of flaps**

The deflection of the flaps induces a diving moment. On a classic configuration, this diving moment is easily compensated by trimming the elevator. On a canard configuration the canards already have a high loading and so they do not have enough range of  $C_z$  left to compensate the diving moment. That is why a lot of canard configurations do not have flaps, since their efficiency is limited.

## ➔ **Flying wing configuration**

The flying wing configuration is one of the most spectacular aircraft configurations. Even if we are not used to this kind of configuration, it is by definition the most aerodynamically efficient.



Northrop Grumman B-2 Spirit  
(<http://www.airliners.net/>, 24th June 2007)

### **- *More efficient design***

Theoretically, the flying wing is a better design: the idea is to remove all what does not contribute to the lift. In this way, there is a decrease of the structural mass and of the drag. The fact that the fuselage and the tail are removed reduces the wetted surface.

### **- *Large storage volume***

The flying wing gives a very large inside volume, however, this does not increase the global weight that the flying wing is able to carry compared to a conventional configuration, so the superiority compared to a conventional configuration can be contested. Furthermore, this works for aircraft with a large size, while the gain for the smallest aircraft is negligible.

### **- *Practical issues***

The aerodynamic efficiency is better in theory, but in practice there are huge issues concerning the stability of flying wings. Thus the flying wings are not equipped with high lift devices, which induces practical problems. The CG range is also very low. To achieve a large payload capability, a high span is required. This raises issues concerning the airports capabilities.



## ➔ Colab configuration



Colab microlight prototype  
(Colab system property)

### - *Very high aerodynamic efficiency*

The Colab design is based on biplane wing joined at its tips. There are some complex interferences between the two wings which give the design a very high efficiency.

### - *Optimized structure*

As we can see on the picture here above, the Colab wing is naturally triangulated. This is an enormous advantage compared to a cantilever wing, since it reduces a lot the loads in the structure and so it is possible to design lighter structures.

➔ **The Colab design will be studied in detail in CHAPTER 4 of this thesis.**

### 3.1.2. *Engine arrangements*

#### ➔ **One front engine puller propeller configuration**

This is actually the most common design in general aviation. This design has a lot of advantages:

- ***Better propeller efficiency***

In this configuration the propeller of the aircraft gets a nice and undisturbed air flow. On the contrary the propeller at the rear of the aircraft gets the flow which is disturbed by the fuselage and the wings. This gives the front propeller an efficiency of about 0.80 to 0.85 compared with an efficiency of 0.72 to 0.76 for an engine mounted at the rear of an aircraft, and so reduces the fuel consumption etc.

- ***Easier mounting and larger diameter***

With standard aircraft configuration it is much easier to put a propeller at the front. The rear fuselage reduces the room for the propeller at the rear and so limits the propeller diameter.

- ***Better wing efficiency***

The propeller blows air into the wing which gives it an additional lift. However, in the same time the propeller induces disturbances in the air flow (prop wash) and slightly reduces the wing efficiency.

- ***Better engine cooling***

The propeller blows air into the engine intakes. This helps the engine cooling. Furthermore, the forward position of the engine provides a better airflow into the engine air intakes.

#### ➔ **One propulsive engine configuration**

This design is really common in the microlights area. It is a simple design, often easy to implement on the aircraft, with good advantages for the pilot.

- ***More comfortable flight***

The propeller at the rear does not interfere with the pilot's view. Furthermore, inside the cabin, the configuration is slightly less noisy.

- ***Better manoeuvrability***

The pusher configuration is less stable in flight than the puller configuration. Therefore, the aircraft is more manoeuvrable. Furthermore, in the puller configuration, the propeller blows air into the empennage, which makes the control surfaces more efficient. This is especially true at low speeds, during take-off and landing.

This configuration is not the most used because it presents also a lot of disadvantages that are explained in the following paragraphs:

**- *Dangerous in case of crash***

In case of a crash, the engine position is bad, since the engine can endanger the occupants of the cabin. On the contrary, when the engine is at the front, it protects the passengers.

**- *Propeller more subjected to foreign objects damages***

In most of the cases, the propeller is behind the main landing gear, and so it is subjected to projections of foreign objects, which make the propeller wear quicker.

**- *Engine overheating***

This configuration does not provide any cooling for the engine: first of all, the propeller does not blow air into the engine, and secondly, the engine is often mounted at the rear of the fuselage, and this position does not provide any cooling airflow for the engine. As a solution, very often aerodynamic fairings are implemented around the engine to make the air circulate and cool the engine. This induces a weight penalty.

**- *Noise***

The disturbed airflow of the fuselage going into the propeller blades makes this configuration noisier than the puller configuration.



Rutan Long-EZ home-built aircraft  
(<http://www.airliners.net/>, 24th June 2007)

**➔ Two puller engines configuration**

This configuration is not frequent for microlights. However, some microlights present this configuration, and it is worth being studied.

**- *Reliability***

The twin engine configuration is in theory more reliable: if one engine fails, the other one allows to still fly the aircraft. In practice, the large yaw moment induced when an engine is lost can be really hard to control and make the flight even more dangerous than with a

conventional single engine aircraft with the engine broken down. To avoid this, the engines are mounted very close to each other spanwise on the microlights.

**- *Performance***

A twin engine configuration gives in general a higher thrust over weight ratio and so better performance, such as climb rate, maximum speed, etc. In some case, a twin engine configuration can reduce the noise of the aircraft compared to a single engine configuration.

**- *Better pilot's view***

This configuration gives the pilot a good visibility and combines some of the advantages of the puller configuration with the advantages of the pusher configuration.

**- *Higher maintenance and cost***

An engine is a non negligible part of the cost of an aircraft, as much for the initial purchase as for the maintenance.

**- *Special flying features***

With a twin engine aircraft the pilot has to take extra care about the engines parameters and it requires more of the pilot's attention.

**➔ *Push Pull configurations***

This configuration is really rare in the microlights area, however it is really interesting since it presents a combination of the characteristics of the different engines configurations studied before. Especially, it provides the safety of a twin engine configuration and in the same time does not have the problem of the yaw moment induced when the engine fails. However, it has the problems of the cooling of the rear engine and the visibility of the pilot reduced by the forward engine.

Below, is one of the most famous push pull configuration, the Cessna 337 Skymaster:



Cessna 337 Skymaster  
(<http://www.airliners.net/>, 24th June 2007)

### 3.1.3. Tail arrangements

#### ➔ **Cruciform tail**

This is by far the most common configuration in light aircraft. This configuration is easy to design and the actuation mechanisms for the control surfaces of the tail are easy to implement in the design.



Piper Pa 28

(<http://www.airliners.net/>, 28th June 2007)

#### ➔ **T tail**

The T tail is the second most common design in general aviation after the cruciform tail. The T tail is a simple design, and it presents the following advantages: The tailplane is not affected by the downwash induced by the wing and by the disturbances of the engine. Furthermore, for the gliders especially, in case of emergency landing in a field, the tailplane is less susceptible to be damaged by foreign objects than with a conventional cruciform tailplane.



Duo Discus

(<http://bestangle.com/blog/wp-content/uploads/2006/07/>, 28<sup>th</sup> June 2007)

### ➔ V tail

The V tail is a very aesthetic configuration. Furthermore, it reduces considerably the drag since there is less wetted surface compared with a conventional empennage. However, on light aircraft this configuration requires a complex mechanism for the coupling of the elevator and the rudder functions. This mechanism is complex, expensive and heavy. This is why this design is not widely used in general aviation.



Beechcraft Bonanza  
(<http://www.airliners.net/>, 29th June 2007)

### ➔ Twin booms

This configuration is used when the designer has specific requirements: for example in the case of a puller configuration, to be able to put a cargo door at the rear of the aircraft or to have a free field for fire from the rear of the aircraft. But this structure can also be used to have an increased structure rigidity, strength and internal volume.



De Havilland dH-110 Sea Vixen D3  
(<http://www.airliners.net/>, 26th June 2007)



### 3.1.4. *Undercarriage arrangement*

#### ➔ **Tailwheel configuration**

This configuration is the oldest in aeronautics. The first airplanes were all designed with this configuration. Some of them did not have the tailwheel but a landing pad. This configuration has a lot of advantages in term of aircraft efficiency: The tailwheel is really light compared to a nose wheel. In case of a retractable landing gear, only the two main wheels are retracted since the tailwheel is very small and does not induce a lot of drag. These characteristics make the weight of the landing gear much lower. Furthermore, this configuration gives much more room for the propeller and so it is possible to have a shorter undercarriage.



Piper Cub

(<http://www.airliners.net/>, 24th June 2007)

#### ➔ **Tricycle configuration**

This configuration appeared later in the aircraft designs. This configuration is much easier to handle: this configuration gives a much better visibility to the pilot of the ground, it is much easier to land and take off with cross wind and it is not possible to tip up the aircraft as can happen with a tailwheel configuration.



Lockheed Super Constellation

(<http://www.airliners.net/>, 24th June 2007)

## 3.2. MATERIALS

### 3.2.1. *Wood and fabric*

The wood and fabric construction is the oldest way of building aircraft. These materials are worth being compared to new materials:

#### ➔ **Advantages**

The wood and fabric materials allow very light designs. In fact the density of the wood varies a lot depending on the kind of wood, but it is always much lower than steel or even aluminium. Typically the density of the wood varies between 350 and 1100 kg/m<sup>3</sup> (compared to 7800 kg/m<sup>3</sup> for steel and 2600 kg/m<sup>3</sup> for aluminium). This explains why wood has been used for aircraft since the beginning of aeronautics.

As it is the oldest technology, it is also the best known: the wood and fabric designs are really spread and the knowledge concerning this technology is huge.

Furthermore, the wood and fabric design does not require complex tooling: a saw, glue, glass paper are the main tools required. That is why a lot of personal aircraft builders use this technology.

#### ➔ **Downsides**

The wood and fabric designs have limits: Usually it is considered that in general aviation wood and fabric designs will not exceed 250km/h.

The wood is a non isotropic material. Its quality can also change depending on provenance. This imposes extra care while designing the aircraft.

The wood is really sensitive to humidity and temperature. While building the aircraft a lot of attention must be paid to ensure that the process is correct.



Fournier RF6-B wood and Fabric Aircraft  
(<http://www.ailleschat.com>, 23<sup>rd</sup> June 2007)



### 3.2.2. *Metallic structures*

The metallic structures started to be used in aeronautics in the 60s. Globally slightly less efficient than wood structures for light aircraft, they present other advantages that make them very popular now.

#### ➔ **Advantages**

The manufacturing of metallic structures can be achieved in any conditions of temperature and pressure. This gives a huge advantage over the wooden constructions. Furthermore, the metallic materials are isotropic.

The metallic structures are usually much simpler than the wooden structures. For example, a typical metal rib would require 2 parts while the wooden rib would need between 20 and 30 components.

All these characteristics make the metallic structure manufacturing process 3 to 4 times faster than the wooden structures.

#### ➔ **Downsides**

The metallic structures are usually heavier than the wooden structure. The extra weight induces bad penalties on the aircraft performance.

The metallic materials are subjected to corrosion: it is important to use the correct protections to ensure that the material remains in good shape.

It is harder to get complex shapes with metallic structures without expensive tooling. However, it has been shown that efficient aircraft can be made with simple metallic structures like the ZENITH from Chris Heintz, which was the first very popular metal aircraft. (cf. picture below)



Zenith

(<http://www.zenithair.com/zen1.htm>, 29<sup>th</sup> June 2007)

### 3.2.3. *Composite materials*

The composite materials are more and more used in modern aircraft designs: they can achieve great mechanical properties with light weight which is exactly what is wanted for aircraft structures.

The composite materials have great mechanicals properties: high stiffness, high static strength, great fatigue resistance, good damage tolerance properties and low weight. Furthermore, the composite materials are not subjected to corrosion. The composite materials allow the manufacturing of very complex shapes, which is important for the aerodynamic surfaces for instance.

The most common composite materials in aerospace are:

- Glass fibre: Cheap, easy to manufacture, allows for very slick aerodynamic surfaces. However, glass fibre is quite heavy compared to other composite materials and its mechanical properties are quite low. That is why it is usually used for fairings.
- Carbon fibre: Great mechanical properties, light, this is the most used for structural components. However, this material is still expensive and the manufacturing process requires complex tooling and a lot of care.
- GLARE: GLass ALuminium REinforced. This new material is used for a big part of the A380. It has better mechanical properties than aluminium and it is at the same time lighter. It has a better resistance to corrosion. It has better fatigue and damage tolerance properties than aluminium and finally it has a better resistance to fire. However, this material is not available for small aircraft manufacturer since it is still a cutting edge technology.

The composites materials have also their weaknesses: They have a bad resistance to the shocks, they are bad electric conductors, they cannot be used at high temperatures and they have bad ageing with humidity. Below is an example of an outstanding composite aircraft: the Global flyer, realised by the company Scaled Composites. This aircraft flew all around the world without stopping.



Scaled Composites Global Flyer  
(<http://www.scaled.com/>, 26<sup>th</sup> June 2007)

### 3.3. AIRCRAFT DESIGN CHOICE

Based on the studies done in this chapter we can choose the best configuration for our microlight.

#### 3.3.1. *General configuration*

For our aircraft I have selected the following configuration:

- Colab wing design
- Pusher propeller configuration
- Tricycle landing gear configuration
- Cruciform tail

The Colab design will enable us to get a very efficient design and in the same time a light design. This is what we want for our aircraft.

The Pusher propeller and the tricycle landing gear will give the pilot the best visibility, manoeuvrability and comfort to win the competitions. In particular, the tricycle landing gear allows the pilot to land with full breaks and so achieve very short landing.

The pusher configuration is the most common for microlights since it is hard to fit the engine and the propeller at the front. In addition, it is much more comfortable for the pilot.

#### 3.3.2. *Materials*

- The wing the tail plane and the fin will be built with carbon fibre / epoxy composite materials.
- All the aerodynamic fairings will be built with carbon fibre / epoxy composite materials.
- The fuselage structure will be built with aluminium tubes of rectangular and circular sections.

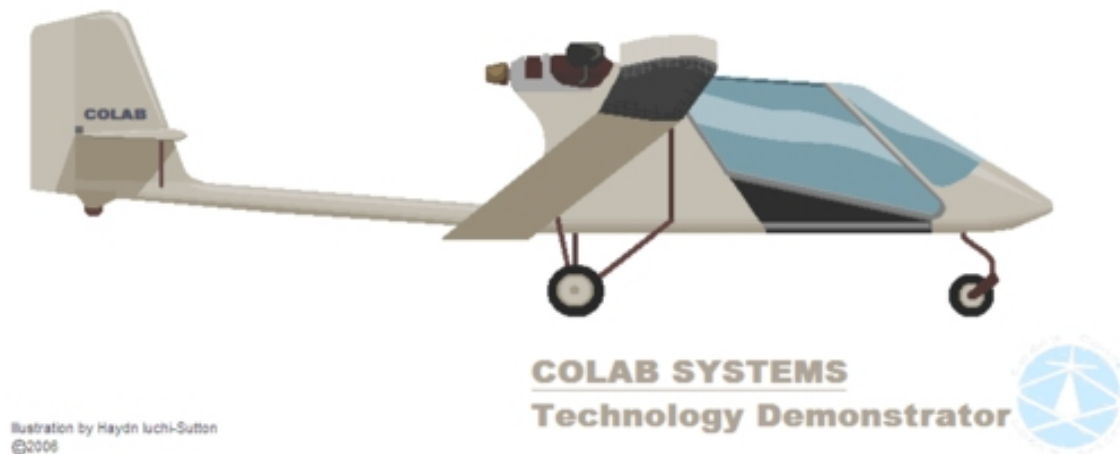
The carbon fibre / epoxy composite materials allow high strength, light weight and nice aerodynamic finishing. We use the aluminium tubes for the fuselage because they are easy to assemble, cheap and light enough.

## 4. THE COLAB DESIGN

### 4.1. PRESENTATION OF THE CONCEPT

#### 4.1.1. *Introduction*

The Colab wing is a patented design which has been developed, tested and optimised by the association Colab system. The invention to Mr Lucien CABROL, who is the main actor of the association and established the patent N° 82-03961 the 9<sup>th</sup> of March 1982 and the patent N°00-14171 the 6<sup>th</sup> of March 2000. This design has been sold to diverse organisations but it is still the exclusive property of Lucien CABROL for all aircraft under 150kg (empty weight).



Colab technology demonstrator digital model  
(Property of Colab concept)

#### 4.1.2. *Design overview*

This design is based on a double wing joined at the tips. On the basic configurations the front wing is horizontal, straight and located at the top of the aircraft while the rear wing has a negative swept and a positive dihedral. Other arrangements can be considered, but this one is simple and efficient. This is the design which has also been the most tested.

On the next page you can see the three views design for the conventional configuration.



Colab technology demonstrator digital model 3 views  
(Property of Colab concept)

#### 4.1.3. *Why can we trust this design?*

##### ➔ **A validated theory**

The Colab team has worked with physicists to establish the mathematical model of the wing. The Colab system team has established the algorithms which give the optimised parameters for the geometry to get the best aerodynamic performance. These algorithms are patented. However it is possible to get information for the geometry of a particular design and that is how this aircraft has been designed.

In addition a lot of wind tunnel tests have been performed to prove the properties of the Colab wing. The Colab team has also performed lab tests with Onera (the French research centre in aerospace) to study the dynamic properties of the structure to check if there were eventual flutter issues.

##### ➔ **A practically tested concept**

The Colab design has been tested and optimised for now more than 25 years. It has been observed and proved that this design has great advantages over conventional designs. But, the theory is not enough to show that a design works, there is also the need of practical experience.

The Colab experience is based on more than 20 model aircraft with a span up to 6m for the “Edelweiss Colab glider” and 1 full scale twin seat microlight. The pictures on the next page show some of the models realized.



Edelweiss Colab (6m span)  
(Property of Colab concept)

2 seater Colab microlight  
(Property of Colab concept)



### ➔ **An award winning design**

In 2005, Jean-Michel BOUQUET, won a prize at the aeronautic models meeting of La Ferté Alais. Its flight demonstration of the Edelweiss Colab was received with a lot of enthusiasm. (Cf. picture below).



Jean Michel Bouquet with the prize for its Edelweiss Colab glider  
(Property of Colab concept)

The Colab team also won the Micro UAV competition in 2005 in France. This competition was organised by the DGA (Délégation Générale pour l'Armement) which is part of the Ministry of Defence. The Ministry of Defence has now taken part into the Colab association to realize UAV. As a consequence, all aircraft using this concept with an empty weight of more than 150 kg are now under contract.

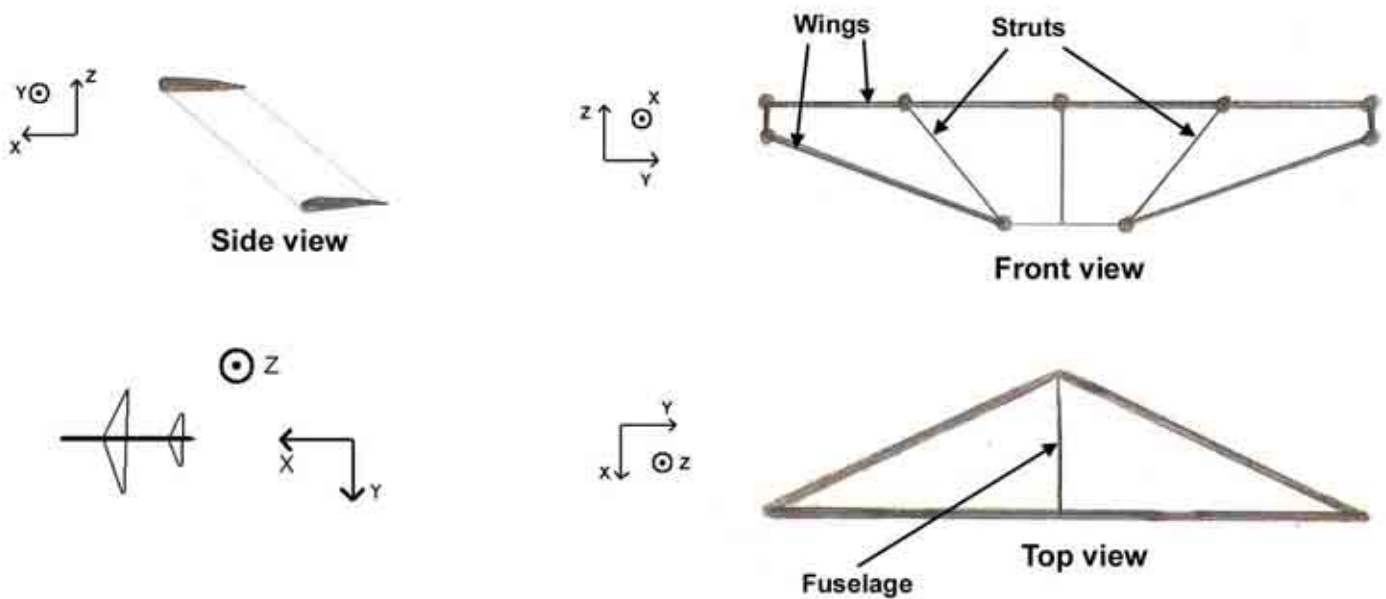


## 4.2. ADVANTAGES OF THE CONCEPT

### 4.2.1. *Structural advantages*

#### ➔ **Stiff geometry**

The position of the wings makes the structure naturally stiff. There are no cantilever beams like in a conventional design. The structure is triangulated and this allows weight reduction with the same stiffness and weight. The figure below illustrates how the structure works and allows us to understand why we get large moment of area in the 3 axis:



Colab wing structure

The front view shows that the structure has a large moment of area on the X axis: therefore the structure is much stiffer for the spanwise bending. The top view shows the sweepback of the rear wing: this gives a large moment of area in the Z axis. Finally, the side view shows that the height difference between the wings and the difference of position along the X axis of the plane gives the wings a very high torsional stiffness along the Y axis. Even at high velocities, the torsion in the wing is negligible.

It has been demonstrated that the most efficient structure is obtained with struts which provide extra stiffness to avoid the buckling of the top wing.

➔ This structure reacts much better to the aerodynamic loads than a conventional cantilever structure.

➔ **Flutter**

The flutter on this wing has been studied and it appears that because of the difference in length of the top and bottom wings, they do not have the same vibration frequencies. As a consequence, when one wing vibrates the energy is damped by the other wing.

➔ This structure is safer than a conventional wing concerning the flutter

#### 4.2.2. *Conception advantages*

➔ **Ultra simple wing geometry**

The wings are not twisted. Furthermore, the cross section is constant spanwise. This is an enormous advantage compared with traditional wings. The ribs are all the same and we can even consider producing wings in large quantity, cutting them at the right span for each aircraft!

➔ No twist, constant cross section, the simplest wing design.

➔ **Ailerons and variable camber flaps simple actuation**

The design is fitted with full span variable camber flaps on the top wing and full span ailerons on the bottom wing. On this design it has been proven that it is feasible to actuate the ailerons and the flaps from the root. This makes the actuation simpler.

➔ **Better pilot's visibility**

The front wing is a top wing while the down wing is attached backward: this gives the pilot a good visibility on the ground.

➔ **Easier fuselage design**

The wing position gives by default a good volume where the pilot can fit: just under the top wing and in front of the low wing. There is no need for complex fuselage structure; the pilot is just sitting under the wing.

#### 4.2.3. *Aerodynamics and performance advantage*

➔ **No stall**

It has been observed than at high angle of incidence the root of the wings start to stall before the tips. As a consequence the pressure centre moves toward the tip of the wings, which increases the aircraft stability. The aircraft does not stall brutally but shrinks slowly and remains perfectly controllable in roll and pitch. Just putting back the stick in the neutral positions stops the shrinking.

➔ **No sideslip at high angle turns**

There is very few side slip at high angle turns. This makes the aircraft very safe since non controlled turns at high roll angle are a large source of accidents.

➔ The Colab aircraft has a very safe behaviour.



### ➔ **Huge velocity and glide ratio range**

Because of its variable camber flaps and the special geometry of its wing this aircraft has a flying velocity range which is impossible to achieve with conventional configurations. With the flaps deflected at  $45^\circ$  (landing configuration) we get such a high lift increment that it is possible to land at speeds as low as 10 kt. In the same time the drag increases a lot and so the glide ratio decreases. On the contrary, with the flaps at  $-10^\circ$  (high speed configuration), the very low drag of the aircraft allows to cruise at 100kt with low engine power.

➔ This configuration provides a velocity range not achievable with classical configurations.

### ➔ **Very manoeuvrable in roll**

The wing design reinforces the ailerons efficiency. Basically when the pilot wants to turn on the left, the right aileron moves downward and the left aileron moves upward; while moving upward the left aileron closes the “box” between the 2 wings, reducing the lift and increasing the drag, while the right aileron increases the lift on the right wing. Although the aircraft is really stable in roll, this property makes the aircraft very manoeuvrable. In addition while on a conventional wing the roll induces an opposite yaw moment that the pilot has to compensate with the rudder, on this configuration, the induced yaw is in the same direction as the roll because of the drag induced when the left aileron closes the wing “box”; the pilot does not need the rudder anymore while performing a turn manoeuvre. It has also been noted that the aircraft does not have a tendency to sideslip in the curves. This decreases the wetted surface in turn manoeuvre, and so the drag decreases, and the aircraft efficiency increases.

➔ Because of the wing geometry the aircraft is more manoeuvrable and easier to fly, with more performance.

### ➔ **Very high glide ratio**

This wing configuration has an amazing glide ratio: first of all this configuration has a very low drag. There is no separation of the boundary layer on the extrados of the wings, which implies that we can get a laminar flow on the entire chord of the airfoil. In addition, the tip vortices almost disappear. All these parameters make the drag very low. Furthermore, this wing has very high lift properties. That is how it is possible to get a glide ratio of 30 with a conventional 8m span wing.

➔ Basically this configuration allows us to get the high glide ratios of gliders with the high lift and low speed capabilities of STOL aircraft, in the same time.

### ➔ **Large CG range**

Because of the configuration of the wing, this aircraft allows a large CG range and so more longitudinal stability. Because of the negative sweepback of the rear wing, the lift is distributed along a long part of the fuselage, and that is how the stability is increased.

## 4.3. UNDERSTANDING OF THE CONCEPT

### 4.3.1. *Basics of aerodynamics*

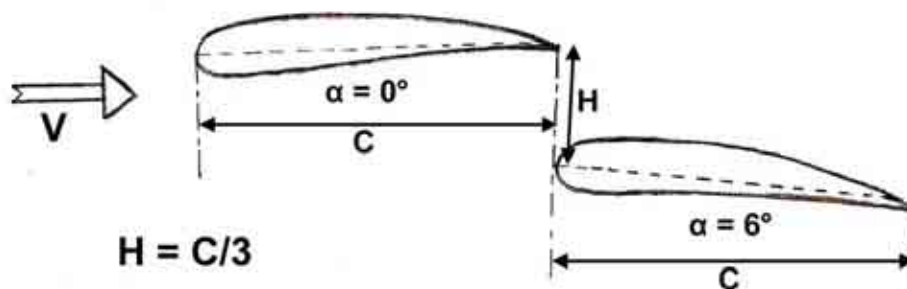
We often forget that the aircraft does not fly thanks to the solid surfaces, but thanks to the aerodynamic disturbances that are generated by the solid surfaces. We need to keep this in mind when trying to understand how the Colab wing works.

### 4.3.2. *The Nenadovitch effect*

This effect has been discovered by the Professor of Aerodynamics at the Prague University, Mr Nenadovitch, during the years 1920-1940. This effect was studied on biplane aircraft in order to optimise the aerodynamics between the top and the low wing. We can summarize the effect with these formulae:

If we consider 2 airfoils with a chord  $C$  and if we move the front wing forward and the rear wing backward, with a difference of height between the wings of  $H=C/3$  and if we increase the angle of attack of the rear wing of  $6^\circ$  compared to the front wing (as illustrated on the figure below, we observe the following effect:

➔ **For the same total lift as a monoplane aircraft, we get a lower drag.**



Nenadovitch geometry

Basically the idea is to transform the negative interaction between the wings into a positive interaction. In the Colab design the interferences between the 2 wings have been optimised, based on the work produced by Mr Nenadovitch.

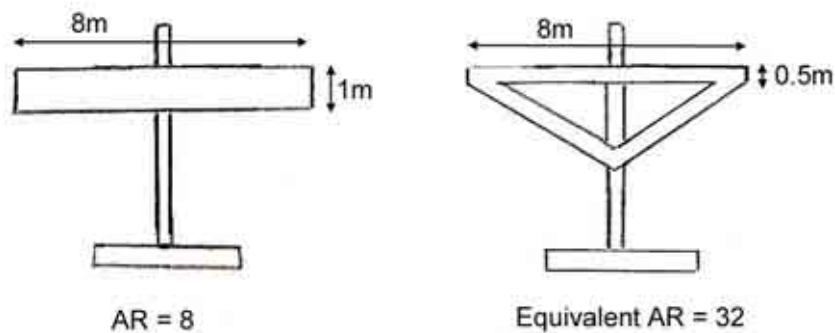
#### 4.3.3. The closing coefficient

The Colab team has developed with numerical methods a theory for the Colab wing, and one of the most important parameters is the closing coefficient. This coefficient is called  $C_b$  (from “Coefficient de Bouclage” in French). The coefficient is expressed with the following formula:

$$C_b = \frac{\text{Length of the equivalent wing}}{\text{Length of the unfolded Colab wing}}$$

For example, with a closing coefficient equal to 1, if we consider 2 wings with the same area and the same span, the performance of the Colab wing will be equivalent to a wing with an aspect ratio 4 times higher.

This formula can be understood better with the following picture. This represents the equivalent aspect ratio for a closing coefficient equal to 1:



Closing

#### coefficient and equivalent wing

Basically when  $C_b = 1$ , the Colab aircraft has the properties of an aircraft with a span equal to the sum of the lengths of all the wing segments. Typically the closing coefficient is between 0.7 and 1.2.

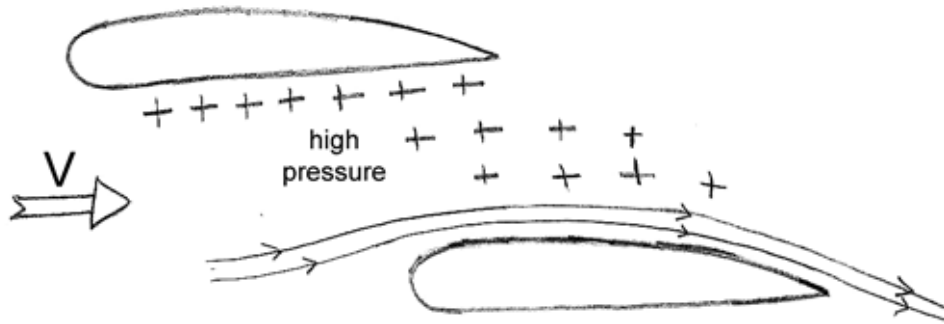
#### 4.3.4. Conceptual explanations

In this part we are going to illustrate the phenomena that make this design so efficient. The explanations given in this part are simple and they are just for the understanding of the global aerodynamic mechanism. In reality, the interferences between the wings are complex and cannot be easily described.

### ➔ No flow separation

One of the main characteristics of the Colab wing is its very low drag. This is due to the fact that the amount of aerodynamic turbulences has been reduced; the flow remains laminar everywhere and there is no separation of the boundary layer on the extrados, as happens on conventional wings.

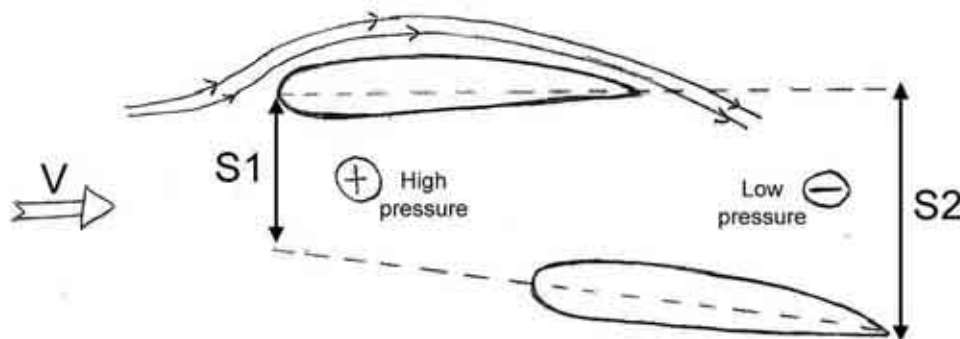
The figure below illustrates how the boundary layer is maintained on the extrados:



Compression of the extrados boundary layer on the low wing

The high pressure on the intrados of the top wing makes the boundary layer of the extrados of the low wing stick to the surface. When there is no flow separation, there is much less turbulence generated, and so less drag.

On the extrados of the top wing, another phenomenon appears; it is illustrated by the following figure:



Suction of the extrados boundary layer on the top wing

We can consider a tube of air between the 2 wings, the entrance of the tube has the area  $S1$  and the exit has the area  $S2$  (cf. illustration). We have  $S1 < S2$ . If we consider that the flow rate and the air density remain constant in this tube, then there is a pressure drop. The low pressure at the end of the tube sucks the air on the extrados of the top wing, and therefore makes the boundary layer stick the surface.

### ➔ **Reduction of the tip vortices**

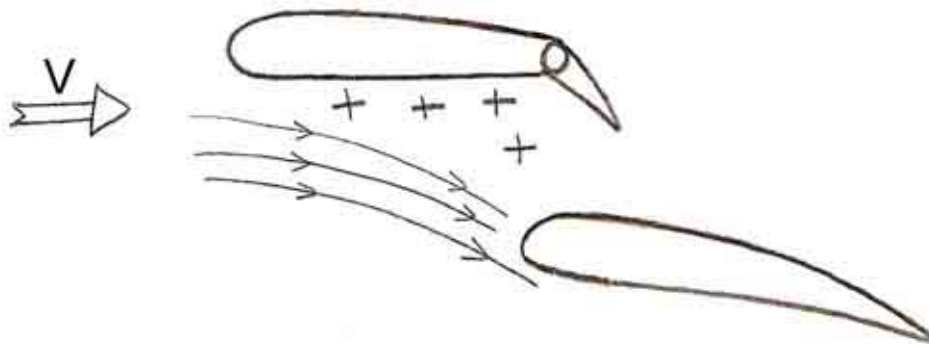
The shape of the tips of the wings has been optimised to increase the wing efficiency. This part increases the closing coefficient and reduces the tip vortices. The shape has been tested and improved and it has a lot of impact on the efficiency of the aircraft. Below you can see pictures that I took when I visited the inventor of the concept, Lucien Cabrol.



Pictures of the wing tip of a Colab wing

### ➔ **High lift capabilities**

The figure below illustrates how it is possible to get the very high lift capabilities with the variable camber flaps:

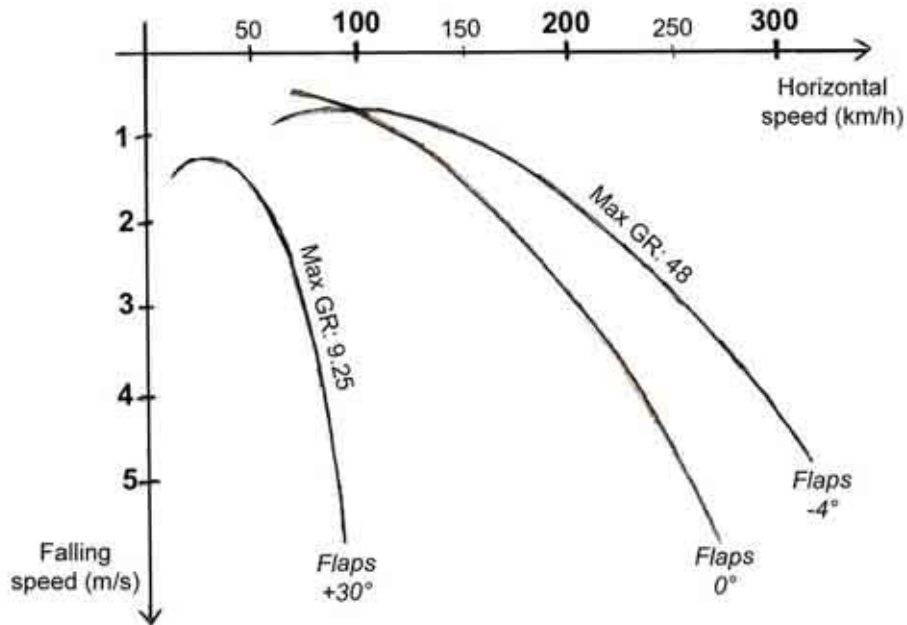


Colab wing with flaps deflected

The deflection of the flaps induces a very high pressure on the intrados of the top wing and so a lift increment. At the same time, the downwash induced increases the angle of attack of the low wing and so the low wing lift increases. Even at high angle of attack the low wing does not stall since the boundary layer remains stuck to the low extrados thanks to the high pressure induced by the top wing. This effect allows the Colab wing to have incredible STOL capabilities.

#### 4.3.5. *Large range of velocities*

One of the most amazing capabilities of the Colab wing is to enable us to get a very large range of velocities and of glide ratios. The speed polar below illustrates what the performance of the Colab wing are:



**Theoretical speed polar for a Colab wing**

- Glider type airfoil
- 8m span and 0.8m chord
- Wing loading 20 kg/m<sup>2</sup>

#### Theoretical Colab drag polar

This polar shows how the variable camber flaps enable the pilot to control the glide ratio of the aircraft. This curve is theoretical; it means that it works for a naked wing, without fuselage. However it is really interesting to see that with a reasonable aspect ratio of 10 we get glide ratios comparable to glider wings with very high aspect ratio.

Furthermore, because of the geometry of the Colab wing, an aspect ration of 10 is much easier to design, from a structural point of view, than with a cantilever wing.

#### 4.3.6. *Smart fuselage design*

The fuselage is a very important source of drag. An optimised fuselage will produce a much more efficient aircraft. The fuselage of the HLM aircraft has been carefully designed to get an aircraft with the best performance.

##### ➔ **Reducing the fuselage interferences on the wing**

The fuselage aerodynamic interferences on the wing reduce a lot the wing efficiency in the inboard area. It is important to reduce them:

- The Colab top wing is mounted on a pod.
- The negative sweepback of the rear wing limits the interference area.



Colab fuselage interferences reduction  
(Property of Colab concept)

##### ➔ **Increasing the propeller efficiency**

The rear mounted engines have a lot of advantages; they give a better pilot visibility, they blow air into the empennage, making the aircraft more manoeuvrable and they are slightly less noisy inside the cabin. However, one of the major issues is that the propeller efficiency is reduced because it is behind the fuselage, in a disturbed area. The rear fuselage is going to have a shape which gives a lot of airflow into the propeller, to increase the efficiency. Basically the shape is similar to the inside shape of a NACA air intake. You can see the illustration on the pictures of a model below:



HLM Colab fuselage propeller efficiency optimisation



## 4.4. MEETING WITH THE COLAB INVENTOR

I went to visit Mr Lucien CABROL at his house, for two days. This part explains the reasons of this visit and the consequences.

### 4.4.1. *Purpose of this visit*

The Colab wing is an amazing concept. So amazing that it seems almost too good to be true. Before starting the design of a microlight with this wing, it was important to check that the Colab team was a serious association and that their design has the properties they claim.

Furthermore, the design is patented worldwide, and no one is authorized to use it without the agreement of the owner of the patent, Lucien CABROL. This visit was also meant to establish an agreement with the Colab team, to work in collaboration.

### 4.4.2. *Results of the visit*

The visit was very rich and interesting. Lucien CABROL and I had very long discussions during the entire 2 days. I was also able to have a look at some of the models built and at the prototype of the structure of a future single seater Colab microlight (cf. pictures below).



Pictures taken during the visit to see Lucien CABROL

### 4.4.3. *Terms of the collaboration*

All the people working with the information contained in this thesis must contact the Colab team first. All new work done using the Colab concept must be communicated to the Colab team. No microlight using the Colab concept can be sold without an agreement of the Colab team. You can contact Lucien CABROL at the following address: [fantacopter@hotmail.com](mailto:fantacopter@hotmail.com) . A copy of this thesis has been sent to the Colab team. The Colab association is a team; I am also in touch with different members of this team. Each member has his specific skills, it is important to be aware of that as they can answer to a lot of questions.

## 5. PARAMETRIC ANALYSIS

In this part we are going to do a parametric analysis based on the aircraft data that we have collected. This analysis based on aircraft under 115kg will allow us to predict the general average properties of our aircraft. For this analysis we will use the method established by L.K. LOFTIN in the NASA paper: *Subsonic Aircraft: Evolution and the Matching of Size to Performance*, [Ref. 9]. This analysis will also enable us to compare the aircraft efficiencies for different parameters.

### 5.1. NOTATIONS AND UNITS RELATIVE TO THIS PART

#### 5.1.1. General notice

For more convenience, and to avoid mistakes, since the NASA paper uses imperial units, in this part all the calculations are going to be done with the imperial units listed below except when mentioned otherwise.

All the calculations are done with the standard atmosphere model at sea level.

#### 5.1.2. Notations and units

|                     |                              |                         |
|---------------------|------------------------------|-------------------------|
| W:                  | Aircraft gross weight        | [lb]                    |
| S:                  | Gross wing area              | [ft <sup>2</sup> ]      |
| P:                  | Engine power                 | [hp]                    |
| V:                  | Speed                        | [ft/s]                  |
| P:                  | Air density                  | [slug/ft <sup>3</sup> ] |
| C <sub>D</sub> :    | Drag coefficient             | [ - ]                   |
| C <sub>D0</sub> :   | Drag coef. at zero lift      | [ - ]                   |
| η:                  | Propulsive efficiency        | [ - ]                   |
| C <sub>L</sub> :    | Lift coefficient             | [ - ]                   |
| C <sub>Lmax</sub> : | Maximum lift coef.           | [ - ]                   |
| C <sub>Lt</sub> :   | Take-off lift coef.          | [ - ]                   |
| l <sub>T,g</sub> :  | Take-off ground run distance | [ ft ]                  |
| A:                  | Aspect Ratio                 | [ - ]                   |
| E:                  | Aircraft efficiency          | [ - ]                   |

#### 5.1.3. Notations for the graphs

The graphs are plotted with the interpolation curves:

- The RED curves correspond to the average interpolation curve.
- The GREEN curves give the envelope of the MOST efficient aircraft.
- The BLUE curves give the envelope of the LESS efficient aircraft.

## 5.2. AIRCRAFT SPEED PREDICTION

### 5.2.1. Equations

We can find a linear correlation between the aircraft engine power and the maximum level velocity with the following equation:

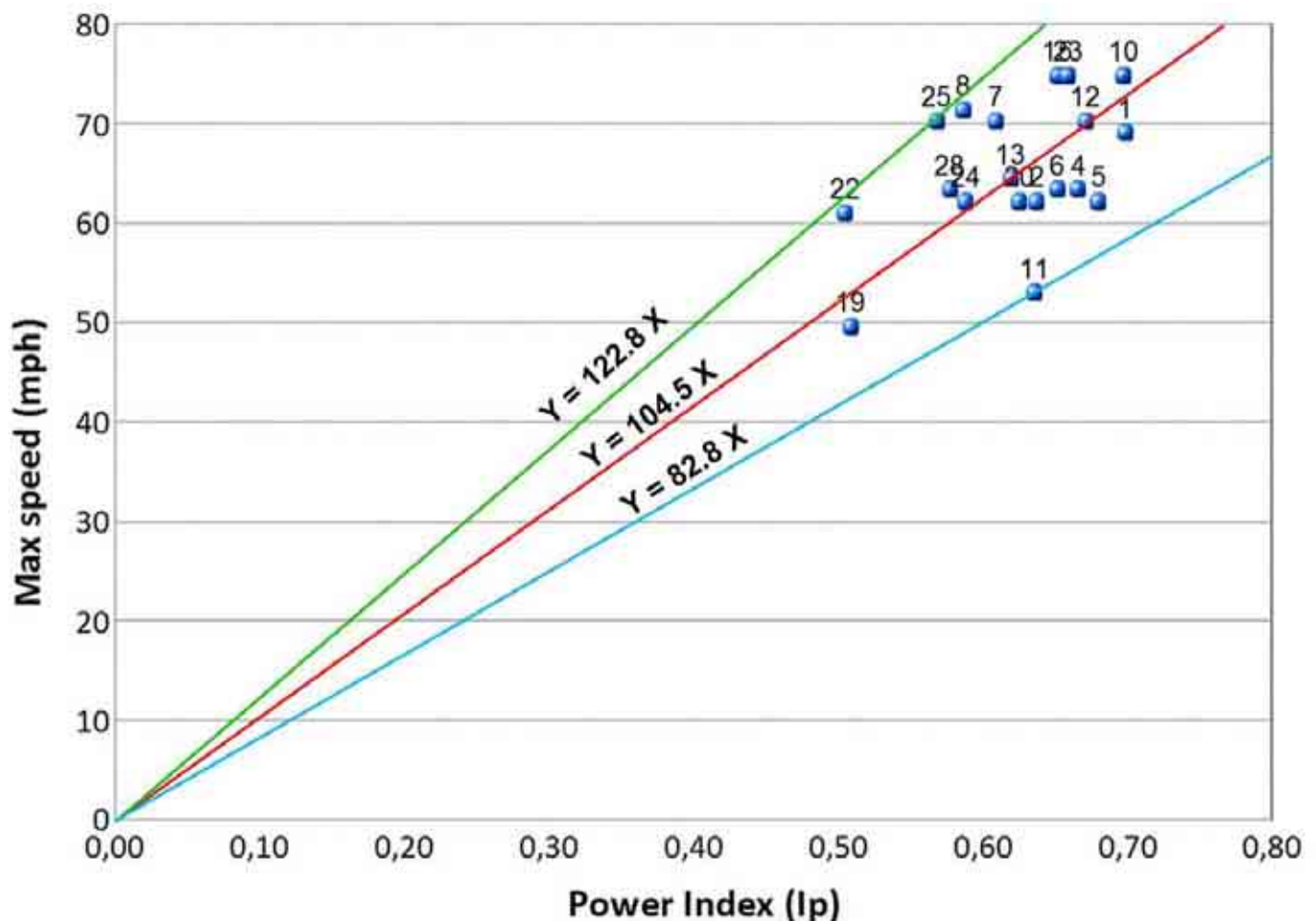
$$V = K \times \sqrt[3]{\frac{W/S}{W/P}} \times \sqrt[3]{\frac{\eta}{C_{D0}}}$$

The propulsive efficiency can be considered as constant and equal to 0.85. Loftin makes the assumption that the  $C_{D0}$  can be considered as constant. This is not really true in our case since we have very different designs with a large range of performance. However, if we want to be able to get correlations, we need to make this assumption. We will need to remember that to understand the results. We can create a parameter called  $I_p$  which is expressed:

$$I_p = \sqrt[3]{\frac{W/S}{W/P}}$$

We then get the following relation that we can plot on a graph:  $V = K \times I_p$

### 5.2.2. Graph



Graph: Variation of speed with power index  
(See Table page 84 for aircraft numbers)

### 5.2.3. Conclusion

On this graph we can notice as we did in the previous parts that the aircraft are not homogeneous in performance: we can observe the very good performance of the number 8 (sirocco, good aerodynamics), the number 25 (onyx CP 150, canard configuration), and the number 22 (Lazair, smart design with V-tail).

This graph allows us to get the following correlation:  $V_{(mph)} = 104.5 \times \sqrt[3]{\frac{W/S}{W/P}}$

This value is based on the average 0.85 propulsive efficiency. We need to incorporate the propulsive efficiency into the equation, we then get:

$$V_{(mph)} = 104.5 \times \sqrt[3]{\frac{\eta}{0.85} \times \frac{W/S}{W/P}}$$

We can also calculate the  $C_{D0}$  for the aircraft. If we put the velocity in miles per hour instead of feet per second the theory gives us:

$$C_D = \eta \times \left( \frac{77.3}{1.47} \right)^3 \times \left( \frac{I_P}{V} \right)^3 = 0.108 \quad (V \text{ in mph})$$

It is assumed that  $C_{D0} = 0.9 \times C_D$ , and  $\eta = 0.85$ , then we get:

$$C_{D0} = 1.1140 \times 10^5 \left( \frac{I_P}{V} \right)^3 = 0.097 \quad (V \text{ in mph})$$

These are the values based on the average slope obtained from the graph: they represent the average performance of the microlights.

## 5.3. AIRCRAFT STALLING SPEED PREDICTION

### 5.3.1. Equations

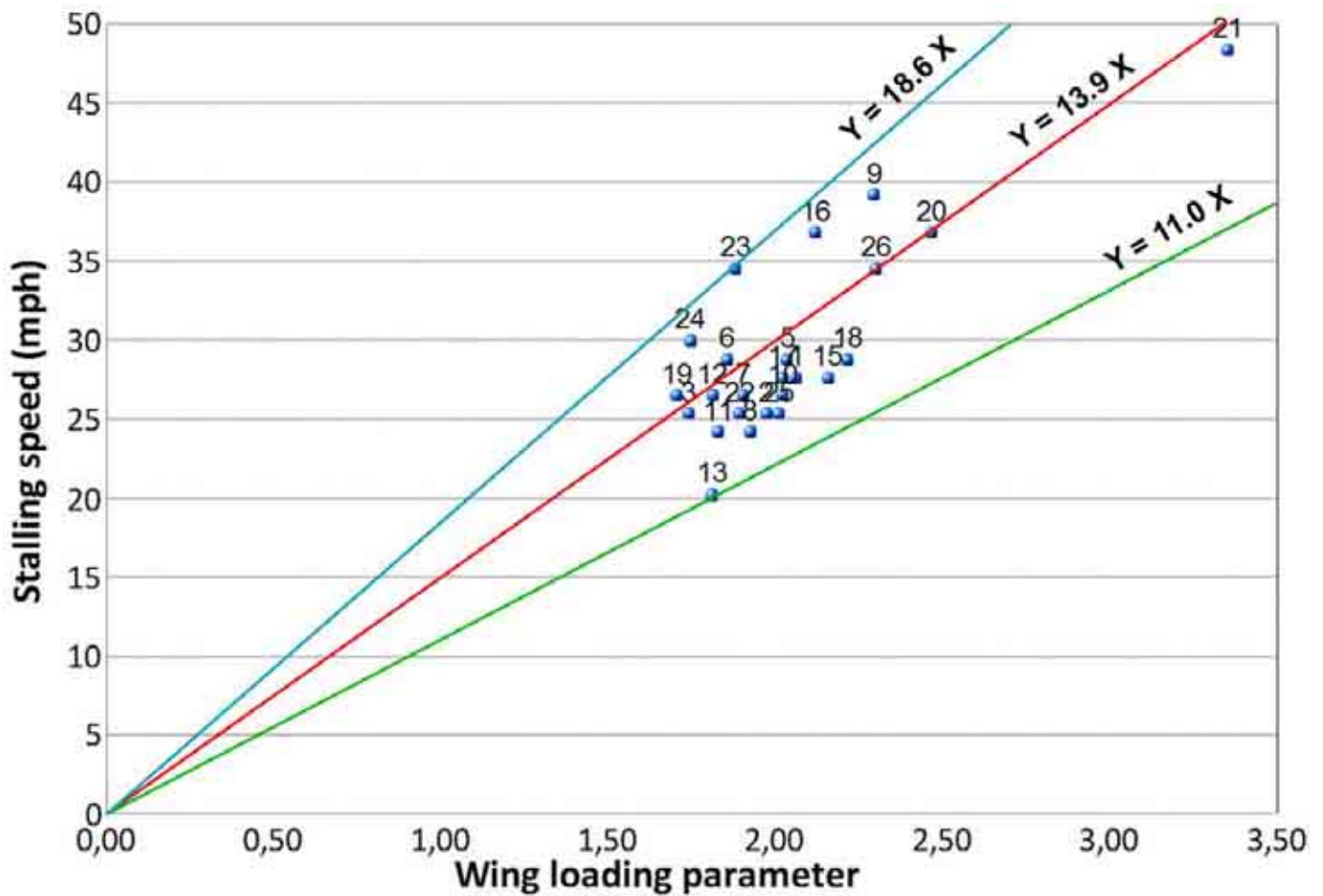
This part is based on the following lift equation at stall speed:

$$W = \frac{1}{2} \cdot C_{L_{\max}} \cdot \rho \cdot S \cdot V_{\text{stall}}^2 \quad (\text{with ISU})$$

Therefore we can deduce that:  $V_{\text{stall}} = K \times \sqrt{W/S}$   
 $\sqrt{W/S}$  is called the wing loading parameter.

We can plot this on a graph to find the linear correlation coefficient. (cf. next page).

### 5.3.2. Graph



Graph: Variation of stalling speed with wing loading parameter  
(See Table page 84 for aircraft numbers)

### 5.3.3. Conclusion

With this graph we obtain the following correlation:  $V_{stall} = 13.9 \times \sqrt{W/S}$  ( $V_{stall}$  in mph)

We can now deduce the average  $C_{Lmax}$  and  $C_{Lt}$  for our microlights:

$$C_{Lmax} = 390.963 \times \frac{W}{S} \cdot \frac{1}{V_{stall}^2} = 2.02 \quad (V_{stall} \text{ in mph})$$

To calculate  $C_{Lt}$  we consider the take-off speed which is assumed to be  $1.1 \times V_{stall}$ :

$$C_{Lt} = 390.963 \times \frac{W}{S} \cdot \frac{1}{(1.1 \times V_{stall})^2} = 1.67 \quad (V_{stall} \text{ in mph})$$

## 5.4. TAKE OFF GROUND RUN PERFORMANCE

### 5.4.1. Equations

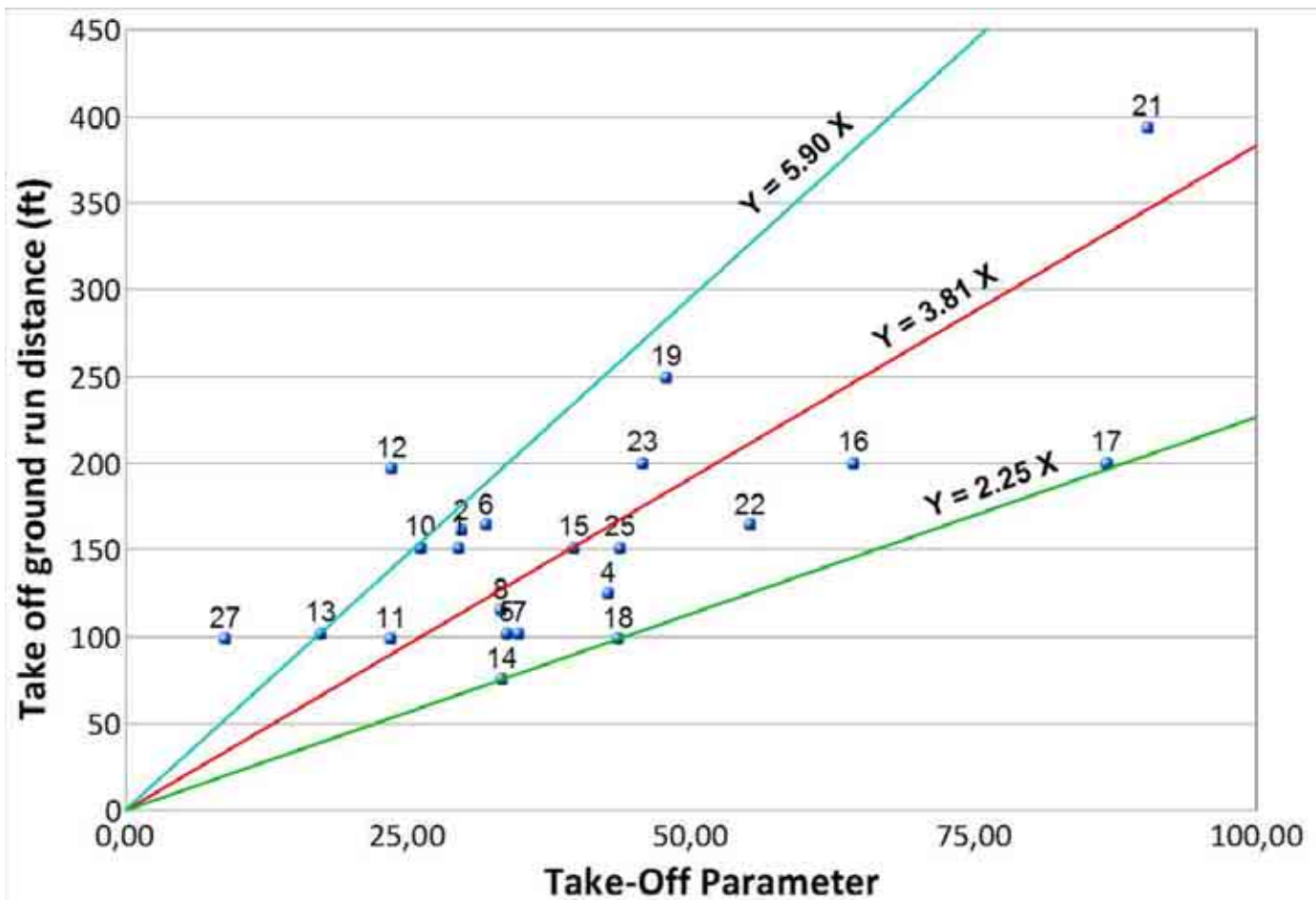
In this part we are going to establish a correlation between the aircraft general characteristics and the take-off field length. The data given by the aircraft manufacturer concerning the take-off field lengths are not accurate, and we can expect some dispersion in the graphs.

The Loftin method predicts that the take-off ground run distance is proportional to the following parameter:

$$l_{T,g} = K \times \frac{(W/S).(W/P)}{C_{Lt}}$$

We know we can determine the  $C_{Lt}$  with the method explained in the previous paragraph. Therefore, we are able to plot the graph and to determine the constant K.

### 5.4.2. Graph



Graph: Variation of Take-off distance with take-off parameter  
(See Table page 84 for aircraft numbers)

### 5.4.3. Conclusions

As we guessed, the dispersion is very bad on this graph. However, in the Loftin analysis, this graph also gives the worst dispersion. The data given concerning the take-off distances are bad, but they are the only parameters we have. Therefore, we must cope with these data.

These data enable us to establish the following correlation:

$$l_{T,g} = 3.81 \times \frac{(W/S).(W/P)}{C_{Lt}}$$

Like we did for the maximum speed we need to incorporate in this equation the propulsive efficiency. We suppose that the average efficiency is equal to 0.85.

$$l_{T,g} = 3.81 \times \frac{0.85}{\eta} \times \frac{(W/S).(W/P)}{C_{Lt}}$$

## 5.5. CLIMB PERFORMANCE

### 5.5.1. Equations

The aircraft rate of climb is proportional to the difference between the maximum power available ( $P_a$ ) and the power required for the flight in steady level ( $P_r$ ). It can be expressed this way:

$$\dot{h} = \frac{33000 \times (P_a - P_r)}{W}$$

The power available can be determined easily with the following relation:  $P_a = \eta.P$ , where  $P$  is the maximum shaft power of the engine.

The power required for the steady level flight is equal to the drag multiplied by the velocity in steady level flight:  $P_r = D.V/550$ . Then we substitute with the drag and the lift equations and we get the following formula:

$$\frac{P_r}{W} = \frac{\sqrt{W/S}}{19 \times (C_L^{3/2} / C_D)}$$

Finally we can express  $\dot{h}$  with the following expression:

$$\dot{h} = 33000 \times \left[ \frac{\eta.P}{W} - \frac{\sqrt{W/S}}{19 \times (C_L^{3/2} / C_D)} \right] = 33000 \times \bar{P}$$



We now need to determine  $(C_L^{3/2}/C_D)$ . What we want in our case is the maximum value, to be sure to get the critical case, i.e. the minimum climb rate. We start from the basic drag equation:

$$C_D = C_{D0} + K.C_L^2, \quad K = \frac{1}{\pi.A.\epsilon}.$$

Then we replace this in the formula and we get:

$$\frac{C_L^{3/2}}{C_D} = \frac{C_L^{3/2}}{C_{D0} + K.C_L^2}$$

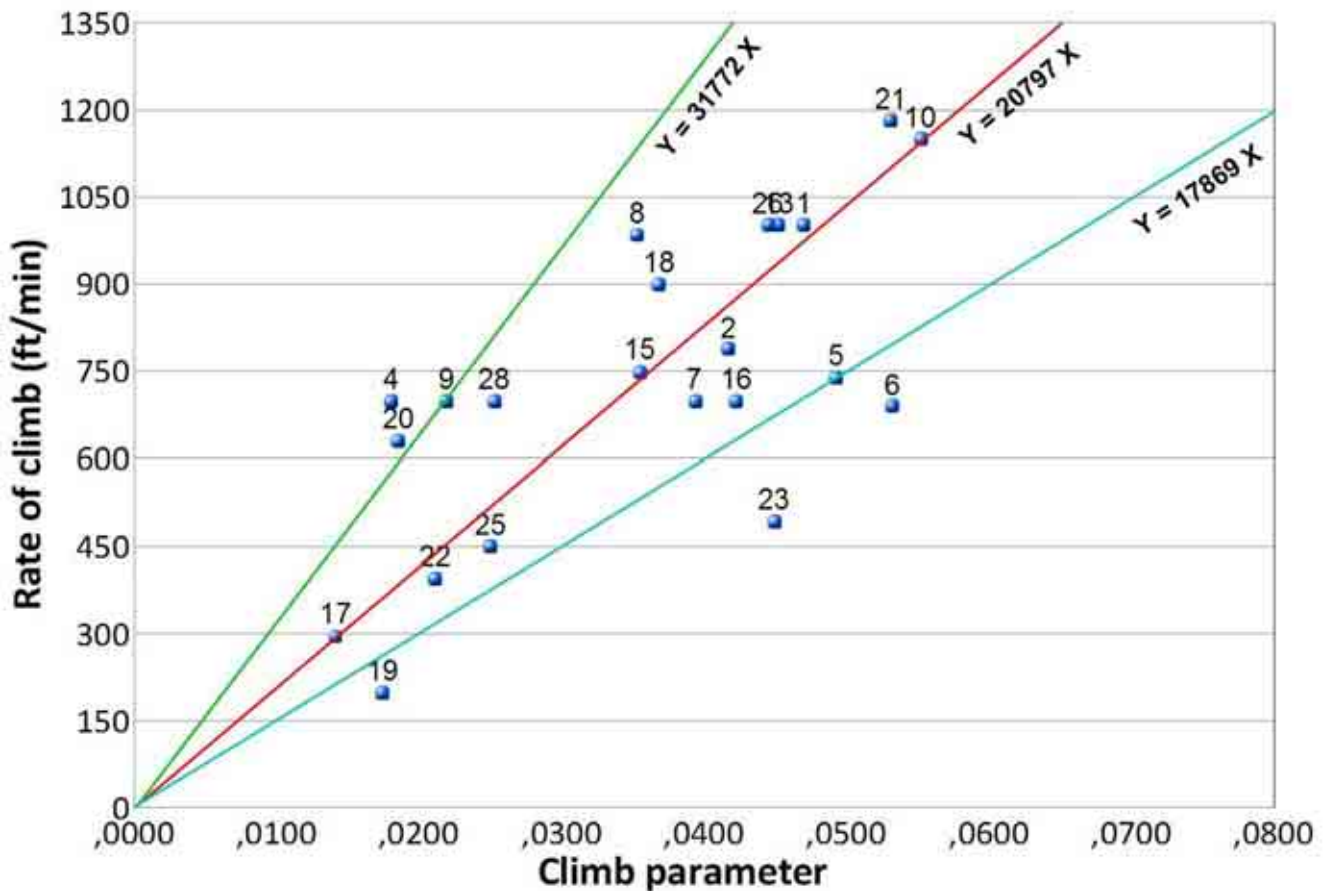
We derive this equation with respect to  $C_L$  and we equate the resulting equation to zero. After simplification we obtain the following formula:

$$\left( \frac{C_L^{3/2}}{C_D} \right)_{\max} = \frac{1.35 \times (A.\epsilon)^{3/4}}{C_{D0}^{1/4}}$$

Now we can plot the graph between  $\dot{h}$  and  $\bar{P}$  to find the linear correlation:

$$\dot{h} = K \times \left[ \frac{\eta.P}{W} - \frac{\sqrt{W/S}}{19 \times (C_L^{3/2}/C_D)} \right]$$

### 5.5.2. Graph



Graph: Variation of climb rate with climb parameter  
(See Table page 84 for aircraft numbers)

### 5.5.3. Conclusions

With this graph we get the following correlation:

$$\dot{h} = 20797 \times \left[ \frac{\eta \cdot P}{W} - \frac{\sqrt{W/S}}{19 \times (C_L^{3/2}/C_D)} \right]$$

If we substitute  $(C_L^{3/2}/C_D)$  by the expression calculated before we get:

$$\dot{h} = 20797 \times \left[ \frac{\eta \cdot P}{W} - \frac{\sqrt{W/S}}{19 \times (1.35 \times (A \cdot \varepsilon)^{3/4} / C_{D0}^{1/4})} \right]$$

As we did for the previous parts we need to incorporate the propulsive efficiency in this equation. We consider in our case than the average propulsive efficiency is 0.85. Then we get:

$$\dot{h} = 20797 \times \left[ \frac{\eta}{0.85} \cdot \frac{P}{W} - \frac{\sqrt{W/S}}{19 \times (1.35 \times (A \cdot \varepsilon)^{3/4} / C_{D0}^{1/4})} \right]$$

## 5.6. MATCHING DIAGRAM

### 5.6.1. Introduction

We have determined the correlations based on existing data for the following parameters:

- Max speed vs. power index
- Stalling speed vs. wing loading parameter
- Take-off run distance vs. take-off parameter
- Rate of climb vs. climb parameter

We are now going to plot all these equations on a single graph W/P vs. W/S.

### 5.6.2. Parametric equations

The first step is to determine the equation  $\frac{W}{P} = f\left(\frac{W}{S}\right)$  for all the parameters.

➔ **Max speed vs. power index**

$$V_{(mph)} = 104.5 \times \sqrt[3]{\frac{\eta}{0.85} \times \frac{W/S}{W/P}} \quad \rightarrow \quad \left(\frac{W}{P}\right) = \left[ \frac{\eta}{0.85} \times \left(\frac{104.5}{V_{(mph)}}\right)^3 \right] \times \left(\frac{W}{S}\right)$$

Input parameters:

- $\eta$
- $V_{\max}$

➔ **Stalling speed vs. wing loading parameter**

$$V_{stall} = 13.9 \times \sqrt{W/S} \rightarrow \left( \frac{W}{S} \right) = \left[ \frac{V_{stall}}{13.9} \right]^2$$

Input parameters: -  $V_{stall}$

➔ **Take-off run distance vs. take-off parameter**

$$l_{T,g} = 3.81 \times \frac{0.85}{\eta} \times \frac{(W/S) \cdot (W/P)}{C_{Lt}} \rightarrow \left( \frac{W}{P} \right) = \left[ \frac{\eta}{0.85} \times \frac{l_{T,g} \times C_{Lt}}{3.81} \right] \times \frac{1}{(W/S)}$$

Input parameters: -  $\eta$   
-  $C_{Lt}$   
-  $L_{T,g}$

➔ **Rate of climb vs. climb parameter**

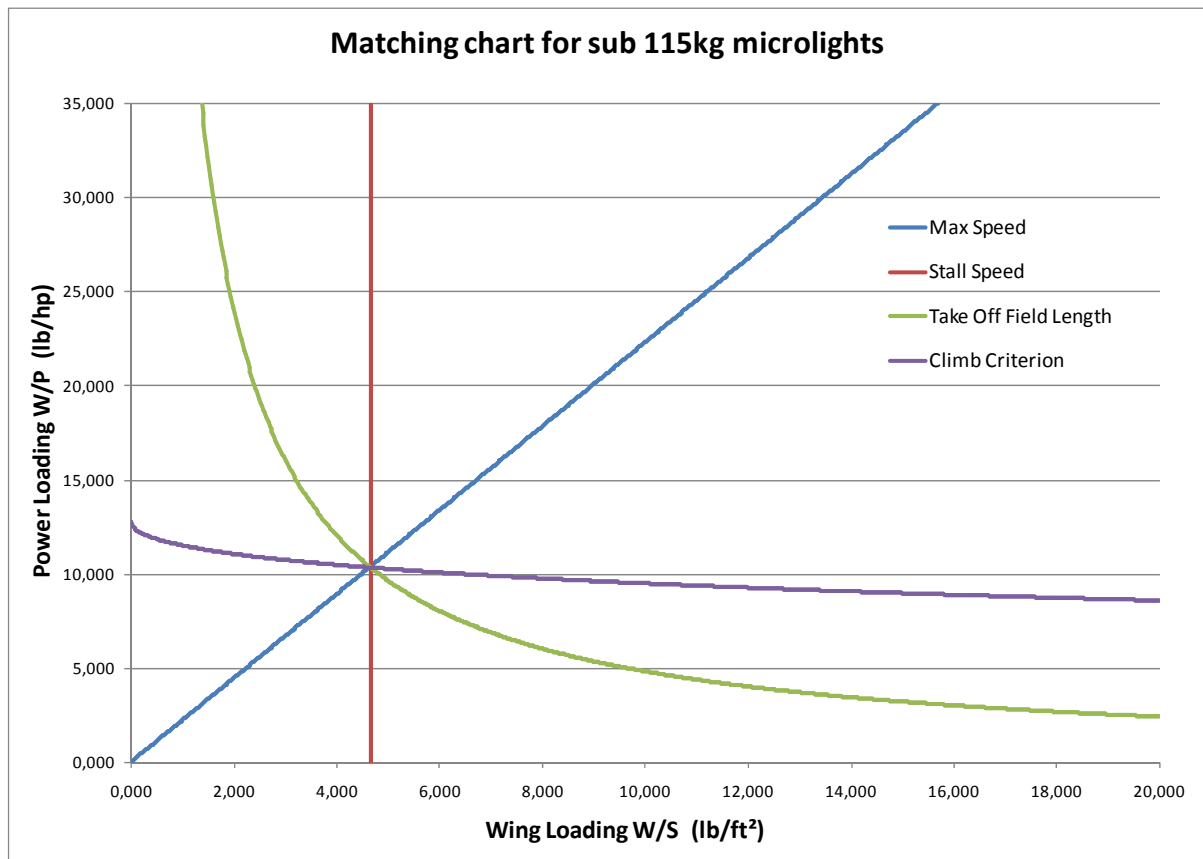
$$\dot{h} = 20797 \times \left[ \frac{\eta}{0.85} \cdot \frac{P}{W} - \frac{\sqrt{W/S}}{19 \times (1.35 \times (A \cdot \epsilon)^{3/4} / C_{D0}^{1/4})} \right]$$

$$\rightarrow \left( \frac{W}{P} \right) = \frac{\frac{\eta}{0.85} \times 20797 \times 19 \times (1.35 \times (A \cdot \epsilon)^{3/4} / C_{D0}^{1/4})}{19 \times \dot{h} \times (1.35 \times (A \cdot \epsilon)^{3/4} / C_{D0}^{1/4}) + 20797 \times \left( \sqrt{\frac{W}{S}} \right)}$$

Input parameters: -  $\eta$   
-  $C_{D0}$   
-  $A$   
-  $\dot{h}$   
-  $\epsilon$

### 5.6.3. Graph

Now that we have the equations, we can calculate the values on a spreadsheet and plot the curves.



Parametric analysis matching chart

This diagram is the key to the parametric analysis: it shows the W/S and W/P values matching for the given input parameters. The parameters have to be adjusted so that all the curves cross in one single point: this point is the configuration in which all the input parameters can be verified. When we have a matching point, we can then deduce a lot of properties of the aircraft. But for this we need to have a weight estimation; that is what we are going to calculate in the following part.

## 5.7. WEIGHT ESTIMATION

### 5.7.1. Equations

First we need to define the weight parameters:

Ws: Structure weight  
Wt: Engine weight  
Wp: Payload weight  
Wf: Fuel weight  
We: Empty weight  
Wg: Gross weight

We have the following equations:

$$W_e = W_s + W_t$$

$$W_g = W_s + W_t + W_p + W_f = W_e + W_p + W_f$$

Now, we can define the useful load fraction which correspond to the payload + the fuel that the aircraft can carry. You can write this parameter:

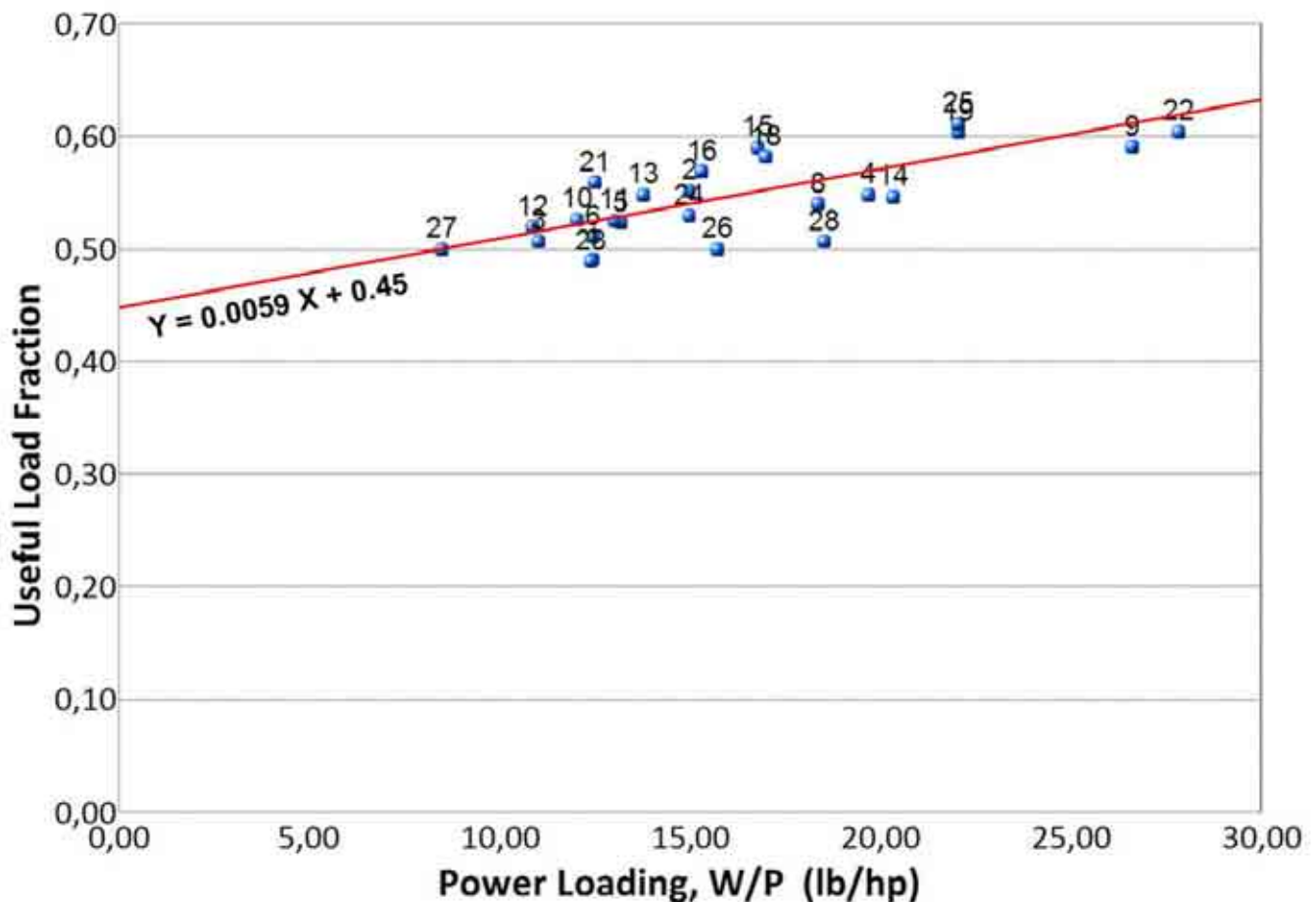
$$\bar{U} = 1 - \frac{W_e}{W_g}$$

The Loftin paper assumes that a linear correlation can be found between the Power loading and the Useful load fraction:

$$\bar{U} = K \cdot \frac{W}{P}$$

We can plot this value on a graph to find the coefficient.

### 5.7.2. Graph



Graph: Variation of Useful load fraction with power loading  
(See Table page 84 for aircraft numbers)

It is interesting to note that the most efficient aircraft in term of payload is the one with the highest power loading. However, this does not take into account the fuel efficiency of the aircraft configuration.

### 5.7.3. Conclusion

With this graph we can have an estimation of the useful load ratio if we know the power loading:

$$\bar{U} = 0.0059 \times \frac{W}{P} + 0.45$$

The power loading is given by the matching chart.

The empty weight is an input parameter.

The payload is also an input parameter.

We can get the gross weight with the relation:  $Wg = We \times (1 - \bar{U})$

The Engine weight can be determined by the following correlation:  $Wt = 1.1 \times P_{(hp)}$

The structure weight is determined by the following equation:  $Ws = We - Wt$

The fuel weight is determined by the following equation:  $Wf = Wg - Wt - Ws - Wp$

➔ We now have an average mass estimation for microlights. With the weight and the matching diagram we can calculate the most important aircraft parameters:

- Engine Power
- Wing area
- Wing Loading
- $Cl_{max}$
- Power index

## 5.8. CROSS CHECKING OF THE RESULTS

This method uses a lot of different parameters and multiple units. The sources of mistakes are numerous and it is important to cross check the results.

### 5.8.1. $C_{Lt}$ equation

We can recalculate the take-off lift coefficient with the output parameters of the analysis and see if we get a coefficient close to the input parameter:

$$C_{Lt} = 390.963 \times \frac{W}{S} \cdot \frac{1}{(1.1 \times V_{stall})^2}$$

### 5.8.2. *Engine power drag equation*

We can use the well known equation of power for a steady flight:

$$\eta.P_{\max} = \frac{1}{2}.C_D.\rho.S.V_{\max}^3$$

We proceed as following: We calculate the engine power with this equation and then we check that the value corresponds to the value calculated with the matching chart. For this equation we use the units from the international system and so it allows us to check that there are no conversion mistakes in the analysis. Our spreadsheet gives an error of 2%.

## 5.9. PARAMETRIC ANALYSIS EXAMPLES

For better understanding, two examples of the use of the parametric analysis are presented on the appendix B of this thesis.

## 5.10.CONCLUSIONS

### 5.10.1. *Validity of the model*

This analysis will provide results for very light aircraft only (less than 150 kg) with average performance.

We can question ourselves about the validity of the model since we have a very large dispersion in the data and it might not produce the most accurate correlations. This dispersion is hard to avoid since this area of microlight aircraft has plenty of different designs. There are huge differences between a design made of steel tubes with a single skin fabric wing and a design made out of aluminium tubes, fitted with composite wings and an optimized airfoil. If we take the example of large airliners, the correlations give much better results, since all the modern airliners have very similar designs. These are the reasons which explain the dispersion we get in the data.



### *5.10.2. Utility of the analysis*

This parametric analysis allows us to have a real estimation of the performance of the microlight aircraft under 115kg for the deregulated regime. The strength of this analysis is that the correlations are based on existing data from sub 115kg aircraft. Therefore, we know that the performance given by this analysis correspond to what we can expect for our design. This is especially important since one can see that in this category of very light aircraft the performance for a given wing loading and power loading, are usually much lower than for standard 4 seater aircraft. This comes from the designs, which are made to be very light, very cheap and simple, to be affordable by a large number of people. The trade off is that these designs are usually not efficient. However, we have seen in our aircraft market study that there are some outstanding designs which are very efficient. The aircraft we want to produce is meant to have very high performance rather than being cheap. Therefore, the parametric analysis will give us lower performance compared to the reality, since it is based on the average performance of the aircraft. This is not a big issue: we have plotted the envelope curves on each graph to have an estimate of what the performance of the extreme designs are. We can use these envelope curves to have an idea of the limits of performance we can reach. In addition, it is more conservative from a safety point of view to have pessimistic predictions than too optimistic.

5.11.TABLE OF RESULTS

This table summarizes the most important results calculated for the parametric analysis.

|                               | N°      | Type of aircraft       | Empty weight (lb) | Gross Weight (lb) | U bar | Engine power (hp) | Wing span (ft) | Wing area S (ft²) | Aspect Ratio | W/T Max (lb / hp) | T/W (hp/lb) | Max W/S (lb/ft²) | Empty W/S (lb/ft²) | Stall speed (mph) | Stall speed (ft/s) | Take Off Speed (mph) | Cruise speed (mph) | Cruise speed (ft/s) | Max Speed (mph) | Max Speed (ft/s) | Climb rate (ft/min) | Take-off run (ft) | Landing run (ft) | Glide Ratio | Metal or wood |
|-------------------------------|---------|------------------------|-------------------|-------------------|-------|-------------------|----------------|-------------------|--------------|-------------------|-------------|------------------|--------------------|-------------------|--------------------|----------------------|--------------------|---------------------|-----------------|------------------|---------------------|-------------------|------------------|-------------|---------------|
| Top wing propulsive propeller | 1       | Kolb firefly           | 254               | 498               | 0.49  | 40.00             | 22.01          | 117.00            | 4.1          | 12.46             | 0.08        | 4.26             | 2.17               | 28                | 41                 | 30                   | 63                 | 93                  | 69              | 101              | 1001                | 151               | 151              | -           | M             |
|                               | 2       | Golden Circle T Bird   | 269               | 600               | 0.55  | 40.00             | 31.17          | 153.92            | 6.3          | 14.99             | 0.07        | 3.90             | 1.75               | 25                | 37                 | 28                   | 61                 | 89                  | 62              | 91               | 787                 | 161               | 151              | 7.0         | M             |
|                               | 3       | Seahawk Condor         | 234               | 474               | 0.51  | 43.00             | 32.15          | 156.07            | 6.6          | 11.02             | 0.09        | 3.04             | 1.50               | 25                | 37                 | 28                   | 35                 | 51                  | 44              | 64               | 525                 | 249               | 299              | -           | M             |
|                               | 4       | Gull 2000              | 249               | 551               | 0.55  | 28.00             | 20.01          | 94.72             | 4.2          | 19.68             | 0.05        | 5.82             | 2.63               | 26                | 39                 | 29                   | 63                 | 93                  | 63              | 93               | 699                 | 125               | 75               | 12.0        | M             |
|                               | 5       | Rans S-17 Stinger      | 251               | 527               | 0.52  | 40.00             | 29.49          | 127.01            | 6.8          | 13.17             | 0.08        | 4.15             | 1.98               | 29                | 42                 | 32                   | 55                 | 81                  | 62              | 91               | 738                 | 102               | 177              | -           | M             |
|                               | 6       | Interplane Griffon 103 | 254               | 518               | 0.51  | 41.60             | 29.53          | 150.26            | 5.8          | 12.45             | 0.08        | 3.45             | 1.69               | 29                | 42                 | 32                   | 56                 | 83                  | 63              | 93               | 689                 | 164               | 115              | -           | M             |
|                               | 7       | Aerolite               | 251               | 450               | 0.44  | 28.00             | 26.84          | 123.78            | 5.8          | 16.06             | 0.06        | 3.63             | 2.03               | 26                | 39                 | 29                   | 45                 | 66                  | 70              | 103              | 699                 | 102               | 102              | 9.0         | M             |
|                               | 8       | Sirocco                | 254               | 551               | 0.54  | 30.00             | 33.20          | 148.54            | 7.4          | 18.37             | 0.05        | 3.71             | 1.71               | 24                | 35                 | 27                   | 49                 | 73                  | 71              | 105              | 984                 | 115               | 131              | 10.0        | M             |
|                               | 9       | Shadow                 | 348               | 851               | 0.59  | 32.00             | 32.81          | 161.45            | 6.7          | 26.59             | 0.04        | 5.27             | 2.16               | 39                | 57                 | 43                   | 86                 | 127                 | 113             | 165              | 699                 | 262               | -                | -           | M             |
|                               | 10      | Carrera 150            | 260               | 549               | 0.53  | 45.60             | 27.66          | 134.01            | 5.7          | 12.04             | 0.08        | 4.10             | 1.94               | 26                | 39                 | 29                   | 60                 | 88                  | 75              | 110              | 1148                | 151               | 151              | -           | M             |
|                               | 11      | Quicksilver            | 247               | 520               | 0.53  | 40.00             | 27.95          | 155.21            | 5.0          | 13.01             | 0.08        | 3.35             | 1.59               | 24                | 35                 | 27                   | 53                 | 78                  | 53              | 78               | 420                 | 98                | 98               | 4.5         | M             |
|                               | 12      | Drifter Rocket         | 240               | 500               | 0.52  | 46.00             | 29.99          | 151.98            | 5.9          | 10.88             | 0.09        | 3.29             | 1.58               | 26                | 39                 | 29                   | 55                 | 81                  | 70              | 103              | 801                 | 197               | -                | -           | M             |
| Top wing pushing propeller    | AVERAGE |                        | 259.23            | 549.14            | 0.53  | 37.85             | 28.57          | 139.50            | 5.88         | 14.51             | 0.07        | 4.00             | 1.86               | 27.43             | 40.23              | 30.17                | 56.87              | 83.41               | 67.99           | 99.72            | 765.79              | 156.38            | 145.01           | X           | X             |
|                               | 13      | Weedhopper             | 249               | 551               | 0.55  | 40.00             | 27.89          | 167.91            | 4.63         | 13.78             | 0.07        | 3.28             | 1.48               | 20                | 30                 | 22                   | 55                 | 81                  | 64              | 95               | 1001                | 102               | 102              | -           | M             |
|                               | 14      | Flying K sky raider    | 249               | 549               | 0.55  | 27.00             | 26.21          | 110.00            | 6.25         | 20.33             | 0.05        | 4.99             | 2.26               | 23                | 34                 | 25                   | 64                 | 95                  | 81              | 118              | 1050                | 75                | 75               | -           | M             |
|                               | 15      | Aerolites Bearcat      | 287               | 699               | 0.59  | 41.60             | 29.99          | 150.05            | 5.99         | 16.80             | 0.06        | 4.66             | 1.91               | 28                | 41                 | 30                   | 68                 | 100                 | 75              | 110              | 748                 | 151               | 151              | -           | W             |
|                               | 16      | Spyder                 | 278               | 644               | 0.57  | 42.00             | 29.92          | 143.26            | 6.25         | 15.33             | 0.07        | 4.49             | 1.94               | 37                | 54                 | 41                   | 64                 | 95                  | 85              | 125              | 699                 | 200               | 299              | 8.0         | M             |
| 3 axis low wing               | AVERAGE |                        | 265.66            | 610.68            | 0.56  | 37.65             | 28.50          | 142.81            | 5.78         | 16.22             | 0.06        | 4.36             | 1.86               | 26.90             | 39.45              | 29.59                | 63.01              | 92.41               | 76.24           | 111.82           | 874.33              | 132.05            | 156.66           | X           | X             |
|                               | 17      | MB02 Souricette        | 209               | 441               | 0.53  | 12.00             | 29.53          | 107.64            | 8.10         | 36.74             | 0.03        | 4.10             | 1.95               | 28                | 41                 | 30                   | 62                 | 91                  | 75              | 110              | 295                 | 200               | -                | 14.0        | W             |
|                               | 18      | Avenger                | 249               | 595               | 0.58  | 35.00             | 26.90          | 121.20            | 5.97         | 17.01             | 0.06        | 4.91             | 2.06               | 29                | 42                 | 32                   | 60                 | 88                  | 94              | 138              | 899                 | 98                | 200              | -           | W             |
|                               | AVERAGE |                        | 229.28            | 518.09            | 0.56  | 23.50             | 28.21          | 114.42            | 7.04         | 22.05             | 0.05        | 4.50             | 2.00               | 28.19             | 41.35              | 31.01                | 60.99              | 89.46               | 84.58           | 124.06           | 597.11              | 149.28            | 200.13           | X           | X             |
|                               | 19      | Whing Ding II          | 122               | 309               | 0.60  | 14.00             | 18.67          | 106.02            | 3.29         | 22.05             | 0.05        | 2.91             | 1.15               | 26                | 39                 | 29                   | 40                 | 59                  | 49              | 73               | 197                 | 249               | 131              | -           | M             |
| Less than 55 kg               | 20      | E-12n                  | 106               | 353               | 0.70  | 14.20             | 21.33          | 57.91             | 7.85         | 24.84             | 0.04        | 6.09             | 1.83               | 37                | 54                 | 41                   | 49                 | 73                  | 62              | 91               | 630                 | 197               | -                | 7.0         | M             |
|                               | AVERAGE |                        | 114.09            | 330.70            | 0.66  | 14.10             | 20.00          | 81.97             | 5.57         | 23.45             | 0.04        | 4.50             | 1.39               | 31.65             | 46.42              | 34.81                | 44.88              | 65.83               | 55.81           | 81.86            | 413.38              | 223.09            | 131.23           | X           | X             |
| Non conventional designs      | 21      | MC-12 Cricket          | 165               | 375               | 0.56  | 30.00             | 16.08          | 33.37             | 7.75         | 12.49             | 0.08        | 11.23            | 4.96               | 48                | 71                 | 53                   | 112                | 164                 | 155             | 228              | 1181                | 394               | -                | 13.0        | M             |
|                               | 22      | Lazair                 | 209               | 529               | 0.60  | 19.00             | 36.42          | 147.46            | 8.99         | 27.85             | 0.04        | 3.59             | 1.42               | 25                | 37                 | 28                   | 40                 | 59                  | 61              | 89               | 394                 | 164               | 164              | 12.0        | M             |
|                               | 23      | Pou du ciel            | 254               | 496               | 0.49  | 40.00             | 19.68          | 139.93            | 2.77         | 12.40             | 0.08        | 3.54             | 1.81               | 35                | 51                 | 38                   | 69                 | 101                 | 75              | 110              | 492                 | 200               | -                | 9.0         | W             |
|                               | 24      | Pouchel                | 176               | 375               | 0.53  | 25.00             | 17.85          | 122.71            | 2.60         | 14.99             | 0.07        | 3.05             | 1.44               | 30                | 44                 | 33                   | 62                 | 91                  | 62              | 91               | -                   | -                 | -                | -           | M             |
|                               | 25      | Onyx CP 150            | 154               | 397               | 0.61  | 18.00             | 23.95          | 97.95             | 5.86         | 22.05             | 0.05        | 4.05             | 1.58               | 25                | 37                 | 28                   | 60                 | 88                  | 70              | 103              | 449                 | 151               | 102              | -           | W             |
|                               | 26      | PUL 9                  | 331               | 661               | 0.50  | 42.00             | 29.53          | 124.86            | 6.98         | 15.75             | 0.06        | 5.30             | 2.65               | 35                | 51                 | 38                   | 106                | 155                 | 139             | 204              | 1001                | 492               | -                | -           | M             |
|                               | 27      | Zipper                 | 220               | 441               | 0.50  | 52.00             | 27.99          | 143.05            | 5.47         | 8.48              | 0.12        | 3.08             | 1.54               | 18                | 27                 | 20                   | 35                 | 51                  | 45              | 66               | 528                 | 98                | 79               | -           | M             |
|                               | 28      | Hiperlight             | 247               | 500               | 0.51  | 27.00             | 22.01          | 140.04            | 3.46         | 18.54             | 0.05        | 3.57             | 1.76               | 39                | 57                 | 43                   | 60                 | 88                  | 63              | 93               | 699                 | 174               | 174              | 12.0        | W             |

| Power Index (IP) | Cd0   | Ip^3  | ((W/S)/σ) <sup>0.5</sup> | CL T  | Climax | (W/S)*(W/P) / (1*CLT) | CL^{1.5}/CD max | P bar  |
|------------------|-------|-------|--------------------------|-------|--------|-----------------------|-----------------|--------|
| 0.70             | 0.116 | 0.342 | 2.06                     | 1.804 | 2.183  | 29.41                 | 5.12            | 0.0470 |
| 0.64             | 0.121 | 0.260 | 1.97                     | 1.964 | 2.376  | 29.74                 | 6.95            | 0.0418 |
| 0.65             | 0.367 | 0.276 | 1.74                     | 1.531 | 1.852  | 21.87                 | 5.46            | 0.0603 |
| 0.67             | 0.130 | 0.296 | 2.41                     | 2.684 | 3.247  | 42.68                 | 5.06            | 0.0181 |
| 0.68             | 0.146 | 0.315 | 2.04                     | 1.619 | 1.960  | 33.74                 | 7.05            | 0.0493 |
| 0.65             | 0.122 | 0.277 | 1.86                     | 1.346 | 1.629  | 31.90                 | 6.52            | 0.0533 |
| 0.61             | 0.073 | 0.226 | 1.91                     | 1.676 | 2.028  | 34.83                 | 7.42            | 0.0394 |
| 0.59             | 0.062 | 0.202 | 1.93                     | 2.053 | 2.484  | 33.21                 | 9.28            | 0.0353 |
| 0.58             | 0.015 | 0.198 | 2.30                     | 1.112 | 1.346  | 126.00                | 12.12           | 0.0220 |
| 0.70             | 0.091 | 0.340 | 2.02                     | 1.889 | 2.286  | 26.10                 | 6.93            | 0.0552 |
| 0.64             | 0.194 | 0.258 | 1.83                     | 1.855 | 2.244  | 23.51                 | 5.22            | 0.0469 |
| 0.67             | 0.097 | 0.303 | 1.81                     | 1.519 | 1.838  | 23.59                 | 6.99            | 0.0645 |
| 0.65             | 0.10  | 0.28  | 2.00                     | 1.72  | 2.08   | 33.78                 | 6.95            | 0.0434 |
| 0.62             | 0.099 | 0.238 | 1.81                     | 2.615 | 3.164  | 17.30                 | 5.79            | 0.0452 |
| 0.63             | 0.052 | 0.245 | 2.23                     | 3.044 | 3.683  | 33.33                 | 8.50            | 0.0280 |
| 0.65             | 0.074 | 0.277 | 2.16                     | 1.973 | 2.387  | 39.66                 | 7.56            | 0.0356 |
| 0.66             | 0.053 | 0.293 | 2.12                     | 1.071 | 1.295  | 64.33                 | 8.48            | 0.0423 |
| 0.65             | 0.07  | 0.27  | 2.09                     | 1.95  | 2.35   | 36.32                 | 7.53            | 0.0378 |
| 0.48             | 0.030 | 0.111 | 2.02                     | 1.735 | 2.100  | 86.75                 | 11.91           | 0.0142 |
| 0.66             | 0.038 | 0.289 | 2.22                     | 1.917 | 2.320  | 43.57                 | 8.89            | 0.0369 |
| 0.59             | 0.04  | 0.20  | 2.12                     | 1.83  | 2.22   | 54.24                 | 10.10           | 0.0275 |
| 0.51             | 0.121 | 0.132 | 1.71                     | 1.343 | 1.625  | 47.80                 | 4.26            | 0.0175 |
| 0.63             | 0.114 | 0.245 | 2.47                     | 1.451 | 1.756  | 104.26                | 8.31            | 0.0186 |
| 0.58             | 0.12  | 0.19  | 2.12                     | 1.45  | 1.76   | 72.70                 | 6.30            | 0.0185 |
| 0.97             | 0.027 | 0.899 | 3.35                     | 1.554 | 1.880  | 90.33                 | 11.82           | 0.0531 |
| 0.51             | 0.063 | 0.129 | 1.89                     | 1.809 | 2.189  | 55.24                 | 10.66           | 0.0212 |
| 0.66             | 0.076 | 0.286 | 1.88                     | 0.961 | 1.163  | 45.75                 | 4.21            | 0.0450 |
| 0.59             | 0.095 | 0.204 | 1.75                     | 1.102 | 1.334  | 41.54                 | 3.80            | 0.0325 |
| 0.57             | 0.059 | 0.184 | 2.01                     | 2.042 | 2.471  | 43.74                 | 7.86            | 0.0251 |
| 0.70             | 0.014 | 0.336 | 2.30                     | 1.436 | 1.738  | 58.09                 | 12.88           | 0.0446 |
| 0.71             | 0.448 | 0.364 | 1.76                     | 2.938 | 3.554  | 8.90                  | 4.50            | 0.0797 |
| 0.58             | 0.085 | 0.193 | 1.89                     | 0.754 | 0.913  | 87.82                 | 4.84            | 0.0253 |

Interpolated values

Aircrafts matching the deregulated regime

Parametric analysis results table

## 6. AIRCRAFT GENERAL LAYOUT

### 6.1. PARAMETRIC ANALYSIS

#### 6.1.1. Input data

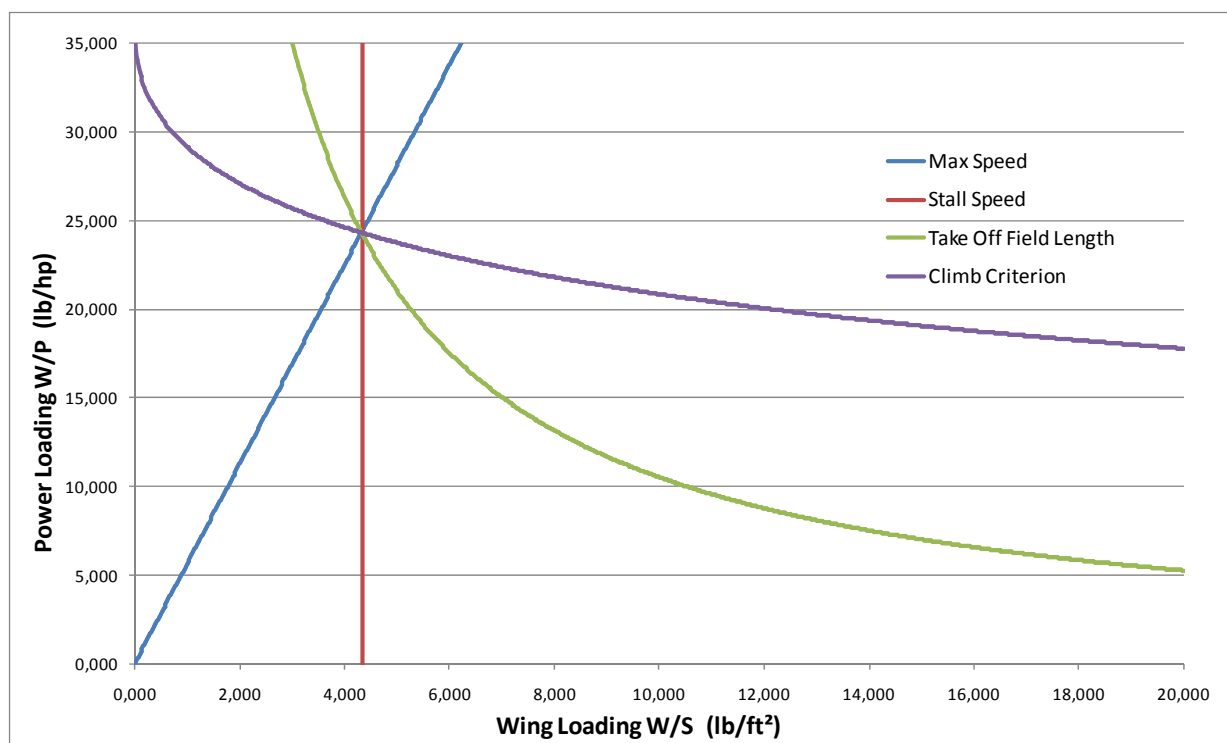
The table below shows the input data for the microlight parametric analysis. These data are based on the aircrafts we studied previously. The designs we studied had on average very low performance, and we can expect our aircraft to be much more efficient than what is predicted by the parametric analysis. However, this analysis gives us a starting point with coherent data. You can find the details concerning the parametric analysis in appendix B.

|                  |   |       |       |         |
|------------------|---|-------|-------|---------|
| Input parameters | V max (mph)                               | 61    | 53    | (kt)    |
|                  | V stall (mph)                             | 29    | 25    | (kt)    |
|                  | TO run (ft)                               | 215   | 66    | (m)     |
|                  | C LT                                      | 1.67  | 1.67  |         |
|                  | Climb Rate (ft/min)                       | 650   | 198   | (m/min) |
|                  | Aspect Ratio                              | 5.00  | 5.00  |         |
|                  | Propulsive efficiency ( $\eta_p = 0.85$ ) | 0.95  | 0.95  |         |
|                  | Aircraft efficiency ( $\eta_a = 0.7$ )    | 0.90  | 0.90  |         |
|                  | CD0                                       | 0.097 | 0.097 |         |
|                  | MAX Fuel consumption (L/h)                | 14.00 | 3.70  | gal/h   |

HLM-Colab-Cranfield parametric analysis input data

We can note that the aircraft efficiency and the propulsive efficiency have been set up higher than the average, to be closer to the real performance of the HLM-Colab-Cranfield microlight.

#### 6.1.2. Matching diagram



HLM-Colab-Cranfield Matching diagram

### 6.1.3. Parametric analysis results

| Output Results | MATCHING DIAGRAM                        |                   |                    |
|----------------|---|-------------------|--------------------|
|                | W/P                                     | kg/hp             | lb/hp              |
|                |   | 11.02             | 24.30              |
|                | W/S                                     | kg/m <sup>2</sup> | lb/ft <sup>2</sup> |
|                |   | 21.24             | 4.35               |
|                |   |                   |                    |
|                | IP                                      | 0.56              |                    |
|                | Useful Load Fraction                    | 0.59              |                    |
|                | Engine Power (hp)                       | 26                |                    |
|                | Range at max speed (km)                 | 363               |                    |
|                | Wing Area (m <sup>2</sup> )             | 13.32             |                    |
|                | Empty Wing Loading (kg/m <sup>2</sup> ) | 8.64              |                    |
|                | Clmax                                   | 2.02              |                    |

| MASS BREAK DOWN |                      |                        |         |
|-----------------|----------------------|------------------------|---------|
|                 |                      | kg                     | lb      |
| WE              | WG                   | Structure Weight       | 87 191  |
|                 |                      | Engine Weight          | 28 62   |
|                 |                      | Payload Weight (Input) | 100 220 |
|                 |                      | Fuel Weight            | 68 150  |
|                 | Empty Weight (Input) | 115 254                |         |
| Gross Weight    |                      | 283 623                |         |

HLM-Colab-Cranfield parametric analysis results

These tables give a prediction of the aircraft performance. However, we need to mention that the empty weight and the payload are the only input parameters. The gross weight is determined thanks to the correlation established with the other aircraft. In our case we consider:

- Empty weight: 115 kg
- Fuel weight: 25 kg
- Payload: 100kg
- ➔ Gross weight: 240 kg

With this mass breakdown and the W/P and W/S ratios we can recalculate the wing gross area and the engine power:

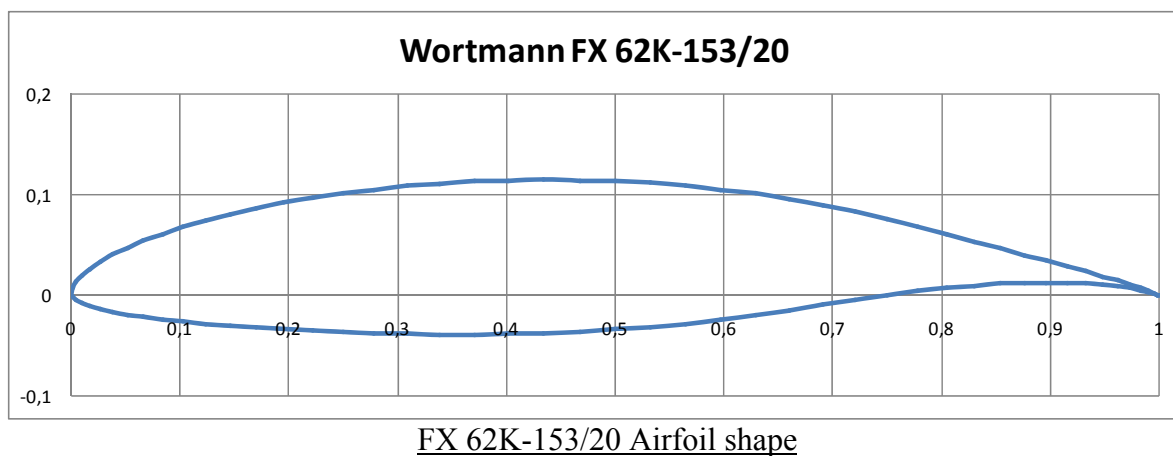
- Wing gross area: 11.29 m<sup>2</sup>
- Engine power: 21.78 hp

## 6.2. WING LAYOUT

### 6.2.1. Wing airfoil and gross area

#### ➔ Airfoil selection

The Colab team has performed a lot of tests and they have determined that the concept works for a large range of airfoils. However, some airfoils are better than others; for our aircraft we will use a Wortmann airfoil, the FX 62K 153/20. The airfoil shape is represented on the figure below. The airfoil thickness is 15.27%. The maximum thickness position is located at 40.30% of the chord. This airfoil is designed to be fitted with flaps (or ailerons). The airfoil is optimised for flaps hinges located at 80% of the chord.



#### ➔ Wing area

The parametric analysis gave us a gross area of 11.29 m<sup>2</sup>. In our design we will use the Colab optimised geometry with a span of 7.6m and a chord of 0.76m. With this geometry we get an area of:

$$S = (7.6 \times 0.76) \times 2 = 11.52 \text{ m}^2$$

This wing area gives us an empty wing loading of 9.98 kg/m<sup>2</sup>, considering an empty weight of 115kg. This meets the requirements of the maximum 10kg/m<sup>2</sup> and gives a wing loading high enough to have good performance.

We can check the lift properties and calculate the stall speed to see if we get a reasonable value:

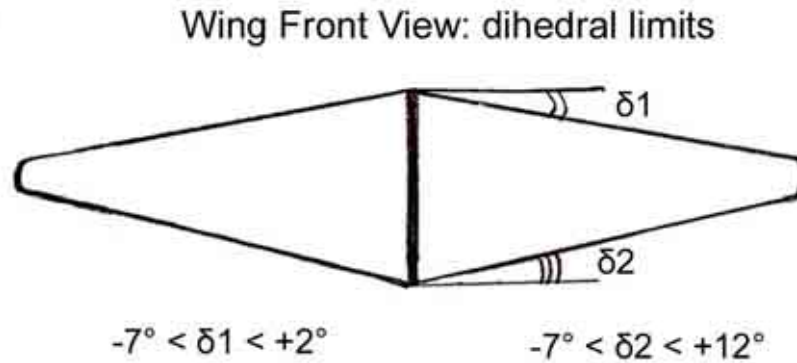
$$V = \sqrt{\frac{W}{\frac{1}{2} \times \rho \times S \times C_{L_{\max}}}} = \sqrt{\frac{240 \times 9.81}{\frac{1}{2} \times 1.2 \times 11.52 \times 1.3}} = 16.18 \text{ m/s} = 31 \text{ kt}$$

We use a value of 1.3 for the  $C_{L_{\max}}$  which corresponds to a conservative value, and, in addition, we do not consider at all the effect of the flaps.

### 6.2.2. Colab wing parameters

The Colab wings have been tested and an optimal geometry has been determined. The parameters are now well known and it is important to follow them exactly.

#### → Wing dihedral



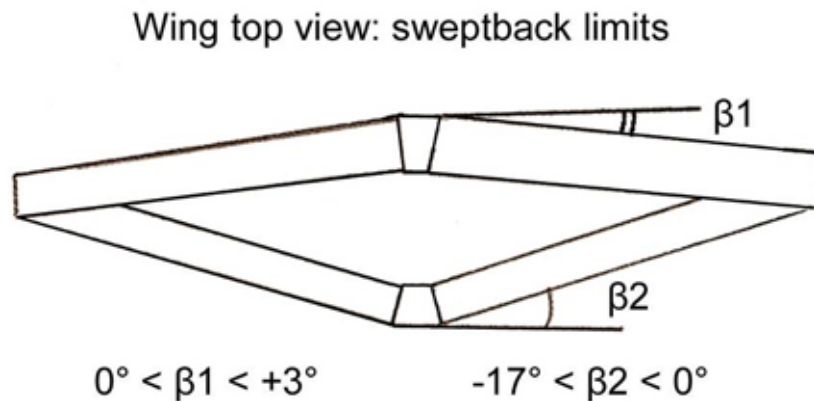
#### Colab wing dihedral limits

The picture above illustrates the range for the dihedral of the wing. In our design the wing has the following parameters:

- $\delta_1 = 0^\circ$
- $\delta_2 = 14^\circ$

The dihedral for the low wing is higher than the max value. However, this value is still acceptable if we take a dihedral equal to 0 on the top wing. This is due to the fact that we need enough room for the pilot.

#### → Wing sweepback



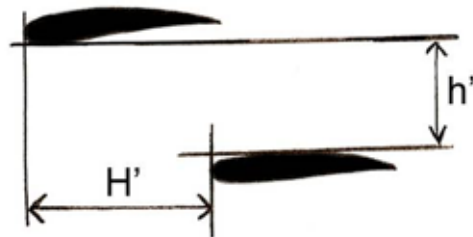
#### Colab wing sweepback limits

As we did for the dihedral, we need to choose the sweepback according to the picture above. In our design the wing has the following parameters:

- $\beta_1 = 0^\circ$
- $\beta_2 = -15^\circ$

➔ **Wing tip geometry**

Wing tip: geometrical limits



$$h' > 0.3 \times \text{chord} \quad H' \neq 0.2 \times \text{chord}$$

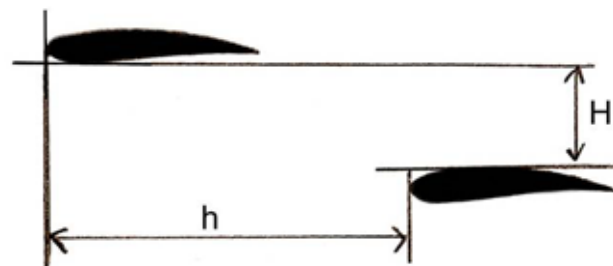
Colab wing tip geometrical limits

To match these parameters, we have chosen the following figures for our wing:

- $H' = 0.16\text{m}$
- $h' = 0.3\text{m}$

➔ **Wing root geometry**

Wing root: geometrical limits



$$H < 3 \times \text{chord} \quad h < 3 \times \text{chord}$$

Colab wing root geometrical limits

The values illustrated on the figure above are already determined with the previous data. We just have to check that we are within the margins. After the calculations we get:

- $H = 1.30\text{m}$
- $h = 1.23\text{m}$

➔ **Wing angle of incidence**

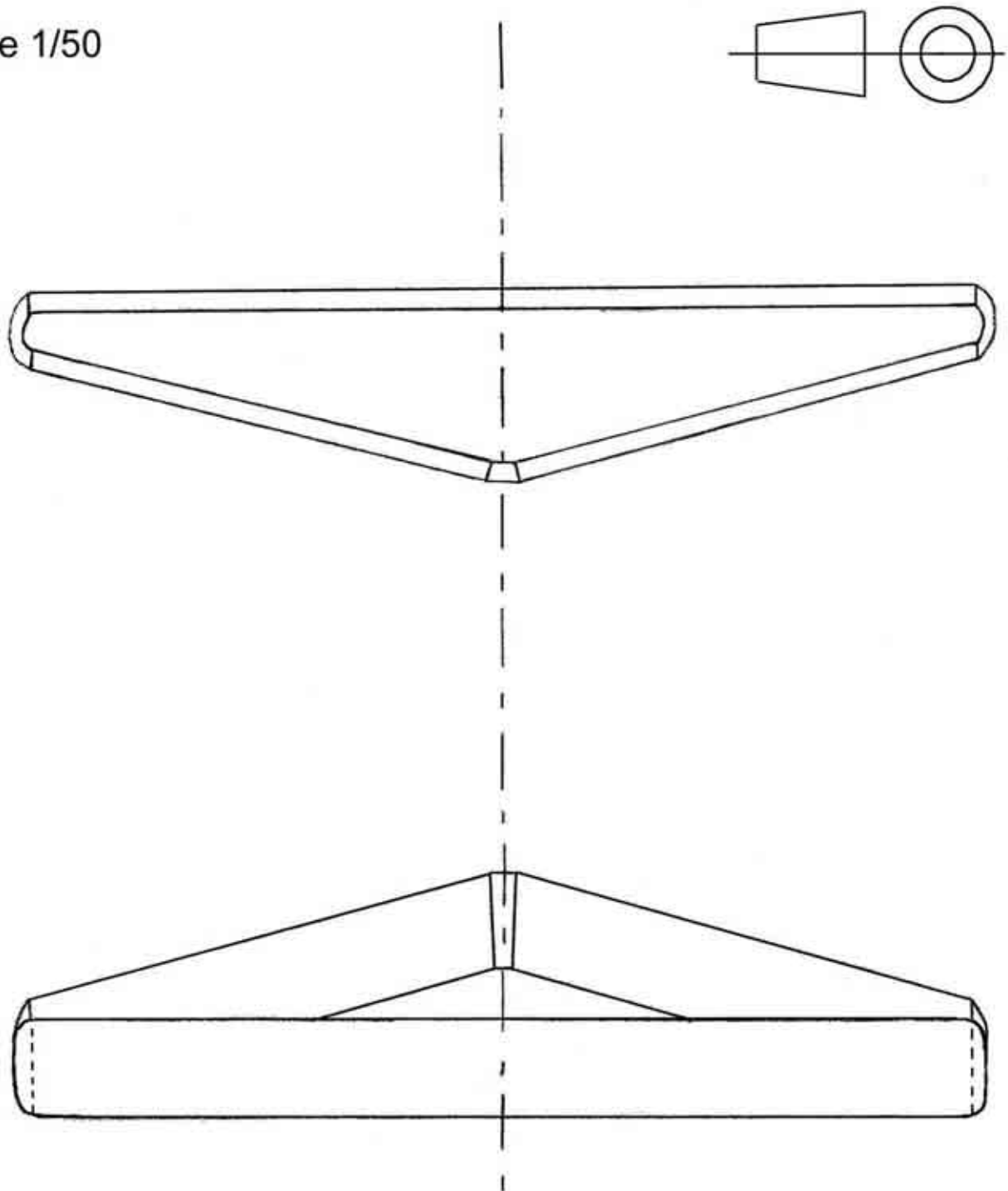
- Both wings have an incidence of  $2^\circ$ .

➔ The geometry of the wing is now completely determined. The wing is plotted on the next page.

### 6.2.3. *Wing layout*

Wing layout

Scale 1/50





## 6.3. CONTROL SURFACES AND TAIL

### 6.3.1. Ailerons

#### ➔ Existing designs

I have studied the aileron areas of different microlight aircraft and determined the percentage of the wing area that they represent. The results are summarized in the table below:

| AILERONS         |             |             |             |
|------------------|-------------|-------------|-------------|
|                  | S           | S ailerons  | %           |
| Kolb firefly     | 10.87       | 2.00        | 0.18        |
| Spyder           | 13.31       | 2.30        | 0.17        |
| Rans S18         | 14.10       | 2.44        | 0.17        |
| Rans S17         | 11.80       | 2.08        | 0.18        |
| Griffon 103      | 13.98       | 2.74        | 0.20        |
| AVERAGE          |             |             | 0.18        |
| <b>HLM Colab</b> | <b>12.8</b> | <b>1.28</b> | <b>0.10</b> |

Microlights ailerons surfaces data

#### ➔ Colab ailerons

The Colab has ailerons on only 10% of the total wing area. This seems very low compared to the other microlights. However, the Colab ailerons have a high efficiency (cf. explanations given before). Several models have been tested with this configuration and this is the parameter which has been selected. The ailerons have the following properties:

- Located on the low wing trailing edge
- Full span
- 20% of the chord (Airfoil optimised for 20%)
- +/- 15° deflection

### 6.3.2. Tail design

For the tail, I have worked with the lecture note “Initial sizing of longitudinal and lateral stabilisers”, by HOWARD SMITH [Ref. 11]. I have studied the data on different aircraft. The aim was to calculate the coefficients  $V_F$  and  $V_T$  explained below:

$$V_T = \frac{S_T \cdot l'_T}{S \cdot c} \quad V_F = \frac{S_F \cdot l'_F}{S \cdot b}$$

- S: Wing gross area
- $S_T$ : Tailplane area
- $S_F$ : Fin area
- c: Wing mean chord
- b: Wing span
- $l'_T$ :  $\frac{1}{4}$  of wing chord to  $\frac{1}{4}$  of tailplane chord length
- $l'_F$ :  $\frac{1}{4}$  of wing chord to  $\frac{1}{4}$  of fin chord length

The data for the aircraft studied are presented in the table on the next page:

| FIN AND TAILPLANE |              |             |             |             |             |             |             |             |             |             |             |             |             |              |               |
|-------------------|--------------|-------------|-------------|-------------|-------------|-------------|-------------|-------------|-------------|-------------|-------------|-------------|-------------|--------------|---------------|
|                   |              |             |             | St          |             |             |             |             |             |             |             | Sf          |             |              |               |
|                   | S            | b           | c           | Tailplane   | Elevator    | Total       | %           | L't         | Fin         | Rudder      | Total       | %           | L'f         | VT           | VF            |
| Kolb firefly      | 10.87        | 6.71        | 1.62        | 0.90        | 1.21        | 2.11        | 0.57        | 3.36        | 0.50        | 0.64        | 1.14        | 0.56        | 3.36        | 0.403        | 0.0525        |
| Spyder            | 13.31        | 9.12        | 1.46        | 0.92        | 1.30        | 2.22        | 0.59        | 2.76        | 0.58        | 0.64        | 1.22        | 0.52        | 2.76        | 0.315        | 0.0277        |
| Rans S18          | 14.10        | 9.42        | 1.50        | 1.25        | 0.86        | 2.11        | 0.41        | 3.13        | 0.71        | 0.68        | 1.39        | 0.49        | 3.13        | 0.313        | 0.0328        |
| Rans S17          | 11.80        | 8.99        | 1.31        | 1.25        | 0.86        | 2.11        | 0.41        | 2.86        | 0.75        | 0.58        | 1.33        | 0.44        | 2.86        | 0.390        | 0.0359        |
| Griffon 103       | 13.98        | 9.00        | 1.55        | 1.46        | 1.18        | 2.64        | 0.45        | 2.90        | 0.66        | 0.83        | 1.49        | 0.56        | 2.90        | 0.353        | 0.0343        |
| AVERAGE           |              |             |             |             |             |             | 0.48        |             |             |             |             | 0.51        |             | 0.355        | 0.0366        |
|                   |              |             |             |             |             |             |             |             |             |             |             |             |             |              |               |
| <b>HLM Colab</b>  | <b>12.80</b> | <b>8.00</b> | <b>1.60</b> | <b>1.20</b> | <b>1.30</b> | <b>2.50</b> | <b>0.52</b> | <b>2.90</b> | <b>0.70</b> | <b>0.55</b> | <b>1.25</b> | <b>0.44</b> | <b>2.90</b> | <b>0.354</b> | <b>0.0354</b> |

#### Microlights tail surfaces data

For the tailplane, the data are chosen to match exactly the  $V_T$  coefficient average, but with a slightly larger elevator area percentage to be sure that the aircraft has enough pitch control since it is more stable than a conventional design. For the rudder the  $V_F$  coefficient is slightly lower than the average since the aircraft is very manoeuvrable in yaw. The calculations for the tail areas are detailed below:

$$\begin{aligned}
 \text{tailplane} : \frac{2.5+0.3}{2} \times 0.7 + 0.1 \times 2.5 &= 1.23m^2 & \text{elevator} : \left[ \frac{1.2+1.0}{2} \times 0.5 + \frac{1.0 \times 0.2}{2} \right] \times 2 &= 1.3m^2 \\
 \text{fin} : \frac{0.4+0.8}{2} \times 1.15 &= 0.69m^2 & \text{rudder} : \frac{1.15+0.95}{2} \times 0.45 + \frac{0.95 \times 0.2}{2} &= 0.57m^2
 \end{aligned}$$

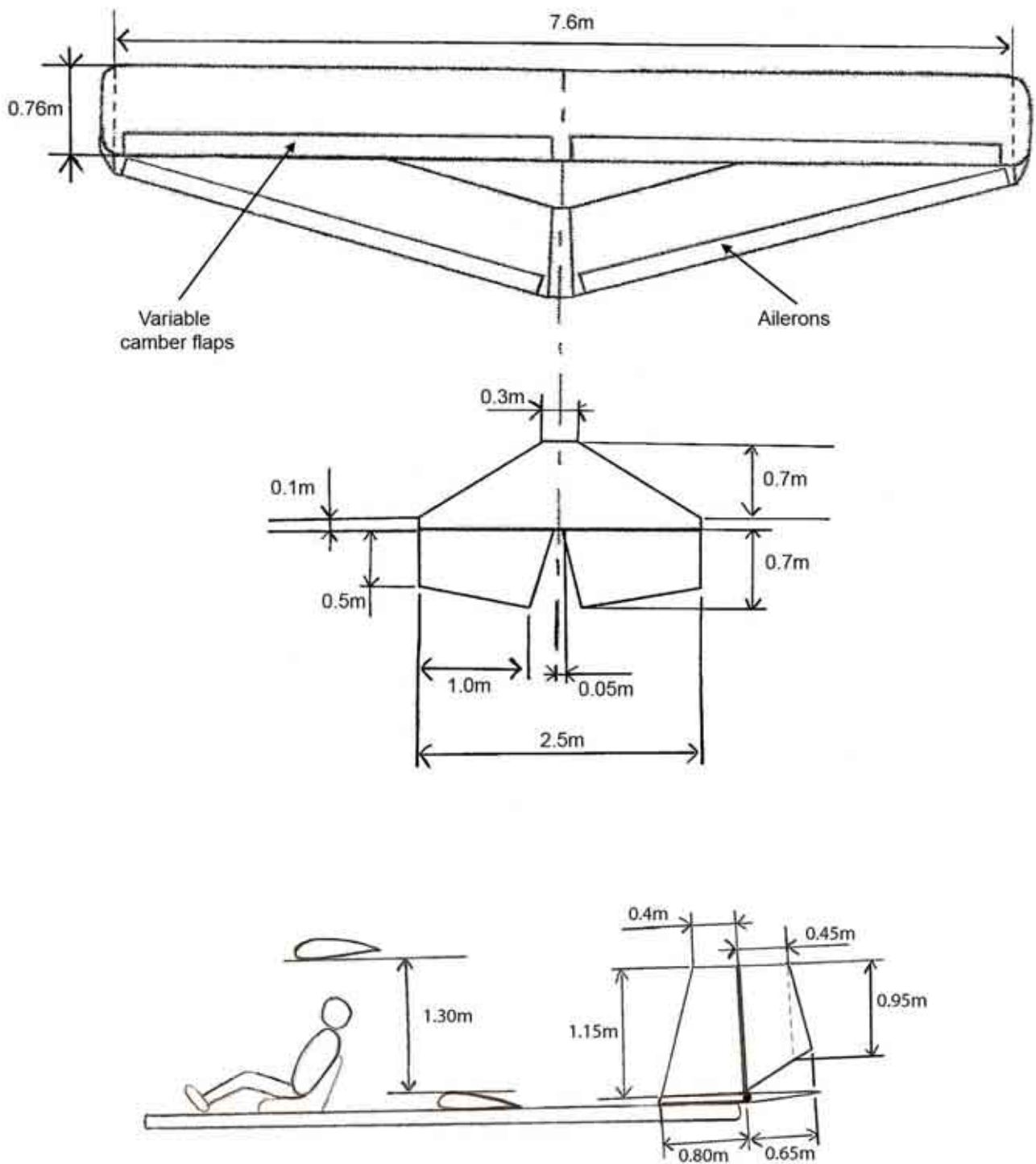
#### 6.3.3. Variable camber flaps

The Colab design requires variable camber flaps to be the most efficient. The optimal geometry of the flaps has been determined with models and we cannot predict them with current empirical methods since their effect is completely linked with the two wings aerodynamic interferences. Therefore, we will rely on the experimental data provided by the Colab team and use the following properties:

- Located on the top wing trailing edge
- Full span
- 20% of the chord (Airfoil optimised for 20%)
- +45° / -10° deflection

#### 6.3.4. Drawings

The control surfaces are plotted on the page below with the main dimensions. The wing dimensions are not all reported on the drawing. They can be found in the “wing layout” paragraph.



☑ Note: The fuselage layout is NOT the final layout. These drawings only illustrate the dimensions of the rudder and the elevator.

## 6.4. ENGINE SELECTION

The aircraft is meant to be flown in competition. Therefore, it is important to remember that we want performance. We want to have an engine that is as powerful as possible within the weight limits so that our aircraft is less than 115 kg.

### 6.4.1. *Engine selection list*

I have selected the following suitable engines for the aircraft:



|               |                     |
|---------------|---------------------|
| Name:         | Mini 3              |
| Manufacturer: | Simonini Flying     |
| Power:        | 31 hp               |
| Total Weight: | 20 kg               |
| Displacement  | 240 cm <sup>3</sup> |
| Type:         | 2 strokes           |

Mini 3 engine



|               |                           |
|---------------|---------------------------|
| Name:         | Black Devil Engine (M25Y) |
| Manufacturer: | Aerocorsair               |
| Power:        | 24.5 hp                   |
| Total Weight: | 14 kg                     |
| Displacement  | 172.5 cm <sup>3</sup>     |
| Type:         | 2 strokes                 |

Corsair M25Y engine

### 6.4.2. *Engine choice*

The Corsair engine has the best power to weight ratio on the microlight engine market. However, we can wonder if it is not worth trying a more powerful engine to increase the take-off and climbing performance of our microlight. The 30 hp engine is a very small market. The Simonini Mini 3 is the best compromise on this market. It provides 31 hp with only 20 kg. This is the engine we chose for our aircraft.

**➔ We chose the Simonini Mini 3 engine**

### 6.4.3. *Propeller choice*

Because of their very light weight and their high aerodynamic performance, the carbon propellers are now the most efficient propellers for the microlights.

Detailed calculations need to be done on the propeller to optimise the properties, but the following parameters give an idea of the propeller required for the aircraft:



|                  |                                    |
|------------------|------------------------------------|
| Material:        | Carbon fibre                       |
| Type:            | 2 blades, adjustable on the ground |
| Diameter:        | 150 cm                             |
| Angle of attack: | 8° (equivalent 13.25 inches pitch) |
| Weight:          | 2.5 kg                             |

Carbon propeller

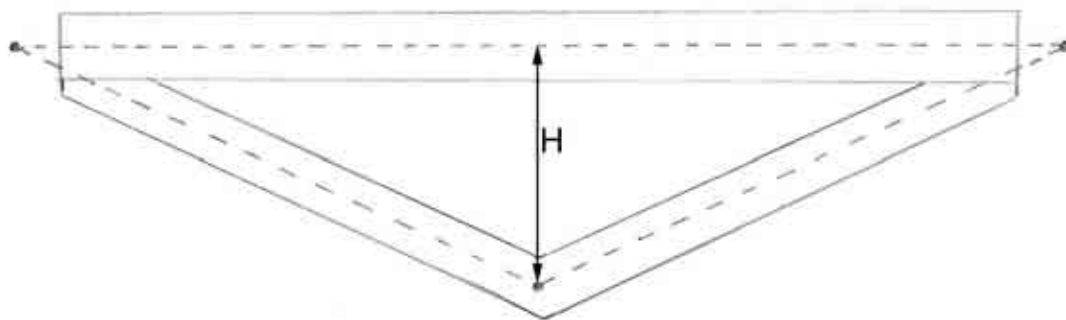
**➔ A carbon propeller with ground adjustable pitch is the most efficient solution for our aircraft fitted with the mini 3 engine.**

## 7. MASS BALANCE AND STABILITY

### 7.1. LONGITUDINAL STATIC STABILITY

#### 7.1.1. *Main wing aerodynamic centre position*

The Colab has a very specific geometry and therefore we can not deduce the position of the aerodynamic centre easily. However, the numerous models built allowed us to determine experimentally what the stability margins will be. The picture below illustrates the wing shape of our aircraft:



Colab wing shape and CG position

With experience it has been established that the wing aerodynamic centre is located at the barycentre of the wing area. As we can see on the picture above, we can draw a triangle if we join the mid chords of the wings. The barycentre of the wing area is very close of the barycentre of the triangle, which is located at one third of the chord.

This property is very interesting since it gives a “virtual chord” of a length  $H$  which is very large (in our case 1.23m). With this large “virtual chord” we get a large CG range, but in the same time, the real wing chord is only 0.76m!

- ➔ **The Colab wing gives a very large CG range even with small chord!**
- ➔ **The aerodynamic centre is located at 1/3 of the “virtual chord”.**

The aerodynamic centre is located at one third of the virtual chord which is 1.23m. Therefore, the aerodynamic centre is located at 0.41m of the front wing leading edge.

- ➔ **Wing aerodynamic centre position: 0.41m of the front leading edge.**

We will consider that the fuselage does not have a big impact on the aerodynamic centre. Therefore, the aircraft aerodynamic centre is equal to the wing aerodynamic centre.

- ➔ **Aircraft aerodynamic centre position: 0.41m of the front leading edge.**

### 7.1.2. Main wing lift curve slope and pitching moment

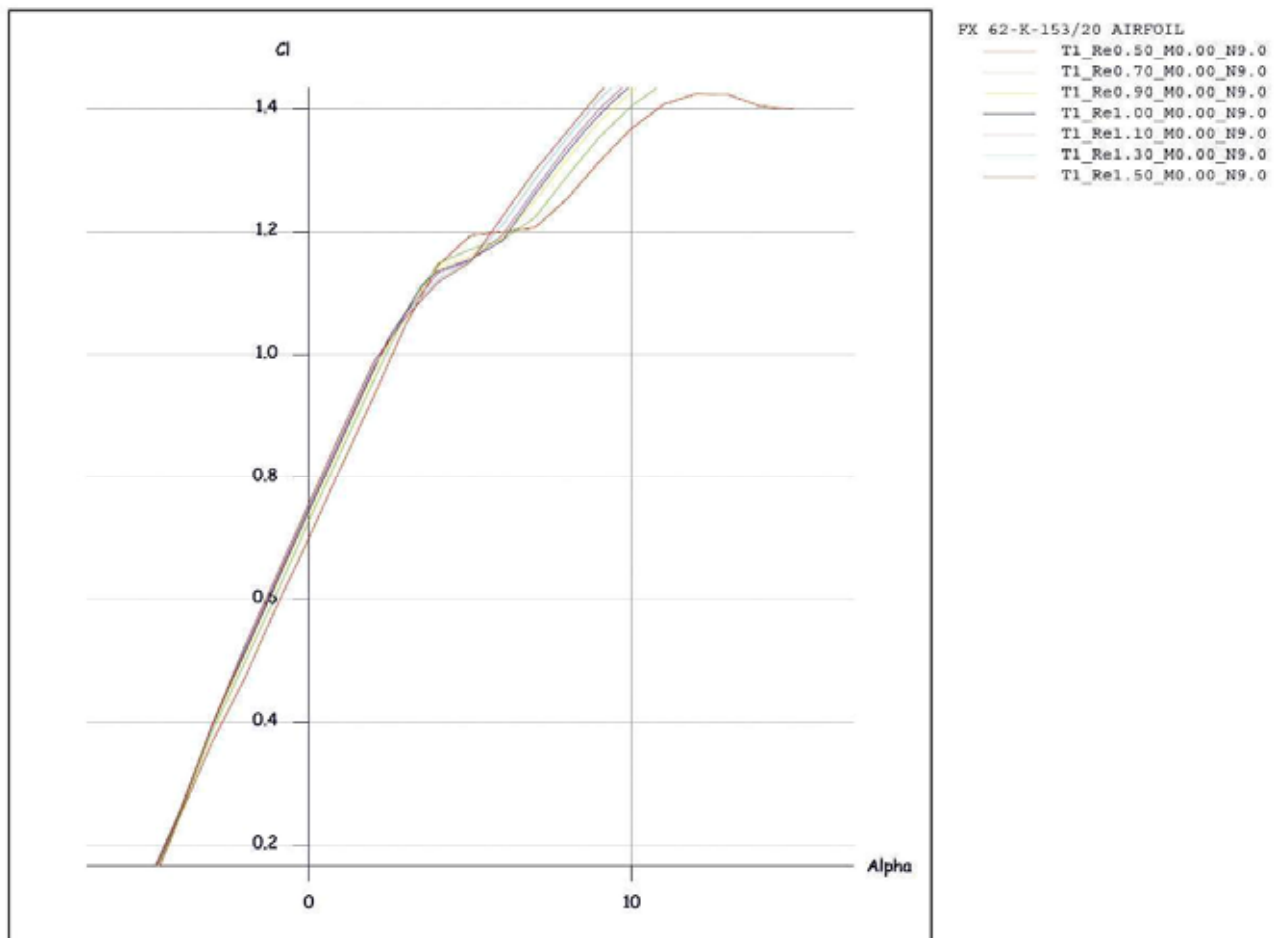
#### ➔ Main wing lift

The main wing lift curve slope should be determined with wind tunnel testings. However, after a discussion with the Colab team, it has been decided to consider that the lift curve slope is close to the curve slope of the FX-62K153-20. In fact, the wing section is constant—there is no twist and the angles of incidence of the top and the low wing are the same. This is why the assumption can be made. The first step consists of calculating the typical Reynolds number for our aircraft:

$$Re = \frac{c.V}{\nu} = \frac{0.76 \times 30}{15.6 \times 10^{-6}} \approx 1,400,000$$

- V is the typical cruise speed (taken equal to 30m/s)
- C is the wing chord
- N is the air kinematic viscosity at 20°C

The aerodynamic properties of the airfoil have been determined using numerical aerodynamics software under GNU licence called XFLR5. The airfoil has been tested for Reynolds number between 500,000 and 1,500,000. The program gives us the results below:



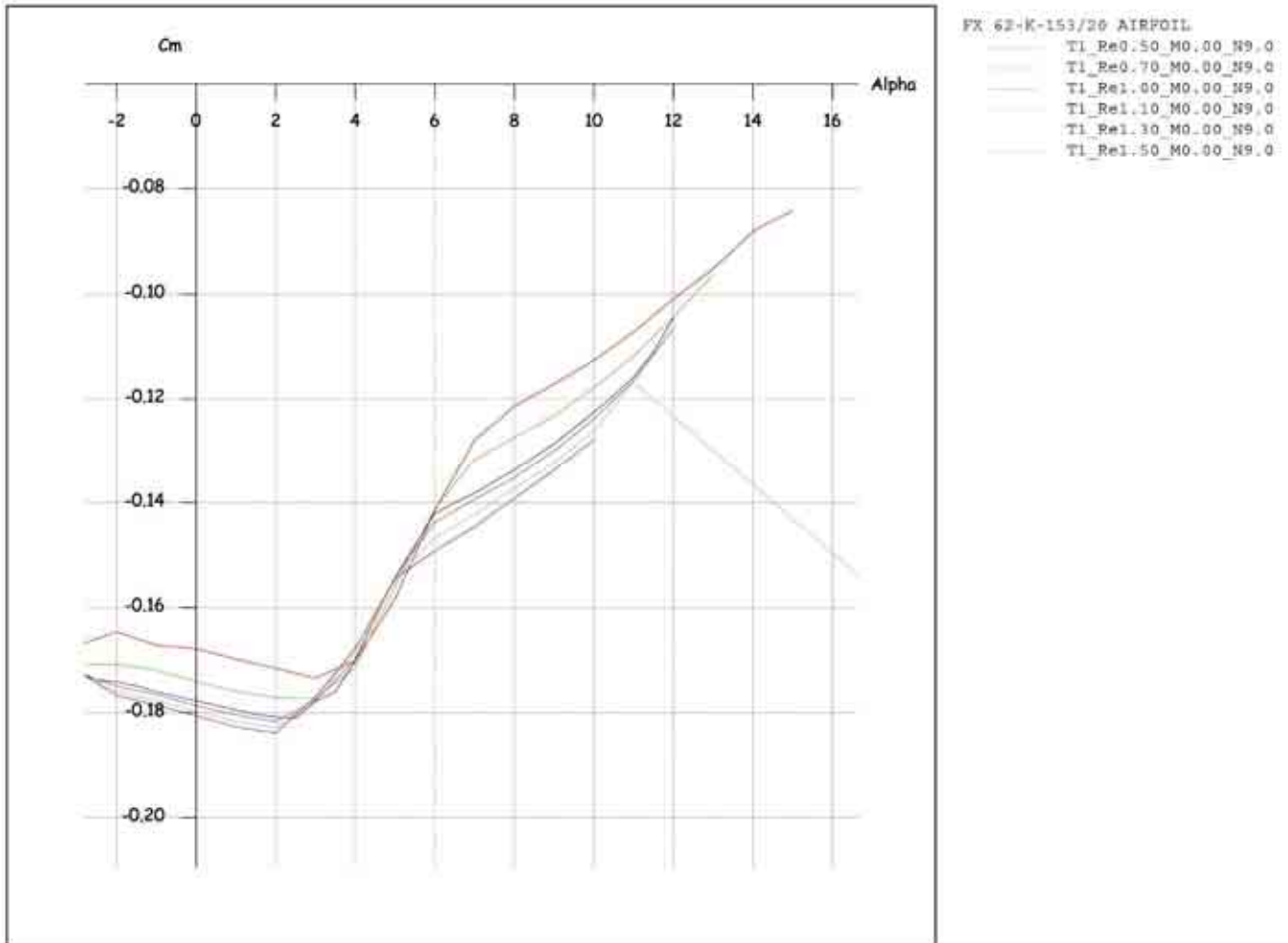
Airfoil lift coefficient polar

We can see that the lift coefficient does not depend on the Reynolds number.

### → Main wing pitching moment

As we did for the lift coefficient, we will consider that we can determine the pitching moment coefficient based on the data of the FX62K153-20. This assumption will give results which are not accurate in theory. On the other hand, the Colab wing has been tested with a lot of models, and this assumption gives workable results.

As we did for the lift coefficient, we will use XFLR5, and the airfoil has been tested for Reynolds number between 500,000 and 1,500,000. We get the results illustrated on the diagram below:



Airfoil pitching moment coefficient polar

The pitching moment coefficient does not depend on the Reynolds number either. As for the lift coefficient, we can consider it as constant.

### → Main wing properties

$$C_{L0} = 0.73 \quad a = \frac{\partial C_L}{\partial \alpha} = 6.8 \text{ rad}^{-1}$$

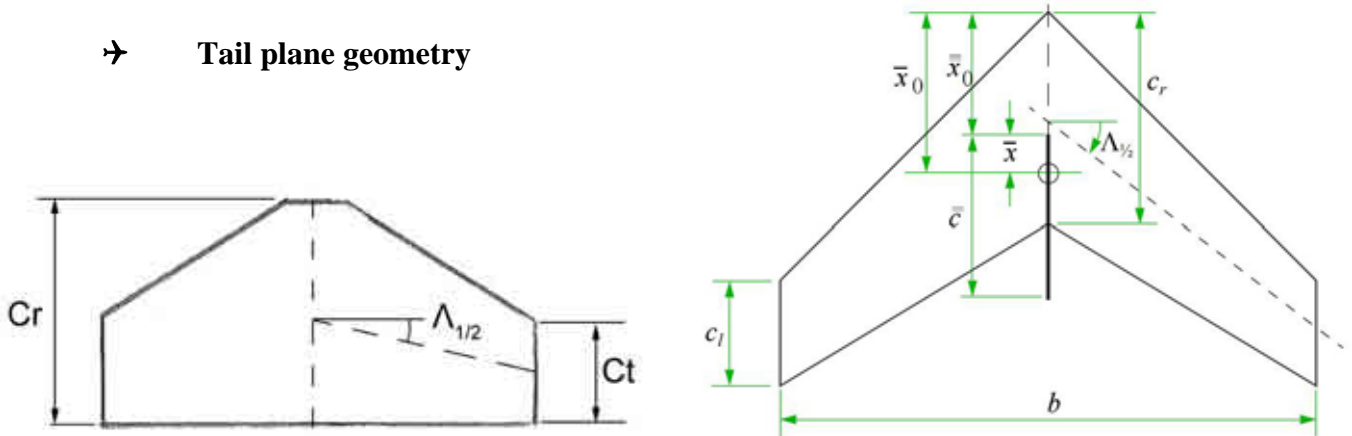
$$C_{M0} = -0.18 \quad \frac{\partial C_M}{\partial \alpha} = 1.67 \text{ rad}^{-1}$$



### 7.1.3. Lift curve slope of the tailplane

We will use the ESDU datasheet 70011: “Lift-curve slope and aerodynamic centre position of wings in inviscid subsonic flow” [Ref. 18]. This allows us to determine the lift curve slope of the tailplane without the elevator deflection. This datasheet is given with a Fortran software. To save time, we will use the software to do our calculations.

#### → Tail plane geometry



Tail geometry: Real tail model (left), ESDU notations (right)

In our case we have the following values:

- Aspect ratio:  $A=2.47$
- Taper ratio:  $\lambda=0.46$
- $\Lambda_{1/2}$ :  $15.6^\circ$
- Cr:  $1.3\text{m}$
- Ct:  $6\text{m}$
- b:  $2.5\text{m}$

The aerodynamic mean chord can be calculated with the following expression given in the datasheet:

$$\bar{c} = \frac{2}{3} \times \frac{1 + \lambda + \lambda^2}{1 + \lambda} \times Cr = 0.99\text{m}$$

Then we can calculate the distance of the leading edge of aerodynamic mean chord aft of wing apex with the following formula given in the datasheet:

$$\bar{x}_0 = \frac{(1 + 2\lambda)(1 + \lambda)}{1 + \lambda + \lambda^2} \times \left[ A \cdot \tan(\Lambda_{1/2}) + 2 \frac{1 - \lambda}{1 + \lambda} \right] \times \bar{c} = 0.30\text{m}$$

#### → Aerodynamic low properties

We take a Reynolds number of 1,400,000.

The speed of sound at sea level is 340.3m/s

This gives us a Mach number of 0.088.

The compressibility parameter  $\beta = \sqrt{1 - M^2} = 0.996 \approx 1.0$

## ➔ Software calculations results

The software gives us the following result for the tail plane lift slope:

$$a_1 = \frac{\partial C_L}{\partial \alpha_1} = 2.85 \text{ rad}^{-1}$$

In addition, as we use a symmetrical airfoil for the tail plane, we know that:

$$C_{L0} = 0$$

### 7.1.4. Lift curve slope of the tailplane with elevator deflection

For this part we will use the ESDU datasheet 74011: “Rate of change of lift coefficient with control deflection for full span plain controls” [Ref. 17]. This allows us to determine the effect of the elevator on the lift of the tailplane. The notations and the method followed are as described in the ESDU 74011 datasheet.

## ➔ Elevator geometry

- Mean tail plane chord:  $c = 0.95\text{m}$
- Mean elevator chord:  $c_f = 0.5\text{m}$

## ➔ Calculations

The ESDU datasheet gives us the following formula:

$$\frac{\partial C_L}{\partial \delta} = \left[ \frac{\partial C_L}{\partial \delta} / \frac{\partial C_L}{\partial \alpha_1} \right]_{TH} \times \frac{\partial C_L}{\partial \alpha_1} \times [1 - k_1 k_2] \cdot$$

With the figure 1 of the datasheet we get:

$$\left[ \frac{\partial C_L}{\partial \delta} / \frac{\partial C_L}{\partial \alpha_1} \right]_{TH} = 0.90$$

With the figures 2 and 3 of the datasheet we get:

$$k_1 = 0.05 \text{ and } k_2 = 0.45$$

This gives us the following result:

$$\frac{\partial C_L}{\partial \delta} = 2.50 \text{ rad}^{-1}$$

### 7.1.5. Average downwash at the tailplane

The downwash at the tail induced by the Colab wing is difficult to predict because of the complex aerodynamics of the Colab wing. However, we need this parameter to have an estimation of the aircraft longitudinal stability. To estimate the downwash we will use the ESDU datasheet 80020 “Average downwash at the tailplane at low angles of attack and subsonic speeds” [Ref.19]. To be able to use this datasheet we will make the following assumptions:

- The Colab wing is modeled by a rectangular wing of 7.6m span and 1.52m chord
- We consider that the height of the tail is equal to the height of the wing ( $Z_T=0$ ).

#### → Wing parameters

- Wing semi span:  $s = 3.8\text{m}$
- Tailplane semi span:  $s_T = 1.25\text{m}$
- Wing lift curve slope:  $a = 6.8 \text{ /rad}$
- Root chord:  $C_r = 1.52\text{m}$
- Tip Chord:  $C_t = 1.52\text{m}$
- Gross area:  $S = 11.55\text{m}^2$
- Aspect ratio:  $A = 5$
- $\Lambda_{1/2}$ :  $0^\circ$
- $x_T$ :  $2.9\text{m}$

#### → Calculations

At low angles of attack the downwash is given by the following expression:

$$\bar{\varepsilon} = \varepsilon_0 + \left( \frac{d\bar{\varepsilon}}{d\alpha} \right) (\alpha - \alpha_0) \quad \boxed{\varepsilon_0 = -0.2^\circ} \text{ (Figure 10)}$$

If we consider the tailplane and the wing at the same height we have:

$$\left( \frac{d\bar{\varepsilon}}{d\alpha} \right) = \left( \frac{d\bar{\varepsilon}}{d\alpha} \right)_0 = B \times \left( \frac{d\bar{\varepsilon}}{d\alpha} \right)_0^* \quad B=1.2, \text{ can be determined with figure 8.}$$

$$\left( \frac{d\bar{\varepsilon}}{d\alpha} \right)_0^* = \frac{2.a}{\pi A} (H_p + \Delta H_p) F = 0.78$$

$$F = \left( \frac{d\bar{\varepsilon}/d\alpha}{d\varepsilon/d\alpha} \right)_0^* = 1.01 \quad \text{Figure 4.d}$$

$$H_p = H_{p_e} - (1 - H_{p_\infty}) = 0.92 \quad \text{Figures 1, 2, 3, } \Delta H_p = -0.02$$

Finally we get:

$$\boxed{\left( \frac{d\bar{\varepsilon}}{d\alpha} \right) = 0.93}$$

### 7.1.6. Stick fixed stability

#### ➔ Stability equation

The theory of flight gives us the following equation:

$$K_n = (h_0 - h) + \bar{V} \frac{a_1}{a} \left( 1 - \frac{d\bar{\varepsilon}}{d\alpha} \right)$$

#### ➔ Aircraft parameters

- Tailplane lift curve slope:  $a_1 = 2.85 / \text{rad}$
- Wing lift curve slope:  $a = 6.8 / \text{rad}$
- Aircraft aerodynamic centre:  $h_0 = 0.33\%$
- Virtual wing chord (Cf. 3.2.1):  $c = 1.23\text{m}$

$$\bar{V} = \frac{S_r}{S} \cdot \frac{L_r}{c} = \frac{2.52}{11.55} \cdot \frac{2.9}{1.23} = 0.51$$

$$\left( \frac{d\bar{\varepsilon}}{d\alpha} \right) = 0.93$$

$$K_n = (0.33 - h) + 0.51 \times \frac{2.85}{6.8} \times (1 - 0.93) = 0.33 - h + 0.015$$

#### ➔ Stick fixed neutral point

The stick fixed neutral point is when  $K_n = 0$ . In our case the stick fixed neutral point is at: 0.34% of the virtual chord = 0.42m. In addition, there is an offset since the virtual chord starts at mid-chord of the front wing, which is at 0.38m from the leading edge.

$$h = 0.34\% \rightarrow 0.80\text{m after the top wing leading edge}$$

### 7.1.7. Maximum CG range

From the previous paragraph we can deduce the maximum CG range:

The most forward CG position is:

- $h = 0.16\%$
- $K_n = 0.215$
- 0.58m from the leading edge

The most rearward CG position is:

- $h = 0.26\%$
- $K_n = 0.085$
- 0.70m from the leading edge

➔ 8.5% stability margin

➔ 0.12m CG range

## 7.2. MASS BREAKDOWN

The biggest part of the wing is made with carbon fibre-epoxy laminates. The ribs are made with Herex foam. The density of the carbon fibre-epoxy laminates is around  $1600\text{kg/m}^3$  but never more. The density of the Herex is  $80\text{kg/m}^3$ . The wing tips are made out of S45000 Steel with a density of  $7800\text{kg/m}^3$ . The tailplane and elevator are made with honeycomb structure. The core is made with high strength aramid honeycomb with a density of  $48\text{kg/m}^3$ . The skin is made with the same laminates as the wing. The fuselage and tail beam and all the primary structure is made out of 2014 T6 aluminium alloy with a density of  $2700\text{kg/m}^3$ . The masses have been calculated using the geometry calculated in the detailed design chapter (later in this thesis) and using Patran. The results are presented in this chapter since they have an impact on the aircraft stability and manoeuvrability.

These data give us the following mass breakdown:

| Wing             |      | Engine            |      |
|------------------|------|-------------------|------|
| Wing skin        | 11.9 | Engine            | 21   |
| Wing spars       | 3.4  | Propeller         | 2.5  |
| Mass booms       | 7.8  | SUBTOTAL (kg)     | 23.5 |
| Ribs             | 11   | Tailplane and fin |      |
| Tips brackets    | 5.5  | Tailplane         | 7.2  |
| Ailerons & flaps | 4.2  | Fin               | 3.9  |
| SUBTOTAL (kg)    | 43.8 | Hinges + brackets | 2.1  |
| Fuselage         |      | SUBTOTAL (kg)     | 13.2 |
| Main Frame       | 10.2 | Equipment         |      |
| Engine mount     | 1.1  | Seat              | 0.7  |
| Tail beam        | 5.6  | Instruments       | 1.5  |
| Undercarriage    | 5    | Controls          | 5    |
| Aero fairings    | 4    | SUBTOTAL (kg)     | 7.2  |
| SUBTOTAL (kg)    | 25.9 |                   |      |
|                  |      | TOTAL (kg)        |      |
|                  |      | 113.6             |      |

Mass breakdown table

All of the masses have been rounded up to take into account the mass of the fasteners which are not negligible. There is a margin of 1.5 kg which is very little. However, it is possible to reduce the weight if necessary with the following points:

- Using the alternative Corsair engine, which would save 6 kg but also reduce the power from 31 to 24.5 hp and so reduce the aircraft performance.
- It is also possible to put cables to maintain the main structural elements, and so it is possible to reduce the thickness of the fuselage beams. However, cables would have a negative impact on the aerodynamic performance.
- The tailplane and fin have been designed to make the aircraft controllable and stable. However, depending on the 1/3<sup>rd</sup> scale model results it might be possible to reduce the tail surfaces area, which would reduce the weight AND the loads on the structure, making it possible to save extra weight.

### 7.3. CG CALCULATION

The airframe CG has been calculated with Patran. Patran also provides the inertia axis of the aircraft. To calculate the global CG of the aircraft we then add the pilot's mass and the engine's mass to the airframe mass. The repartition is plotted below:



#### Aircraft main CGs positions

The CG positions are given as distances from the leading edge of the top wing, in the longitudinal direction of the aircraft. With this data we can calculate the CG position for a pilot mass of 70 kg.

$$X_G = \frac{1545 \times 86.9 + 300 \times 23.5 - 450 \times 70}{70 + 23.5 + 86.9} = 684 \text{ mm}$$

The CG range is between 580mm and 700mm behind the leading edge. The pilots lighter than 60kg would have to add extra mass in the front of the aircraft.

## 8. LOADING ACTIONS AND AIRWORTHINESS

### 8.1. N-V DIAGRAM

#### 8.1.1. Design air speeds

The design air speeds are determined according to chapter S335 of section S of the CAP 482 [Ref.15].

##### → Stall speed at 1G, VS1:

The first important velocity we need to know to design our flaps is the stall speed. This velocity is a key point in the n-V diagram. The method obtained to calculate this velocity is described below. The stall starts when the maximum lift is equal to the weight. The stall velocity depends on the mass and on the flaps configurations. In our case we will consider the case in which the flaps are not deflected.

$$V_{S1} = \sqrt{\frac{W}{\frac{1}{2} \times \rho \times S \times C_{L_{\max}}}} = \sqrt{\frac{240 \times 9.81}{\frac{1}{2} \times 1.2 \times 11.52 \times 1.3}} = 16.18 \text{ m/s} = 31 \text{ kt}$$

Colab wing allows lift coefficients as high as 4 with the flaps fully deflected at 45°. However, to be conservative we will consider a maximum lift coefficient of 3.5. This gives us the following stall speed:

$$V_{SF} = \sqrt{\frac{W}{\frac{1}{2} \times \rho \times S \times C_{L_{\max}}}} = \sqrt{\frac{240 \times 9.81}{\frac{1}{2} \times 1.2 \times 11.52 \times 3.5}} = 9.86 \text{ m/s} = 19 \text{ kt}$$

##### → Design wing-flap speed Vf:

The Vf velocity is the limit load that our flaps will be able to resist. Vf is the structural design velocity. This velocity does not depend on the mass of the aircraft. It depends solely on the aircraft configuration. There is a unique limit velocity for each position of the flaps. Flaps must be used only at velocities lower than Vf.

Below are the criteria for the calculation of Vf according to chapter S335 of section S of the CAP 482 . Vf may not be less than:

- 1.4 Vs1 with the flaps in take-off position at maximum take-off weight = 22.65m/s
- 2.0 Vsf with the flaps in approach position at maximum landing weight = 19.72m/s

→ We take  $V_F = 22.7 \text{ m/s}$

➔ **Design maximum level speed at full throttle  $V_C$**

The parametric analysis gives us a maximum speed of 25m/s. However, this is based on the average of the less than 115 kg aircraft studied. This is not representative of the Colab performance. The Colab maximum speed has been estimated at 50m/s.

➔ We take  $V_C=50\text{m/s}$

➔ **Design diving speed  $V_D$**

$V_D$  is the velocity for which the aircraft structure is designed. It corresponds the maximum velocity that the aircraft can ever fly at in extreme condition. This velocity is take as  $1.4 \times V_C = 70\text{m/s}$ .

➔ We take  $V_D=70\text{m/s}$

➔ **Design manoeuvring speed**

$V_A$  is the minimum manoeuvring velocity at the maximum positive load factor ( $n_1$ ). In the same time we can define  $V_G$  as the minimum manoeuvring speed at the minimum load factor ( $n_4$ ). In our case we will consider  $V_G=V_A$ .  $n_1$  and  $n_4$  are defined in chapter S337 of section S of the CAP 482.

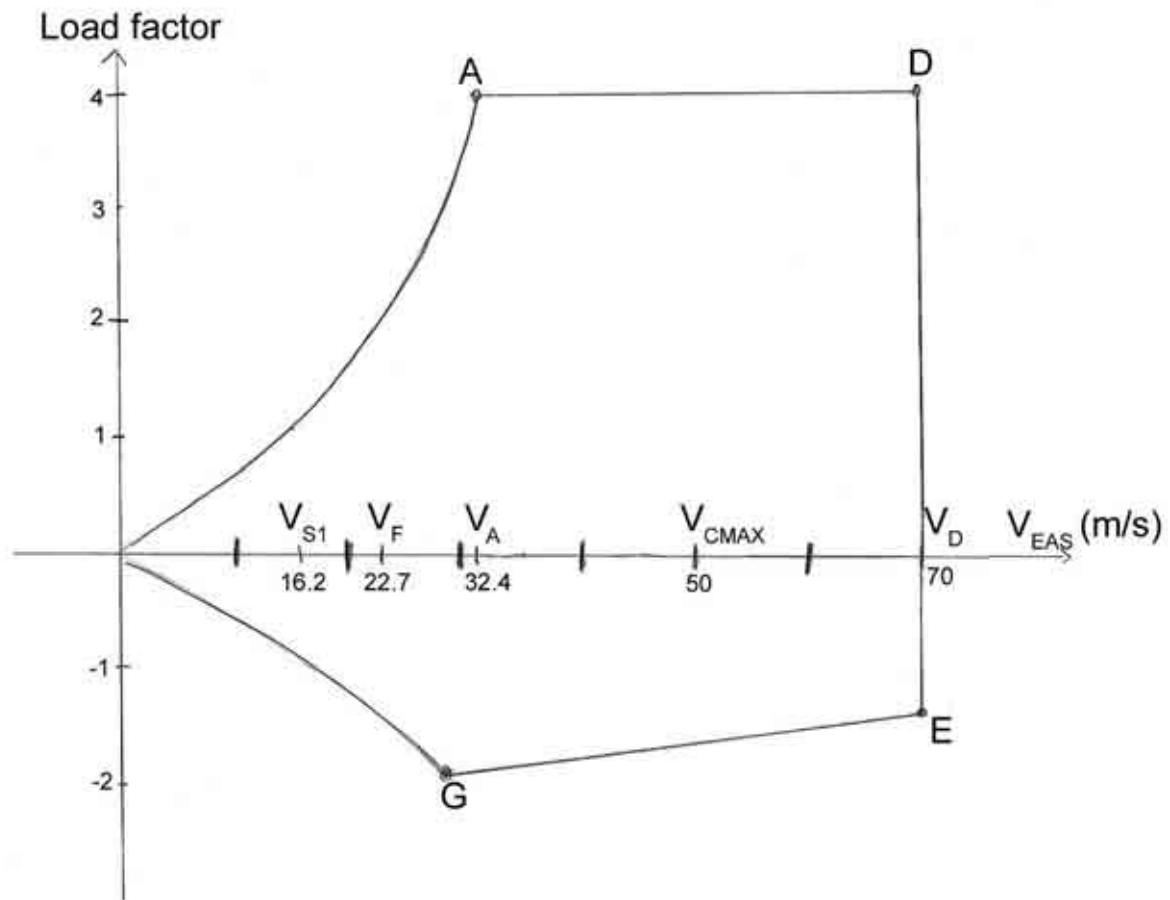
$$\rightarrow V_A = V_G = V_{s1} \sqrt{n_1} = 32.36 \text{ m/s}$$

### 8.1.2. *Gusts cases*

The section S of the CAP 482 does not consider any gust cases. However they take load factors as high as +4 and -2 to be sure that the gust envelope is contained inside the n-V diagram by default.



### 8.1.3. *n-V diagram*



HLM-07 n-V diagram

☒ **Note:** The velocities are given in equivalent air speed, which means that they are considered with an air density at sea level.

## 8.2. WING LOADS

### 8.2.1. Wing load cases

The wing load cases can be defined with the load factors. In case of a 4g acceleration, the mass of the aircraft is multiplied by 4. The wings have to withstand this load. However, in this case, we do not need to consider the wing mass; when the aircraft has a 4g acceleration, the loads on the wing are directed downward, which means that these loads are opposite the lift.

We can calculate the loads on the wing with the following formulas:

$$\begin{aligned} \text{Aircraft maximum mass:} & 240\text{kg} \\ \text{Wing mass:} & 30\text{kg} \\ \text{Aircraft weight without wing:} & (240 - 30) \times 9.81 = 2060.1 \text{ N} \\ \text{Total lift with load factor:} & F = n \times 2060.1 \text{ N} \end{aligned}$$

**These loads are applied on the total wing area, and 4 independent wing surfaces.**

**The wing is not twisted and the cross section is constant, which means that we have a CONSTANT LIFT DISTRIBUTION SPANWISE.**

**The top and low wings have the same angle of incidence.**

**➔ As a consequence we can consider that each wing sees  $\frac{1}{4}$  of the total load:**

$$\text{Lift per wing: } L = \frac{n \times 2060.1}{4} \text{ N}$$

Each wing has a length of 3.8 m, we can now deduce the shear force span wise:

$$\text{Limit Shear Force per wing: } SF = \frac{n \times 2060.1}{4 \times 3.8} \text{ N/m}$$

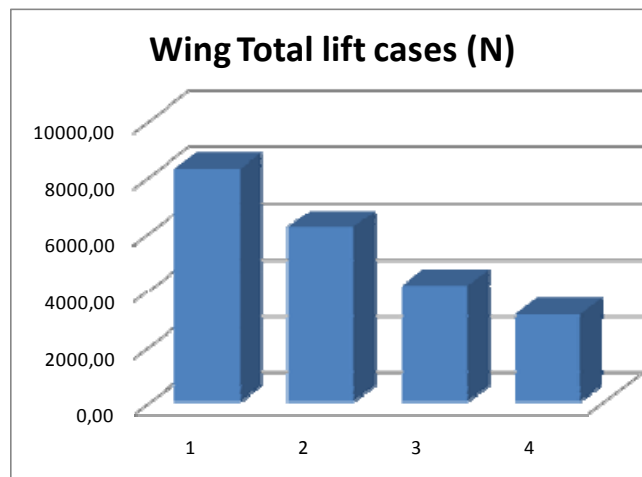
$$\text{We multiply by 1.5 to get the Ultimate shear force: } SF_{ULT} = \frac{n \times 2060.1}{4 \times 3.8} \times 1.5 \text{ N/m}$$

The load cases are summarized in the following table:

| Case | Aircraft without wing mass (kg) | n    | speed (m/s) | Wing lift load (N) | LIMIT SF per wing per side (N/m) | ULTIMATE SF per wing per side (N/m) |
|------|---------------------------------|------|-------------|--------------------|----------------------------------|-------------------------------------|
| 1    | 210                             | 4    | 32          | 8240.40            | 542.13                           | 813.20                              |
| 2    | 210                             | 3    | 70          | 6180.30            | 406.60                           | 609.90                              |
| 3    | 210                             | -2   | 32          | 4120.20            | 271.07                           | 406.60                              |
| 4    | 210                             | -1.5 | 70          | 3090.15            | 203.30                           | 304.95                              |

Wing load cases summary

The cases are plotted on the following diagram:

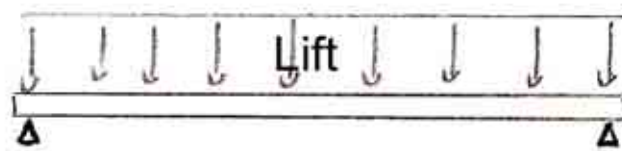


Wing load cases diagram

We can see on this diagram that the most critical case is the case 1 at 4g, as we could expect it. That is the case we are going to study for the wing design.

### 8.2.2. *Low wing shear force diagram*

The low wing is mounted with pivots at the tip; it can be modelised as a beam not restrained at the tips, as illustrated on the picture bellow:



Low wing beam model

Ultimate shear force on the wing: 813.20 N/m

Total load:  $SF = 813.20 \times 3.8 = 3090.16 \text{ N}$

Tips reactions:  $F_{tips} = 3090.16/2 = 1545.08 \text{ N}$

We know that the shear force spanwise is given by:  $Sf(y) = \int_y^s L(y).dy$

We can now plot the shear force diagram (cf. next page)



Bottom right wing shear force diagram

### 8.2.3. Low wing bending moment diagram

The bending moment can be expressed with the following formula:

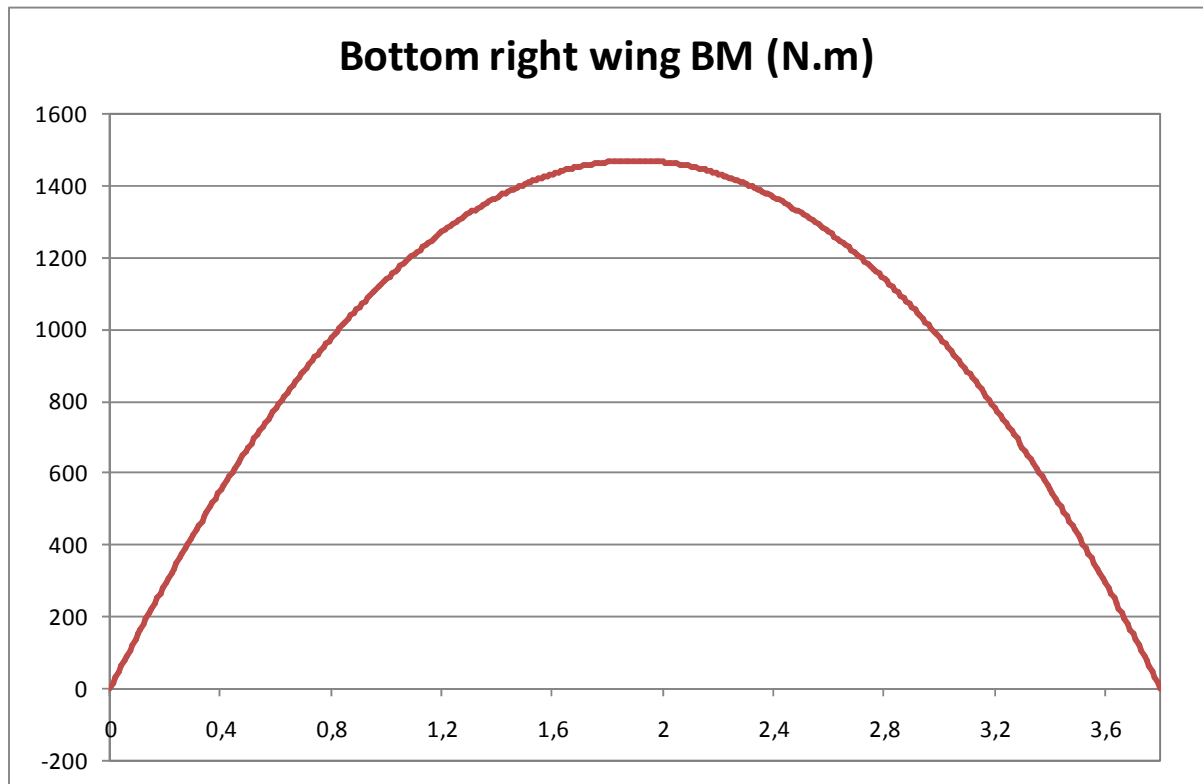
$$Bm(y) = -\int_y^s Sf(y).dy$$

To calculate the shear forces and bending moment we are going to use a numerical integration with an excel spreadsheet. This is much easier and faster than a polynomial interpolation and an analytic integration. We have split our interval in 380 parts. Then we use the trapezoids method to calculate our integrals:

$$\int_0^s f(y).dy = \sum_{i=1}^{380} \frac{s}{380} \cdot f(y_i)$$

This is a discrete method and so we have errors, but the theory gives us an error of around 1% in the integration which does not affect our calculations.

We can now plot the bending moment diagram (cf. next page).



Bottom right wing bending moment diagram

We can note that the numerical integration gives us a bending moment equal to 0. This allows us to verify that the calculations are correct. The moment is indeed equal to 0 at the tips since they are mounted with pivots.

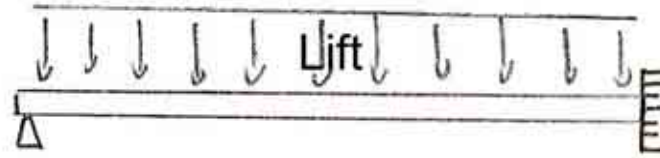
#### 8.2.4. *Maximum loads in the low wings*

We can summarize the maximum loads in the low wing:

- ➔ **Maximum shear force:**      **1545.1 N**
- ➔ **Maximum bending moment:**    **1467.9 N.m**

### 8.2.5. Top wing shear force diagram

The top wing is mounted with one pivots at the root and it is restrained at the tip; it can be modelised as a beam, as illustrated on the picture bellow:



Top wing beam model

Ultimate shear force on the wing: 813.20 N/m

Total load:  $SF = 813.20 \times 3.8 = 3090.16 \text{ N}$

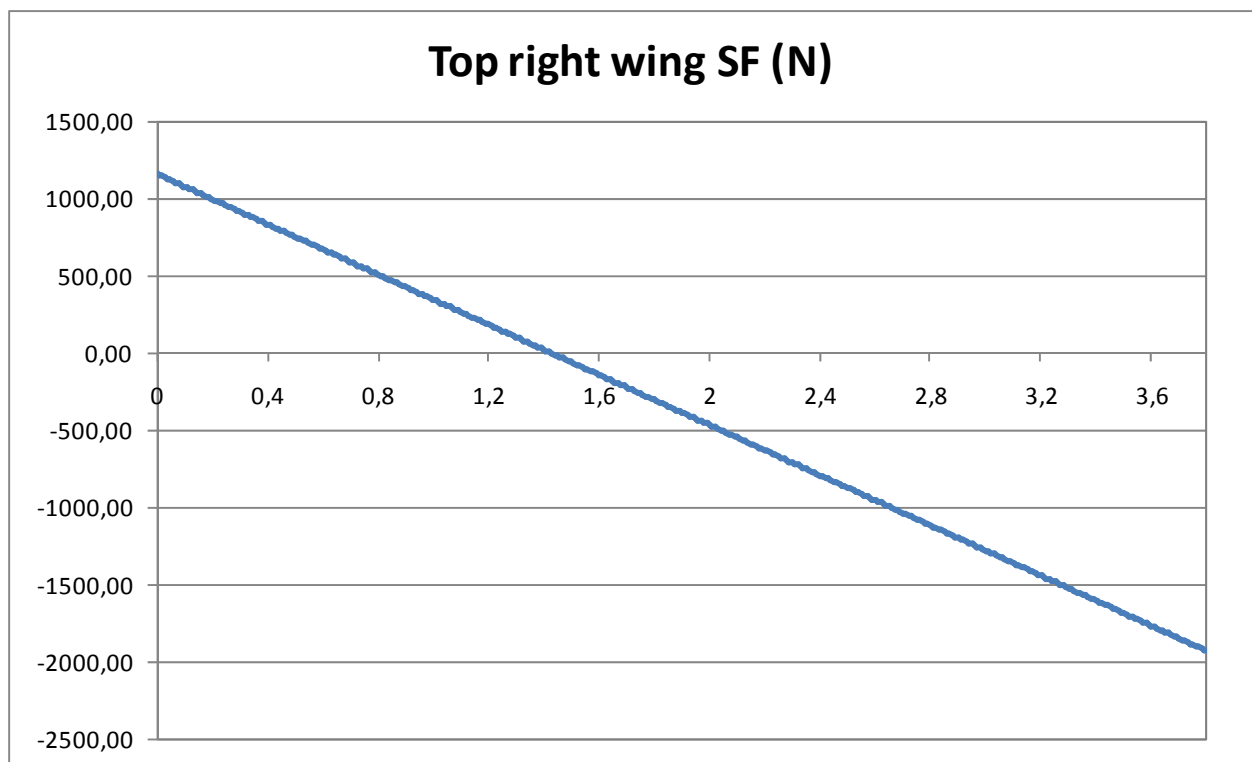
Restrained tip reactions:  $F_{tip} = 3090.16 \times (5/8) = 1931.35 \text{ N}$

Restrained tip reactions:  $F_{root} = 3090.16 \times (3/8) = 1158.81 \text{ N}$

As for the low wing, we know that the shear force spanwise is given by:

$$Sf(y) = \int_y^s L(y) \cdot dy$$

We can now plot the shear force diagram :



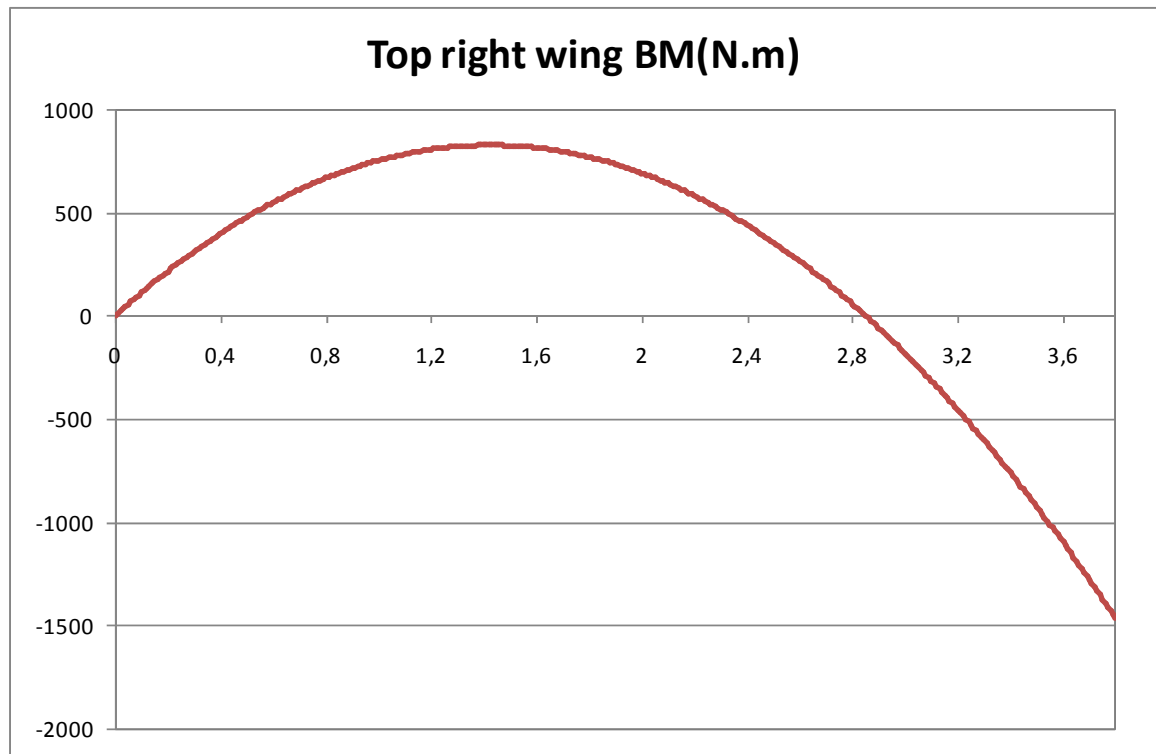
top right wing shear force diagram

### 8.2.6. Low wing bending moment diagram

The bending moment can be expressed with the following formula:

$$Bm(y) = -\int_y^s Sf(y).dy$$

As we did for the low wing, we will use a numerical integration to calculate the bending moment in the top wing:



Bottom right wing bending moment diagram

We can note that the numerical integration gives us a bending moment equal to 0. This allows us to verify that the calculations are correct. The moment is indeed equal to 0 at the tips since they are mounted with pivots.

### 8.2.7. Maximum loads in the top wings

We can summarize the maximum loads in the low wing:

- ➔ **Maximum shear force:** 1931.4 N
- ➔ **Maximum bending moment:** 1467.82 N.m

We can see that the wing with the restrained tip is the most loaded. We are going to make the calculations using this wing loads.

## 8.3. CONTROL SURFACES LOADS

### 8.3.1. Ailerons and flaps loads

#### → Airworthiness requirements

The chapter S455 of section S of the CAP 482 requires that the ailerons must be designed for the following control loads:

- Full deflection of roll control at  $V_A$  (Case 1)
- One third deflection of the roll control at  $V_D$  (Case 2)

In addition, the CS-VLA 397 requires that the control surfaces loads need not exceed the pilot forces. The maximum loads allowable are given in the table on page 1-C-6 of the CS-VLA.

→ The pilot force on the stick should always be less than 300 N.

#### → Ailerons properties

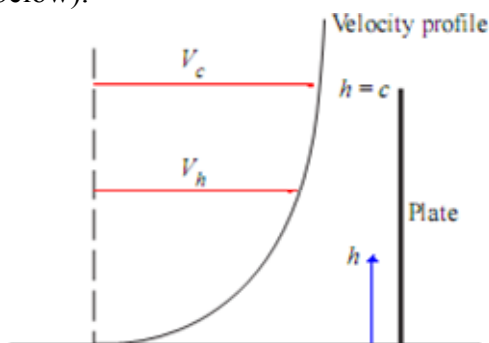
The ailerons are fitted on the low wing of the aircraft. They are on the entire span and they use 20% of the chord. The properties are summarised below:

- Aileron length (per wing): 3800mm
- Aileron width: 152mm
- Aileron max deflection:  $\pm 15^\circ$

#### → Aerodynamic model

As the chord is constant, we will make the assumption that the load is distributed constantly spanwise.

The value of the aerodynamic force is calculated thanks to the ESDU 70015 [Ref. 14] datasheet. We make the assumption that the ailerons are a long, flat plate inclined in the flow. We also have to consider the fact that the plate is mounted on a surface since it affects the velocity on the spoilers because of the boundary layer effect (Cf. figure below).



$$\frac{V_h}{V_c} = \left(\frac{h}{c}\right)^{\frac{1}{n}}$$

$$V_{eff}^2 = \frac{n}{n+2} V_c^2$$

Velocity profile on a flat plate mounted on a surface

We get this formula to calculate the effort:  $F = \frac{1}{2} \cdot \rho \cdot c(y) \cdot V^2 \cdot C_N \cdot \sin(\alpha)$

The  $C_N$  is a coefficient which depends on the air flow properties, the ailerons geometry and the ailerons inclination.

→ In our case we get  $C_N = 1.86$



### → CS-VLA loading requirements

Chapter A11 of CS-VLA requirements gives an alternative mean of calculations for the ailerons loads. Since the method we used previously is really empirical, we will check the values given by the CS-VLA.

The value of the force is given by the curve 5 of the figure A5 of the JAR VLA. This gives us the following value:

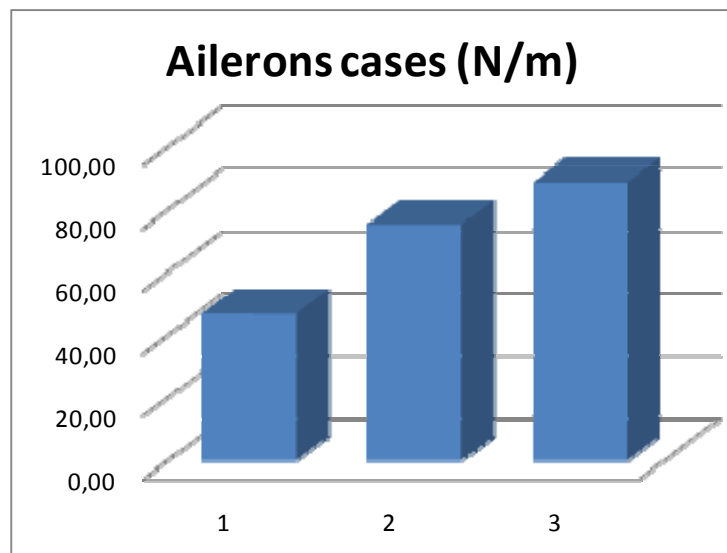
- **Limit aileron load = 60 kg/m<sup>2</sup> → 883 N/m<sup>2</sup> ultimate.**
- **Triangular chordwise distribution.**
- **The aileron chord is constant so the spanwise loading is constant.**

### → Ailerons cases

The results are summarised in the table below:

| AILERONS |             |             |      |                     |                           |                              |
|----------|-------------|-------------|------|---------------------|---------------------------|------------------------------|
| Case     | Angle (deg) | speed (m/s) | CN   | S (m <sup>2</sup> ) | LIMIT Load per side (N/m) | ULTIMATE Load per side (N/m) |
| 1        | 15          | 32          | 1.86 | 0.578               | 46.86                     | 70.30                        |
| 2        | 5           | 70          | 1.86 | 0.578               | 75.51                     | 113.27                       |
| 3        | -           | -           | -    | 0.578               | 89.00                     | 134.00                       |

Ailerons load results table



Ailerons limit loads cases

On the graph above we can compare the intensity of the loads.

We can see that the case 3 from the CS-VLA is the most critical. This is the case that we are going to consider for the calculations. Since the ailerons and the flaps have the same geometry and they operate at the same speeds, their designs are identical

### 8.3.2. *Horizontal tail surfaces symmetrical loads*

#### ➔ **Airworthiness requirements**

The section S of the CAP 482 requires that the horizontal stabilizing surfaces must be designed for:

- Balancing loads (Chapter S421)
- Manoeuvring Loads (Chapter S423)
- Unsymmetrical loads (Chapter S427)

However, the Section S of the CAP 482 does not provide any method to calculate the loads on the horizontal surfaces. This is why we will use the method given in the CS-VLA [Ref. 16]. The CS-VLA follows the same steps as the CAP 482.

#### ➔ **Balancing loads**

For this load we will make the assumption that the CG is located at the most forward position (0.20m from the top wing leading edge). The lift centre is located at 0.41 m from the leading edge. We consider a downward load at 4g and an upward load at 4g. Now we calculate the moment induced by the weight at the aerodynamic centre:

$$\text{Downward: } M_w = (0.41 - 0.20) \times 240 \times 4 \times 9.81 = 1978 \text{ N.m}$$

$$\text{Upward: } M_w = (0.41 - 0.20) \times 240 \times 2 \times 9.81 = 989 \text{ N.m}$$

This moment has to be balanced by the lift on the tailplane. We know that the tailplane moment arm is 2.9m. Now, we can calculate the lift force on the tailplane:

$$\text{Downward: } L_T = 1978 / 2.9 = 682 \text{ N} \quad 682 / 2.53 = 270 \text{ N / m}^2 \text{ (LIMIT)}$$

$$\text{Upward: } L_T = 989 / 2.9 = 341 \text{ N} \quad 341 / 2.53 = 135 \text{ N / m}^2 \text{ (LIMIT)}$$

- ➔ **For this load we use a chordwise triangular distribution.**
- ➔ **We assume that the spanwise distribution is proportional to the local chord.**
- ➔ **The ultimate downward loading for the balancing loads is 404 N/m<sup>2</sup>.**
- ➔ **The ultimate upward loading for the balancing loads is 202 N/m<sup>2</sup>.**

#### ➔ **Maneuverings loads**

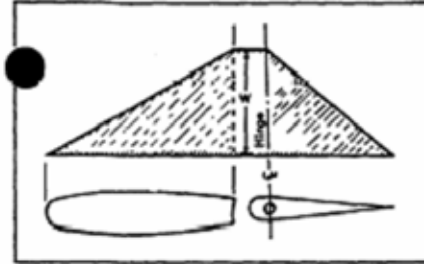
For this case we use the method given in the CS-VLA 423. We need to consider the two following cases:

- Case a: “A sudden deflection of elevator at VA [...] The average loading of B11 of appendix B can be used and the distribution in figure B7 of Appendix B can be used”.
- Case b: “A sudden upward deflection [...] followed by a downward deflection resulting in the following combinations of normal angular accelerations”. The accelerations are given in table 1 of CS-423 VLA.

-Case a:

The figure B11 of appendix B of CS-VLA gives us a maximum loading for both upward and downward directions of:

- ➔  $W = 59 \times 1.5 \text{ kg/m}^2 = 868 \text{ N/m}^2$  Ultimate upward and downward.
- ➔ We assume that the spanwise distribution is proportional to the local chord.
- ➔ The figure B7 gives us the chordwise distribution of the manoeuvring load, as illustrated below:



Manoeuvring load distribution (CS-VLA Figure B7)

-Case b:

The table page 1-C-7 of the CS-VLA gives us the following normal angular and angular accelerations for the tail ( $n_m$ =positive limit manoeuvring load factor=4g):

|           |                        |   |
|-----------|------------------------|---|
| Download: | - Normal acceleration: | 1g  |
|           | - Angular acceleration | $+\frac{20.1}{V_A} n_m (n_m - 1.5) = 6.3 \text{ rad / s}^2$ |
| Upload:   | - Normal acceleration: | 4g  |
|           | - Angular acceleration | $-\frac{20.1}{V_A} n_m (n_m - 1.5) = 6.3 \text{ rad / s}^2$ |

The distance between the CG of the tail and the CG of the aircraft is 2.9 m. Therefore, we get the following accelerations on the tail:

|           |                       |  |
|-----------|-----------------------|--|
| Download: | - Total acceleration: | $9.81 + 6.3 \times 2.9 = 28.8 \text{ m / s}^2$           |
| Upload:   | - Total acceleration: | $9.81 \times 4 + 6.3 \times 2.9 = 57.51 \text{ m / s}^2$ |

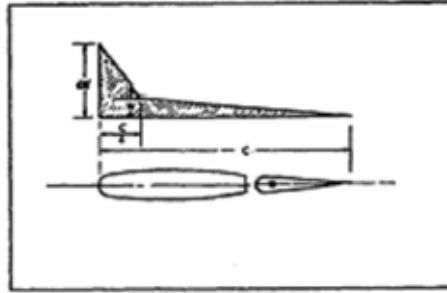
We estimate that the weight of the tailplane is less than 10 kg. Therefore, we can calculate the inertia loads if we consider that the maximum weight on one side is 5kg:

- ➔ **Download:**  $28.8 \times 5 = 144 \text{ N} \rightarrow 144 / 2.53 \times 1.5 = 86 \text{ N / m}^2$  **ultimate**
- ➔ **Upload:**  $57.51 \times 5 = 286 \text{ N} \rightarrow 286 / 2.53 \times 1.5 = 171 \text{ N / m}^2$  **ultimate**
- ➔ **The inertia loads are uniformly distributed on the tailplane.**
- ➔ **The spanwise distribution is proportional to the local chord.**

### → Gust loads

The gust loads can be determined thanks to figure B3 of the CS-VLA requirements. In this case we consider that upward and downward gust loads are the same. From figure B3 with  $W/S=12 \text{ kg/m}^2$  and  $V_c=50\text{m/s}$  we get:

- $W=60 \times 1.5 \text{ kg/m}^2 = 883 \text{ N/m}^2$  upward and downward.
- The spanwise distribution is proportional to the local chord.
- The chordwise distribution is given by the figure B8 illustrated below:



Gust load distribution (CS-VLA Figure B8)

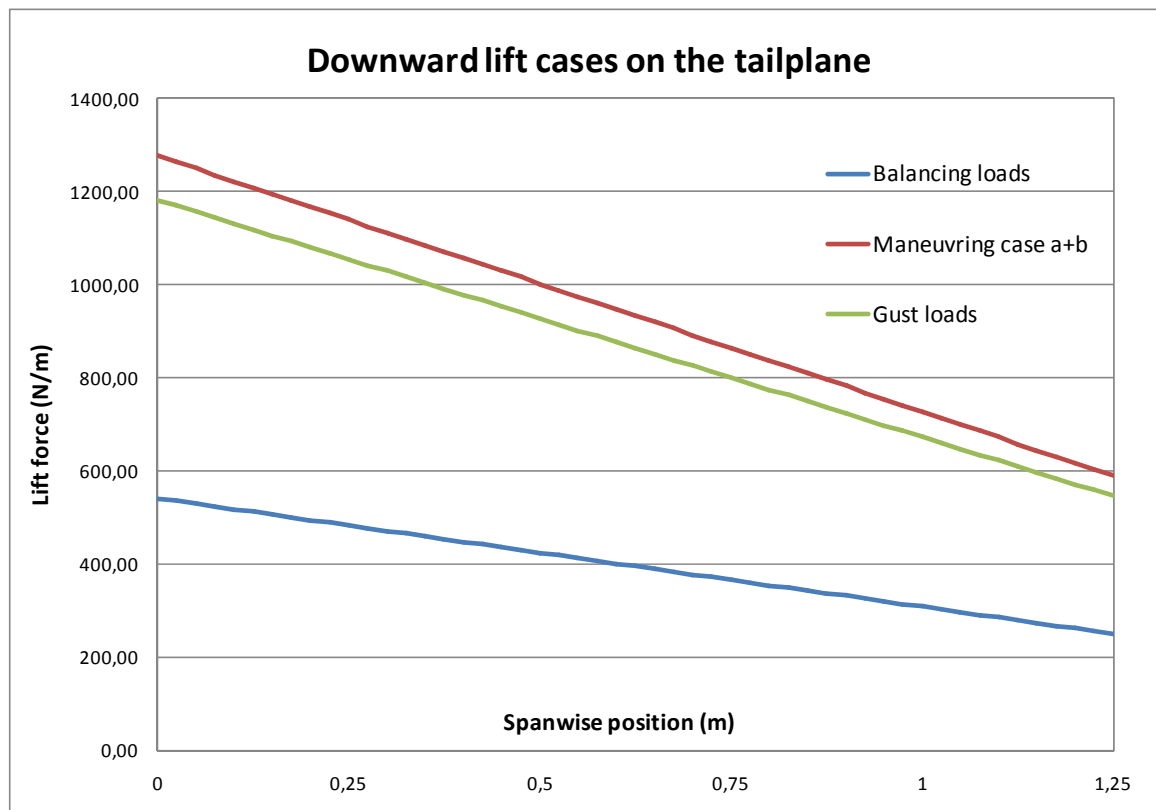
### → Summary of the loads

|                               | Downward                             |                 |                      | Upward                            |                 |                      |
|-------------------------------|--------------------------------------|-----------------|----------------------|-----------------------------------|-----------------|----------------------|
|                               | av. Ult. Lift<br>(N/m <sup>2</sup> ) | Max Ult. SF (N) | Max Ult. BM<br>(N.m) | av. Ult. Lift (N/m <sup>2</sup> ) | Max Ult. SF (N) | Max Ult. BM<br>(N.m) |
| Balancing loads               | 404                                  | 494             | 271                  | 202                               | 247             | 136                  |
| Maneuvering loads<br>case a   | 868                                  | 1162            | 583                  | 868                               | 1162            | 583                  |
| Maneuvering loads<br>case b   | 86                                   | 105             | 59                   | 171                               | 209             | 115                  |
| Maneuvering loads<br>case a+b | 954                                  | 1267            | 642                  | 1039                              | 1371            | 698                  |
| Gust loads                    | 883                                  | 1080            | 592                  | 883                               | 1080            | 592                  |

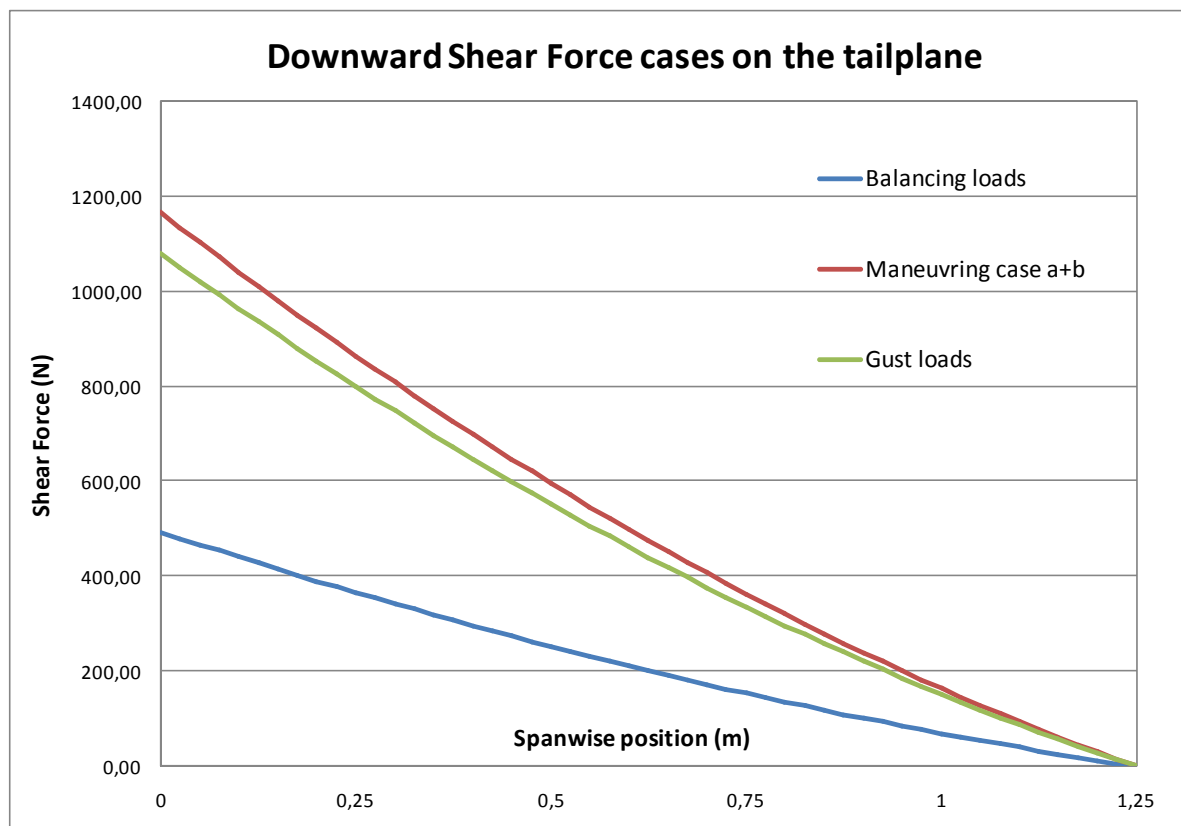
Tailplane loads summary table

We need to remember that the loads are given PER SIDE of the tailplane. The actual shear force on the total tailplane is two times what is given in the table.

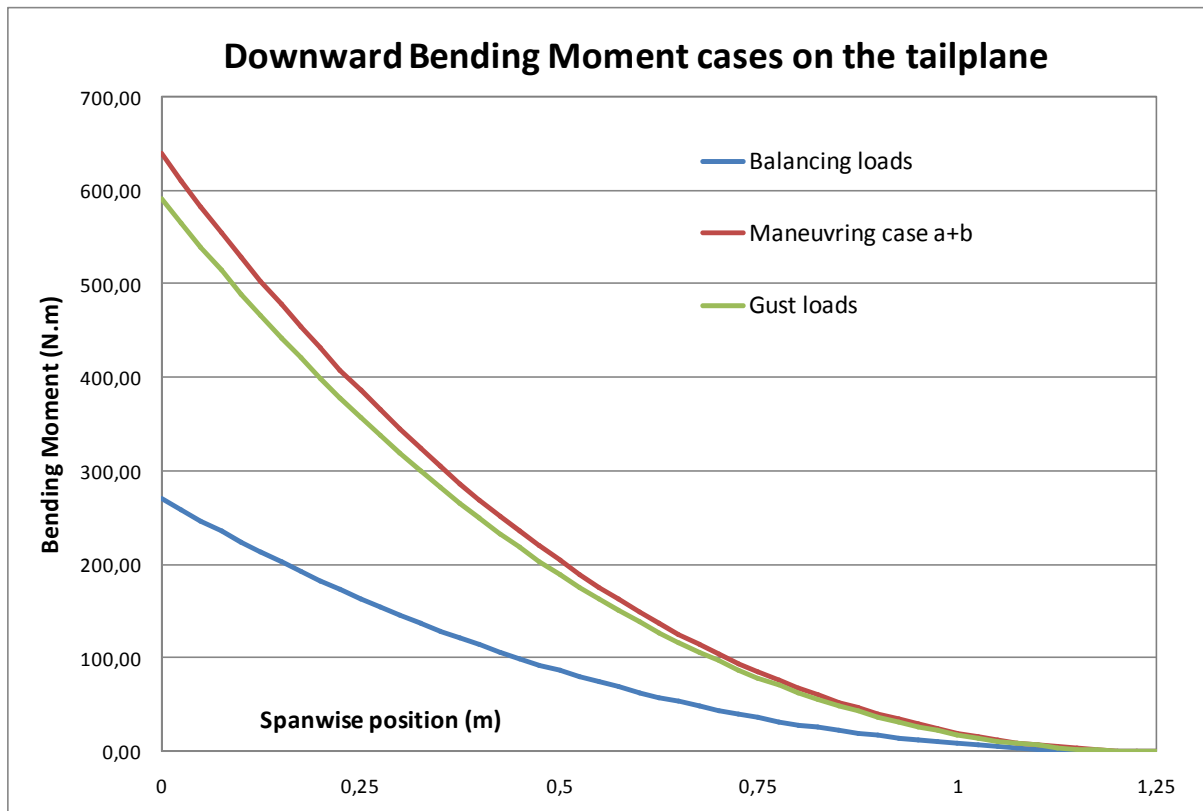
➔ Downward loading diagrams



Downward lift cases diagram

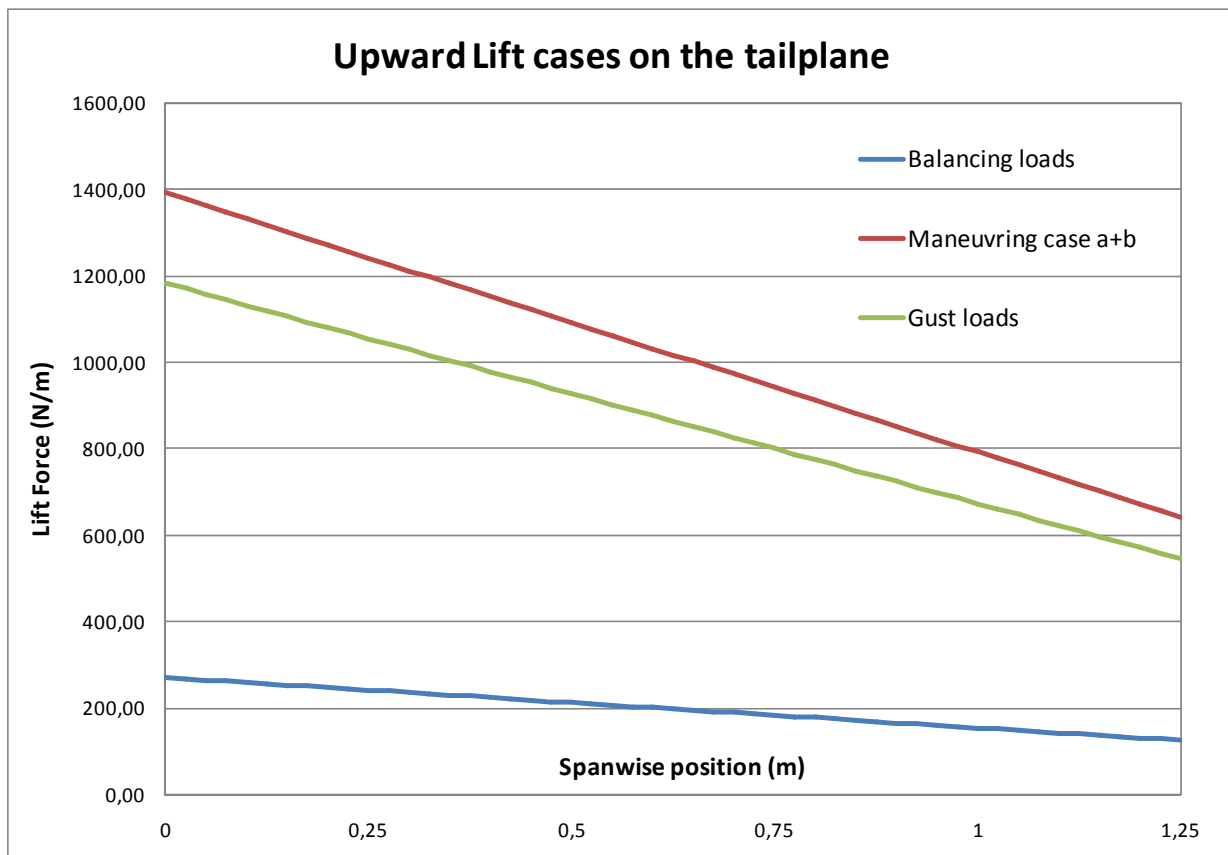


Downward Shear Force diagram

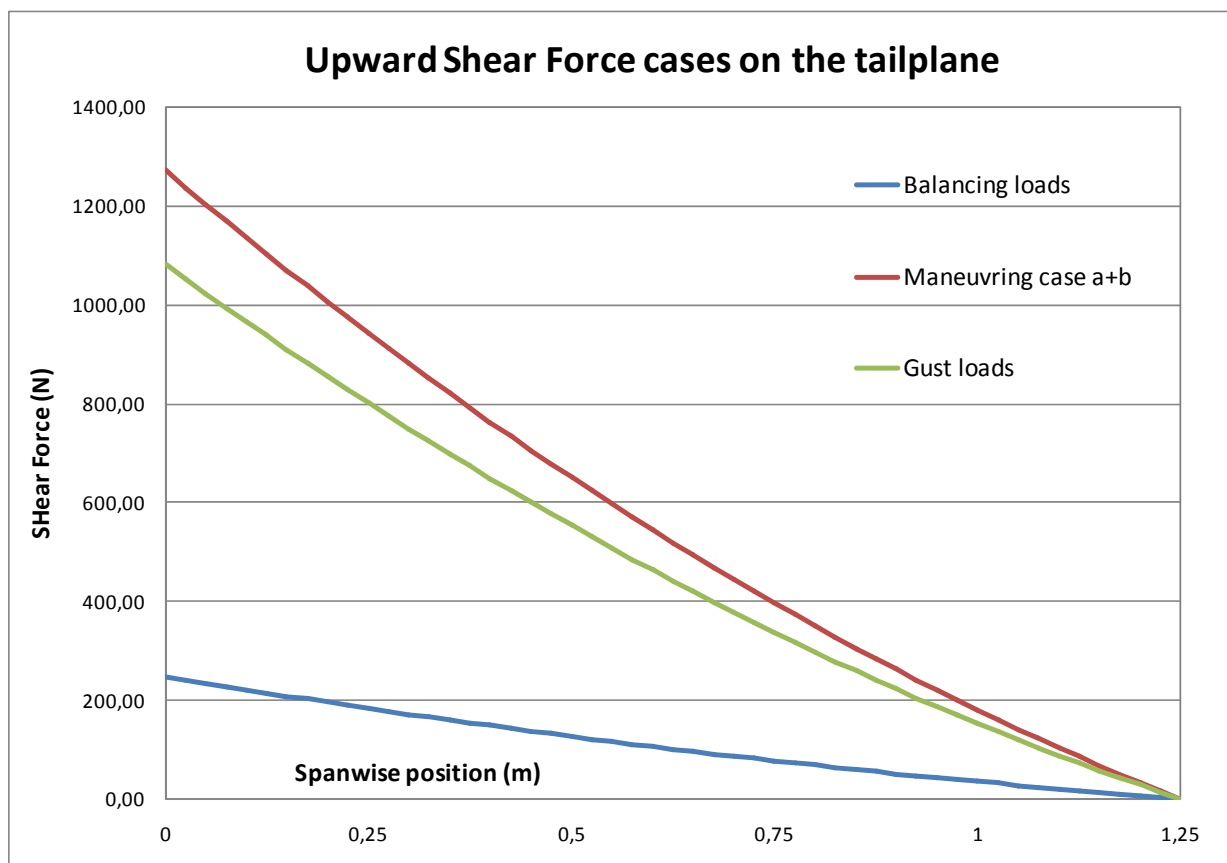


Downward Bending moment diagram

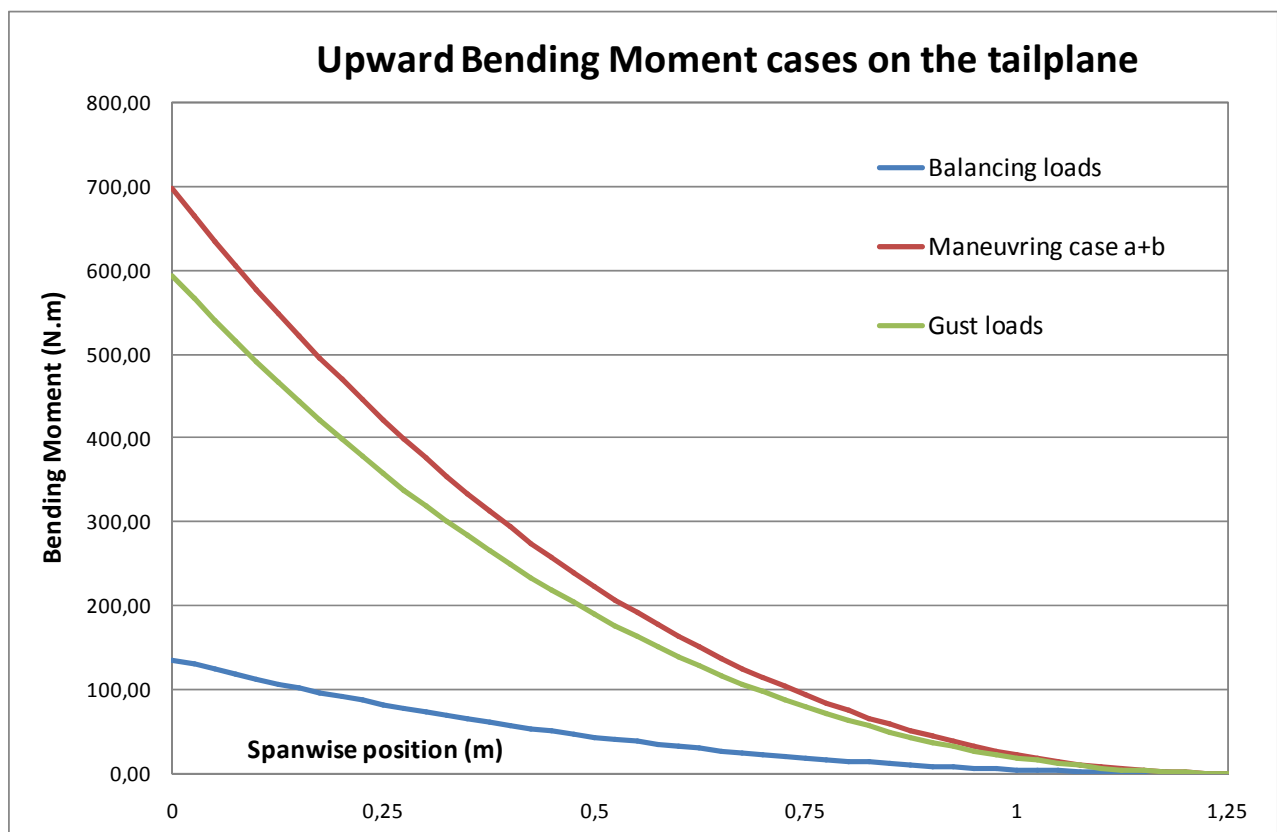
➔ Upward loading diagrams



Upward lift cases diagram



Upward shear force diagram



Upward bending moment diagram

### 8.3.3. *Horizontal tail surfaces unsymmetrical loads*

According to CS-VLA 427 “Horizontal tail surfaces [...] must be designed for unsymmetrical loads”. The loading can be assumed to be :

- 100% of the maximum loading from the symmetrical flight conditions on one side.
- 100-10(n-1) maximum loading from the symmetrical flight conditions on the other side.

➔ **In our case we get:**

- **1039 N/m<sup>2</sup> Ultimate on one side.**
- **70% of 1039 N/m<sup>2</sup> = 727 N/m<sup>2</sup> Ultimate on the other side.**

### 8.3.4. *Vertical tail surfaces loads*

➔ **Maneuverings loads**

According to CS-VLA 441, the vertical tail must be designed to withstand the following conditions:

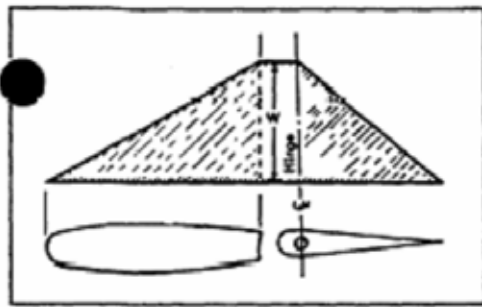
- (1) “With the aeroplane in unaccelerated flight at zero yaw, it is assumed that the rudder control is suddenly displaced to the maximum deflection, as limited by the control stops or by limit pilot forces.” This can be determined with figure 1 of appendix B and distribution B7.
- (2) “With the rudder deflected as specified in sub-paragraph (a)(1) of this paragraph, it is assumed that the aeroplane yaws to the resulting sideslip angle. In lieu of a rational analysis, an overswing angle equal to 1.3 times the static sideslip angle of subparagraph (a)(3) of this paragraph may be assumed.” This can be determined with Figure B1 and distribution B6.
- (3) A yaw angle of 15 degrees with the rudder control maintained in the neutral position (except as limited by pilot strength). This can be determined with figure 1 and distribution B8.

- ➔ **For the three cases we get a loading of 59kg/m<sup>2</sup> = 868N/m<sup>2</sup> Ultimate.**
- ➔ **The spanwise distribution is proportional to the local chord.**
- ➔ **The chordwise distributions are illustrated on the figures on the next page.**

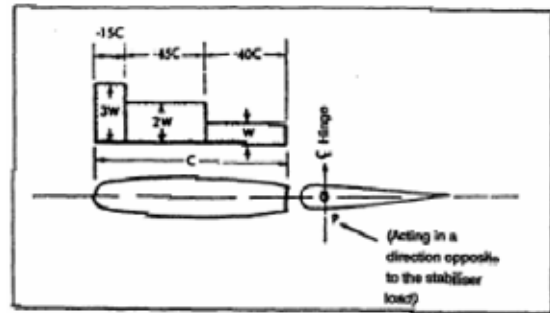
|                   | av. Ult. Lift (N/m <sup>2</sup> ) | Max Ult. SF (N) | Max Ult. BM (N.m) |
|-------------------|-----------------------------------|-----------------|-------------------|
| Maneuvering loads | 868                               | 1223            | 593               |
| Gust loads        | 1250                              | 1617            | 854               |

Fin load cases summary

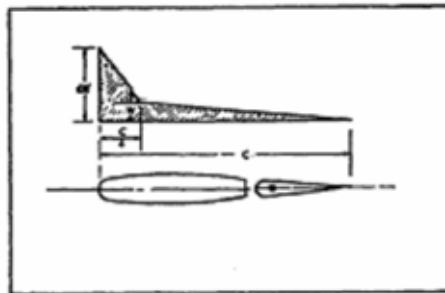




Case (1) distribution (Figure B7)



Case (2) distribution (Figure B6)

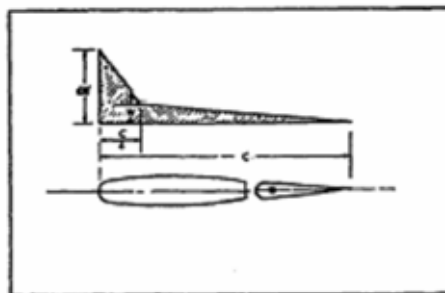


Case (3) distribution (Figure B8)

### → Gust loads

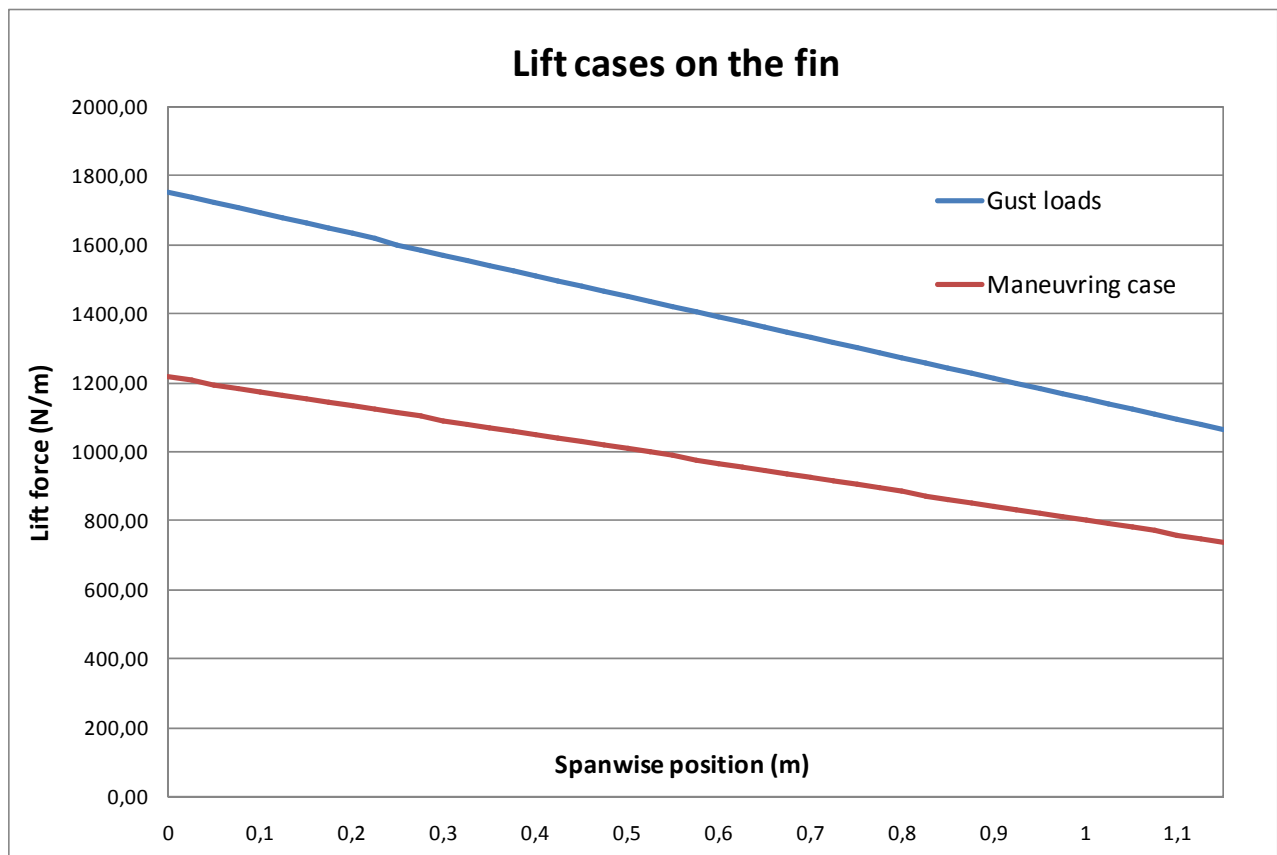
According to CS-VLA 443 the gust loads can be determined using figure B5 of appendix B and the distribution of figure B8. Our fin aspect ratio is 1.92. With the figure B5 we get:

- $W = 105 \times 0.82 = 85 \text{ kg/m}^2 \rightarrow 1250 \text{ N/m}^2$  Ultimate
- The spanwise distribution is proportional to the local chord.
- The chordwise distribution is given by the figure below:

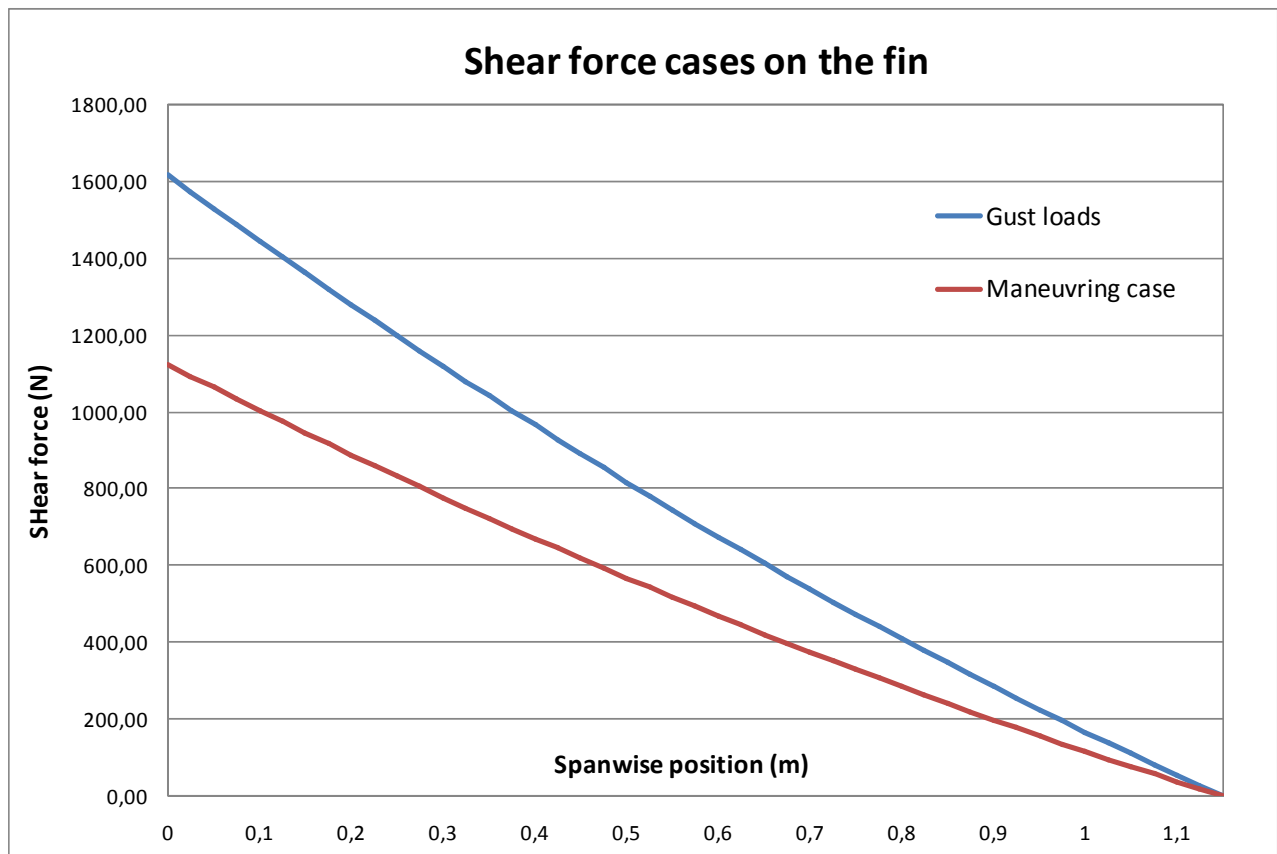


Gust cases distribution (Figure B8)

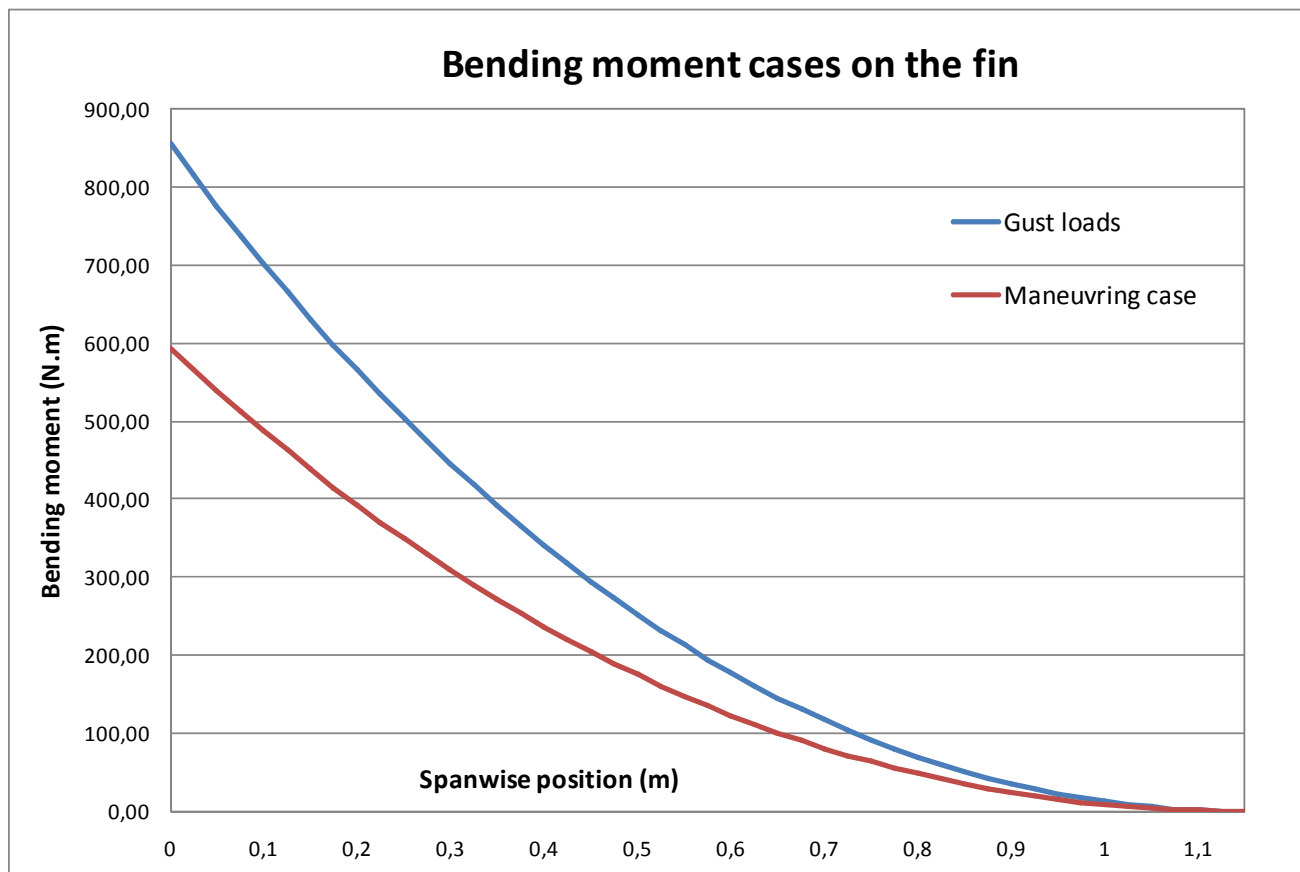
## ➔ Loading diagrams



Lift on the fin diagram



Shear force on the fin diagram



Bending moment on the fin diagram

### 8.3.5. *Rudder and elevator loading*

The CS-VLA specifies special loadings for the tail control surfaces. This can be calculated thanks to the figure A4 curve 2 for the horizontal tail and A4 curve 1 for the vertical tail. This gives us the following results :

- ➔ **Max load is 60 kg/m<sup>2</sup> LIMIT → 883 N/m<sup>2</sup> Ultimate for the elevator.**
- ➔ **Max load is 60 kg/m<sup>2</sup> LIMIT → 883 N/m<sup>2</sup> Ultimate for the rudder.**
- ➔ **Both have a triangular distribution chordwise.**

CS-VLA 397 also requires one to consider the maximum pilot forces on the controls. Thanks to the table page 1-c-6 we get the following results:

- **Maximum elevator stick load: 740 N**
- **Maximum rudder pedals load: 890 N.**

## 9. DETAILED WING DESIGN

### 9.1. WING LAYOUT

#### 9.1.1. Spars layout

##### → Spars structure

We have different possibilities for the wing design. We can choose between the following structures:

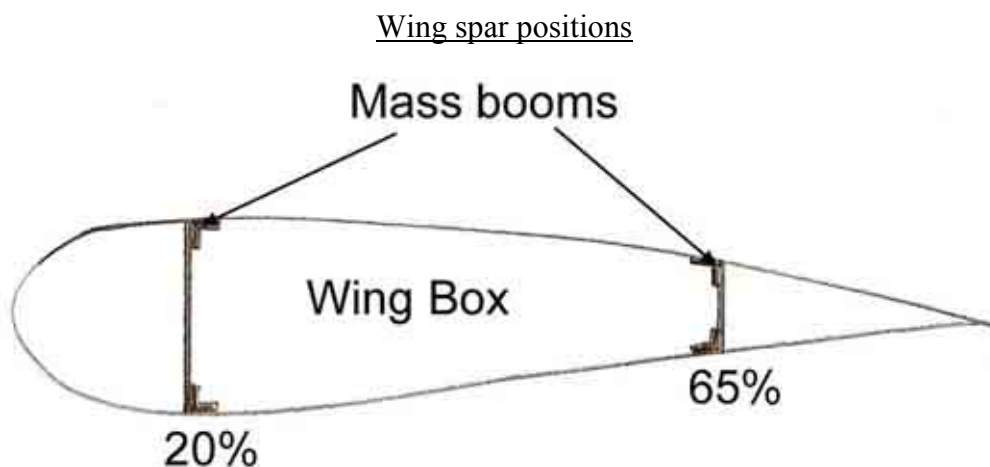
- Single spar D box
- 2 spars distributed flange design (with stringers)
- 2 spars mass booms design

The single spar design with the D box is often used for aircraft in this category. However, with the Colson design we want to be able to mount the wings on pivots. Two spars are much more convenient: we can attach lugs on each of the spars. The distributed flange design is better in theory since the stringers prevent the wing skin from buckling. However they are very expensive to manufacture since they make the structure very complex. That is why I have chosen to make a two spar mass boom design.

##### → 2 spars mass booms design

##### → Spars positions

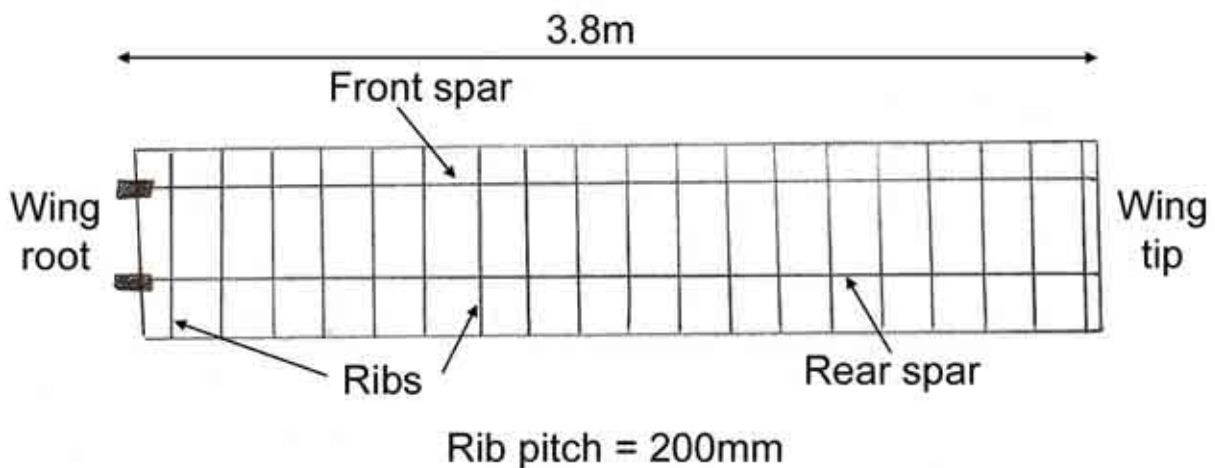
We have decided to use 2 spars in our design. We need to determine their positions chordwise. Typically the first spar position is located between 10% and 20% of the chord length and the second spar between 60% and 70% of the chord length. By moving backward the position of the rear spar we increase the area of the wing box and so we increase the torsional stiffness. On the other hand we reduce the rear spar height and so we deteriorate the bending properties of the flap. As a consequence of all these parameters I have chosen to put the first spar at 20% of the chord and the rear spar at 65% of the chord as illustrated below:



### 9.1.2. Ribs position

The ribs are really important structural components in a wing. Their main role is to react the shear force due to the lift. They do not contribute to the bending stiffness but they prevent the buckling of the skin. The more rib you put in the design the closer they will be and so the smaller the area of skin subjected to buckling will be. Therefore you can have a thinner skin and less weight. The more rib you put the less load each rib will see and so you can put thinner ribs, but the more rib you put the more complex and heavy the design is. In practice it is a trade off. The rib pitch can be determined by the following formula:  $L = 0.55 \cdot \sqrt{dr}$ , where  $dr$  is the maximum depth of the airfoil. In our case we get  $L=190\text{mm}$ , we will take  $200\text{mm}$ .

➔ 20 ribs per wing with a rib pitch of 200mm



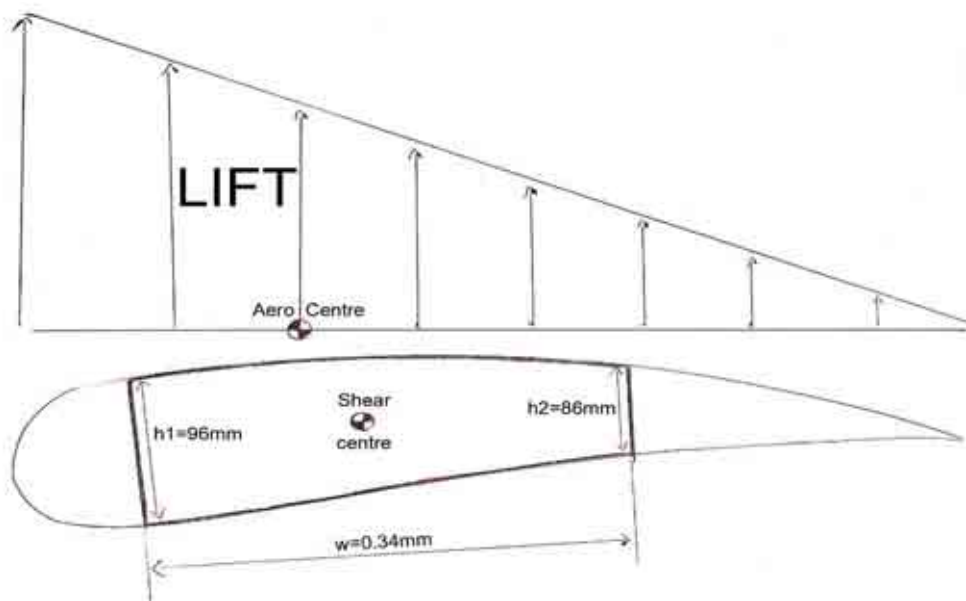
Wing layout

## 9.2. SIZING OF THE SKIN

### 9.2.1. Shear centre and torque diagram

To calculate the shear flow in the wing box we need to determine the position of the shear centre and the position of the aerodynamic centre. The shear centre is the position in which a force can be applied on the box without causing any shear flow in the top and bottom flanges. The aerodynamic centre is the point where the resultant of the lift force is applied. We consider a triangular lift distribution on the flap. In this case the position of the aerodynamic centre is easy to determine and is located at  $1/3$  of the flap chord. For the position of the shear centre, we can make the assumption that the flap box has a horizontal axis of symmetry and so the shear centre is located on this axis. Then the longitudinal location is given by this formula:  $e_c = \frac{h_1}{h_1 + h_2}$  where  $e_c$  is the position of the shear centre forward of the rear spar, as fraction of the width of the box. In our case:

$$e_c = \frac{0.96}{0.96 + 0.86} = 52.7\% , \quad w = 0.34m .$$



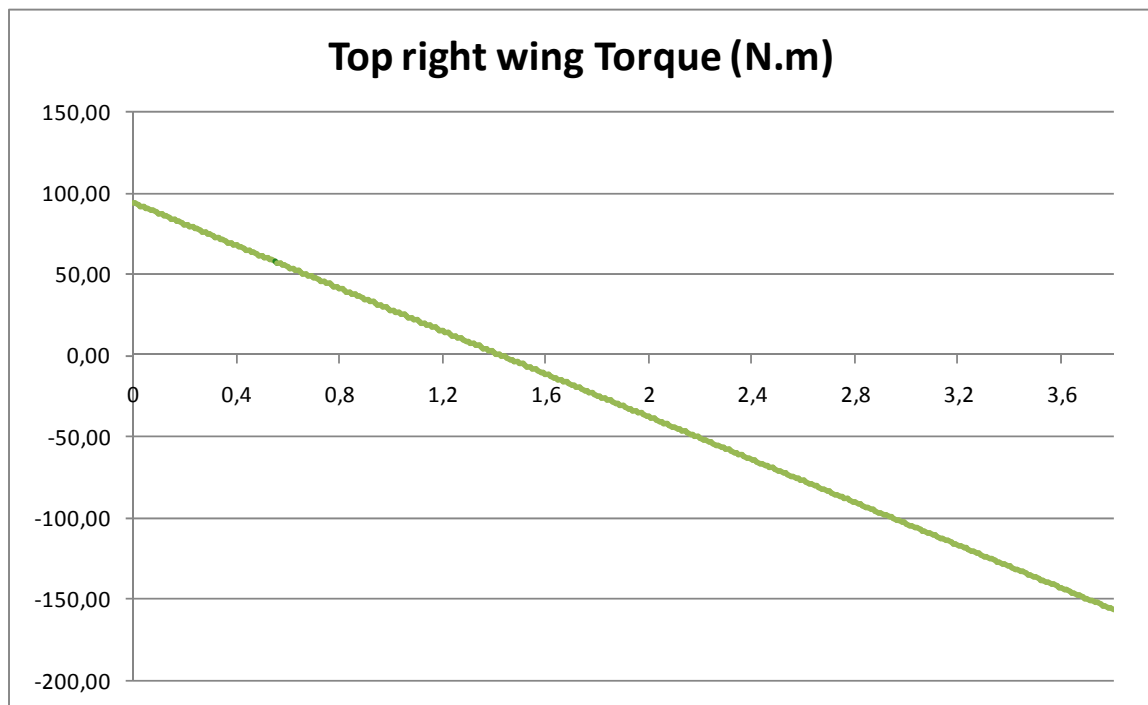
#### Aerodynamic and shear centres

The distance between the shear and the aerodynamic centre gives us the moment arm for the torque:

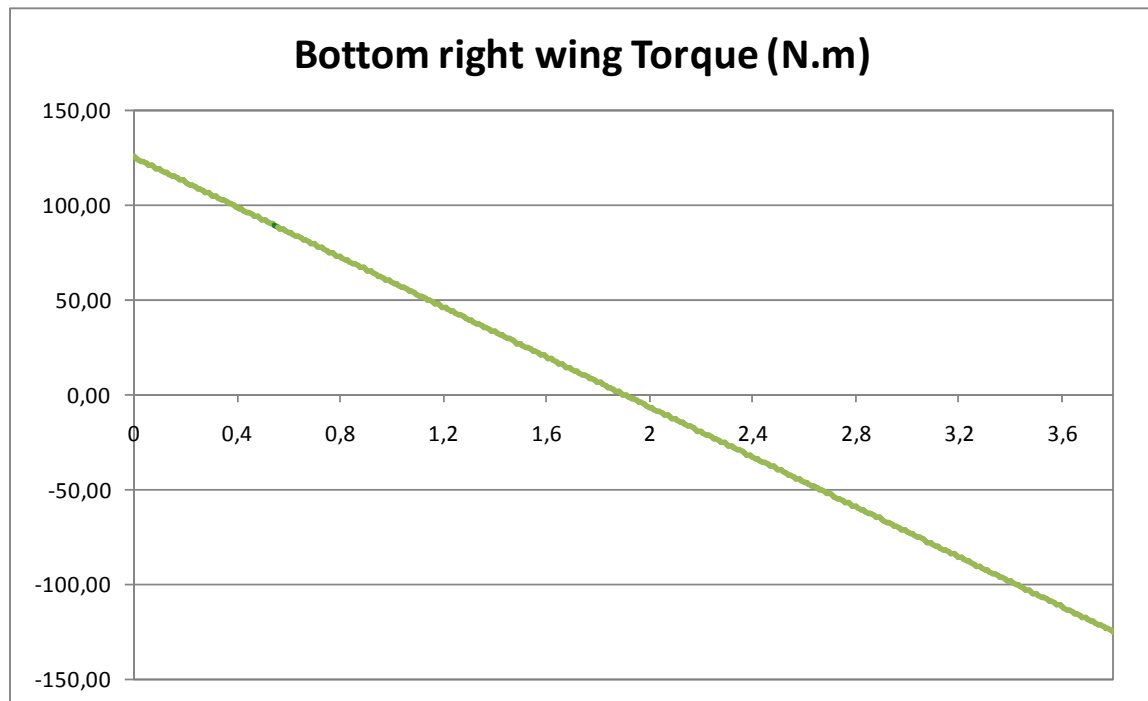
- The position of the front spar is at  $0.76 \times 20\% = 0.152m$  from the leading edge
- The position of the aerodynamic centre is at  $0.76 \times 33\% = 0.255m$  from the leading edge.
- The shear centre is at  $0.34 \times 52.7\% + 0.152 = 0.336m$

➔ **The torque arm is**  $0.336 - 0.250 = 0.081m$

We can now determine the torque diagram (Cf. next page).



Torque diagram of the top right wing (case 4)



Torque diagram of the bottom right wing (case 4)

As illustrated on this diagram the torque has the maximum value at the tips and especially on the tip of the bottom wing, where it is restrained.

- ➔ The maximum value of the ultimate torque is 157N.m.
- ➔ The maximum value of the limit torque is 105N.m.

### 9.2.2. Torsional shear skin thickness

Now that we have the torque values we can calculate the skin thickness required to resist the torsional shear. With the mass boom design we can make the assumption that the skin takes only the loads due to the torsional shear and that the bending loads are taken by the spars. These values vary spanwise. All the calculations are done in a spreadsheet, only the results will be presented.

We can get the shear flow in the flap box with this formula:

$$Qt = \frac{T}{2A}$$

Where T is the ULTIMATE torque and A the wing box area. In our case we get:

$$Qt = \frac{157}{2 \times 0.34 \times \frac{0.0960 + 0.086}{2}} = 2537 N/m$$

Then we can get the skin thickness with this formula:

$$t_q = \frac{Q_t}{\sigma_s}$$

Where  $\sigma_s$  is the allowable shear stress in the composite material. For the composites that I have chosen (0.38mm thick, high strength carbon fibre epoxy woven fabric)  $\sigma_s = 70\text{MPa}$ . We get then:

$$t_q = \frac{2537}{70000000} \cdot 1000 = 0.036\text{mm}$$

The thickness is noticeably small, but it is normal because we have a very small moment arm and so a very small torsional shear flow. We need to remember that this thickness only takes into account the torsional shear flow. In addition this thickness corresponds to the minimum thickness so that the laminate does not brake. This does not take into account the shear buckling of the skin.

**➔ Minimum strength thickness = 0.0036 mm**



### 9.2.3. Torsional stiffness skin thickness

For the stiffness criteria we need to use the LIMIT load. The section S of the CAP 482 does not specify any value of maximum rotation of the structure but it is very common to take this value equal to  $\theta_{\max}=0.05$  rad.

To calculate the torsional stiffness we use this formula:

$$\frac{d\theta}{dL} = \frac{P_r \cdot T_c}{4 \cdot A^2 \cdot G \cdot t_\theta}$$

Where  $P_r$  is the perimeter of the flap box,  $A$  is the area of the flap box,  $G$  is the shear modulus of the material,  $T$  is the limit torque,  $t_\theta$  the skin thickness. With the composites material that I use, (0.38mm thick, high strength carbon fibre epoxy woven fabric),  $G=5$ GPa. We can transform this equation into:

$$\frac{d\theta}{dL} \cdot t_\theta = \frac{P_r \cdot T_c}{4 \cdot A^2 \cdot G}$$

Then we suppose  $t_\theta$  constant and so we can integrate the equation and we get:

$$\theta \cdot t_\theta = \frac{P_r \cdot T_c}{4 \cdot A^2 \cdot G} \cdot L$$

Where  $L$  is the distance between the point of deflection  $\theta$  and the point of deflection  $\theta=0$ . we can deduce:

$$\theta_{\max} \cdot t_\theta = \frac{P_r \cdot T_c}{4 \cdot A^2 \cdot G} \cdot L_{\max} \text{ and then } t_\theta = \frac{P_r \cdot T_c}{4 \cdot A^2 \cdot G} \cdot \frac{L_{\max}}{\theta_{\max}}$$

We are going to take into account the case of the low wing with the 2 tips mounted on pivots. We will consider that the twist angle is not too different for the top wing.

We know that  $\theta_{\max}=0.02$  rad, so we just have to determine  $L_{\max}$ . We know that at the tips position the rotation  $\theta=0$  because the wing box cannot move in torsion.

We also know that the maximum angle is reached in the middle, because of the symmetry. The middle is located at 1.9 meters from the tips, we have  $L_{\max}$ .

$$t_\theta = \frac{(0.34 \times 2 + 0.086 + 0.096) \times 157}{4 \times \left(0.34 \times \frac{0.86 + 0.96}{2}\right)^2 \cdot 5} \cdot \frac{1.9}{0.02} = 0.00027m = 0.27mm$$

This thickness is bigger than what was calculated for the failure since the torsional stiffness criterion is more severe than the failure criterion.

➔ **Minimum torsional stiffness thickness = 0.27mm**

#### 9.2.4. Wing skin buckling

We have designed the wing skin to resist the torsional shear buckling and to meet the stiffness requirements. The lift pressure puts the laminate in tension and therefore will not induce buckling. On the contrary, the torsional shear can induce shear buckling and that is what we are going to check in this part. To check the shear buckling I have used the ESDU datasheet 80023 [Ref.12]. The method is described below. The composite calculations are done with the Cranfield College Of Aeronautic Laminate Analysis software (Coala).

To calculate the maximum allowable shear  $N_{xyb}$  in the plate I will use the figure 5 of the ESDU 80023 datasheet. This figure requires the following parameters:

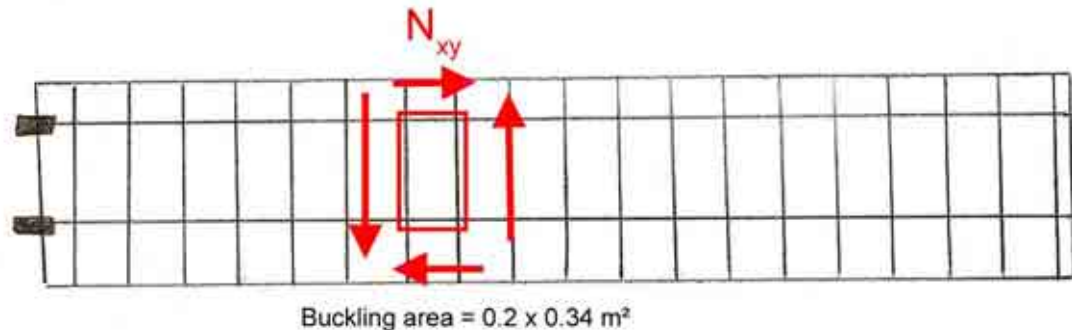
- Plate geometry:  $a=200\text{mm}$ ,  $b=750\text{mm}$
- Laminate properties: D matrix (calculation with a simple software)

We can then calculate the following non dimensional values:

Then we read on  $\frac{a}{b} \cdot \left( \frac{D_{22}}{D_{11}} \right)^{\frac{1}{4}}$  and  $\frac{D_0}{(D_{11} \cdot D_{22})^{\frac{1}{2}}}$  with  $D_0 = D_{12} + 2 \cdot D_{33}$  the graph the value of  $\frac{N_{xyb}}{(D_{11} \cdot D_{22})^{\frac{1}{2}}}$  and we can deduce  $N_{xyb}$ .

##### → Buckling area:

I will study the buckling of the skin between the front spar and the rear spar and between the ribs. This represents a rectangle of 200mm width and 340mm length. This area is represented on the picture below:



Shear buckling of the wing skin

##### → Load case

The wing skin buckling is not dangerous for the aircraft safety. However the deformations on the skin induce aerodynamic disturbances of the flow and can reduce the aircraft performance. This is why we want to check that under LIMIT load, under NORMAL flight conditions (1G steady flight) the skin does not buckle.

→ Maximum shear in the skin in normal flight conditions, case 1 = 0.4N/mm

### → Buckling calculations results

The buckling calculations results are summarized in the following table:

|   |             |  |          |          |
|---|-------------|--|----------|----------|
| D0 (N.mm)                                       | 8.50E+01    | <b>Plain symmetric Woven Fabric 0.38</b> |          |          |
| $D0 / (D22 \cdot D11)^{(1/2)}$                  | 0.216       | 3.93E+02                                 | 3.93E+01 | 0.00E+00 |
| $a/b \cdot (D22/D11)^{(1/4)}$                   | 0.588       | 3.93E+01                                 | 3.93E+02 | 0.00E+00 |
| $Nxb \cdot a \cdot b / (D11 \cdot D22)^{(1/2)}$ | 83          | 0.00E+00                                 | 0.00E+00 | 2.29E+01 |
| Nxb (N/mm)                                      | 0.479       | Ply thickness (mm)                       |          |          |
| <b>RF</b>                                       | <b>1.19</b> | <b>0.38</b>                              |          |          |

Skin buckling results table and laminate D matrix

We have a reserve factor of 1.19 which means that we do not have a lot of margins. However, this calculation is done for the most stressed part of the wing, which is a very small portion of the wing. We can then consider that the skin buckling is not going to cause trouble in normal flight conditions.

### → Laminates selection:

For the skin I have chosen the following laminate:

- Name: Woven Carbon Prepregs (IM7-6K Fibre)
- $E_1=85\text{GPa}$ ,  $E_2=85\text{GPa}$ ,  $G_{12}=5\text{GPa}$ ,  $\nu_{12}=0.1$
- $X_t=700\text{MPa}$ ,  $X_c=400\text{MPa}$ ,  $Y_t=700\text{MPa}$ ,  $Y_c=400\text{MPa}$ ,  $S=50\text{MPa}$
- Layout: 1 layer  $0^\circ$  spanwise
- Ply thickness: 0.380mm
- Total thickness: 0.380mm

#### 9.2.5. Wing skin strength

In this part I am going to check that the strength of the fabric chosen is high enough. This step is important since we have only checked the buckling under the case 1 at limit load. We need to check the worst case (Case 4) at ultimate load.

The ultimate shear flow is : 2.43 N/mm.

The laminate thickness is 0.38 which means that the maximum stress is:  $2.43/0.38=6.4\text{MPa}$ .

The laminate shear strength is 50 MPa which gives us a reserve factor of 7.82.

From a damage tolerance and fatigue point of view we want to limit the strain to 0.004.

We need to check that we meet this requirement:  $\varepsilon = 6.4 / 5000 = 0.00128 < 0.004$ .

**→ The structure is safe: Max strain: 0.0013, Stress RF: 7.82**

### 9.3. SPARS SIZING

The spars are not used to take the bending. The spars will only react the shear force due to the lift. Based on these considerations we can calculate the shear flow in the front spar and in the rear spar and then size them. As I did for the torque I am going to present the calculations done for only the max case. The detailed calculation all along the span are done in an excel matrix. For these calculations we use the ULTIMATE loads and the load Case 4.

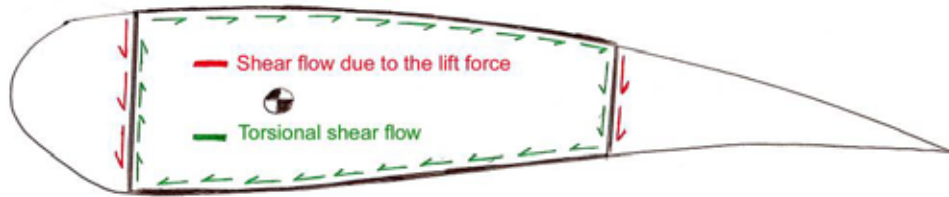
#### 9.3.1. Shear force repartition between the front spar and the rear spar

The first step of the analysis is to determine the loads in each spar. We can get this repartition with the following formulas:

$$F_{\max} = V_{\max} \cdot \frac{h_1^2}{h_1^2 + h_2^2} = 1072 \text{ N} \quad R_{\max} = V_{\max} \cdot \frac{h_2^2}{h_1^2 + h_2^2} = 860 \text{ N} \quad (V_{\max} = 1931.4 \text{ N})$$

Where F is the load on the front spar, R the load on the rear spar and V the shear force.

But the spars also react the shear flow due to the torque (calculated before) and we need to take this into consideration in our calculations.



Shear flows in the spars

We can note that you add the shear flows in the rear spar but you subtract them in the front spar.

$$\text{Shear flow in the front spar: } q_F = \frac{F}{h_1} - Q_t = \frac{1072}{0.096} - 2425.19 = 8740 \text{ N/m}$$

$$\text{Shear flow in the rear spar: } q_R = \frac{R}{h_2} + Q_t = \frac{8040}{0.12} + 1097 = 12430 \text{ N/m}$$

#### 9.3.2. Preliminary thickness calculation

Then to get the thickness you need to divide the shear flow by the allowable shear stress, which in our case we take it equal to 150MPa, which corresponds to a standard laminate. We get these results:

$$t_F = \frac{q_F}{\sigma_s} = 0.058 \text{ mm} \quad t_R = \frac{q_R}{\sigma_s} = 0.083 \text{ mm}$$

The spars thicknesses are very small but we did not take into account the possibility of buckling in the spars. We will study this in the next part.

### 9.3.3. Spars shear buckling

To check the buckling in the spars we are going to use the ESDU datasheet 80023 [Ref.12], as we did for the skin.

#### → Buckling area:

The buckling area is the surface of the spar located between 2 ribs. This corresponds to a rectangle of the size of spar height (96mm for the front spar and 86mm for the rear spar) times the rib pitch which is 200mm.

#### → Loads :

For the wing skin we considered that the buckling wasn't critical since it only affects the aerodynamic performance. For the spars, this is not the case at all; we do not want any shear buckling in the spars at ultimate load, on the maximum case (Case 4).

→ Max ultimate shear flow in front spar: 8.74 N/mm

→ Max ultimate shear flow in rear spar: 12.43 N/mm

#### → Buckling calculations results for the front spar

|   |             |
|---|-------------|
| D0 (N.mm)                                       | 1.19E+03    |
| $D0 / (D22 \cdot D11)^{(1/2)}$                  | 0.58        |
| $a/b \cdot (D22/D11)^{(1/4)}$                   | 0.36        |
| $Nxb \cdot a \cdot b / (D11 \cdot D22)^{(1/2)}$ | 150         |
| Nxb (N/mm)                                      | 16.0        |
| <b>RF</b>                                       | <b>1.83</b> |

| <b>LAM_1-1 (0,1/60,1/120,1)s 0.75</b> |          |              |
|---------------------------------------|----------|--------------|
| 3.69E+03                              | 3.50E+02 | 1.16E+02     |
| 3.50E+02                              | 1.13E+03 | 3.27E+02     |
| 1.16E+02                              | 3.27E+02 | 4.20E+02     |
| Ply thickness (mm)                    |          | <b>0.125</b> |

Front spar buckling results table and laminate D matrix

#### → Buckling calculations results for the rear spar

|   |             |
|---|-------------|
| D0 (N.mm)                                       | 1.19E+03    |
| $D0 / (D22 \cdot D11)^{(1/2)}$                  | 0.58        |
| $a/b \cdot (D22/D11)^{(1/4)}$                   | 0.32        |
| $Nxb \cdot a \cdot b / (D11 \cdot D22)^{(1/2)}$ | 155         |
| Nxb (N/mm)                                      | 18.4        |
| <b>RF</b>                                       | <b>1.48</b> |

| <b>LAM_1-1 (0,1/60,1/120,1)s 0.75</b> |          |              |
|---------------------------------------|----------|--------------|
| 3.69E+03                              | 3.50E+02 | 1.16E+02     |
| 3.50E+02                              | 1.13E+03 | 3.27E+02     |
| 1.16E+02                              | 3.27E+02 | 4.20E+02     |
| Ply thickness (mm)                    |          | <b>0.125</b> |

Rear spar buckling results table and laminate D matrix

From a cost point of view we want to use the same laminates for both spars and that is why the reserve factor is slightly higher on the front spar than on the rear spar. We can see that the reserve factors are quite high, but the laminate thickness is only 0.75mm and it is not practical to have a lower thickness if we want to keep a symmetrical lay-up.

### → Laminate selection

For both spars I have chosen the following carbon fiber-epoxy laminate:

- Name convention : LAM\_1-1
- $E_1=140\text{GPa}$ ,  $E_2=10\text{GPa}$ ,  $G_{12}=5\text{GPa}$ ,  $\nu_{12}=0.3$
- $X_t=1.5\text{GPa}$ ,  $X_c=1.2\text{GPa}$ ,  $Y_t=50\text{MPa}$ ,  $Y_c=250\text{MPa}$ ,  $S=70\text{MPa}$
- Layout:  $(0_1/60_1/120_1)_s$
- Ply thickness: 0.125mm
- Total thickness: 0.75mm

### 9.3.4. Spar strength checking

In theory, if the spars do not buckle they won't fail under the same load. However it is useful to have an idea of the reserve factors. We will check the strength with the highest shear flow (in the front spar) which is equal to 12.43N/mm. The results of the Coala analysis are summarized in the table below:

|                                       |               |
|---------------------------------------|---------------|
| <b>LAM_1-1 (0,1/60,1/120,1)s 0.75</b> |               |
| <b>Shear flow</b>                     | <b>12.43</b>  |
| <b>Tsai-Wu stress RF</b>              | <b>19.6</b>   |
| <b>Tsai_wu strain RF</b>              | <b>19.6</b>   |
| <b>max strain</b>                     | <b>0.0004</b> |

Spars strength analysis results

As we can see, the reserve factors are really high, but this is because of the buckling criterion. The maximum strain is less than 0.004, so the structure is safe.

## 9.4. BOOM SIZING, WING STIFFNESS

### 9.4.1. Minimum boom area calculation

To design the wings with the mass booms, we make the assumption that only the booms react the bending. In fact the skin between the spars is flexible and so does not contribute to the bending stiffness.

First of all we want to calculate the effective direct load  $P$  in the top and bottom surfaces of the wing box with the following formula:

$$P_{\max} = \frac{M_{\max}}{h_{\text{mean}}} = \frac{1468}{0.091} = 16132N$$

To get the total area of the booms we need to divide  $P$  by the allowable stress and multiply by 2. In our case, for high strength carbon laminate we can take an allowable proof stress of 300MPa.

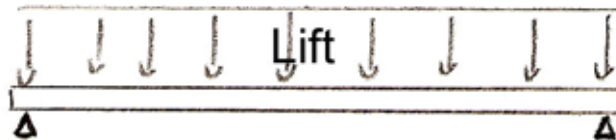
$$A_{\text{booms}} = 2 \times \frac{P_{\max}}{\sigma_b} = 2 \times \frac{16132}{300} = 107\text{mm}^2 \quad \frac{107}{4} = 27\text{mm}^2 \text{ per boom}$$

➔ The minimum boom area is 27mm<sup>2</sup>.

### 9.4.2. Wing stiffness criterion

We have calculated the boom area to withstand the ULTIMATE loads of the maximum case (case 4). However we do not want that the wing have a large deflection because of the bending moment. We need to check the wing maximum deflection. To check the deflection we are going to use the LIMIT loads of the case 4.

The wing which is the most stressed is the top wing, with one tip restrained. On the contrary, the wing which will have the largest deflection is the bottom wing mounted on 2 pivots. As we did previously we are going to consider the bottom wing as a beam simply supported on each side (cf. bellow)



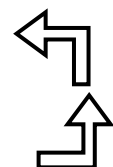
Wing maximum deflection beam model

The maximum deflection of this beam is achieved in the middle. It is given by the following formula:

$$l_{\max} = \frac{5 \times p \times L^4}{384 \times E \times I_z}$$

We can see that we need to iterate the following steps:

- Select a first young modulus  $E_1$  of the laminate
- Look at the  $I_z$  required
- Calculate the boom geometry
- With the booms thickness calculate the new laminate and the new  $E_1$



### → Boom Iz calculation

We consider that the wing box is roughly symmetrical. Then we can say that the axe of inertia of the section is in the middle. The moment of inertia is given by the following formula:  $I_z = \sum d^2 \times A$ , where

- d is the distance between the booms centre of inertia and the wing box inertia axe
- A is the area of the boom.

|                     |                            |
|---------------------|----------------------------|
| For the front spar: | $d=96/2 - 4 = 44\text{mm}$ |
| For the rear spar:  | $d=86/2 - 4 = 39\text{mm}$ |
| Booms area:         | $80\text{mm}^2$            |
| Iz:                 | $553120\text{mm}^4$        |
| p limit case 4:     | $542 \text{ N/m}$          |
| E:                  | $93 \text{ GPa}$           |
| L:                  | $3.8\text{m}$              |

$$\rightarrow l_{\max} = \frac{5 \times 0.842 \times 3800^4}{384 \times 93 \times 10^3 \times 553120} = 28.6\text{mm} \Leftrightarrow 0.75\% \text{ of the wing length}$$

### → Booms materials

The material that I have used for the booms has the following properties:

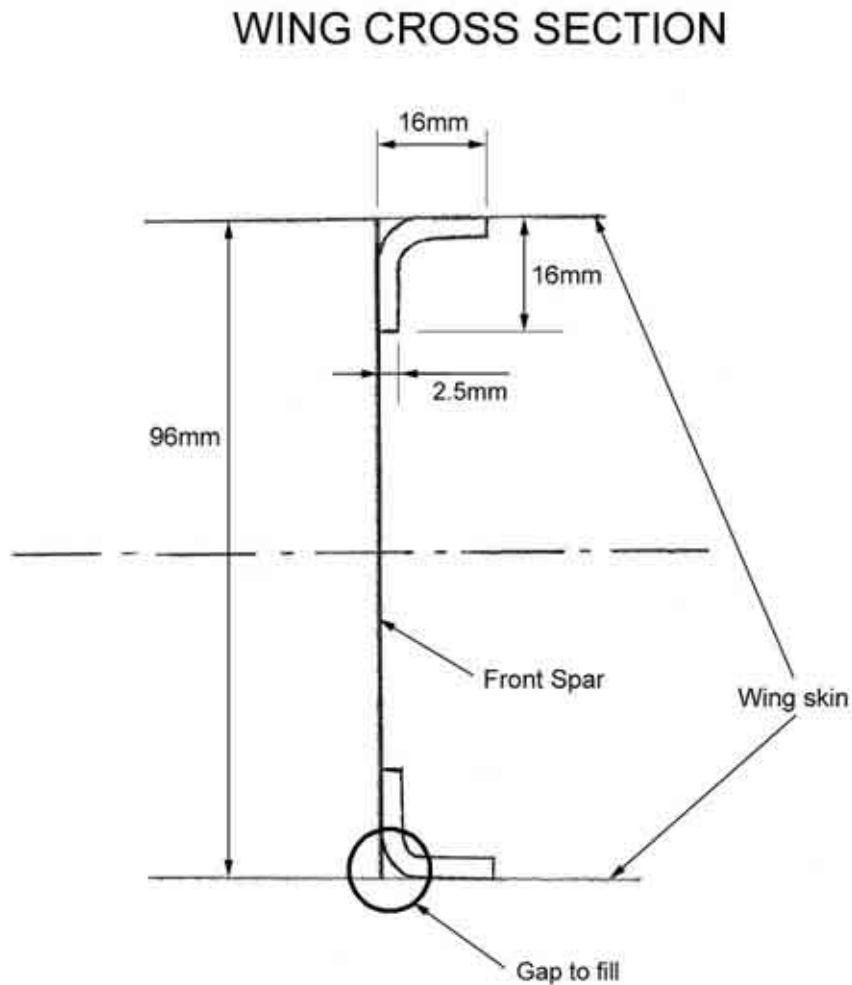
- Naming convention: LAM\_3-1
- $E_1=140\text{GPa}$ ,  $E_2=10\text{GPa}$ ,  $G_{12}=5\text{GPa}$ ,  $\nu_{12}=0.3$
- $X_t=1.5\text{GPa}$ ,  $X_c=1.2\text{GPa}$ ,  $Y_t=50\text{Mpa}$ ,  $Y_c=250\text{MPa}$ ,  $S=70\text{MPa}$
- Layout:  $(0_6/45_1/-45_1/90_2)_s$
- Ply thickness:  $0.125\text{mm}$
- Total thickness:  $2.5\text{mm}$

We can note that this laminate has a high proportion (60%) of fibres in the  $0^\circ$  direction. With this property we get a high modulus  $E_1=93\text{GPa}$  which gives the laminate a very high stiffness in the  $0^\circ$  direction and so improves the efficiency of the material in the structure and so saves weight.



### 9.4.3. Booms layout

The picture below represents a cross section of the wing at the front spars. They show the layout of the booms. The design is to scale.



- ➔ The booms are located **INSIDE** the wing box
- ➔ The gap **MUST BE FILLED** either with special aeronautic adhesive or with the adapted Nail Head shaped uncured thermoset.
- ➔ **WARNING: THE 0° FIBRES HAVE TO BE IN THE SPANWISE DIRECTION.**
- ➔ The booms are made in **ONE PIECE** on the full length.

#### 9.4.4. Boom strength

We need to check that the booms won't fail under ULTIMATE load in the maximum case (Case 4) with the lay-up that we have selected.

We have calculated that the tensile force  $P_{\max}=16132\text{N}$ .

The load in the laminate is  $\frac{P_{\max}}{\text{Length}} = \frac{16132}{32} = 504.2\text{N/mm}$

With Coala we will check that the laminate is safe in traction and in compression with this load. The results are summarized in the tables below:

| LAM_3-1 (0,6/45,1/-45,1/90,2)s 2.5 |        |
|------------------------------------|--------|
| Tensile load (N/mm)                | 505    |
| Tsai-Wu stress RF                  | 2.39   |
| Tsai_wu strain RF                  | 2.63   |
| max strain                         | 0.0022 |

| LAM_3-1 (0,6/45,1/-45,1/90,2)s 2.5 |        |
|------------------------------------|--------|
| Compressive load (N/mm)            | 505    |
| Tsai-Wu stress RF                  | 3.44   |
| Tsai_wu strain RF                  | 3.44   |
| max strain                         | 0.0022 |

Booms strength results

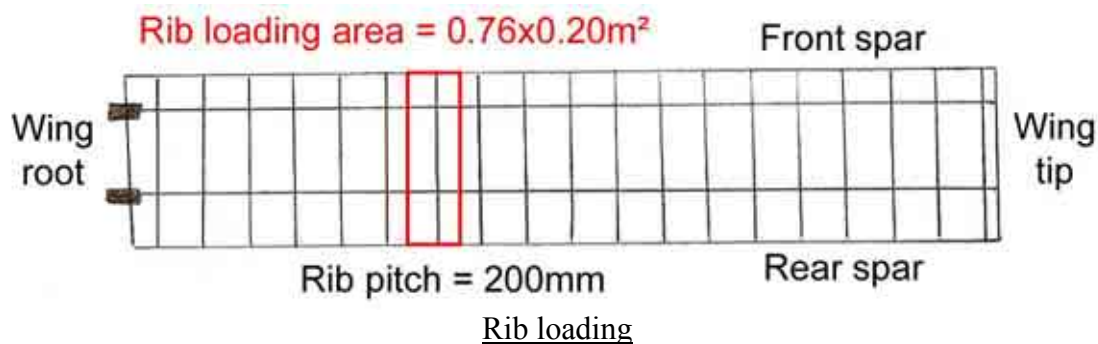
- ➔ The maximum strain is 0.0022, which is less than 0.004
- ➔ The minimum reserve factor is 2.39

### 9.5. RIBS SIZING

#### 9.5.1. Wing rib air load

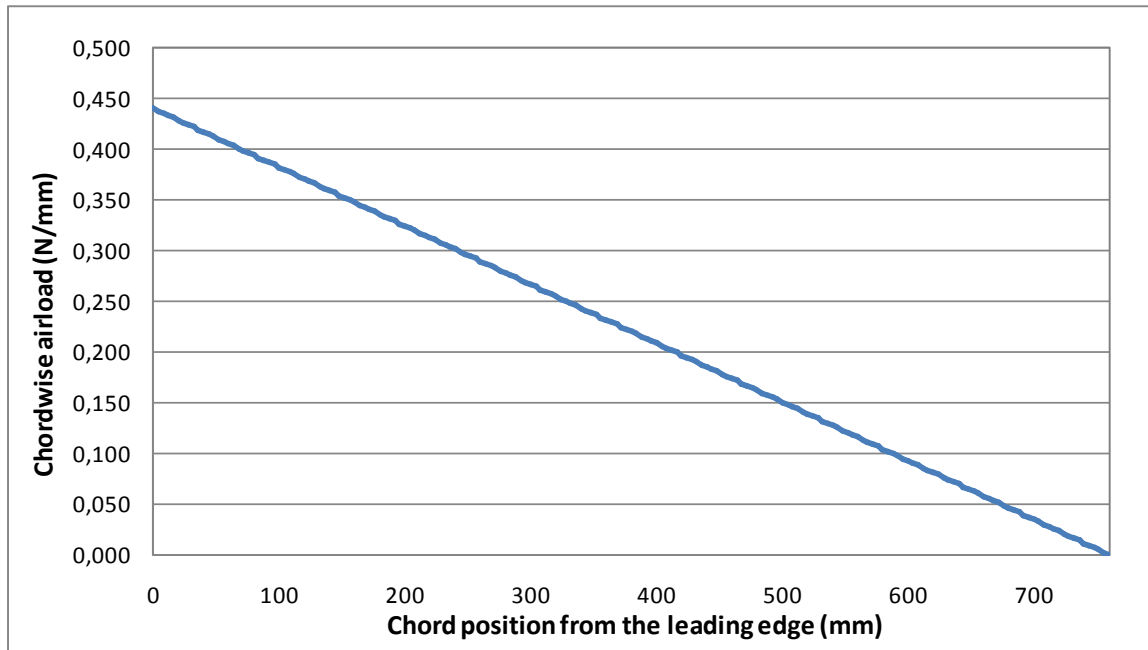
For all the calculations in this part we will make the assumption that only the wing box carries loads. The leading edge and the trailing edge do not have an important role as structural components of the wing. We are going to study the loads on the ribs submitted to air load. For this calculation we will assume a triangular airload repartition. We will work with the ULTIMATE loads.

The main role of a rib is to react the shear force due to the airload. The rib pitch is 200mm and therefore each rib will see the load applied on the 200mm wide area between the leading edge and the trailing edge, as illustrated below:



We have a spanwise loading on the main flap so we can deduce the load on one rib. The spanwise loading is 826N/m. the rib pitch is 200mm and the mean chord length is 760mm. We get the distribution plotted below.

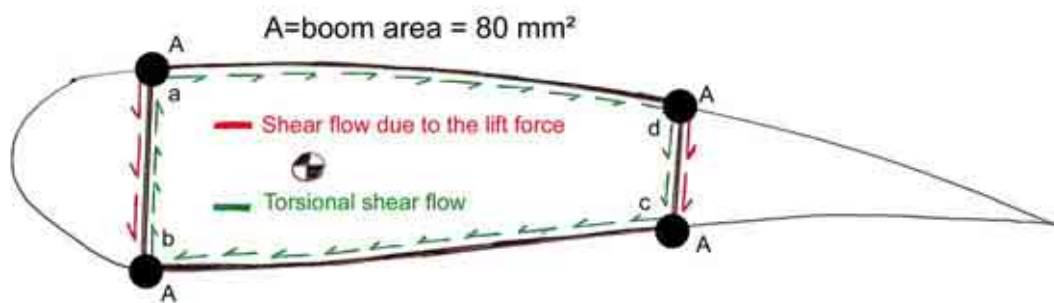
$$V_y = 0.826 \times 200 = 165.2\text{N} \text{ and } F_{\text{mean}} = \frac{0.826 \times 200}{760} = 0.22\text{N/mm}$$



Rib airload distribution chordwise

### 9.5.2. Shear flow distribution:

Then we need to calculate the shear flow distribution in the rib. We know that we have the following distribution:



Shear flow in a rib submitted to airload

We will start by calculating the vertical shear flow. The first step is to calculate the second moment of inertia of the section. To do this we will take into account only the booms areas:  $I_{xx} = \sum_i A_i \times y_i^2 = 664480 \text{ mm}^4$

Then we can calculate the shear flow in the sections a-b, b-c, c-d and d-a. To do this we will use the method explained on the next page:

The shear flow is expressed as following:  $q = \frac{V_y}{I_{xx}} \int y \cdot dA$

We will consider in our case that we only have the concentrated masses of the booms at the positions  $y_a$ ,  $y_b$ ,  $y_c$  and  $y_d$ . So we then get the following formula:  $q = \frac{V_y}{I_{xx}} \sum_i y_i \cdot A_i$

Finally we get:

- $q_{da}=0$
- $q_{ab}=0.955 \text{ N/mm}$
- $q_{bc}=0$
- $q_{cd}=0.855 \text{ N/mm}$

Now we have the shear flow due to the vertical load  $V_y$ . Then we need to calculate the torsional shear flow. For that we will write the equilibrium of moments at point b:

$$\sum \vec{M}_1 + \vec{M}_2 + \vec{T} = \vec{0}$$

We have the moments induced by the following forces:

- Shear flow in the rear spar:  $M_1 = q_{ab} \cdot h_2 \cdot 340 = 25000 \text{ N.mm}$
- Airload:  $M_2 = 99 \cdot V_y = 16355 \text{ N.mm}$
- Torque: T

Where  $h_2$  is the height of the rear spar, 340mm is the moment arm of the first force (= distance between the front spar and the rear spar) and 99mm is the moment arm of the second force (= distance between the centre of pressure and the front spar). These 2 moments have to be balanced by the torque induced by the distance between the point of application of  $V_y$  and the shear centre of the box. So we can determine T. Then with the value of T we can determine the torsional shear flow in the rib:

$$T = 8655 \text{ N.mm} \quad q = \frac{T}{2A} = \frac{8655}{2 \times 340 \times 95} = 0.134 \text{ N/mm}$$

To get the shear force diagram we need to add the contributions of all the shear flow:

$$SF(x) = SF_{airload} + SF_{Reaction \text{ at front spar}} + SF_{Due \text{ to } q} + SF_{Reaction \text{ at rear spar}}$$

$$SF(x) = SF_{airload} + q_{ab} \cdot h_1 + q \cdot y(x) + q_{cd} \cdot h_2$$

For the bending moment we need to integrate all these components. As integration is linear we can separate the bending moment into the following components:

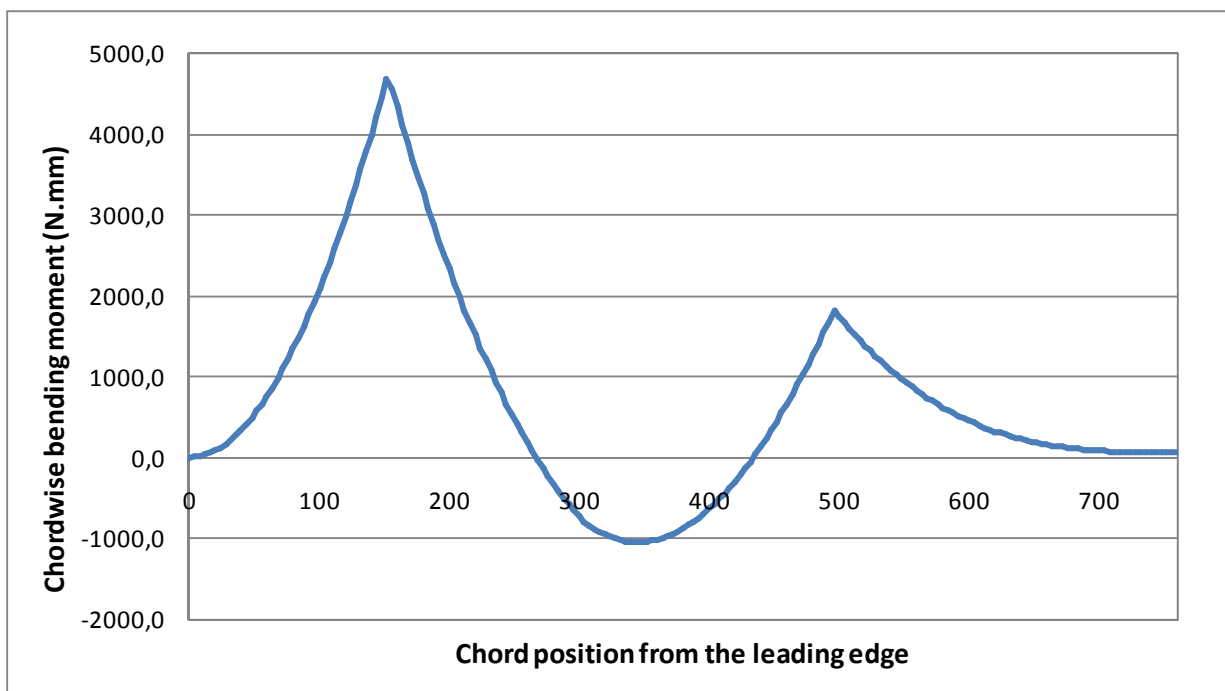
$$BM(x) = BM_{airload} + BM_{Reaction \text{ at front spar}} + BM_{Due \text{ to } q} + BM_{Reaction \text{ at rear spar}}$$

$$BM(x) = BM_{airload} + q_{ab} \cdot h_1 \cdot x + q \cdot y(x) \cdot x + q_{cd} \cdot h_2 \cdot x$$

### 9.5.3. Shear Force and Bending Moment diagrams



Rib under airload shear force diagram



Rib under airload bending moment diagram

- ➔ The maximum Ultimate shear force is 59.5N.
- ➔ The maximum Ultimate bending moment is 4687N.mm.

#### 9.5.4. Strength of the rib:

##### → Material

The rib is made with structural PVC foam with the following properties:

|                        |                     |
|------------------------|---------------------|
| -Shear strength:       | 1.30MPa             |
| -Tensile strength:     | 2MPa                |
| -Compressive strength: | 1.5MPa              |
| -Young modulus:        | 60MPa               |
| -Shear modulus:        | 30MPa               |
| -Density:              | 80kg/m <sup>3</sup> |

##### → Stress due to the bending

The rib has a thickness of  $b=10\text{mm}$ .

The minimum height of the wing box is  $h=86\text{mm}$ .

→ The minimum moment of inertia of the rib section is:  $I_z = \frac{b.h^3}{12} = 530047\text{mm}^4$

→ The maximum bending stress in the rib section is  $\sigma_{xx} = \frac{Mf.y}{I_z} = \frac{4687 \times 40}{530047} = 0.36\text{MPa}$

→ The maximum allowable stress is 1.5MPa in compression and 2MPa in traction. The worst case is the compression. This gives us a reserve factor of:

$$RF_{bending} = \frac{1.5}{0.36} = 4.16$$

##### → Stress due to the shear

→ The maximum shear stress in a rectangular section is given by:

$$\sigma_{xy} = \frac{6}{5} \times \frac{SF_{\max}}{S} = \frac{6}{5} \times \frac{59.5}{80 \times 10} = 0.09\text{MPa}$$

→ The maximum allowable shear stress is 1.30 MPa. This gives us a reserve factor of:

$$RF_{Shear} = \frac{1.3}{0.09} = 14.4$$

The reserve factors are quite high; however, we need to keep a minimum rib thickness to make sure that there is a sufficient area to bind the skin to the rib. That is why we have chosen a minimum thickness of 10mm.

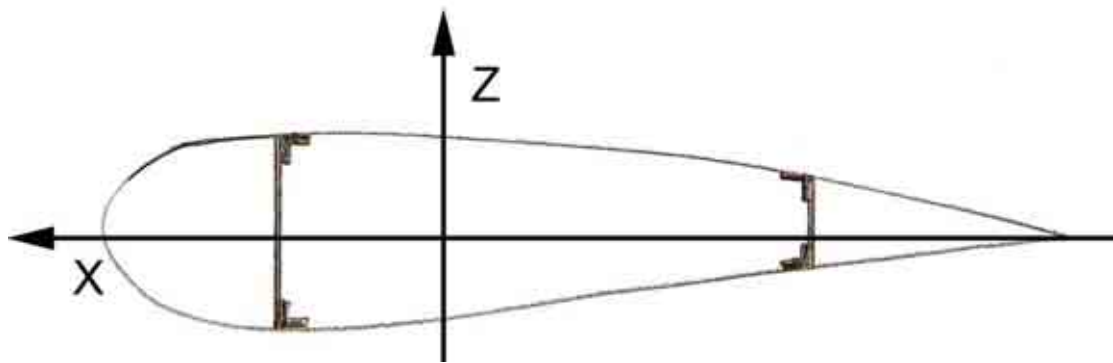
## 9.6. BUCKLING OF THE TOP WING

### 9.6.1. *Presentation of the problem*

Because of the shape of the structure, the top wing is submitted to a compressive load because of the action of the low wing, which is moving upward, because of the lift load. Therefore, we need to check that the top wing won't buckle under this compressive load.

### 9.6.2. *Section properties*

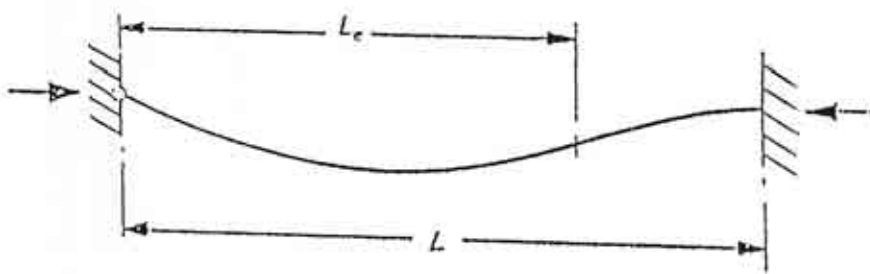
We consider the wing as a beam. The wing has two main axes of inertia that we can consider for buckling: the horizontal X and vertical Z. The axes are illustrated on the figure below:



Wing axes of inertia for buckling

The wing can be considered as a whole ensemble because the ribs and the skin maintain the spars and the booms together and prevent them from buckling individually. To calculate the second moment of area of the section we take only into account the booms area. We can see that the wing lower moment of inertia is along the X axis. If the structure buckles, it will along the X axis. Therefore, we just need to check that the buckling does not occur in this direction.

We know that the top wing is restrained at one extremity and mounted on pivot on the other tip. We can consider that we have the situation illustrated below:



Buckling of a simply restrained beam

### 9.6.3. Calculation of the Euler buckling

The Euler buckling load for a simply restrained beam is given by the formula below:

$$P_{CR} = \frac{2 \cdot \pi^2 \cdot E \cdot I}{L^2}$$

In our case we have the following parameters:

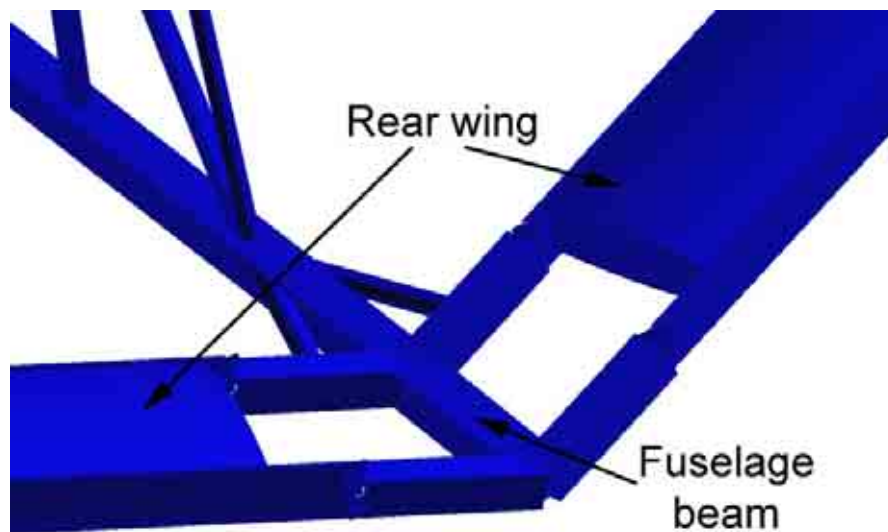
Iz: 553120mm<sup>4</sup>  
E: 93000 MPa  
L: 3800mm

➔ We get **F=70317 N**.

Knowing that the Ultimate lift force for the maximum case on one wing is 813N, we can deduce that the induced compressive load is not going to exceed the maximum Euler force, which is almost 100 times higher.

## 9.7. ATTACHMENT DETAILS

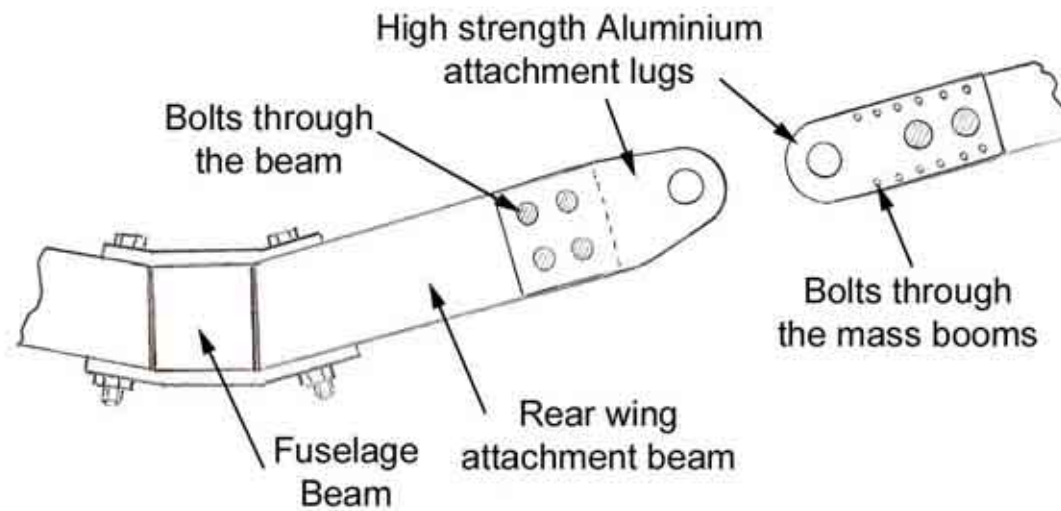
### 9.7.1. Rear wing attachments



Rear wing attachments beams

The rear wing attachment to the fuselage is realized with two aluminium beams. It is important to remember that there is, in fact, a pivot link at this point of the attachment. This pivot link is realized with 2 lugs in high strength aluminium. The shear force must be carried from the boom & spar assembly to the fuselage beam. The figure on the next page illustrates how the assembly is done to ensure this function.





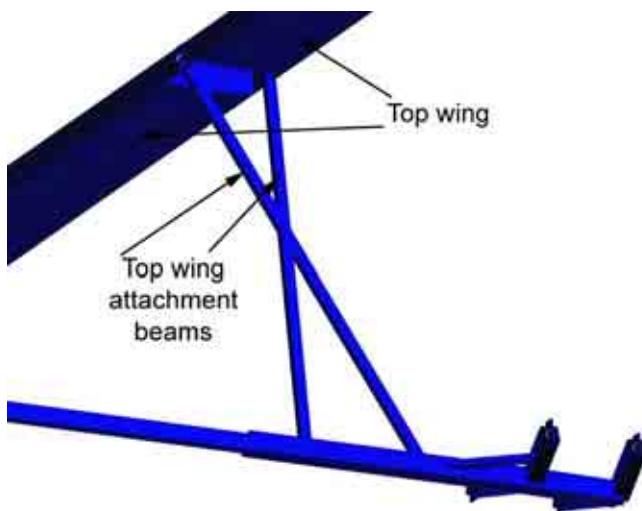
Detailed rear wing assembly

The rear lug plates are clenching the spars on both sides and there are bolts all the way through and in addition, it is bounded to make sure that the loads are distributed on the entire spar web. This is really essential. The spar web is 0.75 mm thick and it would fail under a shear force applied by the bolts. In addition, some small bolts are put through the mass booms to ensure that the spar assembly remains all together.

#### ➔ **Lug material and design**

This part of the structure is critical. It has to be designed very carefully. Aluminium alloy with a strength of not less than 450 MPa has to be used for the lugs and spars attachments. Additional work is necessary to determine the lugs properties and the attachment to the spar required to get the lightest fail-safe structure.

#### 9.7.2. *Top wing root attachment*

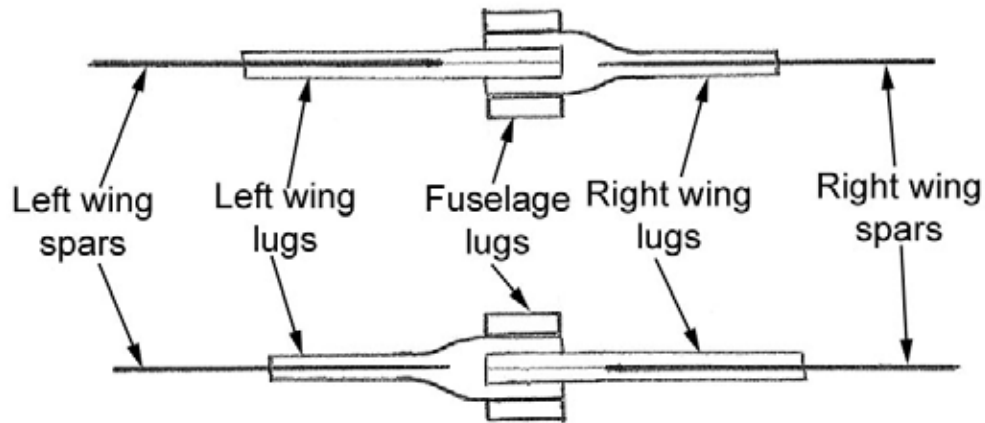


Top wing attachment beams

The top wing is attached to the fuselage with two vertical beams.

The spars are joined together with a pivot link and they are also joined to the two vertical beams. The link is ensured with a lug.

The figure on the next page illustrates how the lug is designed.



Top view of the top wing attachments

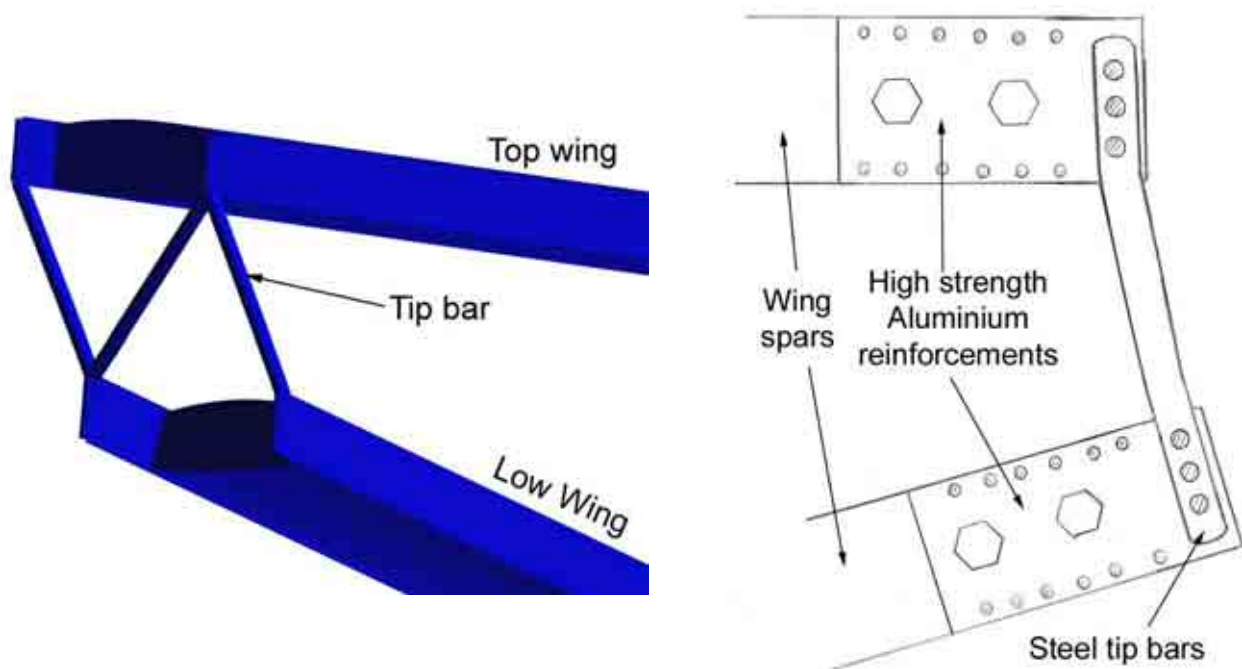
These attachments are similar to the one designed for the rear wing. The difference is that there is a junction of the two wings on the same beam. Each lug is split into two parts. This is to ensure that the design is fail-safe. The lugs must be able to withstand the limit load without failing in case of failure on one side of the lug.

#### ➔ **Material and design**

As for the rear wing attachment, detailed calculations need to be done on this part. However, the spar reinforcement and lug must be in high strength aluminium with a strength not less than 450 MPa.

It is very important to make this part fail-safe. It is a vital element of the aircraft structure.

### 9.7.3. Wing tips attachments



Wing tips attachments

The figures above show how the tips are joined together. The finite element analysis has proven that the loads are actually reduced if both wings are rigidly connected in bending at the tips. This is because the wing structure is not truly triangulated at the tips. The tip reinforcements are in high strength aluminium and they are completely similar to what has been shown for the root before.

#### ➔ **Material and design**

The tips bars have been tested with the finite element model. The geometry and the material have been chosen.

The material required for the tips bar is an S45000 series steel with a strength of not less than 900MPa.

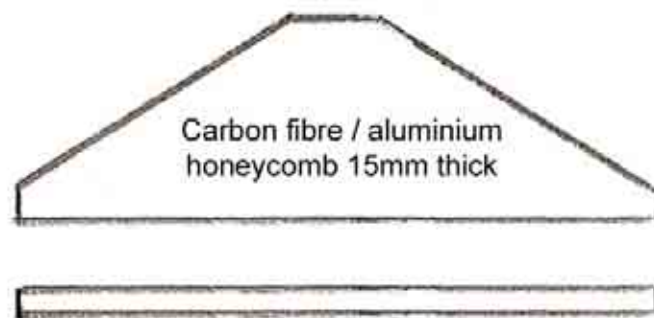
The bars have a diameter of 24 mm and a thickness of 2 mm.

# 10. TAIL AND CONTROL SURFACES DESIGN

## 10.1.TAILPLANE DESIGN

### 10.1.1. Tailplane layout

For most of the very light aircraft designs, the tailplane is made of a flat surface. This allows for a very simple design and does not greatly affect the performance. This is the method we will use for our design. We will use a carbon fibre epoxy skin / aramid core honeycomb structure. The shape of the tailplane is represented below:



Tailplane general layout

### 10.1.2. Tailplane preliminary design

#### → Structural model

The tailplane has an axis of symmetry along the fuselage axe. We can consider only half of the tailplane and consider that the root is fully restrained.

For the design of the tailplane we will use the engineering bending theory and consider that half of the tailplane is a cantilever beam restrained at the root. This is a rough approximation; however, we are going to check our assumptions with a correct finite element model.

#### → Maximum loads

From the loading actions based on the CS-VLA we get that the maximum ultimate bending moment at the root is equal to 698 N.m.

### → Minimum laminate thickness required

The axial force in the top and bottom skin of the sandwich structure can be calculated with the following formula (where h is the sandwich panel thickness):

$$P = \frac{M}{h} = \frac{698}{0.015} = 46534N$$

The length of the root is 800 mm. If we divide P by this length we get a loading of 58 N/mm. Now, we can use Coala to determine the right laminate to choose. The results are summarised in the table below:

| <b>LAM_1-1 (0,1/60,1/120,1)s 0.75</b> |               |
|---------------------------------------|---------------|
| <b>Tensile load (N/mm)</b>            | <b>58</b>     |
| <b>Tsai-Wu stress RF</b>              | <b>5.68</b>   |
| <b>Tsai_wu strain RF</b>              | <b>5.68</b>   |
| <b>max strain</b>                     | <b>0.0014</b> |

Tailplane laminate result table

The reserve factors are quite high. However, we do not want to reduce the laminate thickness too much because it will become hard to find and to manufacture. 0.75 represents a good compromise. The maximum strain is below 0.004 and so the structure is safe from a fatigue and damage tolerance point of view.

### → Laminate selection

For tailplane honeycomb structure I have chosen the following carbon fibre-epoxy laminate:

- Name convention : LAM\_1-1
- $E_1=140\text{GPa}$ ,  $E_2=10\text{GPa}$ ,  $G_{12}=5\text{GPa}$ ,  $\nu_{12}=0.3$
- $X_t=1.5\text{GPa}$ ,  $X_c=1.2\text{GPa}$ ,  $Y_t=50\text{MPa}$ ,  $Y_c=250\text{MPa}$ ,  $S=70\text{MPa}$
- Layout:  $(0_1/60_1/120_1)_s$
- Ply thickness: 0.125mm
- Total thickness: 0.75mm

The high strength aramid honeycomb core has the following properties:

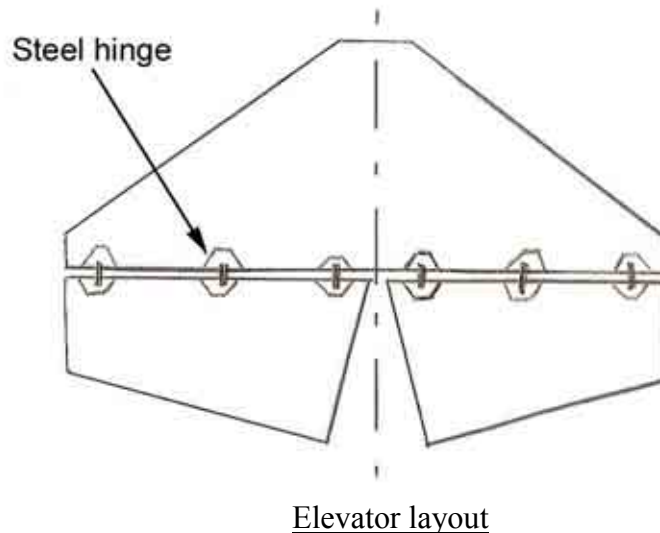
- Compression strength : 0.60 MPa
- L shears strength: 0.50 MPa
- W shears strength: 0.25 MPa
- Compression modulus: 38 MPa
- L shears modulus: 16 MPa
- W shears modulus: 11 MPa

**☑ Note: the composite skin material used is the same as used for the spars, to reduce the cost.**

## 10.2.ELEVATOR DESIGN

### 10.2.1. Elevator layout

Like the tailplane, the Elevator is made with carbon fibre epoxy skin / aramid core honeycomb structure. There are three hinges per side, one at each tip and one in the middle. The elevator layout is illustrated in the figure below:



### 10.2.2. Elevator preliminary design

From the CS-VLA we find that the maximum load on the elevator is  $883\text{N/m}^2$ , whereas the maximum load on the tailplane is  $1039\text{ N/m}^2$ .

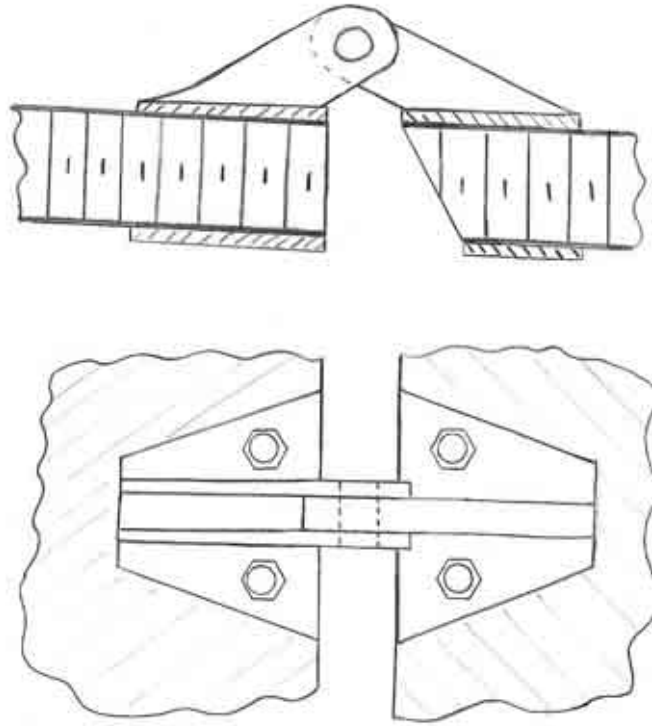
Because of the geometry of the structure, the elevator is not submitted to stress as high as the tailplane; in fact, the tailplane is a cantilever beam, so it has a lot of stress at the root. On the contrary, the elevator has 3 attachment points and so the load is distributed spanwise and the components are less stressed.

➔ It is conservative to use the same sandwich laminate for the elevator and the tailplane and it reduces the costs.

➔ The finite element model of the assembly will allow us to check that the structure is safe.

### 10.2.3. Elevator hinge design

The figure below illustrates a possible configuration for the elevator hinge design. It is made with a steel lug mounted on two steel panels on each side of the sandwich structure to distribute the load on a large area. When the correct position is determined, the steel panels are bounded and bolted on the sandwich panel.



Elevator hinge configuration

There is no need to design each lug to be fail-safe since we have 3 hinges per side. On the other hand, we need to design the hinges so that in the case of failure of one hinge, the two remaining hinges are able to withstand the limit load without failure.

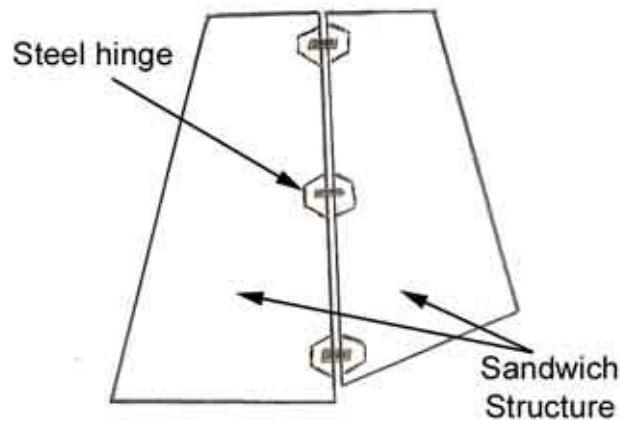
Having three hinges per side is good from a safety point of view, however great care must be taken for the assembly of the control surface; in fact, the three lug axis has to be aligned, which is quite hard to achieve. That is why the hinges have to be designed with some looseness.

The lugs have to be mounted on the top surfaces of the elevator and tailplane. In this way, the pilot can notice easily if the hinges are damaged during the pre-flight visit.

## 10.3.FIN AND RUDDER DESIGN

### 10.3.1. Fin and rudder layout

The fin and rudder structure is going to be very similar to the tailplane and elevator structure. Both the fin and rudder are made with a sandwich structure. The fin and rudder geometry is illustrated on the figure below:



Fin and rudder layout

### 10.3.2. Fin initial design

#### → Fin structural model

As we did for the tailplane, we will use the engineering bending theory for the initial design of the fin. The fin is considered to be a cantilever beam fully restrained at the root. This is a rough assumption, but the finite element model will allow us to check if the structure is safe.

#### → Fin maximum loads

From the loading actions based on the CS-VLA we get that the maximum ultimate bending moment at the fin root is equal to 854 N.m.

#### → Fin minimum laminate thickness required

The axial force in the top and bottom skin of the sandwich structure can be calculated with the following formula (where  $h$  is the sandwich panel thickness):

$$P = \frac{M}{h} = \frac{854}{0.015} = 59934N$$

The length of the fin root is 800 mm. If we divide  $P$  by this length we get a loading of 72 N/mm. Now, we can use Coala to determine the right laminate to choose. The results are summarised in the table on the next page.



| LAM_1-1 (0,1/60,1/120,1)s 0.75 |       |
|--------------------------------|-------|
| Tensile load (N/mm)            | 72    |
| Tsai-Wu stress RF              | 4.46  |
| Tsai_wu strain RF              | 4.46  |
| max strain                     | 0.003 |

Fin laminate result table

We can see that the reserve factors are greater than one and that the strain is less than 0.004. We use the same laminate that we used for the tailplane and elevator, which gives great advantages in terms of cost reduction.

#### → **Fin laminate selection**

For fin skin structure I have chosen the following carbon fibre-epoxy laminate:

- Name convention : LAM\_1-1
- $E_1=140\text{GPa}$ ,  $E_2=10\text{GPa}$ ,  $G_{12}=5\text{GPa}$ ,  $\nu_{12}=0.3$
- $X_t=1.5\text{GPa}$ ,  $X_c=1.2\text{GPa}$ ,  $Y_t=50\text{MPa}$ ,  $Y_c=250\text{MPa}$ ,  $S=70\text{MPa}$
- Layout: (0<sub>1</sub>/60<sub>1</sub>/120<sub>1</sub>)s
- Ply thickness: 0.125mm
- Total thickness: 0.75mm

The high strength aramid honeycomb core has the following properties:

- Compression strength : 0.60 MPa
- L shears strength: 0.50 MPa
- W shears strength: 0.25 MPa
- Compression modulus: 38 MPa
- L shears modulus: 16 MPa
- W shears modulus: 11 MPa

#### 10.3.3. *Rudder initial design*

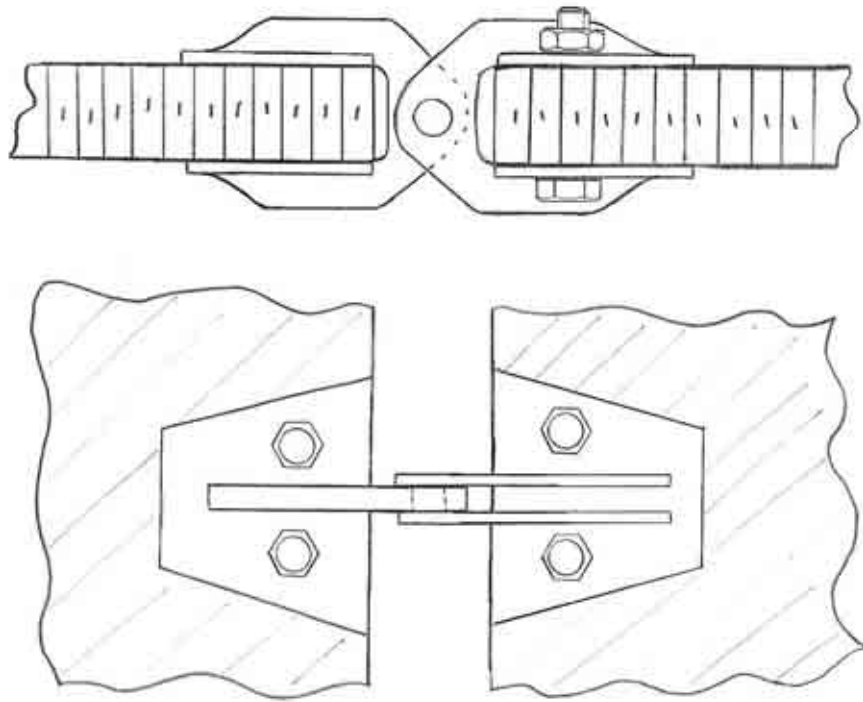
For the exact same reason as the elevator design, we know that the load in the rudder is lower than the stress in the fin. Therefore, we know that it is conservative to use the same sandwich structure for the rudder than for the fin. In addition, it makes the design easier and cheaper.

→ **The rudder uses the same sandwich structure as the fin.**

#### 10.3.4. *Rudder hinge design*

As we did for the elevator, the rudder is fitted with 3 hinges to make the design fail-safe. It has to be proven that the structure is able to withstand limit load without failure in case of one hinge failure.

A possible hinge design is presented on the next page. The hinge is made out of steel.

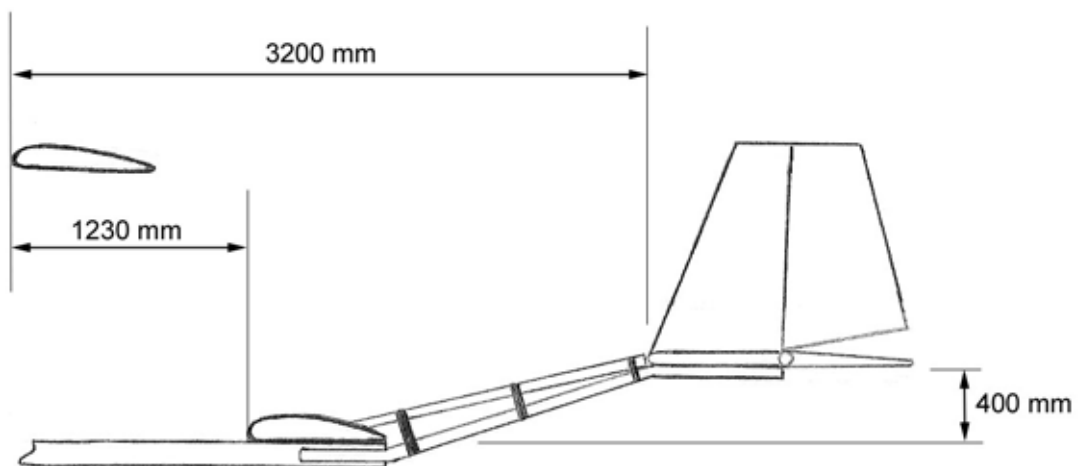


Rudder hinge configuration

The notes that have been made for the elevator hinges are applied on this design too. The hinges panels are bolted and bounded on the sandwich panel.

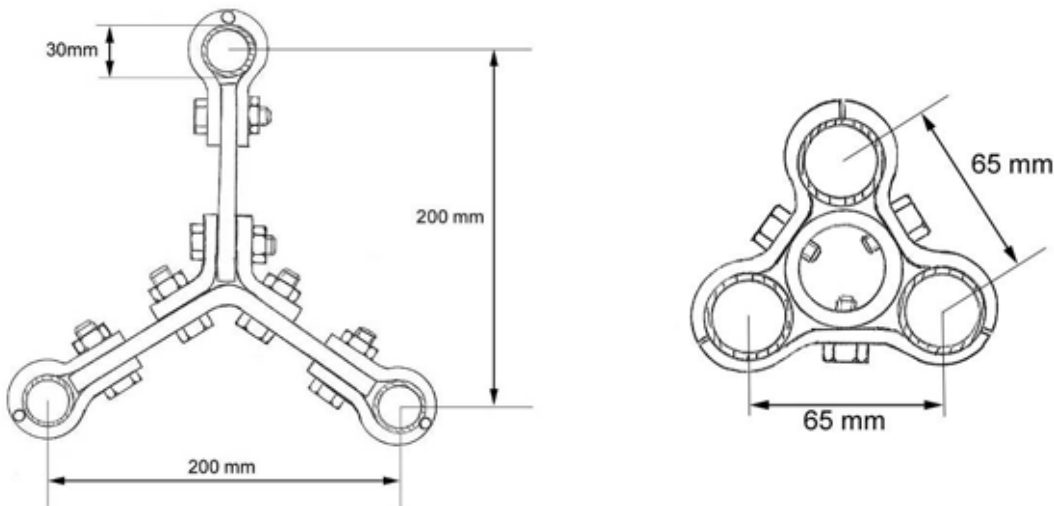
## 10.4.TAIL STRUCTURE DESIGN

### *10.4.1. Tail general layout*



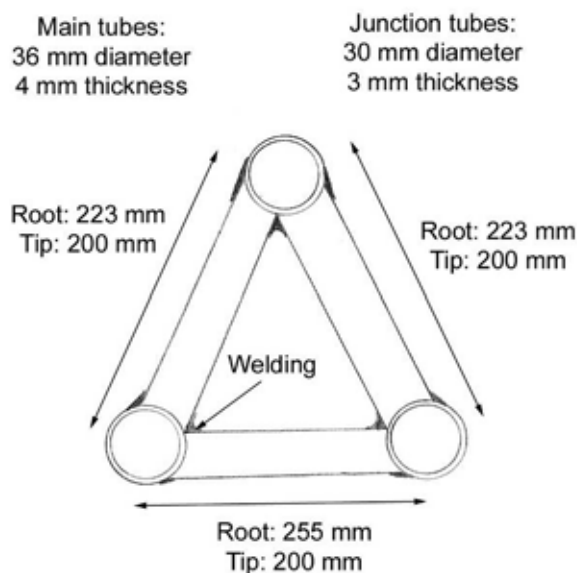
Tail general layout

The tail beam is made of three circular aluminium tubes with a triangular repartition. This allows us to get easily a variable second moment of area, and so an optimised structure. The second moment of area is the biggest at the root, at the junction with the fuselage, where the bending moment arm is the longest. The geometry is illustrated on the figures below:



Tail beam assembly layout, fuselage (left) & tailplane (right) junctions

These drawings show what can be done to assemble the three tubes of the tail beam. The two bottom tubes are attached to the tailplane. The top tube is attached to the fin. At the junction with the fuselage, the bottom tubes and the top tube are attached to the fuselage main beam. The three tubes are wrapped in fabric to give nice aerodynamic properties to the tail. The design on the top left has the advantage to use less material. However, the torsional stiffness of the beam is poor with this design.

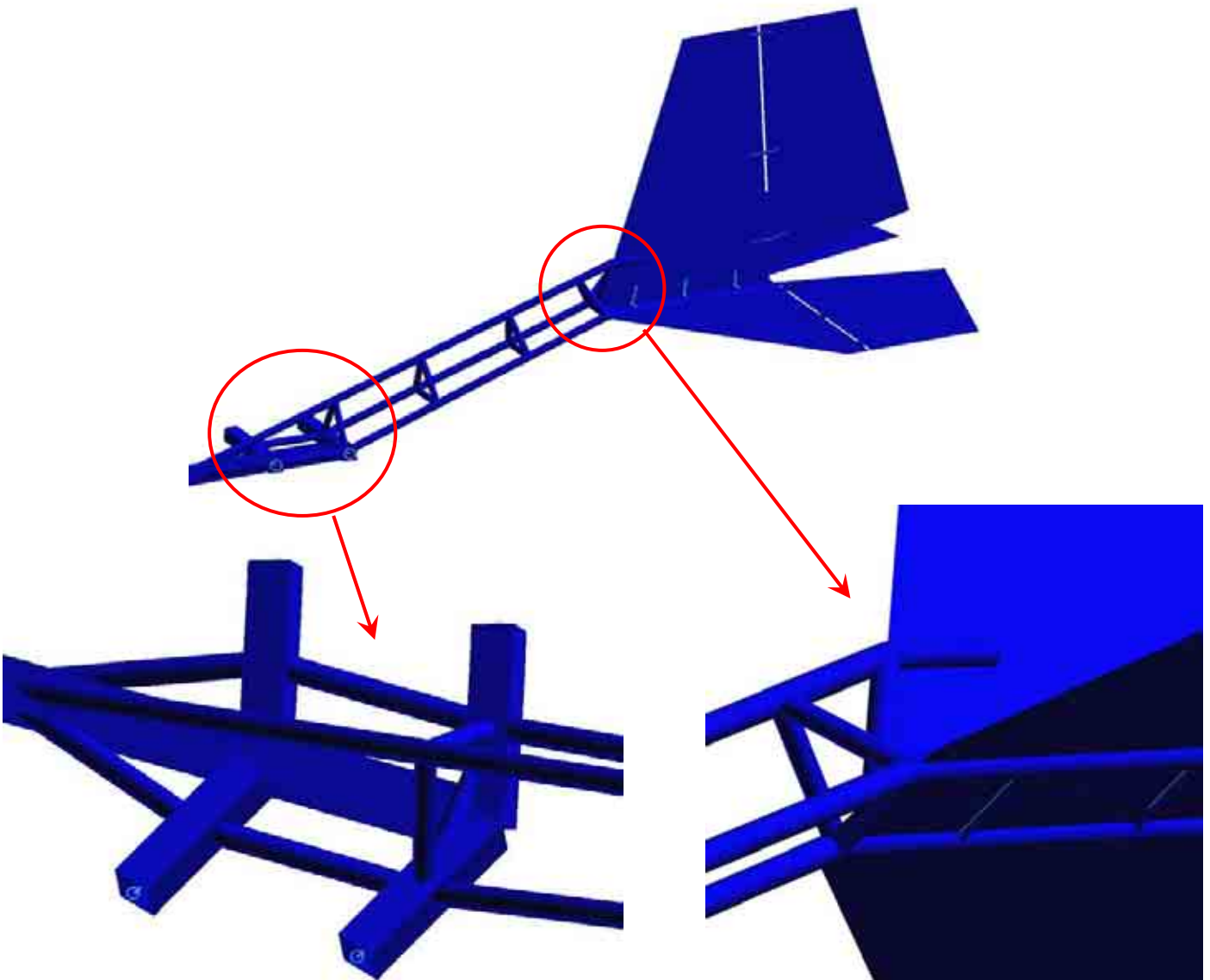


Tail beam layout

It has been verified with finite elements that the best torsional stiffness is achieved by joining the beam as illustrated on the left: the main beams are joined together by aluminium tubes. Everything is welded together.

This section has proven to be efficient in bending and in torsion too, although a continuous circular section is the best for torsion. However, this section is lighter and in the main loads put the tail beam in bending and not in torsion.

#### 10.4.2. Details of the tail beam attachments



Patran tail beam Finite Element model.

The two bottom tubes are attached on the entire tailplane width. There is a distance of 200 mm between them. They are fixed under the tailplane with brackets bolted through the sandwich structure of the tailplane. They transfer the non-symmetrical loads into torque in the tail beam. It is important to notice that the top beam is attached to the fin. This helps to transfer the torque to the tail beam, but it also transfers the vertical bending loads.

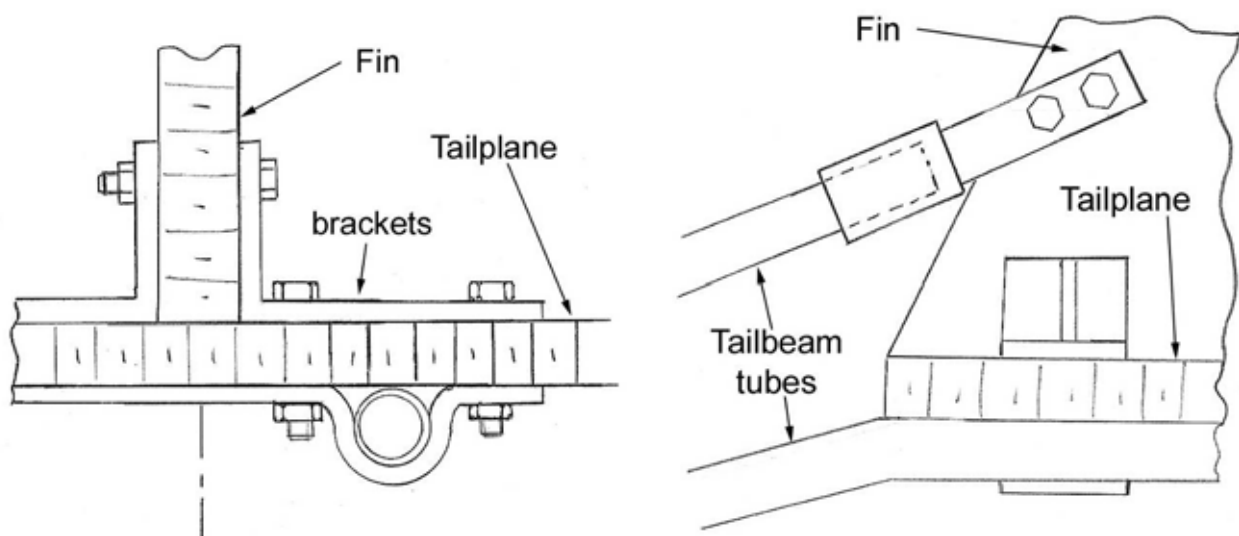
At the root we can notice that the two bottom beams are attached to the rear wing support beam and then they join to the main fuselage tube. The loads are distributed in the fuselage and at the same time, the rear wing support beam assembly is stiffened. This assembly is important since it ensures the lateral stiffness of the tail.

The top beam goes directly to the main fuselage tube. The top beam is stabilized by the triangles joint which maintain the tail beam shape. The top tube ensures the vertical stiffness.



Tailplane / fin brackets attachments

In this view we can see the brackets which hold the fin and the tailplane together. The tubes seem to go through the sandwich section but in reality they are UNDER the tail plane. The fin-tailplane brackets are bolted through the tailplane and they coincide with the brackets which hold the tailplane and the tubes together as illustrated below:



Tail bracket assembly detail

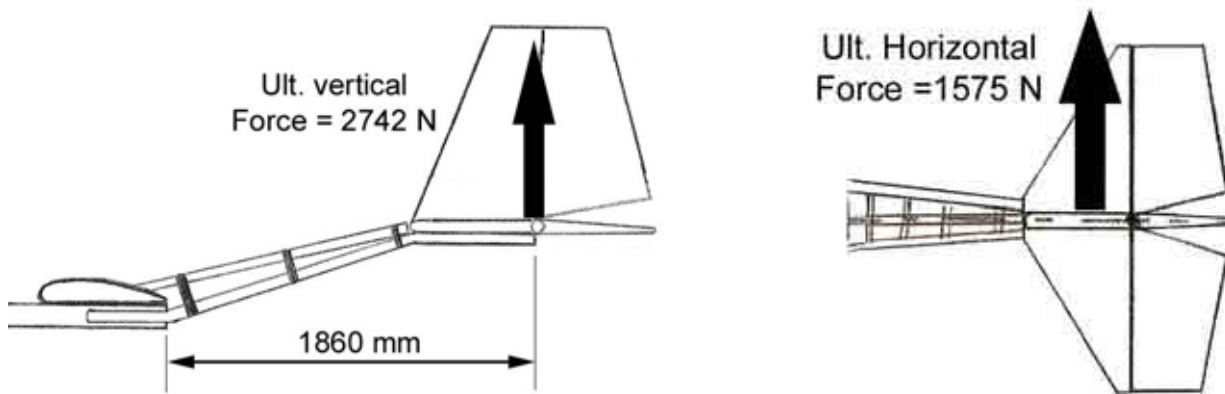
The designs above illustrate how the tail beam can be attached to the tail. The designs are not to scale, but they are given to understand the concepts.

This design has been tested with finite elements and it is safe. However, there is an issue concerning the deflection in case of combined limit loads on the fin and tailplane. It must be possible to optimise the tail beam structure to reduce the deflection.

### 10.4.3. Tail beam initial stress calculation

#### → Tail beam loads

The tail beam is submitted to a bending moment due to the force on the tailplane and fin. The force on the tailplane has been determined in loading actions, according to the CS-VLA. If we suppose that the lift has rectangular distribution chordwise, then the force is applied at mid chord of the tailplane and elevator. The picture below illustrates the forces:

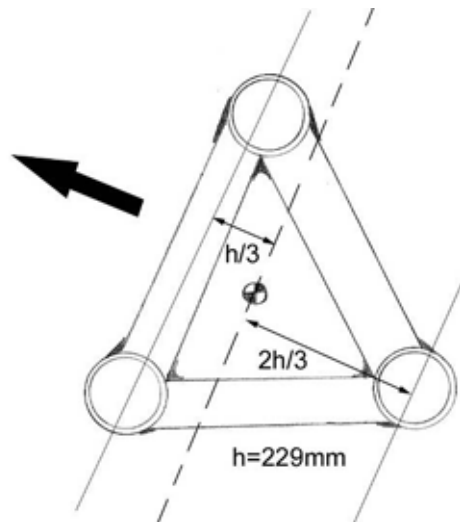


Force on the tail beam

→ The maximum bending moment at the root is  $\sqrt{2742^2 + 1575^2} \times 1.86 = 5888 \text{ N.m}$

#### → Tail beam second moment of area

The geometry of the tail beam at the root is illustrated on the figure below:



Tail beam second moment of area

- The neutral axis is located at one third of the height of the triangle.
- Each tube has a diameter of 36mm and a thickness of 2mm which represents an area of 854 mm<sup>2</sup>.

We consider only the three main tubes for the calculations. The other tubes are just joining the three main beams to give it torsional stiffness. We can now calculate the second moment of area of the section.

$$\Rightarrow I_z = \left(\frac{2}{3}h\right)^2 \times a^2 + 2 \times \left(\frac{1}{3}h\right)^2 \times a^2 = 29.85 \times 10^6 \text{ mm}^4$$

#### ➔ **Maximum stress in the tube**

We can now calculate the bending stress in the tubes:

$$\sigma_{xx} = \frac{M \cdot y}{I_z} = 31 \text{ MPa}$$

The stress seems low, but this does not include the torsion in the tube. In addition, the structure of the tail beam needs to be stiff enough so that the deflection at the tail remains low. These tubes have been selected after several iterations with the finite element model.

#### ➔ **Material selection**

For the tail beam we use an Aluminium 7020 T6 alloy. The average strength is 320MPa. This gives us a reserve factor of:

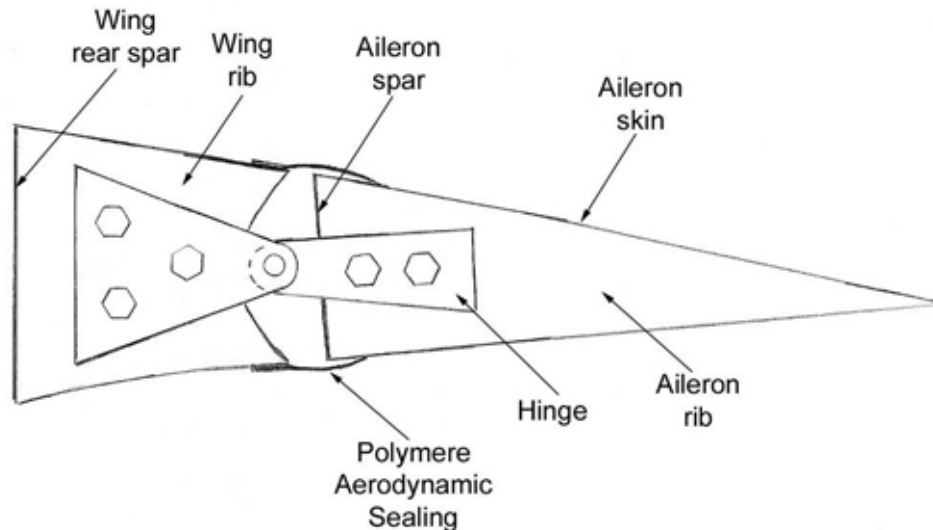
$$RF = \frac{320}{31} = 10.3$$

The reserve factor is quite high, but in this preliminary design we do not want to reduce too much the tubes diameter, so as to be able to drill holes in them and put fasteners.

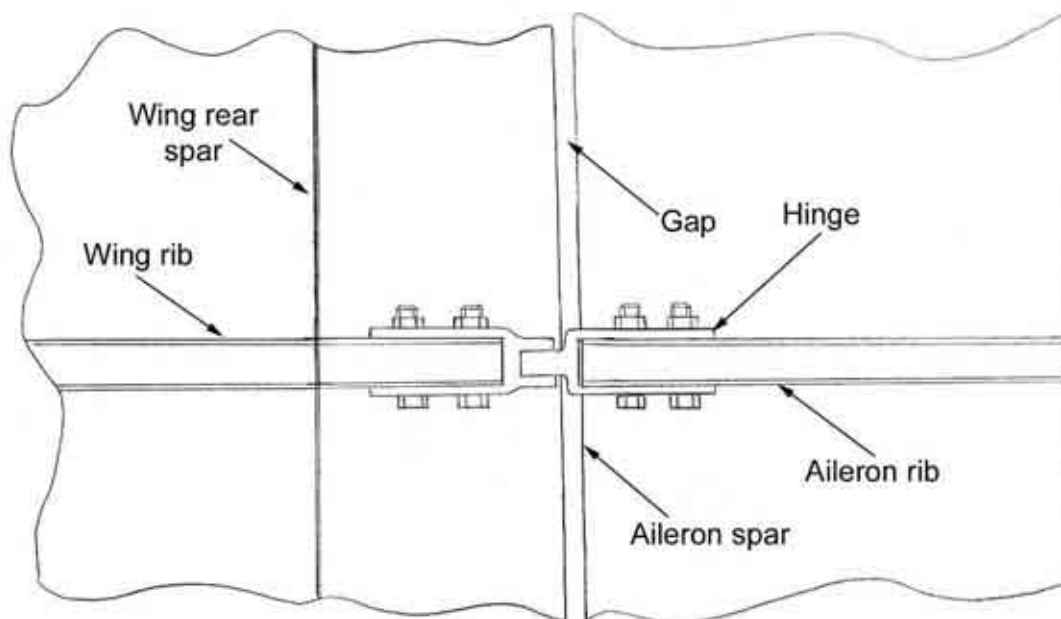
## 10.5.FLAPS AND AILERONS DESIGN

### 10.5.1. Ailerons and flaps general layout

The general layout of the ailerons is illustrated below. It is important to note that the ailerons and the flaps have the same design.



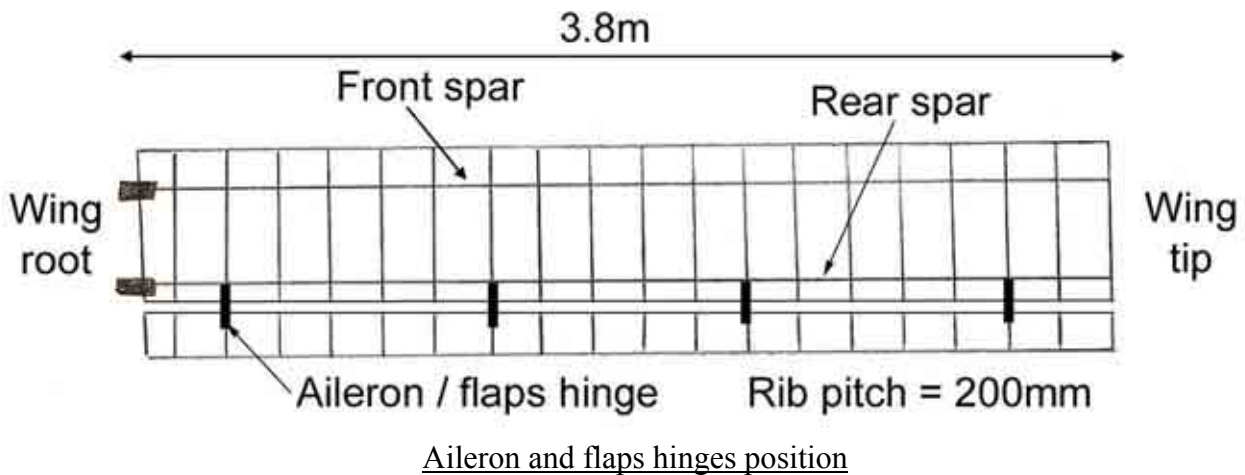
Aileron general layout: side view



Aileron general layout: top view

We can note that there is an aerodynamic sealing to cover the gap so that the airflow is not disturbed. The ailerons and flaps are fitted on the entire span: each member is 3.8 m long. They are fitted with 4 hinges.





The hinges have to correspond to a wing rib. The two extremity hinges are at 400mm from the ailerons tips and the middle hinges are at 1400 mm from the tips.

The hinge line is at 24% of the chord from the trailing edge and the spar is at 22% of the chord from the trailing edge.

### 10.5.2. Ailerons and flaps materials

#### → Ribs

The ailerons ribs and the skin ribs are the same. The rib pitch is the same. For both the ailerons and the wing, the foam ribs at the hinges location are reinforced with a carbon laminate skin on both sides. This skin transfers the loads of the hinges to the rib. The composite layout is the same as previously used. It is given hereafter:

- Name convention : LAM\_1-1
- $E_1=140\text{GPa}$ ,  $E_2=10\text{GPa}$ ,  $G_{12}=5\text{GPa}$ ,  $\nu_{12}=0.3$
- $X_t=1.5\text{GPa}$ ,  $X_c=1.2\text{GPa}$ ,  $Y_t=50\text{MPa}$ ,  $Y_c=250\text{MPa}$ ,  $S=70\text{MPa}$
- Layout:  $(0_1/60_1/120_1)_s$
- Ply thickness: 0.125mm
- Total thickness: 0.75mm

#### → Skin

The aileron skin is the same as the wing skin. It is a woven carbon fabric laminate of 0.38 mm thickness. The properties are given below:

- Name: Woven Carbon Prepregs (IM7-6K Fibre)
- $E_1=85\text{GPa}$ ,  $E_2=85\text{GPa}$ ,  $G_{12}=5\text{GPa}$ ,  $\nu_{12}=0.1$
- $X_t=700\text{MPa}$ ,  $X_c=400\text{MPa}$ ,  $Y_t=700\text{MPa}$ ,  $Y_c=400\text{MPa}$ ,  $S=50\text{MPa}$
- Layout: 1 layer  $0^\circ$  spanwise
- Ply thickness: 0.380mm
- Total thickness: 0.380mm

### → Aileron spar

The aileron spar is made out of the same laminate as the wing spar. The laminate properties are given below:

- Name convention : LAM\_1-1
- $E_1=140\text{GPa}$ ,  $E_2=10\text{GPa}$ ,  $G_{12}=5\text{GPa}$ ,  $\nu_{12}=0.3$
- $X_t=1.5\text{GPa}$ ,  $X_c=1.2\text{GPa}$ ,  $Y_t=50\text{MPa}$ ,  $Y_c=250\text{MPa}$ ,  $S=70\text{MPa}$
- Layout:  $(0_1/60_1/120_1)_s$
- Ply thickness: 0.125mm
- Total thickness: 0.75mm

### → Hinges

The hinges are made out of T6 aluminium.

## 10.5.3. Ailerons and flaps design

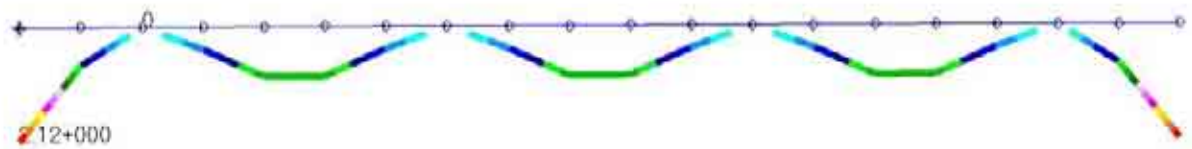
### → Aileron and flaps loads

The ailerons and flaps are submitted to an ultimate load of 134 N/m. We will check the deflection at limit load and the strength at ultimate load.

### → Calculation method

The ailerons and flaps have been calculated with a simple finite element model. We consider that only the spar will react the bending moment. Therefore, for the model we use a beam, submitted to a constant loading spanwise with a second moment of area equal to the spar second moment of area.

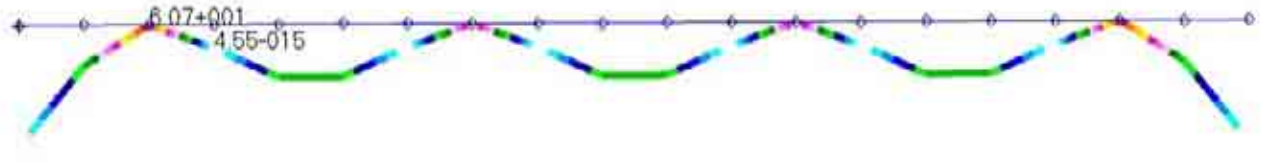
### → Deflection results



### Aileron spar deflection under limit load (mm)

The maximum aileron deflection under limit load is 2.12 mm. This is perfectly reasonable.

→ **Stress result**

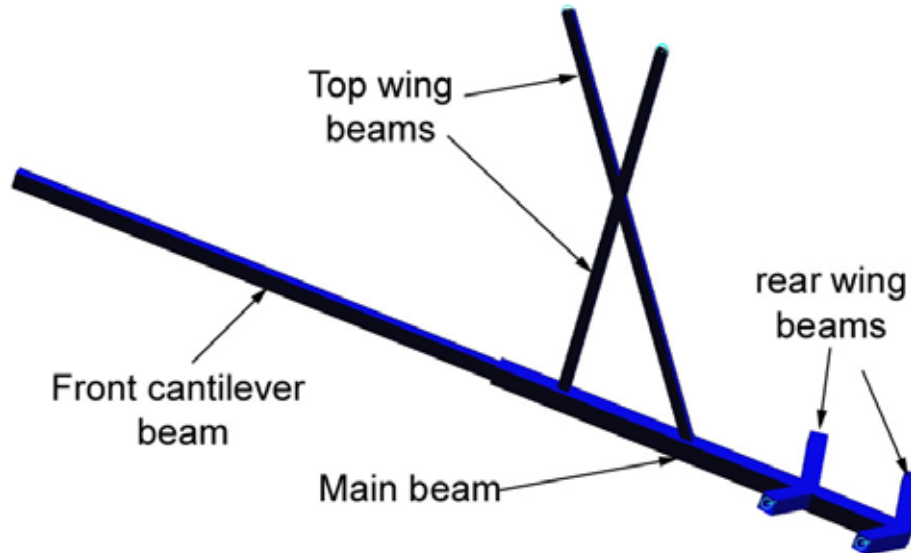


Aileron spar maximum combined stress under ultimate load (MPa)

The maximum aileron spar stress under ultimate load is 60.7 MPa. With Coala we check that this gives us a reserve factor of 3.9 and a maximum strain of 0.002 which is under 0.004, so our structure is safe.

# 11. FUSELAGE AND UNDERCARRIAGE

## 11.1. FUSELAGE GENERAL LAYOUT



Fuselage general layout

The main structure of the fuselage is simple. The four main components are represented on the picture above. The most important component is the main beam. It takes the loads of the wings, of the engine and of the front cantilever. It is also the area where the main undercarriage is mounted.

## 11.2.MAIN COMPONENTS DESIGN

The main beam has a complex loading due to the rear wing, the tail, the top wing and the front beam. The rear beams have also a complex loading due to the rear wings and the tail loads. These beams have been sized with the finite element analysis.

### 11.2.1. Front cantilever beam design

#### → Loading

The front cantilever beam is submitted to the pilot weight. The most critical case is the 4 positive G. In this case, if we consider a maximum pilot mass of 100kg, we get a force equal to:

**$4 \times 9.81 \times 100 = 3924 \text{ N}$  Limit - 5886 N ultimate.**

**The Force is applied at 700mm from the root.**

**The ultimate bending moment is 4120 N.m**

### → Stress and reserve factor

The beam has a square section of 70 x 70 mm. The material has a thickness of 3mm.

→ The second moment of area is equal to: **902289 mm<sup>4</sup>.**

→ The maximum stress is equal to  $\sigma_{xx} = \frac{Mf \cdot y_{\max}}{I_z} = 160 \text{ MPa}$

The strength of the T6 aluminium is 350 MPa. We can now calculate the reserve factor:

→ The reserve factor is equal to **2.18.**

#### *A.1.1. Top wing beams*

The top wings beams are mostly subjected to a tensile load due to the lift. However, it is important to also consider that a lateral force may occur and put the top wing beams in lateral bending. In addition, we need to consider the effect of the drag.

### → Loading

- Case 1: We consider that half the ultimate lift is transmitted in tension to the top wing beams. From the loading actions we know that this represents a vertical force of:

**6180N Ultimate.**

- Case 2: The wing mass is 38 kg. We consider a 4g lateral acceleration on the top wing (half the mass). The moment arm is 1.3 m. The load applied is equal to:

**38/2 x 9.81 x 4 x 1.5 = 1118 N Ultimate.**

**1118 x 1.3 = 1453 N.m Ultimate.**

- Case 3: The drag also needs to be taken into account. The drag will induce a bending moment on the beams. We can make an estimation of the drag and take the very pessimistic case that the drag is equal to 1/10<sup>th</sup> of the maximum lift at 4g. (case 1). The moment arm at the junction of the beam (where the structure is the weakest) is equal to 0.5 m. This gives us the maximum load equal to:

**618N Ultimate.**

**618 x 0.5 = 309 N.m Ultimate.**

➔ **Stress and reserve factor**

The two beams are identical. They have a square section of 40 x 40 mm and a thickness of 1.5 mm.

➔ **The section area is equal to 231 mm<sup>2</sup>**

➔ **The second moment of area on both beam axes is equal to 57153 mm<sup>4</sup>**

- Case 1:  $\sigma_{xx} = \frac{F_{\max}}{A} = 27 \text{ MPa}$

- Case 2: For the lateral bending we need to consider that the two beams are reacting the force. This gives us a second moment of area twice as big.

$$\sigma_{xx} = \frac{Mf \cdot y_{\max}}{I_z} = 254 \text{ MPa}$$

- Case 3: The structure is the weakest where the beam is crossing. At this point the second moment of area is the smallest. However, it is designed to be not less than two times the second moment of area of one beam. Then we deduce:

$$\sigma_{xx} = \frac{Mf \cdot y_{\max}}{I_z} = 54 \text{ MPa}$$

The most critical case is the case 2. All of the cases give us axial stress. Therefore, we can add all the stresses to calculate the most critical stress:

➔ **The total combined axial stress is 335 MPa.**

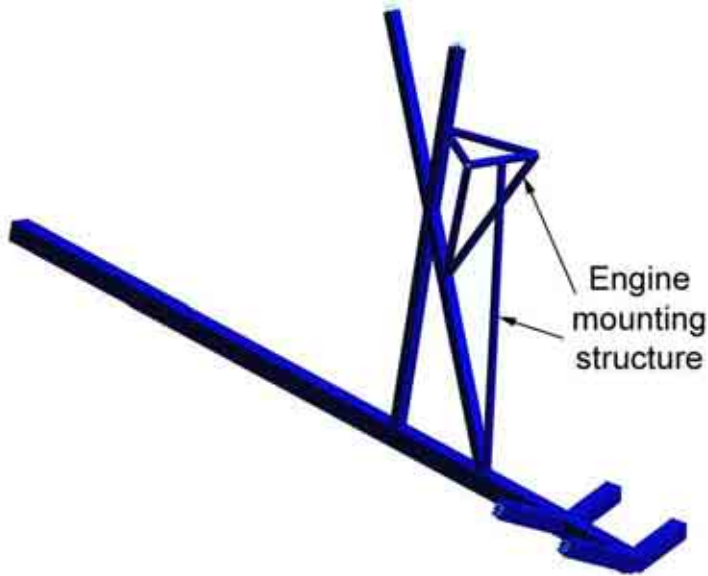
The beams are in T6 aluminium with strength of 350 MPa. We can now calculate the reserve factor:

➔ **The reserve factor is equal to 1.05**

This reserve factor may seem very low. However, we have considered very conservative cases which are unlikely to occur at the same time. Therefore, we can say that the structure is safe.

## 11.3.ENGINE MOUNTING

### 11.3.1. Engine mounting general layout



On the picture on the left we can see the layout of the engine mounting. Basically we can divide the structure into two main parts:

- The top part which will transfer the thrust to the fuselage.
- The vertical beam which ensures the engine structure stability in case of vertical accelerations.

#### Engine mounting layout

This engine mounting structure may seem odd looking; however, it has been carefully optimised to improve the global assembly efficiency:

- The top part of the engine mounting is completely triangulated. This makes the structure very stiff, which is very important to carry the thrust loads of the engine efficiently.

- This triangulated structure is mounted on both sides of the weakest point of the top wing beams, which is the intersection of the beams. This has the effect of reinforcing this area and making the structure globally stiffer.

- Finally, the vertical beam is there to react the vertical loads that occur in case of vertical accelerations. It also makes the structure stiffer for longitudinal accelerations (engine accelerations, for instance), since it increases the second moment of area of the assembly top wing beam and engine mounting for the longitudinal bending.

### 11.3.2. Engine mounting design

The top part of the engine mounting is a very hyperstatic structure and therefore, it is complex to calculate by hand. This part of the structure will be calculated with the finite elements model.

However, it is important to check that the vertical beam will not buckle. It is a very long member, in compression, which would make it a good subject for buckling. For this we will use the Euler buckling theory.

### → Loading

We can consider the following case: We assume that the inertia load due to the engine mass is completely reacted by the vertical beam in case of a 4G positive acceleration. This is very conservative since, in practice, the load would also be reacted by the top structure of the engine mounting.

We can calculate the loads as follows, knowing that the engine + propeller mass is 25kg :

$$\text{Compressive force} = 25 \times 9.81 \times 4 \times 1.5 = 1471 \text{ N Ultimate.}$$

### → Euler buckling

The tube has a diameter of 30 mm and a thickness of 1 mm. This gives a second moment of area of 9588mm<sup>4</sup>.

The tube is in T6 aluminium with a young modulus of 70 GPa.

The beam is restrained at both ends. Therefore, the Euler buckling formula is expressed as follows:

$$P_{cr} = \frac{\pi^2 EI}{(0.5L)^2} = 21898 \text{ N}$$

The Euler critical load is much higher than the applied load. Therefore, we know that the beam will not buckle.

## 11.4.UNDERCARRIAGE

The undercarriage has not yet been designed. However, this part contains the main layout of the undercarriage, and the key ideas in its design.

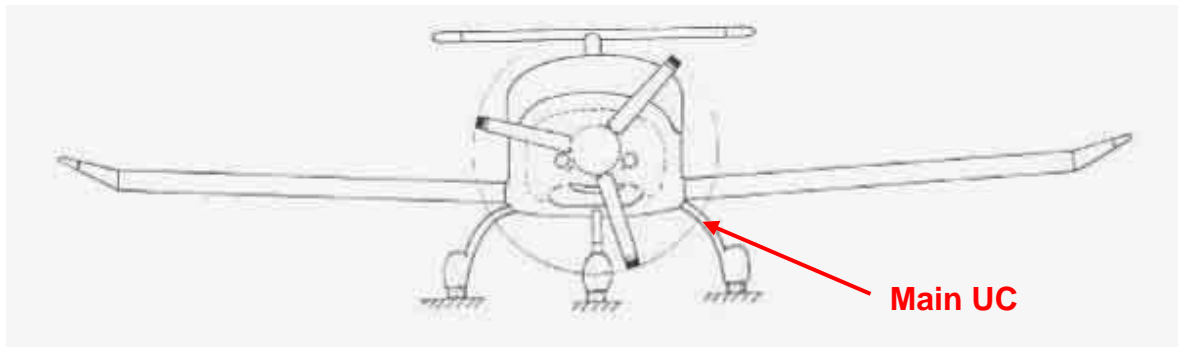
### 11.4.1. Dynaero MCR-01 undercarriage



Dynaero MCR aircraft  
(<http://www.dynaero.com/>, 8<sup>th</sup> August 2007)

The Dynaero MCR aircraft is the fastest microlight currently available on the market. It makes extensive use of composite materials and has a very well thought out structure. The main undercarriage especially is a very smart design.





Dynaero MCR front view  
(<http://www.dynaero.com/>, 8<sup>th</sup> August 2007)

I have contacted the Dynaero design office and they gave me further information concerning the main undercarriage design:

- The main undercarriage is made out of glass fibre composite material. Glass fibre has the best energy absorption over weigh ratio.
- The main undercarriage is made of one single piece of glass fibre.
- The main landing gear has been designed to withstand an impact with a 2.8m/s velocity for an aircraft of 490 kg.
- The weight of the glass fibre beam is 5.2 kg.

#### *11.4.2. Key ideas for the design*

The maximum take-off weight of the microlight is 240 kg, which is slightly less than half of the MCR. The kinetic energy is proportional to the mass; therefore, the maximum landing energy for our aircraft is twice as small.

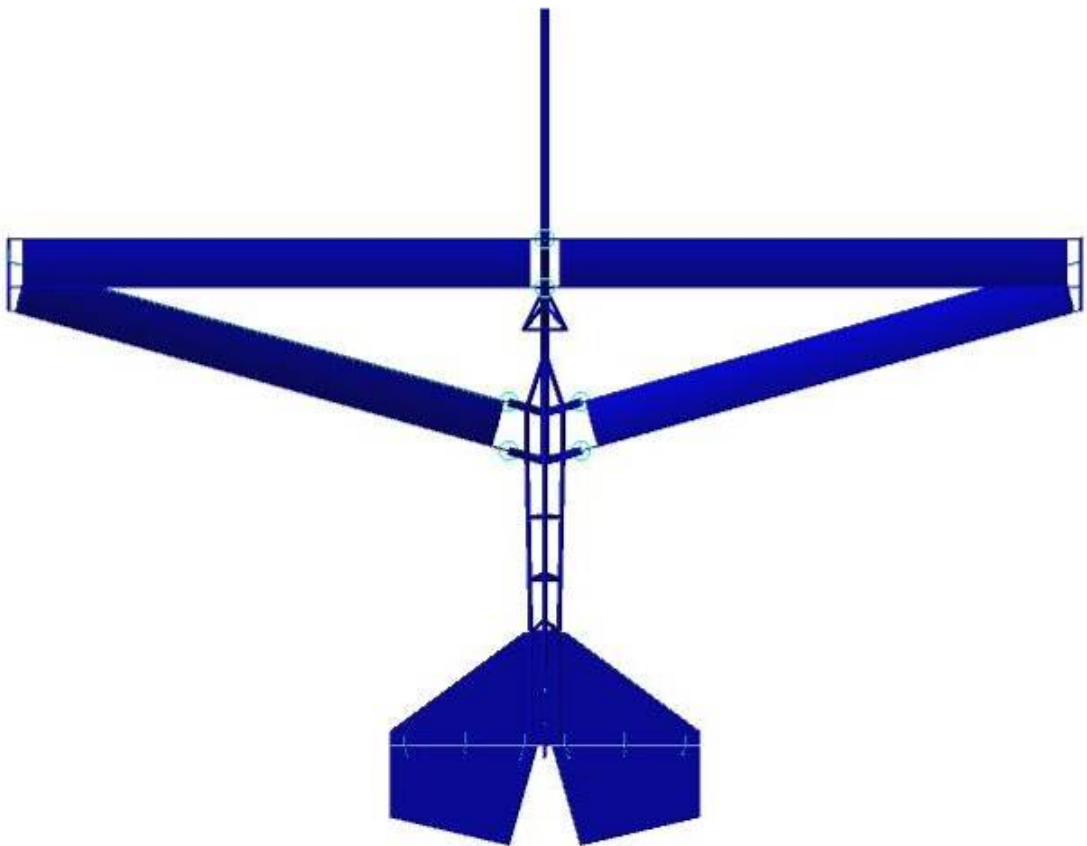
➔ This information shows that it is possible to design a very efficient undercarriage at light weight.

## 12. FINITE ELEMENT ANALYSIS

### 12.1.GLOBAL OVERVIEW OF THE MODEL



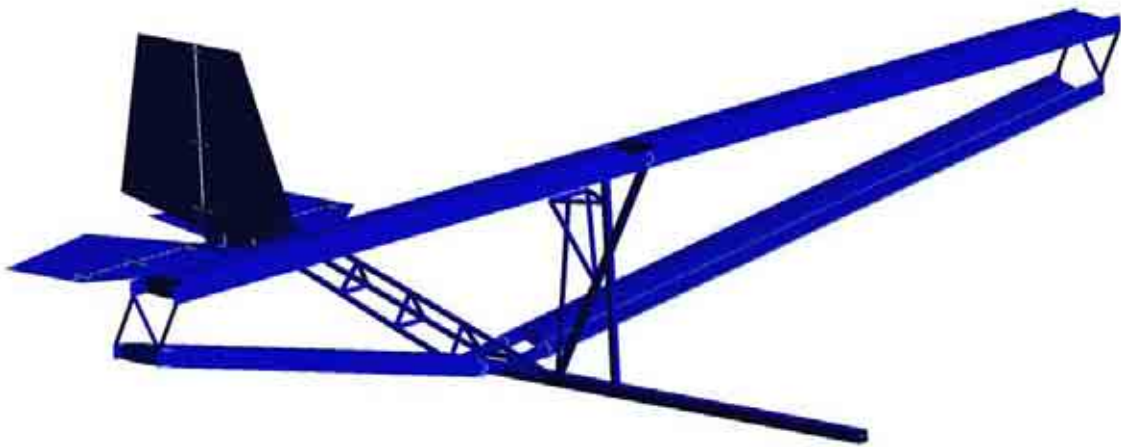
Finite element model side view



Finite element model top view



Finite element model front view



Finite element model iso view

The model has been made using MSc Patran as pre and post processor and Nastran as solver.

The finite element model has been built with 1D and 2D elements only. The finite element model contains MPC elements.

The model contains:

- 24892 nodes
- 3520 CBAR elements
- 25212 CQUAD elements

## 12.2.GEOMETRY AND MESH

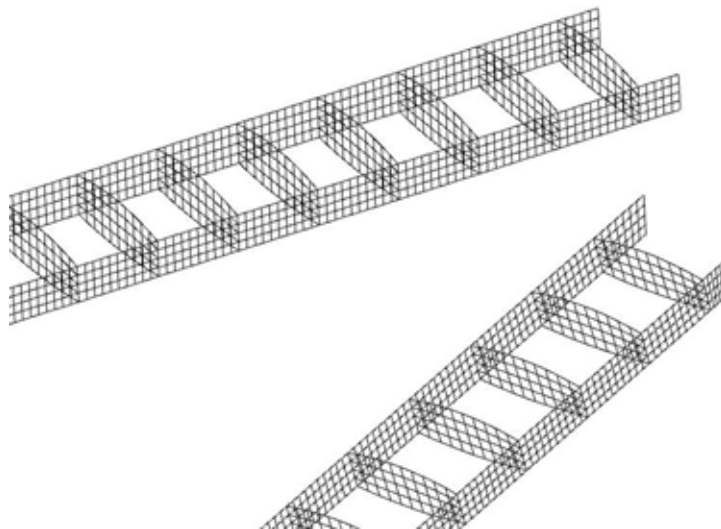
### 12.2.1. Wing

Only the wing box has been modelled. We can assume that the leading edge and the section of the wing after the rear spar will not contribute greatly to the behaviour of the general structure.

The wing has been modelled in 8 different groups:

- Top wing spars (Cquad)
- Rear wing spars (Cquad)
- Top wing ribs (Cquad)
- Rear wing ribs (Cquad)
- Top wing skin (Cquad)
- Rear wing skin (Cquad)
- Mass boom (Cbar)
- Wing tips attachments (Cbar)

It has been decided to use four elements in the depth of the rib. Four elements allows us to check an eventual bending of the rib chordwise. Once this choice has been made it determines the entire wing mesh: the rib mesh determines the spar mesh in the width, then the mesh is determined in the length to avoid distorted elements. Finally, the spar mesh determines the skin mesh and the booms mesh. This is why there are so many elements in the wing mesh.



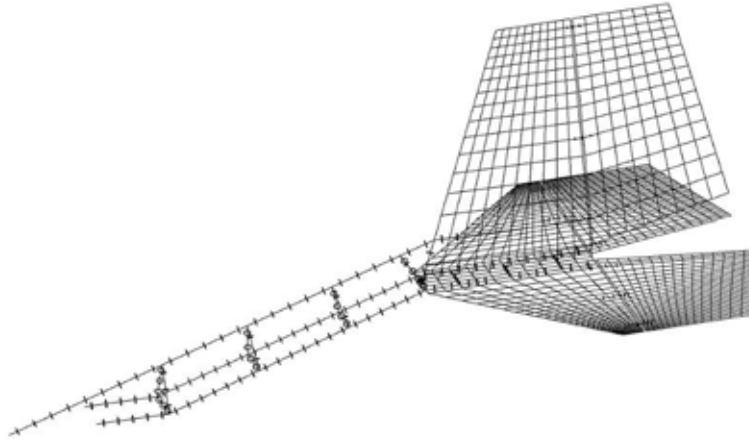
Right wings tips spar and ribs mesh

### 12.2.2. Tail

The tail has been completely modelled, including the hinges. The tail has been modelled using 6 different groups:

- Tailplane (Cquad)
- Fin (Cquad)
- Tailbeam (Cbar)
- Tail beam joints (Cbar)
- Hinges (Cbar)
- Angle brackets (Cbar)

The mesh is presented on the figure below:



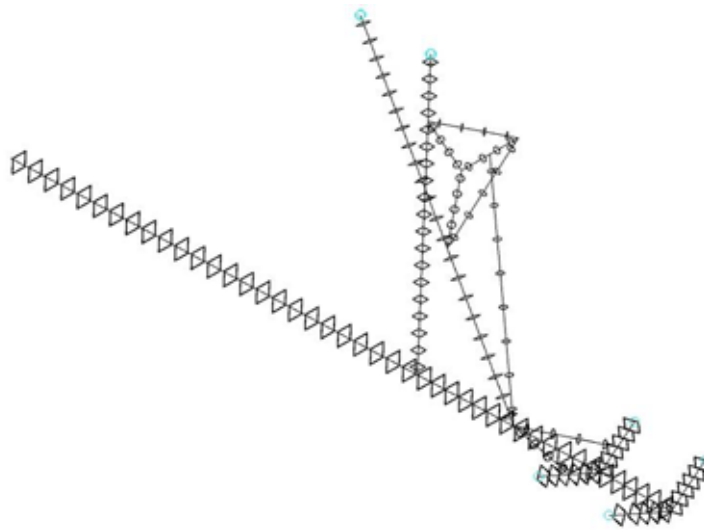
Tail mesh

### 12.2.3. Fuselage

The fuselage has been modelled using only Cbar elements. It is divided into three groups:

- Rear wing beams
- Main fuselage
- Engine Mounting

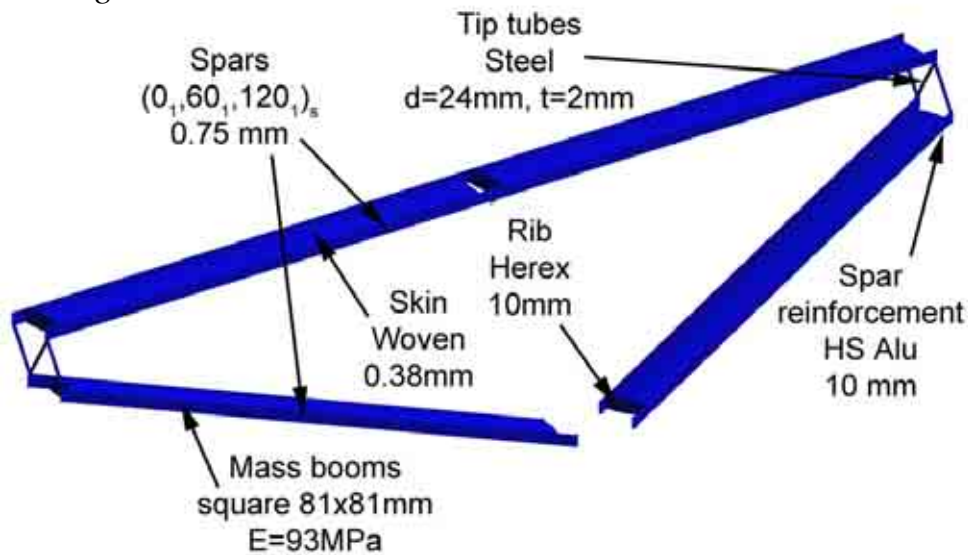
The fuselage mesh comports MPC elements to model the pivot links between the wing spars and the fuselage. The fuselage mesh is represented on the figure below:



Fuselage mesh

## 12.3.ELEMENT PROPERTIES

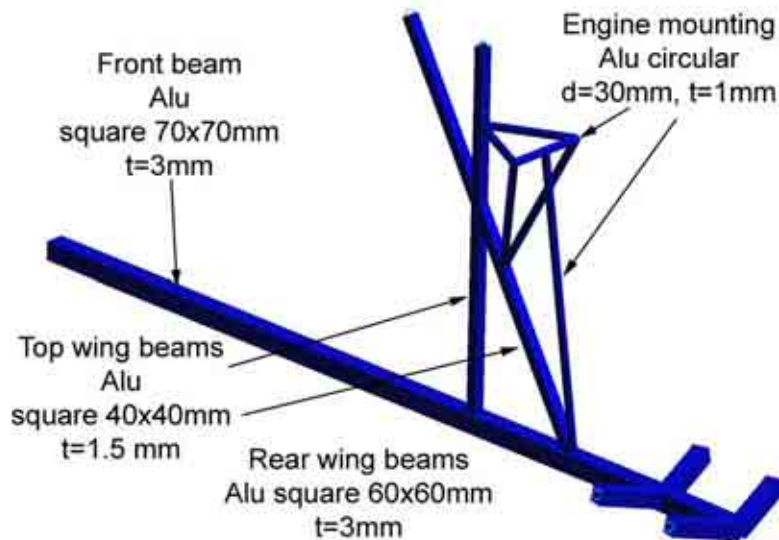
### 12.3.1. Wing



Wing properties

The mass booms have been modelled with Cbar elements. They use an isotropic material with a young modulus equal to the  $E_1$  modulus of the composite. To simplify the model a full square section has been used. The section has been calculated so that the final second moment of area of the wing is the same as the one calculated in the wing detailed design chapter.

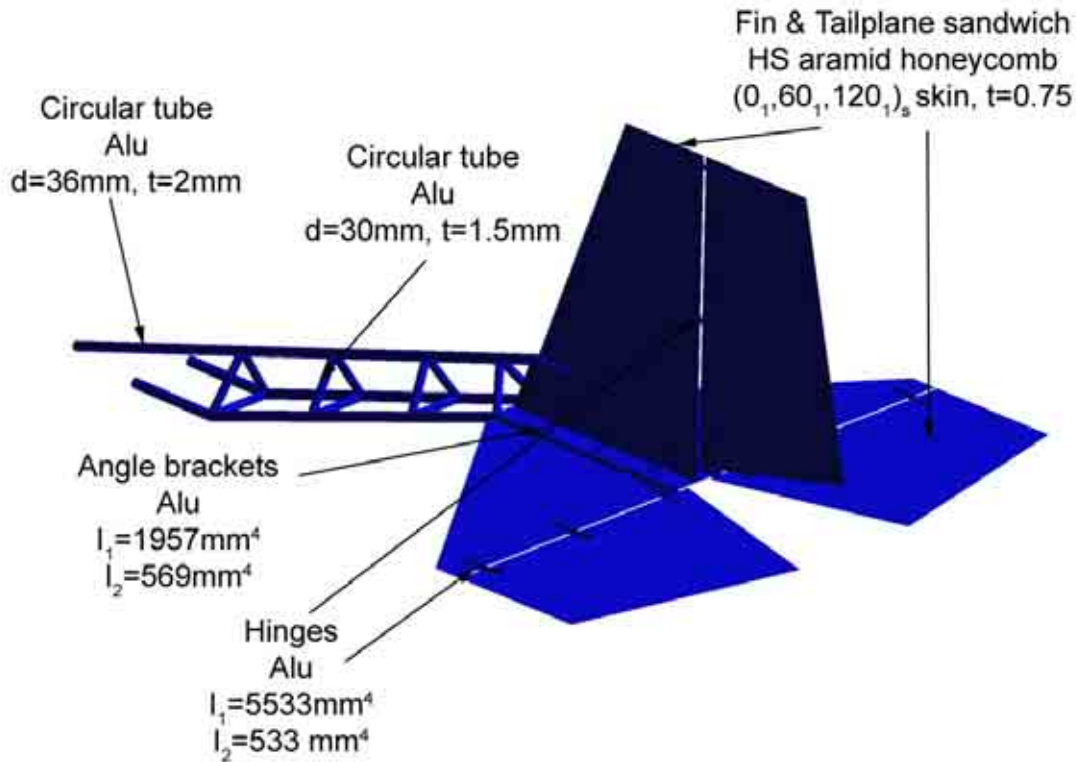
### 12.3.2. Fuselage



Fuselage properties

The entire fuselage is made with bar elements. The fuselage is in aluminium T6 with a minimum strength of 350 MPa.

### 12.3.3. Tail



Tail properties

The angle brackets  $I_1$  axis is the axis parallel to the main fuselage axis. The hinge  $I_1$  axis is the axis parallel to the hinge axis, for both the tailplane and the fin. The hinges have been modelled with rigid bar elements. They show how the shear forces loads are transferred from the elevator and rudder to the tailplane and fin. This is conservative since the bar elements will also transmit the bending to the tailplane and fin. In reality, no bending would be transferred through the hinges.

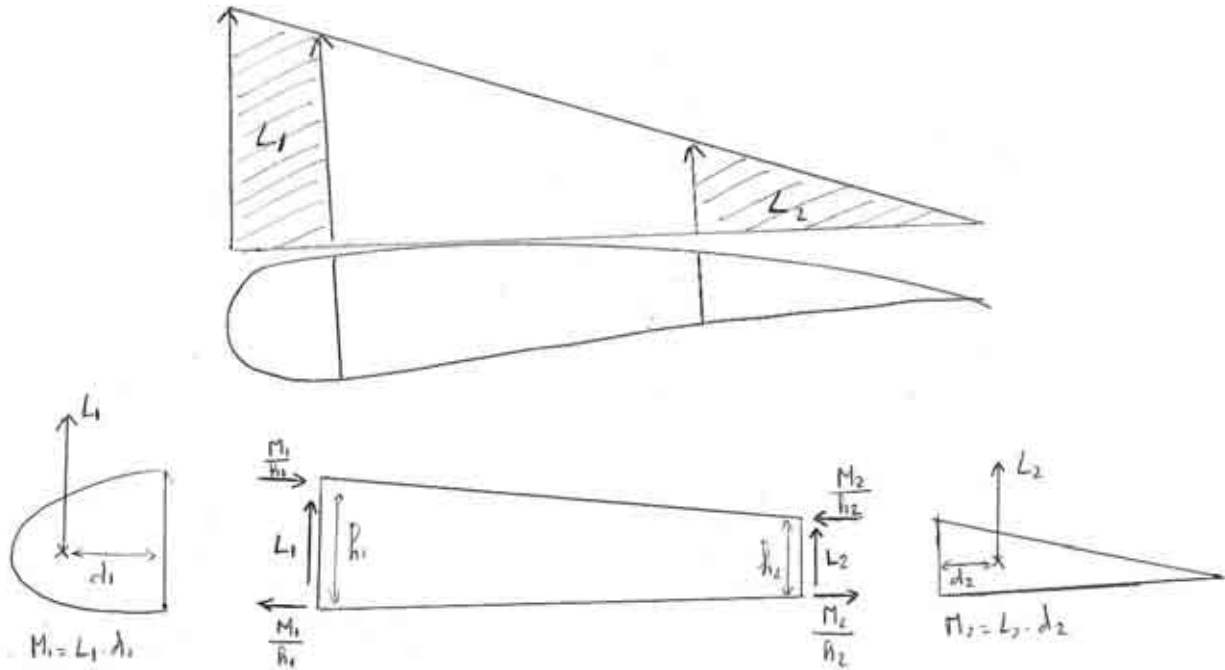
## 12.4.LOADS AND BOUNDARIES CONDITIONS

### 12.4.1. Wing loads

Only the wing box has been modelled, but it is important to take into account all the loads on the wing.

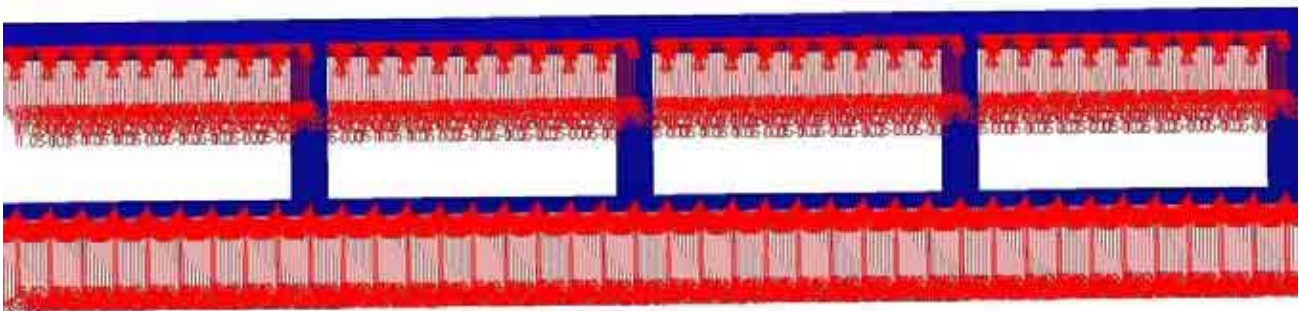
The best equivalent model, if we assume a triangular distribution, is presented below; however, a more approximate method has been used for our model, with a rectangular distribution.

The pictures on the next pages show the equivalent loading on the wing box, taking into account the loads in front of the front spar and behind the rear spar. There is a shear force and a bending moment induced. The shear force is reacted by the ribs. The bending moment is reacted by the skin.



### Wing box equivalent loading

In our model it is assumed that the entire lift is applied directly to the wing box. This has an impact on the torsional flow on the skin and on the pressure load on the skin, which is higher than the actual pressure load. It has also an impact on the shear force in the ribs. However, the shear force and the bending moment in the spars and booms are not greatly affected by this model. These components are the most important from a structural point of view for the safety of the aircraft. We assume that  $2/3^{\text{rd}}$  of the total lift is applied on the extrados of the wing and  $1/3$  of the total lift is applied on the intrados of the wing. The pressure loading is presented on the picture below:

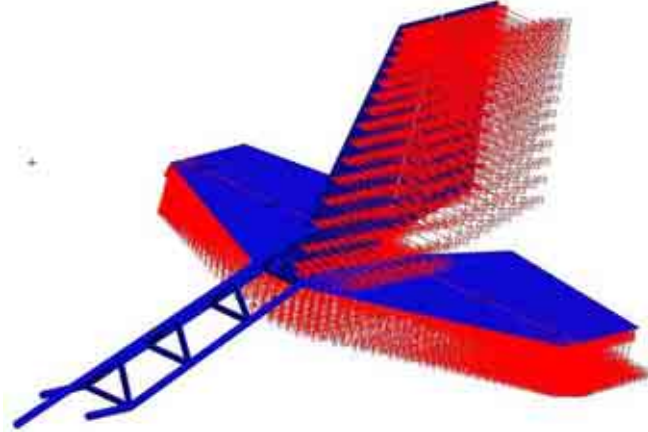


Pressure load on the bottom and top skin (rear view, spars removed)



#### 12.4.2. Tail loads

The tailplane loads come directly from the loading actions chapter. The maximum pressure loads from the CS-VLA requirements have been used and applied on the tailplane and elevator. The loads have been applied simultaneously to check the tail beam strength. The pressure loads on the tailplane and the fin are shown on the picture below:

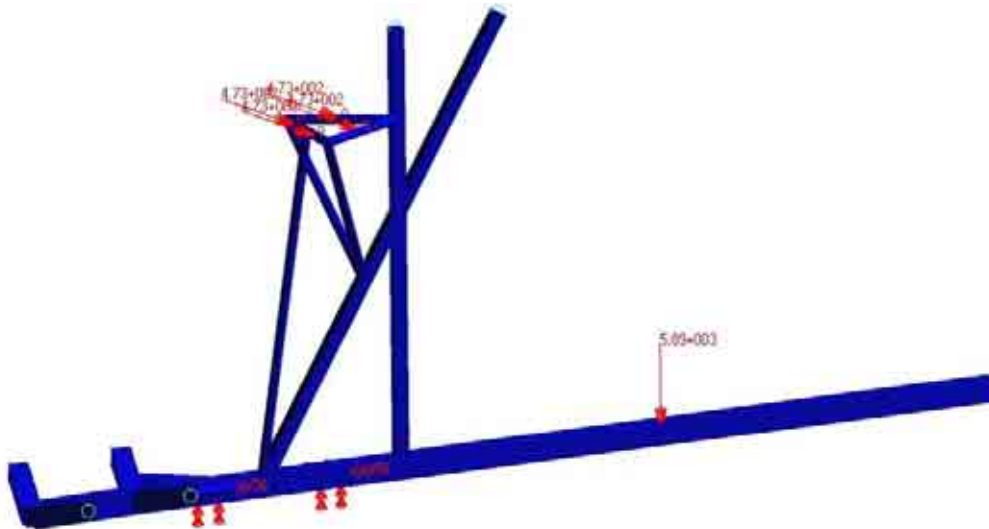


Tail loads

#### 12.4.3. Fuselage loads

The fuselage has been submitted to 3 different loads and boundary conditions listed and illustrated below:

- Ultimate weight at 4G of the passenger on the cantilever beam
- Combined 4G inertia loads and thrust from engine on the engine mounting
- Main beam restrained to prevent any free body movement of the model



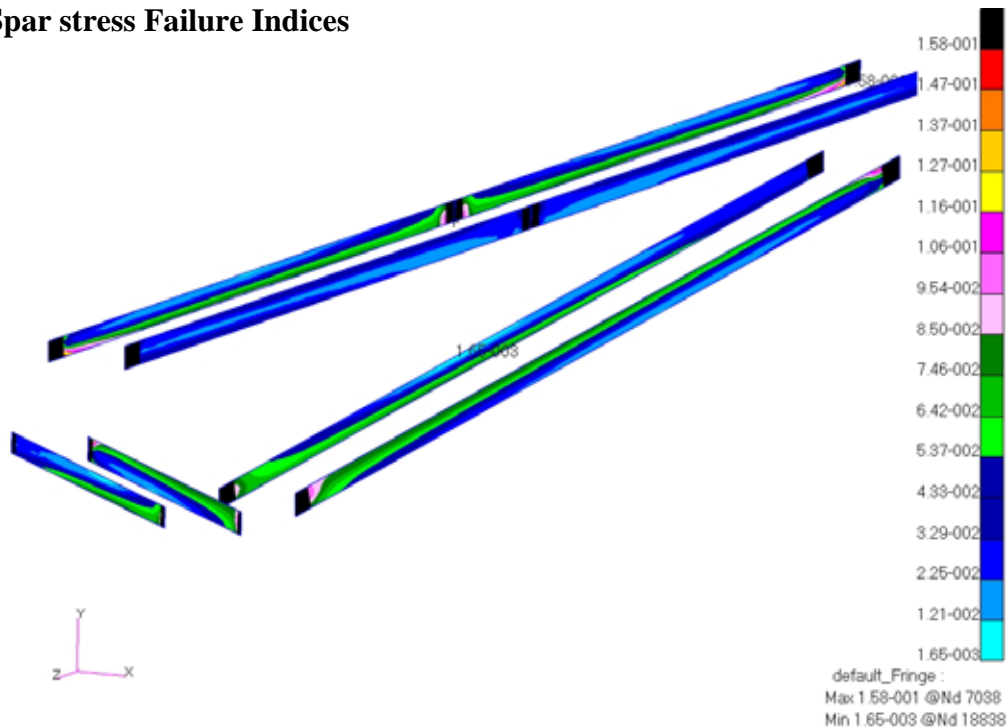
Fuselage loads and boundary conditions

It might be worth determining the torque induced in case of engine seizure and its effect on the engine mount. It might also be useful to consider a side load and look at the torque induced in the wing beams by the engine mount structure.

## 12.5.STRENGH RESULTS (ULTIMATE LOAD)

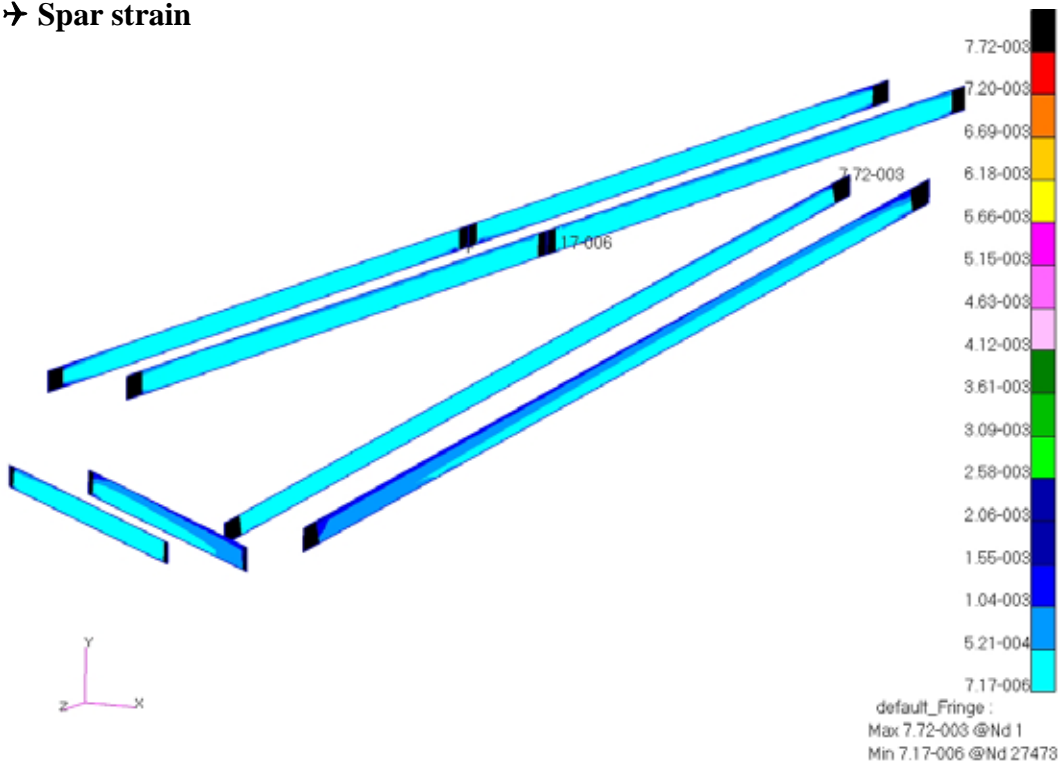
### 12.5.1. Wing structure

#### → Spar stress Failure Indices



Spar Tsai-Wu criterion result (No units)

#### → Spar strain

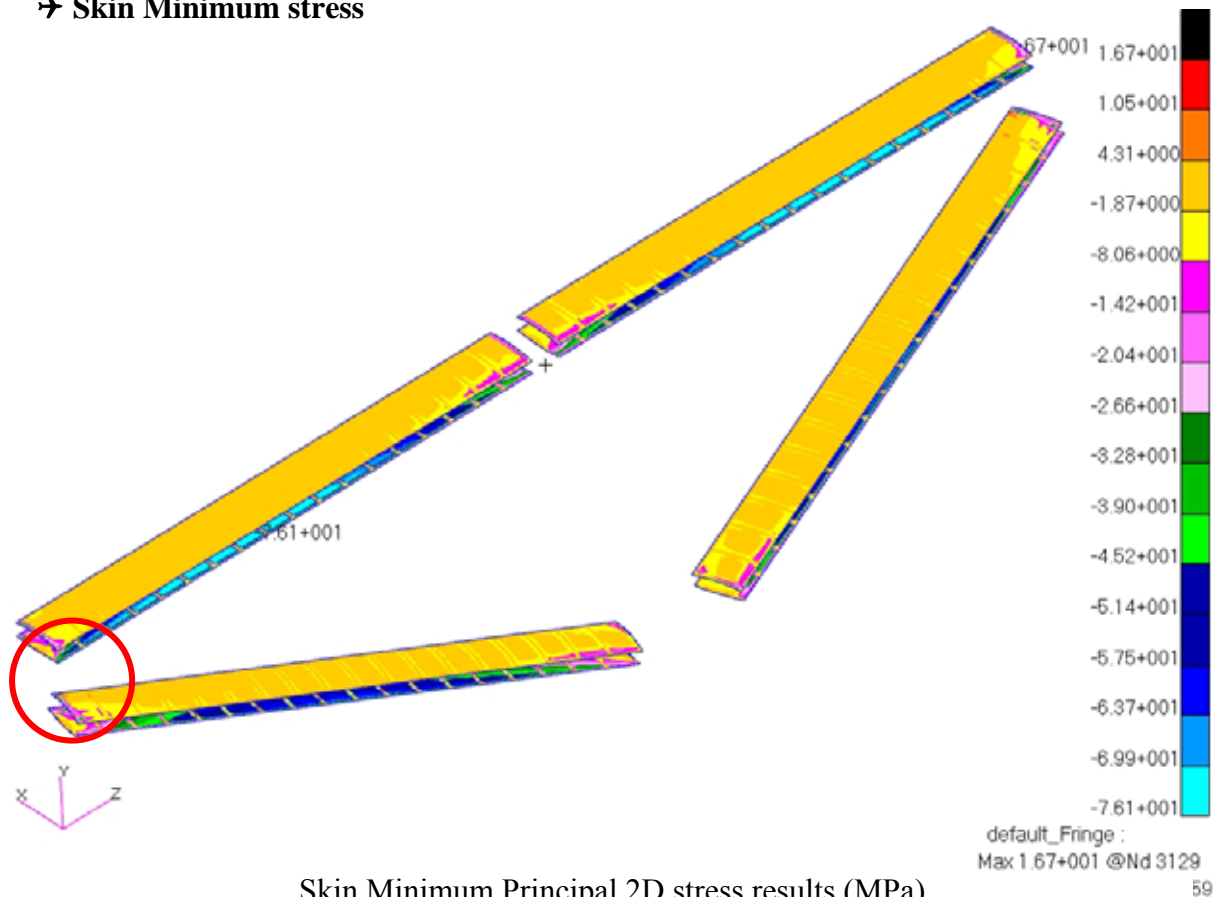


Spar maximum strain results (no units)

The top picture shows that the maximum Tsai Wu failure index for the spar laminate is 0.158. This gives us a reserve factor of 6.3. This seems very high. However, for the composites we want to limit the strain to 0.004 for fatigue and damage tolerance considerations.

The bottom picture shows us the strain in the spars laminate. The black tips are, in fact, the areas reinforced with aluminium. These areas have the maximum strain. The actual maximum strain in the laminates is in green, which is 0.0036. This is just below 0.004, so the damage tolerance criterion is verified.

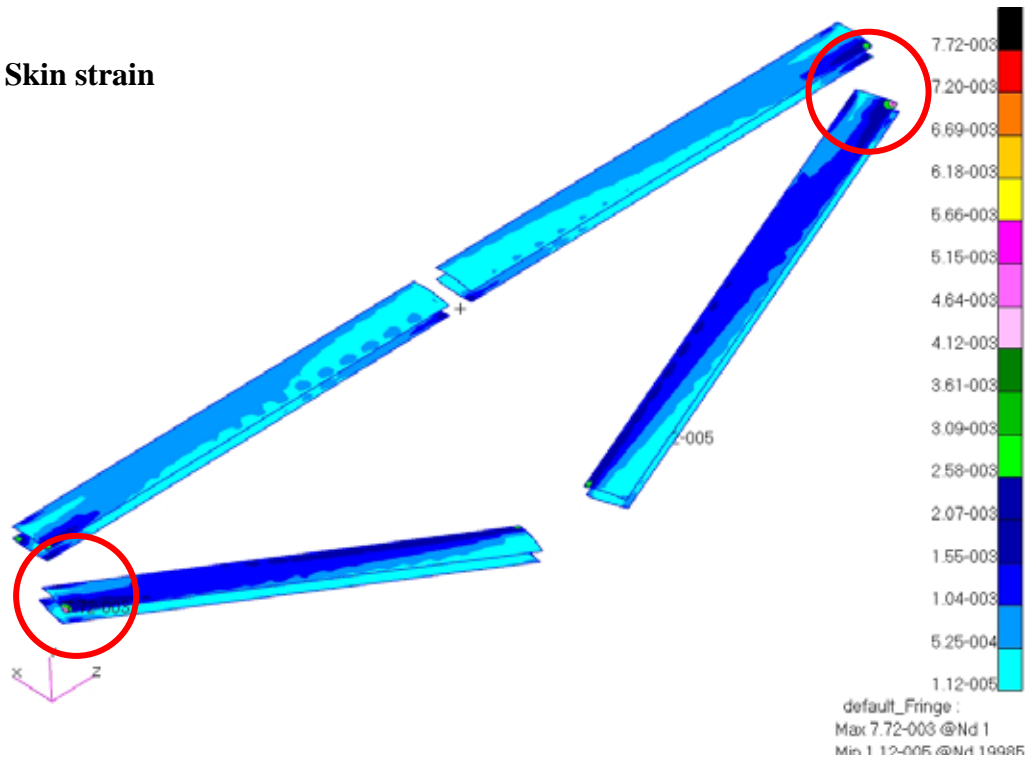
#### → Skin Minimum stress



The picture above shows the minimum stress in the skin laminate. I have chosen to plot the minimum stress because the laminate strength is 450 MPa in compression and 700 MPa in tension. Therefore, we know that the compressive loads are the most critical. The maximum compressive stress is 76MPa. This gives us a reserve factor of 5.8. As for the spars, this reserve factor is high, but it is due to the maximum strain criterion. The most loaded spars are at the tips (red circle). The maximum strain on the wing is 0.007. This is above 0.004. However, the picture on the next page shows that this is for a very small area of the skin (red circle). If we do not consider this region, the strain is below 0.0026. Therefore, we can consider that the structure is safe.

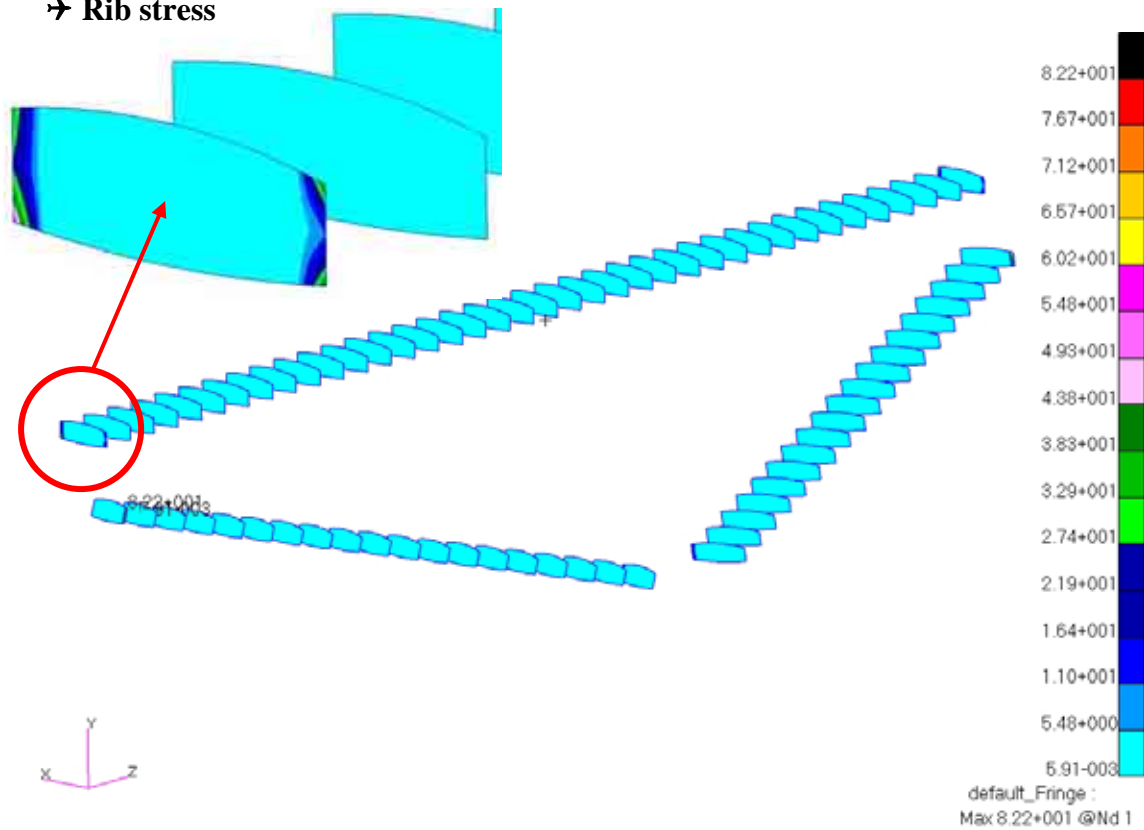
→ For both the spars and the skin we notice that the tip region is, as we could expect, the most stressed. This shows that the design and the manufacture has to be done very carefully in this area. It might be worth trying to reinforce the tips with steel instead of aluminium. The weakness of aluminium is its very low young modulus.

→ Skin strain



Skin maximum strain results (No units)

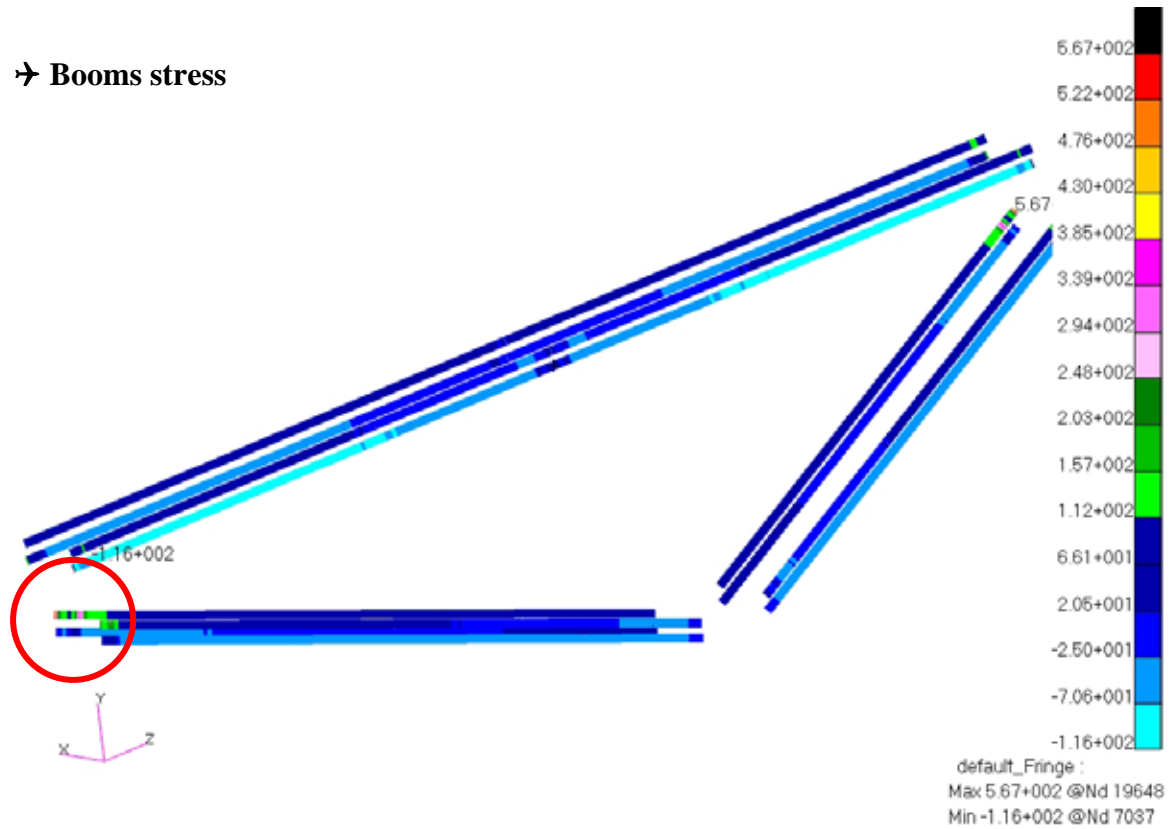
→ Rib stress



Ribs Von Mises stress results (MPa)

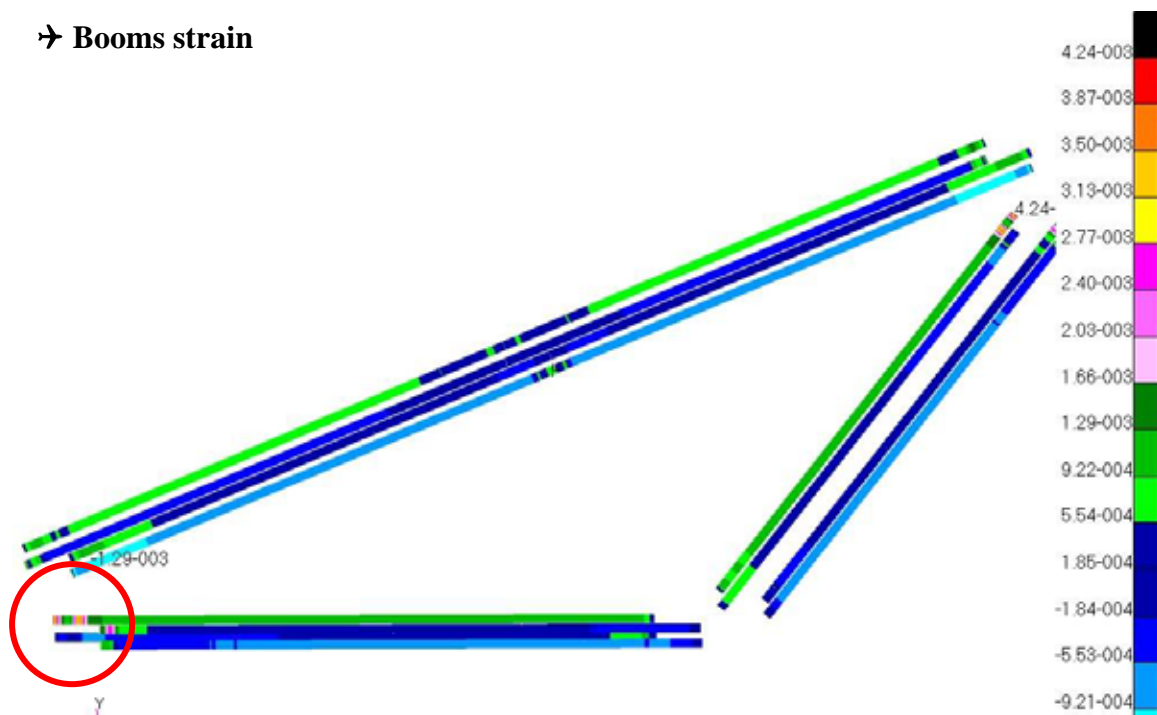
The rib stress is very low. However, we can see that at the tips again, there is a very small area where the rib stress gets very high. It might be considered to reinforce the tip ribs with a carbon skin to get a stronger sandwich structure.

### → Booms stress



Booms bar maximum combined stress (MPa)

### → Booms strain



Booms bar maximum combined strain (No Units)

As we noticed for the other wing components, the tips are the areas the most stressed. We can see that the strain at the tips slightly exceeds 0.004. This is a very local phenomenon, and the tips are reinforced with aluminium so the booms are not reacting all the stress. If we look at the model without the tips the maximum strain is 0.026 which matches the fatigue requirements.

## → Wing tips



Wing tip bar maximum combined stress (MPa)

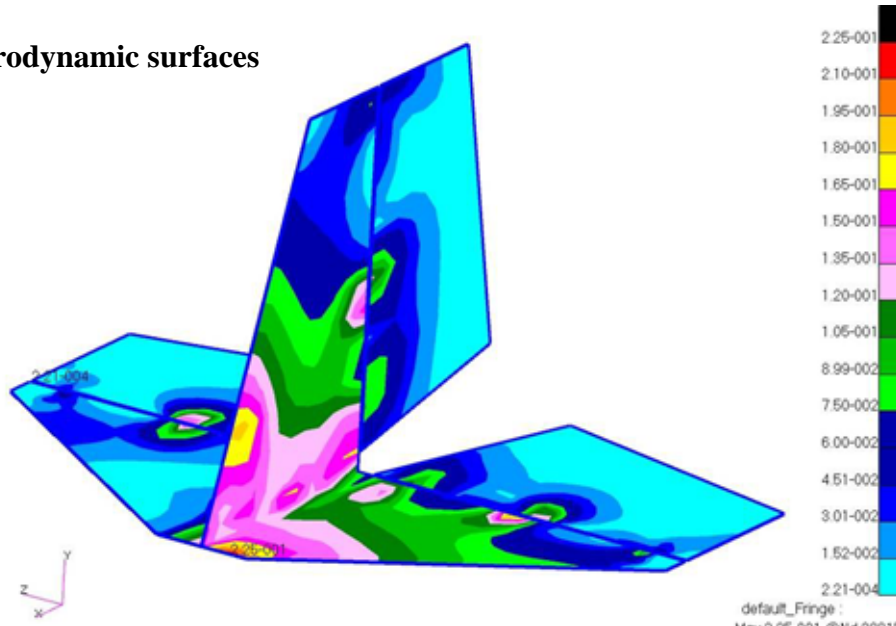
The wing tips are attached to the high strength aluminium reinforcements located on the spars tips. The wing tips are key components of the wing structure. They are highly stressed. That is why they are made out of steel.

The maximum stress in the tips is 567 MPa. This gives us a reserve factor of 1.5, which is high enough to be safe.

The first finite element model had a pivot link between the low wing and the tip bars and a fully rigid link between the top wing and the tip bars. The analysis has shown that BOTH the stress and the wing deflection can be reduced if both wings are rigidly connected at the tips. The global wing structure is not isostatic anymore, but it is a more efficient way to design the wing.

### 12.5.2. Tail

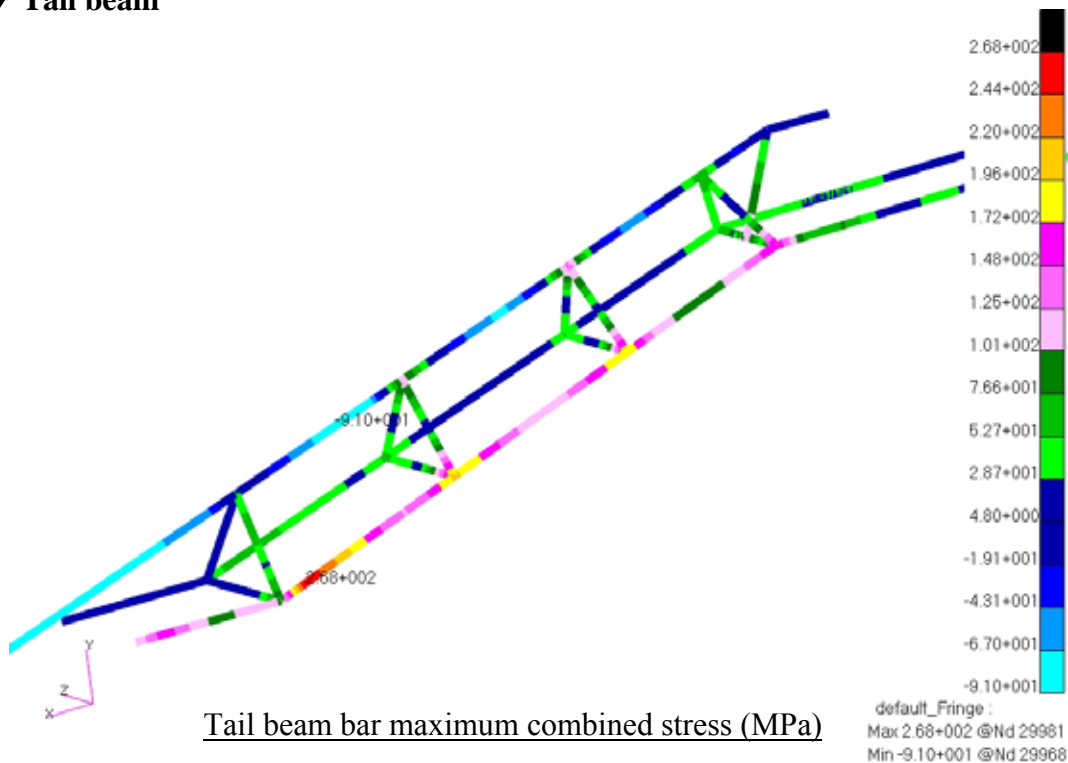
#### → Aerodynamic surfaces



Aerodynamic surfaces Tsai Wu stress criterion (No units)

On the picture above we can see how the stress is distributed through the hinges and through the tail beam attachments. There are stress concentration areas and this shows that it is really important to transfer the concentrated loads (hinges, tail beam) on the largest surface possible, as illustrated in the tail design chapter. The maximum Failure index is 0.25 which gives us a reserve factor of 4. The maximum combined stress in the tail beam (plotted below) is 268MPa. This gives us a reserve factor of 1.3. We can see that the maximum stress is at the root, where the bending moment is the highest. The most stressed beam is in fact reacting the bending moment due to the vertical tailplane load PLUS the bending moment due to the horizontal fin load. This is why we observe that only one beam among three is highly stressed.

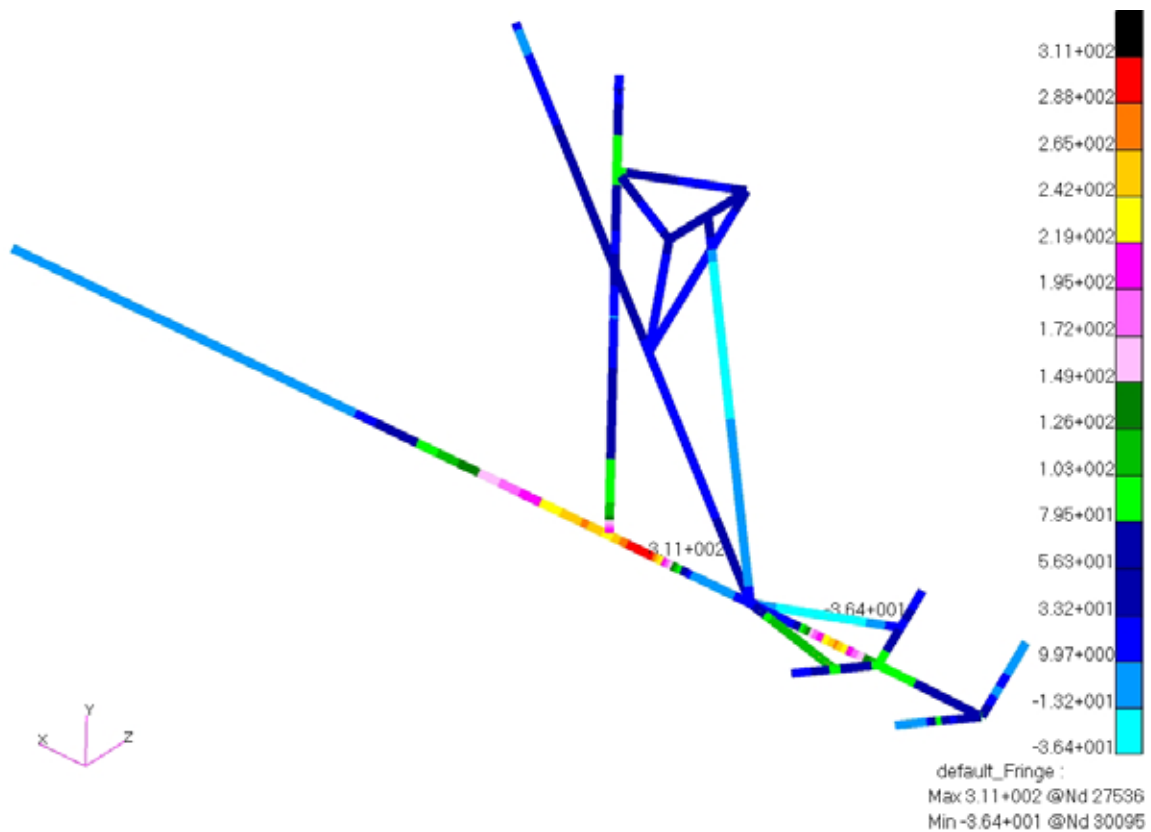
#### → Tail beam



Tail beam bar maximum combined stress (MPa)



### 12.5.3. Fuselage



Fuselage bar maximum combined stress results (MPa)

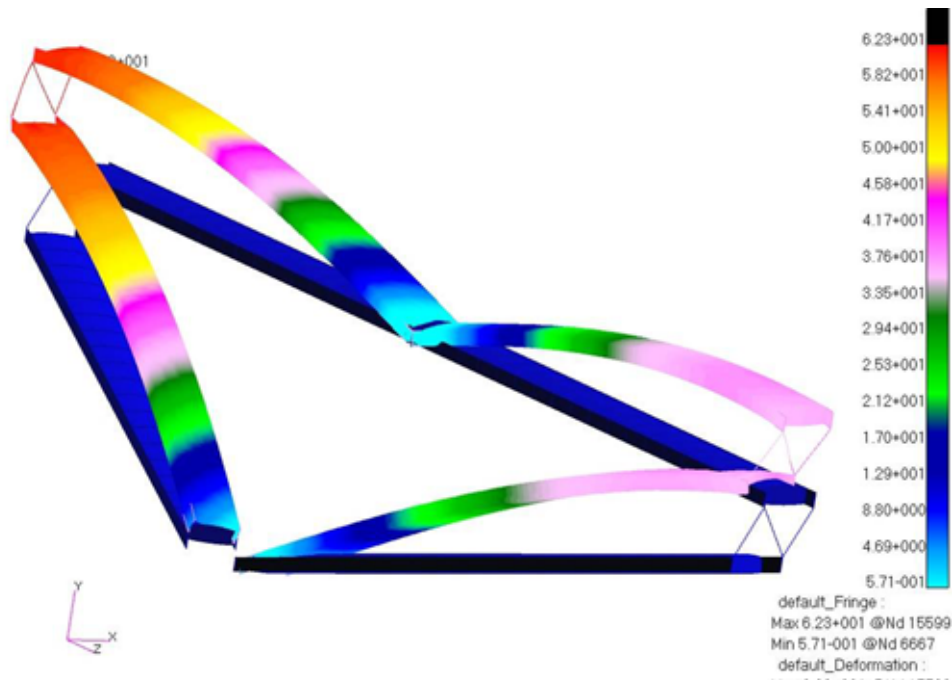
The fuselage maximum stress is 311 MPa. This gives us a reserve factor of 1.3. However, we can expect that in reality the maximum stress in the fuselage is lower than this. The high stresses are due to the fact that we have fully restrained this area of the fuselage, which induces a very high concentrated load, even if it is distributed on three nodes.



## 12.6.DEFORMATIONS (LIMIT LOAD)

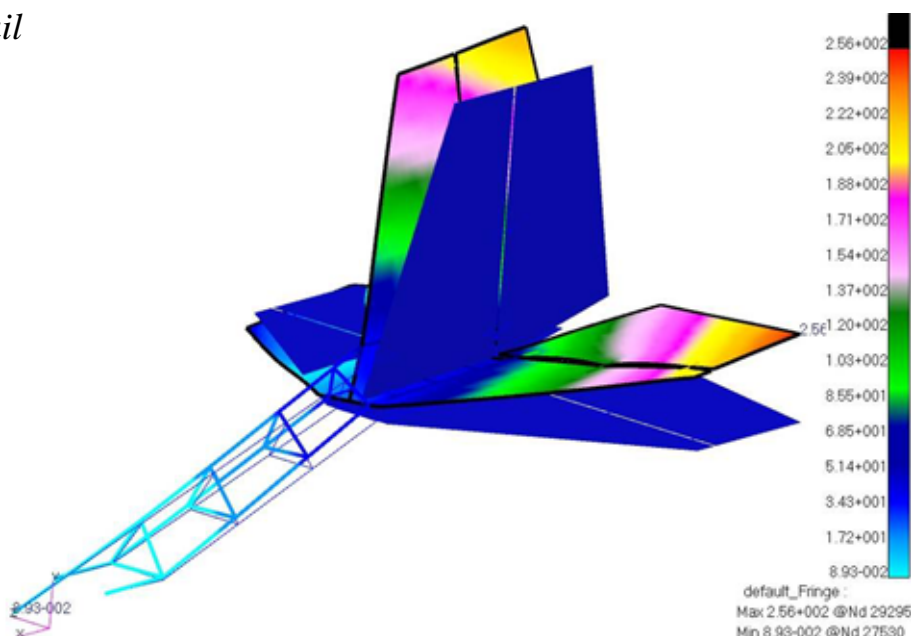
### 12.6.1. Wing

The picture below shows the wing deformation at limit load. There is a deflection of 63 mm at the tips. The wing span is 7600mm. This represents a deflection of 0.8% of the span, which is perfectly acceptable. It is interesting to note that the deflection really shows that the wing roots are mounted with pivot joints while the tips are restrained. This gives the wing a deflection which looks completely different than a conventional cantilever wing.



Wing deflection under limit load (mm), magnified

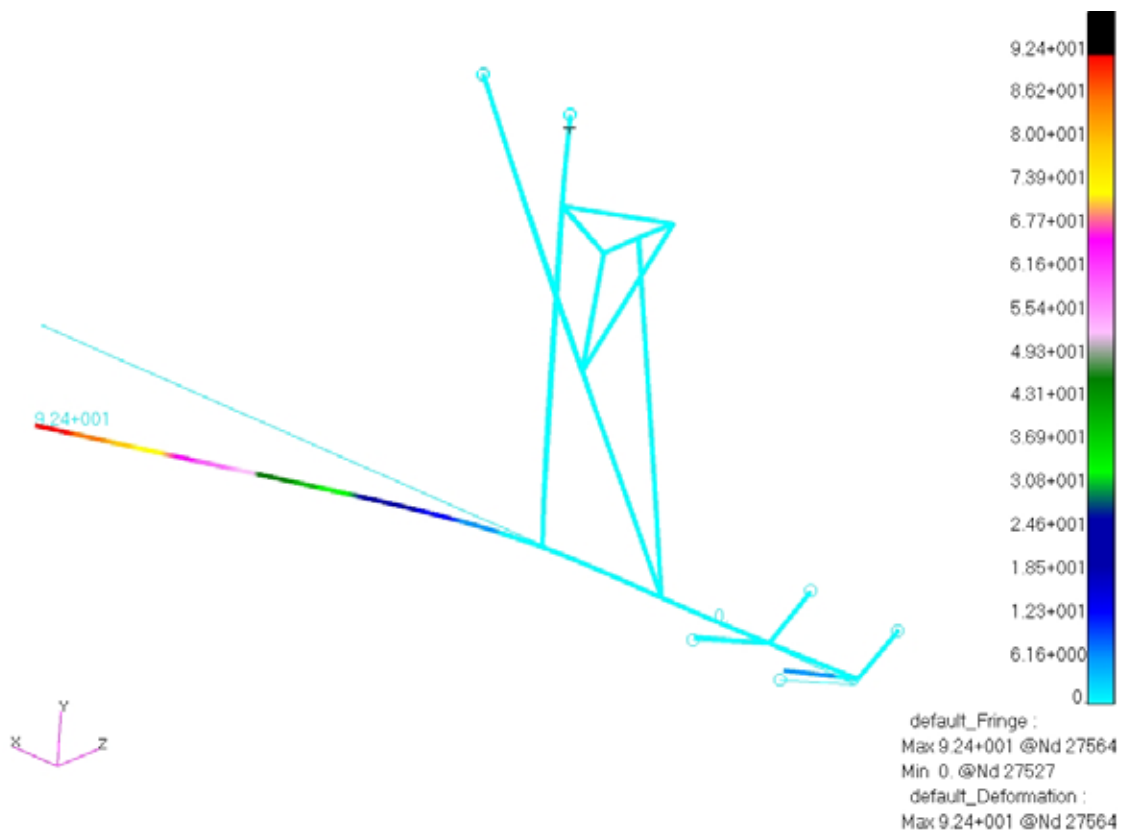
### 12.6.2. Tail



Tail deformations under limit load (mm), magnified

The maximum deformation of the tail is 250mm, it represents 10% of the tailplane span, which is very high. We can explain this easily: The load case used combines the two most severe standard gust cases from the CS-VLA. These load cases are standard for all aircraft, which means that they are not adapted to our aircraft. However, if we want to comply with the CS-VLA, this is the only data we have, since we do not have wind tunnel test data. In addition, the loads are considered simultaneously, which is very severe. Finally, the fuselage is fully restrained on the model. In reality, a load on the tail would make the whole aircraft rotate; the fuselage would not remain fixed. That is why we can say that this displacement is never going to occur in reality. However, it would be good to investigate other ways to design the tail beam, and, if possible, find a lighter and stiffer structure.

### 12.6.3. Fuselage

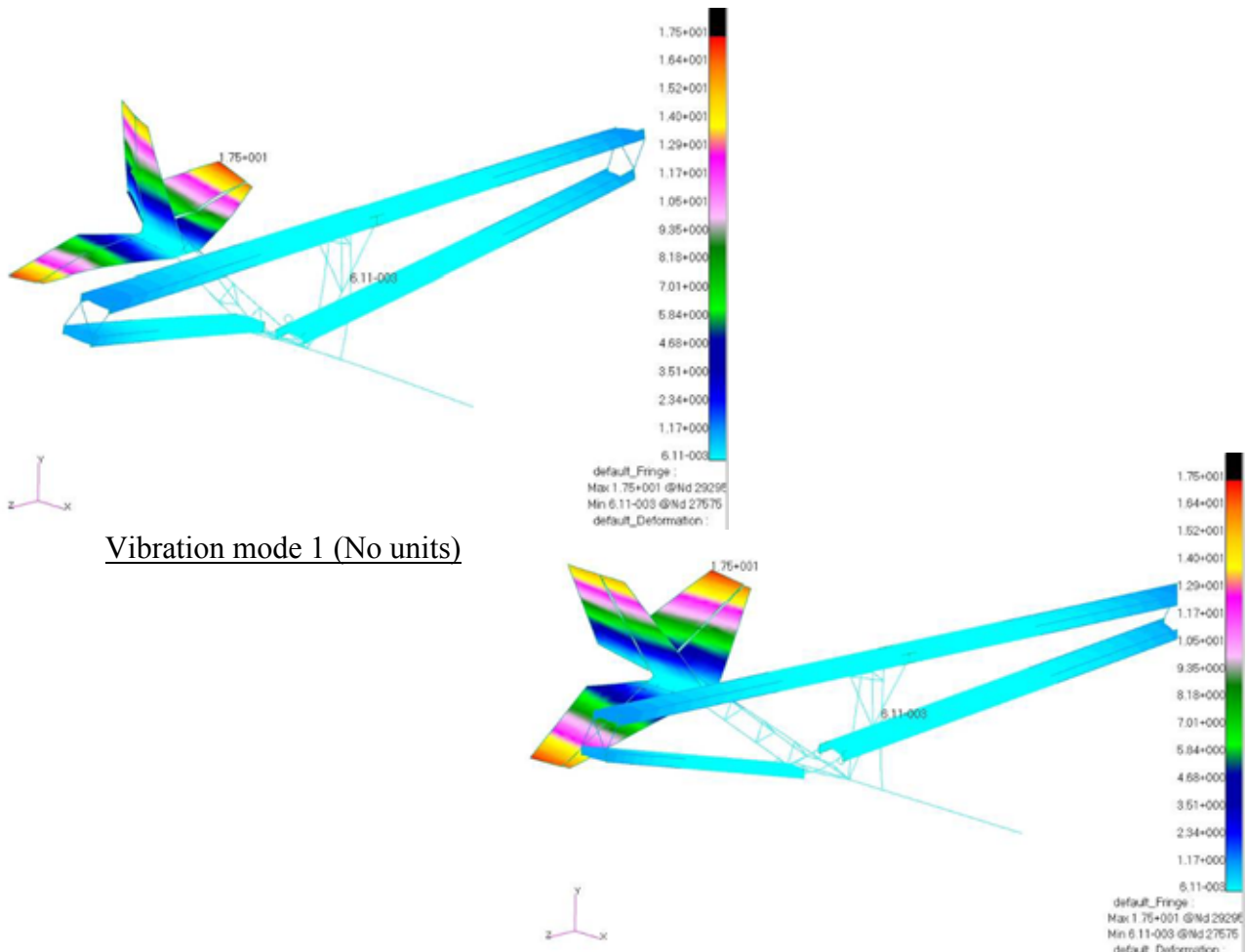


Fuselage deformations under limit load (mm), magnified

The picture on the top shows that the maximum deflection occurs at the tip of the cantilever beam. This deflection can seem very high, however, for the same reason as the tail we know that in reality, the deflection will never reach this value. The load is a 4G acceleration on a 100kg pilot. This is a severe criterion. In addition, the fuselage main beam has been restrained. In reality, the aircraft would have a pitching acceleration and the fuselage would not remain horizontal as it does with the restraints.

## 12.7.DYNAMIC ANALYSIS

The dynamic analysis allows us to check the vibration modes of the aircraft. This is interesting since the lowest frequencies show the weaknesses of the structure. The model has been analysed as a free body, without any loads or restraints, to get an idea of the vibration modes that could occur during the flight. As the model is free, the six first modes are rigid body translations and rotations around the model inertia axis, with a frequency of 0Hz. I have studied the two first modes. The results are presented on the pictures below:



Mode1: The mode 1 has a frequency of 4.0 Hz. The mode one is a lateral bending of the entire tail.

Mode2: The mode 2 has a frequency of 7.9 Hz. The mode two is an overall torsion of the tail.

➔ This analysis shows that the tail is the less rigid assembly of the aircraft. The tail beam is made out of aluminium for weight considerations. The aluminium has a very low Young's modulus and that is why we observe these low frequency vibrations.

## 13. 1/3 SCALE MODEL

### 13.1.PURPOSE OF THE MODEL

The model will help us for the final design; we will look at the following points :

- Checking the stability
- Checking the maximum CG range
- Checking the stall behaviour
- Checking the spin behaviour
- Understanding the low speed capability
- Understanding the effect of the variable camber flaps on the Colab wing
- Checking the maneuverability

This is important to build a model. For instance, if the manoeuvrability is really good we can consider reducing the tail aerodynamic surfaces. If we reduce these surfaces, we reduce the weight, and we also reduce the loads, so we can make the tail beam lighter.

### 13.2.MANUFACTURING OF THE WINGS

You can find below pictures of the wings (there are four segments of 1.34m, the picture shows one segment).



1/3 scale model wings

The wings are made with polystyrene with a balsa skin. They use the same airfoil as the full scale aircraft. We studied the effect of the Reynolds number on the airfoil and in fact this airfoil has good performance for chords as low as 200mm. Our chord is 267mm, so we can use the same airfoil as used for the real aircraft.

### 13.3.GLOBAL WING ASSEMBLY

The pictures below show the wing global assembly. The wing geometry has been perfectly respected to match with the Colab wing requirements.



Global wing assembly and wing tips details

Unfortunately, the construction of the model has not been finished prior to the end of this project. However, the building is still in progress and the model is expected to fly by the end of October 2007.

# CONCLUSIONS AND IMPRESSIONS

## ➔ SUMMARY

The aim of this project was to come up with a very efficient aircraft design under 115 kg. These objectives have been fulfilled; the design presented in this thesis is very efficient, light and simple. It was possible to reach this thanks to the following parameters:

- A very extensive study of the market and detailed analyses done to choose the best aircraft configuration.
- The design makes extensive use of carbon fibre epoxy composites laminates and aluminium tubes.
- The Colab concept wing has very good aerodynamic properties and great structural advantages.
- The structure has been optimised with a complete finite element model.
- The aerodynamic properties can be optimised with the 1/3<sup>rd</sup> scale model.

## ➔ FURTHER WORK

This thesis gives the layout of the aircraft, but further work is required before the aircraft can fly. In particular, the points below need to be considered:

- The attachments have been designed but they need to be stressed and optimised.
- The general layout of the aerodynamic fairings of the fuselage has been given but a wind tunnel testing would be good to optimise the shape and increase the performance.
- The undercarriage needs to be designed and stressed.
- The control surfaces are designed, but the actuation and the cable systems remain to be done.
- The 1/3<sup>rd</sup> scale model needs to be finished and the flight data analysed to optimise the aerodynamic design.
- The tail beam stiffness is rather low and it is useful to check if a lighter or same mass design can be found with a greater stiffness.

The weight margin is quite low to stay under 115kg. However, it is possible to save weight if necessary with the following options:

- Make the structure lighter by using cables.
- Using the alternative lighter 24.5 hp Corsair engine
- Reducing the tail areas if the model test shows that it is possible

➔ In conclusion, this project was a great experience, both from a technical and personal point of view. Designing an aircraft from scratch, choosing the design and stressing it is a great opportunity for an aerospace engineer, passionate by aircraft. This project was a unique chance to apprehend all the aspects of the aircraft design and to use them in a real environment.

# REFERENCES

1. E. TORENBEEK, 1982, *Synthesis of subsonic airplane design*, Delft University Press, Delft The Hague Hingham.
2. DARROL STINTON, 2001, *The Design of the Aeroplane\**, Oxford: Blackwell Science, Oxford.
3. DANIEL P. RAYMER, 2006, *Aircraft Design: A Conceptual Approach\**, American Institute of Aeronautics and Astronautics, Blacksburg.
4. JOHN T. LOWRY, 1999, *Performance of light aircraft*, American Institute of Aeronautics and Astronautics, Reston.
5. E. W. C. WILKINS, 1938, *Aeroplane Design*, Charles Griffin & Company, London.
6. DENNIS HOWE, 2000, *Aircraft conceptual design synthesis*, professional engineering publications, Cranfield.
7. ROMAIN NOYER, 2000, *Analysis and design of an engine installation for the microlight aircraft shadow C series*, MSC Thesis, Cranfield University.
8. F.A.K. LAMBERT, 1994, *Design of a light aircraft for JAR-VLA requirements*, MSC Thesis, Cranfield University.
9. L.K. LOFTIN, 1980, *Subsonic Aircraft: Evolution and the Matching of Size to Performance*, NASA Paper, NASA Reference publication 1060.
10. JANE'S, 1949-2005, *All the world's aircraft*, Jane's Information Group, London.
11. HOWARD SMITH, *Conceptual design course, Initial sizing of longitudinal and lateral stabilizers*, CoA DAeT 9345, Cranfield University, 2007.
12. ESDU 80023. *Buckling of rectangular specially orthotropic plates*. 1995.
13. P. STOCKING. *Detailed stressing, rib analysis*. CoA AVT-AVD 9638. Cranfield University. 2006.
14. ESDU 70015. *Fluid forces and moments on flat plates*. 1970.
15. Section S of the CAP 482 airworthiness regulation, 1999.
16. CS-VLA airworthiness regulation, 2003.
17. ESDU 74011. *Rate of change of lift coefficient with control deflection for full span plain controls*, 1974.
18. ESDU 70011. *Lift-curve slope and aerodynamic centre position of wings in inviscid subsonic flow*, 1970.
19. ESDU 80020. *Average downwash at the tailplane at low angles of attack and subsonic speeds*, 1980.

# APPENDICES



# **A. BMAA TECHNICAL LEAFLET**

## **A.1. INTRODUCTION**

At the end of April 2007, the CAA issued an exemption for a group of microlights to allow them to operate without needing to hold a Permit to Fly. This followed a number of years of campaigning by the BMAA to simplify the airworthiness requirements for lightweight, single-seat microlights.

This document outlines the implications of this rule change and how our members can take advantage of it. It also seeks to explain the operation and responsibilities of owning a deregulated machine, and the framework of support that the BMAA offers.

At issue 1, the document outlines the general philosophy of the rule change. It is anticipated that further details will be added in the near future as the system matures and the finer details are developed.

## **A.2. THE DEFINITION**

The exemption from the Air Navigation Order was issued by the CAA on 30 April 2007 and includes the following text:

General exemption against Article 8 of the Air Navigation Order 2005 for microlight aeroplanes with a maximum weight, without pilot and fuel, of 115kg.

1) The Civil Aviation Authority, in exercise of its powers under Article 153 of the Air Navigation Order 2005, hereby exempts any microlight aeroplane coming within paragraph 2 from the prohibition contained in Article 8(1) of the Order that it shall not fly unless there is in force a certificate of airworthiness.

2) A microlight aeroplane comes within this paragraph if it:

- a) is designed to carry not more than one person;
- b) has a maximum weight without its pilot and fuel of 115 kg; and
- c) has a maximum wing loading without its pilot and fuel of 10 kg per m<sup>2</sup>.

3) This exemption shall only apply where the microlight aeroplane:

- a) is flying on a private flight; and
- b) is not flying over any congested area.

4) This exemption shall have effect from the date on which it is signed until 31 January 2008.

It is anticipated that the intent of this exemption will be included in the Air Navigation Order (ANO) at its next revision.

Of course, the aircraft must also continue to meet the definition of a microlight, which for a single-seater means a maximum take-off weight not exceeding 300 kg (330 kg for an amphibian or floatplane) and a stall speed not exceeding 35 knots at maximum take-off weight. Most conventional designs are unlikely to reach these limitations.

The BMAA considers that the definition of wing area (when calculating the wing loading) includes that portion of the wing contained within the fuselage section of fixed-wing aircraft. The area of the horizontal stabilising surface is not considered to contribute towards the total wing area of a standard fixed-wing configuration, although a 'canard' wing would. The wing area of parafoil-type wings is considered to be the area projected onto a horizontal surface when inflated.

It should be noted that the definition of a 'self-propelled hang-glider' still exists. The definition is as follows: an aircraft comprising an aerofoil wing and a mechanical propulsion device which:

- a) is foot launched;
- b) has a stall speed or minimum steady flight speed in the landing configuration not exceeding 35 knots calibrated airspeed;
- c) carries a maximum of two persons;
- d) has a maximum fuel capacity of 10 litres; and
- e) has a maximum unladen weight, including full fuel, of 60 kg for single place aircraft and 70 kg for two place aircraft.

Separate, more lenient rules govern the use of ‘self-propelled hang-gliders’. The key thing to note is that if the aircraft is launched by use of undercarriage (and not by the legs!) then the aircraft does not qualify as a ‘self-propelled hang-glider’.

### A.3. WHAT THE CHANGE IN RULES MEANS

What the exemption means is that for aircraft that meet the above definition it is not necessary to hold a valid Permit to Fly or associated Certificate of Validity. This in turn implies that the design need not meet a particular design or maintenance standard, and the aircraft doesn’t need an annual inspection or check flight.

Much research has shown that the requirements for a design to be approved and for an aircraft to hold a Permit to Fly represent a large monetary burden which has proven to be an effective barrier to development of single seat types. Research has also shown that similar categories exempted from formally proving compliance with airworthiness codes operating worldwide have similar structural safety records as heavier, regulated sport-aviation types. On the other hand, with the absence of a formal requirement to prove airworthiness a significant safeguard has been removed and more emphasis is placed on the owner to understand and take responsibility for his/her aircraft and its operation. The basic premise, therefore, is that the owner/operator takes full responsibility for the airworthiness of his or her aircraft, and the associated risks. In addition, the energy levels of the aircraft involved are kept low by keeping their empty weight to a minimum, thereby reducing the risk to third parties.

This change also means that owners can design and modify their machines largely without reference to the CAA or BMAA. The only exception to this is changes that may alter the basis of the noise certificate (see the later section on noise certificates).

### A.4. WHAT THE CHANGE IN RULES DOES NOT MEAN

The exemption only allows the aircraft to fly without a Permit to Fly. The rest of the Air Navigation Order (and other legislation) still holds true. In particular, the following rules still apply, as they do to all microlight aircraft:

- The pilot must be in possession of a valid and relevant licence (plus all that goes with it, such as a ‘certificate of experience’ and medical declaration).
- The aircraft must have a noise certificate.
- The aircraft must have appropriate third party insurance (minimum of 750,000 SDRs, approximately £600,000).
- The aircraft must be registered with the CAA (‘personalised’ registration letters are permitted).
- The aircraft must display its registration letters in the normal way (CAP 523 on the CAA’s website gives details).
- A fire-proof metal plate shall be affixed to the aircraft showing the nationality and registration marking (i.e. GABCD).

- Radio equipment must be of a type approved by the CAA and licences for those radios held.
- A CAA approved logbook must be kept for the airframe and engine (the BMAA/Pooley's logbook is an acceptable alternative to the CAA publications).
- The Rules of the Air must be obeyed.
- Accident reporting continues as normal.

#### *A.4.1. Pilot licensing*

Pilots of this class of microlight must be in possession of an appropriate licence. Generally this is an NPPL (Microlight) with training appropriate to the control system being used (flexwing, 3-axis, parachute, etc). Some credit towards obtaining the NPPL can be taken for existing licences and ratings on other classes of flying machine: up-to-date information can be found on the NPPL website: [www.nppl.uk.com](http://www.nppl.uk.com)

#### *A.4.2. What types are there?*

Within the definition above, any configuration of flying machine is possible; however, so far they fall into 4 distinct groups:

1) The flexwing 'trike'. This is the same as the heavier flexwing microlight types, and consists of a single delta-shaped wing, like a hang glider, with a 3-wheel fuselage/trike unit suspended beneath and a pusher engine. Control is by weightshift. The pilot manoeuvres the aircraft by moving the fuselage unit relative to the wing by means of a control frame.

2) The three-axis type. This resembles a conventional aeroplane in layout with wing and tail. Variations may include a 'canard' with the 'tail' at the front, and tractor or pusher engine positions. Three-axis generally refers to the conventional control system of elevator, ailerons and rudder that offer control of all three axes of movement (pitch, roll and yaw). However some types may use linked or single roll/yaw controls.

3) The paratrike (powered parachute). This consists of a fuselage/trike unit suspended from a paraglider style wing. Simple versions can be adaptations to convert paramotors from foot- to wheeled-launch. Control is via control lines which adjust the shape of the canopy.

4) Hybrid types. These can use a combination of weightshift and aerodynamic control, and range from simplifications of three-axis types to sophisticated aerodynamic control additions to flexwing types.

### **A.5. HOW SHOULD I DECIDE WHICH TO BUY?**

Selection of the right type for you will depend on your personal requirements of performance, cost, ease of storage and your own personal flying style aspiration.

When you look at purchasing an aircraft, you should think about the following points:

1) Does the type have a good track record and support? Existing types built in large numbers and having a good reputation provide a good indication of a sound purchase. Email forums provide an opportunity to contact existing owners and learn their experience and hear their recommendations. New types being developed may promise better performance and exciting new features, but also will naturally need some proving time in service to iron out all the small bugs, which may prove to be frustrating for the first customers. In such cases a proven company with good reputation for support will provide reassurance that such a purchase is sensible. Good UK based support is also highly desirable.

2) Does it really comply with the definition of a deregulated microlight? This is especially important when shopping from a foreign supplier who has not designed their aircraft specifically for the UK market. Often specifications on paper or from the internet may not reflect reality or current production. Weights quoted might be inaccurate. Seek a hard and fast assurance/guarantee that it will comply with the UK requirements. Empty weight should include all items fixed to the aircraft – that includes the wing, instruments and all actually present and fitted options. Only items that attach directly to the pilot, and fuel and baggage may be excluded. Don't forget that to have the maximum 115 kg empty weight allowance the wing must be at least 11.5 m<sup>2</sup>.

3) If you're considering buying a used aeroplane - has it been maintained in a safe condition? A thorough look over the aircraft and through its logbook is a good starting point: has it been regularly maintained, has it been in any accidents/have there been any repairs made, etc. Be very wary of aircraft without logbooks!

#### *A.5.1. I've got a microlight on a permit and want use the new rules*

If your aircraft has a valid Permit to Fly (or the powerplant hasn't been modified since it last held a valid Permit to Fly) and it fits into the above definition, then your aircraft can be operated under the new rules.

All you need to do is to complete the form at the back of this handbook and send it to the BMAA to let us know your intentions. There is no need to inform the CAA.

#### *A.5.2. I've got a new microlight that I want to fly under the new rules*

The first step is to check that your aircraft does indeed meet the above definition. If it does, you need to register the aircraft with the CAA using form CA1 which can be downloaded from the CAA's website ([www.caa.co.uk](http://www.caa.co.uk)). The CAA will seek confirmation that the aircraft is suitably insured (if the aircraft is in build then this can be deferred until the aircraft is complete). In addition, you should also complete the form at the back of this handbook and send it to the BMAA to let us know your intentions.

Before flying your aircraft you will also need to arrange a noise certificate to be issued (see section below on noise certificates).

### **A.6. THE BMAA'S INVOLVEMENT**

Once an owner declares to the BMAA that an aircraft is to be operated as 'deregulated' machine, the Association takes no further part in its airworthiness.

It is recognised that in an ideal world technical advice and support should be available from the BMAA. At the current time, until the BMAA seeks further legal advice, the officers and volunteers of the Association (which includes the BMAA permanent staff, inspectors, check pilots and test pilots) must not offer technical advice regarding the airworthiness of a deregulated microlight. Until the Association has clearly defined the extent to which staff and volunteers can get involved, the legal liability risks to the Association are too large to ignore.

As more advice becomes available, it will be published here.

## A.7. MODIFICATIONS AND NOISE CERTIFICATES

The exemption which allows this class of microlight to operate without a permit does not extend to exempting the aircraft from The Air Navigation (Environmental Standards) Order 2002: i.e. to hold a noise certificate.

This means that each individual deregulated microlight must hold its own noise certificate. This certificate lists the registration (and airframe, wing, engine, exhaust, silencer, propeller and gearbox combination) to which it applies and certifies that the combination meets the noise regulations. In theory, if any of the airframe / wing / engine / exhaust / silencer / propeller / gearbox combination change, then the noise certificate needs to be changed to reflect this. This may entail further testing to determine whether or not the noise regulations are still met. Note that modifications that affect the speed at which the aircraft flies will affect the noise certification basis: aircraft that fly slower will be 'louder' as the time taken to fly over a point will be longer.

At the current time, the administration of noise certificates and noise testing of microlights is performed by the CAA free of charge. If you require a new noise certificate for your aircraft (either because its new or because a modification has been made to a part of the aircraft that might affect the noise certification), then the application form can be downloaded from the CAA's website (go to [www.caa.co.uk](http://www.caa.co.uk) and search for 'microlight noise application form'). The CAA will then either issue a new noise certificate using the information you provide them, and existing test data that they have on file, or will contact you to arrange a test. If you believe that the modification is already approved on an identical or very similar aircraft, then give the CAA full details and they will be able to take this into consideration when assessing whether or not a physical noise test will be required. Note that no aircraft in this class may legally fly without a valid noise certificate. In order to fly an aircraft for the purposes of noise testing, or for developing an aircraft prior to fixing its final configuration, you need to arrange an individual exemption from the CAA.

The CAA can be contacted on [department.certification@srg.caa.co.uk](mailto:department.certification@srg.caa.co.uk) or on 01293 573309 or 573306.

## A.8. ADVICE ON DEREGULATED MICROLIGHTS

Whilst the BMAA cannot offer advice on individual aircraft designs or modifications, we can try to point you in the right direction!

In order to fly this class of microlight, it is a requirement that you have a suitable pilot's licence. When you learn to fly you pick up all sorts of useful advice as to how to go about doing so safely: dig out this advice and use it! You will be relying more heavily on your own assessment and observation of the day-to-day condition of your aircraft than you might normally be used to. If something is 'against your better judgement', don't fly, think about it carefully instead – perhaps sleep on it!

Don't forget to record flying hours, maintenance, modifications and other useful information in the logbook(s). This will help you keep your aircraft in tip-top condition, and help you to sell it later down the line.

### *A.8.1. Maintenance*

In terms of maintenance, you are strongly advised to follow the manufacturer's advice. You might also consider using the BMAA's generic microlight maintenance schedule (TIL 020) as a basis or supplement. Operating data for aircraft that operate on Permits to Fly (TADS or operators/maintenance manuals) might give food for thought as to what areas to look at. Other things that might hint towards something becoming unsafe might include:

- visible cracks in parts
- perishing rubber/plastic items
- fabric that is discoloured, fraying or becoming easily damaged
- damaged stitching
- distorted or bent parts
- corrosion
- broken wires/strands/parts

You are strongly advised to source replacement parts from the original manufacturer of the aircraft. Replacement parts such as wires (or other critical items that are 'made up') might best be sourced from manufacturers of 'Approved' aircraft if they're not available from the original manufacturer. The use of correct materials and parts can often be vital in retaining the strength and integrity of a structure.

### *A.8.2. Designing your own aircraft, modification or repair*

When designing your own aircraft, modification or repair, there are almost limitless references you can use to help work out whether something is safe or not. You should bear in mind that it is your responsibility to satisfy yourself that your aircraft is safe to fly and that the design is fit for purpose. Bear in mind that strength is only one aspect of the design: don't forget to consider other aspects such as centre of gravity position, stability, control, aerodynamics, performance, handling and so on. You might consider performing some calculations to work out whether a design is safe, or perform some load testing, or some flight testing. Don't forget that what might seem like a fairly innocuous change can sometimes have a significant knock-on effect on other aspects of the aircraft.

Amongst the references available are the following:

BMAA reference (all available from the BMAA website, [www.bmaa.org](http://www.bmaa.org))

- TIL006 Understanding and using performance data
- TIL007 Fuel systems
- TIL011 Propellers
- TIL012 Weight and balance
- TIL013 Strobes
- TIL015 Sail repairs
- TIL020 Maintenance schedule
- TIL027 Avionics
- TIL029 Designing your own aircraft
- TIL101 & 102 Radio installations
- TIL103 Trike panniers
- TIL104 Transponder installations
- TIL105 Flexwing seatbelts
- TIL107 Auxiliary electrical sockets
- TIL108 Carb heaters
- TIL109 GPS installations

- Forms AW/005, AW/006, AW/007 Aircraft inspection reports
- Form AW/010 Flight test schedule
- Form AW/011 Check flight schedule
- Form AW/027 Flight test schedule
- Form AW/041 Engine installation checklist
- Form AW/051 Flight test schedule

CAA references (all available from the CAA website, [www.caa.co.uk](http://www.caa.co.uk))

- BCAR Section S (CAP 482)
- Civil Aircraft Airworthiness Information and Procedures (CAAIP) (CAP 562)
- Amateur built aircraft (CAP 659)

FAA references (all available from the FAA website, [www.faa.gov](http://www.faa.gov))

- AC43-13 1b Acceptable methods, techniques and practices – aircraft inspection and repair
- AC20-27f Certification and operation of amateur-built aircraft
- AC90-98a Amateur-built aircraft and ultralight flight testing handbook EASA references (all available from the EASA website, [www.easa.eu.int](http://www.easa.eu.int))
- Certification specifications for very light aeroplanes CS-VLA
- Certification specifications for sailplanes and powered sailplanes CS-22
- Certification specifications for normal, utility, aerobatic and commuter category aeroplanes CS-23

Miscellaneous books/references

- Wood handbook, US Department of Agriculture, Forest Service (search on the internet for 'USDA wood handbook')
- Aviation mechanic handbook, Dale Crane
- Analysis and design of flight vehicle structures, Bruhn
- Formulas for stress and strain, Roark
- Understanding aircraft structures, Jeremy Liber
- The design of the aeroplane, Darrol Stinton
- Simplified aircraft design for homebuilders, Dan Raymer
- The properties of aluminium and its alloys, Aluminium Federation Ltd
- Metallic materials properties development and standardization (MMPDS), USDOT (version 1 available from [www.ntis.gov](http://www.ntis.gov))
- ESDU data sheets (available as reference in major libraries)

Note that the above is not an exhaustive list, nor does it guarantee that if these references have been consulted that the design is safe! Finally, it is the owner's responsibility to ensure continued compliance with the definition of this aircraft class. Remember that if weight creeps up (as it often does over time) then at some point it may no longer fit into this category of microlight – check the weight occasionally to make sure.

Approved for issue

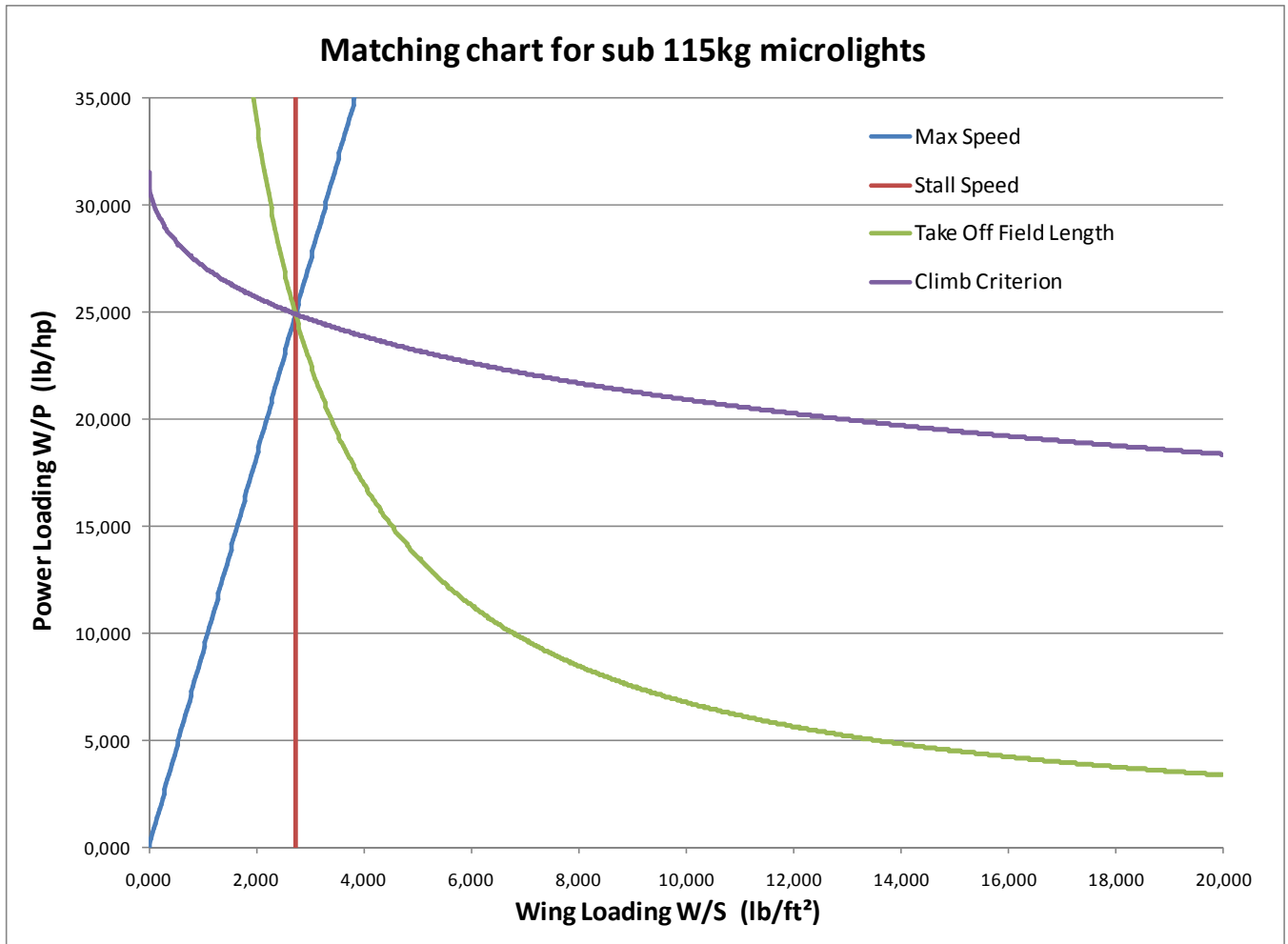


Jon Viner  
Chief Technical Officer  
British Microlight Aircraft Association

## B. PARAMETRIC ANALYSIS EXAMPLES

### B.1. SLOW HIGH ASPECT RATIO AIRCRAFT

#### B.1.1. Matching diagram



Parametric analysis matching chart slow aircraft



### B.1.2. Input parameters

|                  |                                   |        |        |         |
|------------------|-----------------------------------|--------|--------|---------|
| Input parameters | V max (mph)                       | 50     | 43     | (kt)    |
|                  | V stall (mph)                     | 23     | 20     | (kt)    |
|                  | TO run (ft)                       | 155    | 47     | (m)     |
|                  | C LT                              | 1,67   | 1,67   |         |
|                  | Climb Rate (ft/min)               | 660    | 201    | (m/min) |
|                  | Aspect Ratio                      | 10,00  | 10,00  |         |
|                  | Propulsive efficiency (av = 0,85) | 0,85   | 0,85   |         |
|                  | Aircraft efficiency               | 0,70   | 0,70   |         |
|                  | CD0                               | 0,097  | 0,097  |         |
|                  | MAX Fuel consumption (L/h)        | 12,00  | 3,17   | gal/h   |
|                  | $Cl^{3/2}/Cd_{max}$               | 10,372 | 10,372 |         |

Low speed aircraft input parameters table

### B.1.3. Output results

| Output Results | MATCHING DIAGRAM                        |                   |                    |
|----------------|---|-------------------|--------------------|
|                | W/p                                     | kg/hp             | lb/hp              |
|                |   | 11,25             | 24,80              |
|                | W/S                                     | kg/m <sup>2</sup> | lb/ft <sup>2</sup> |
|                |   | 13,33             | 2,73               |
|                |   |                   |                    |
|                | IP                                      | 0,48              |                    |
|                | Useful Load Fraction                    | 0,60              |                    |
|                | Engine Power (hp)                       | 20                |                    |
|                | Range at max speed (km)                 | 301               |                    |
|                | Wing Area (m <sup>2</sup> )             | 16,73             |                    |
|                | Empty Wing Loading (kg/m <sup>2</sup> ) | 5,38              |                    |
|                | Clmax                                   | 2,02              |                    |

| MASS BREAK DOWN        |    |                  |     |     |
|------------------------|----|------------------|-----|-----|
|                        |    |                  | kg  | lb  |
| WE                     | WG | Structure Weight | 68  | 150 |
|                        |    | Engine Weight    | 22  | 48  |
| Payload Weight (Input) |    | 100              | 220 |     |
| Fuel Weight            |    | 33               | 73  |     |
| Empty Weight (Input)   |    |                  | 90  | 198 |
| Gross Weight           |    |                  | 223 | 492 |

|       |              |      |
|-------|--------------|------|
| Check | Cl t         | 1,67 |
|       | Engine power | 19   |

Low speed aircraft output results table

### B.1.4. Interpretation

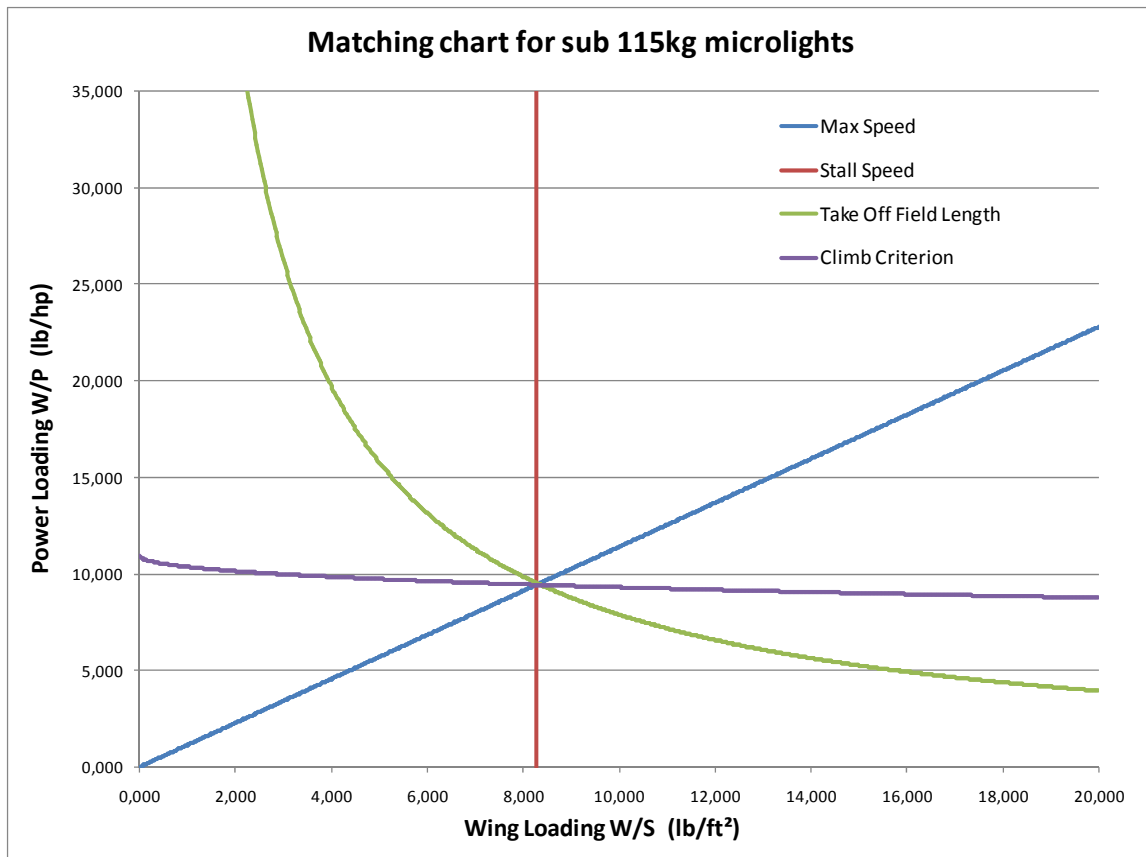
These tables give us the most important parameters: this aircraft has a very low maximum speed, a very low stall speed and a short take-off run. We can note that this induces a very large wing area, a very low empty wing loading, a very small engine power and a large fuel weight. This case is extreme and it would be hard to design an aircraft with these properties. However, it shows how the parameters evolve for very slow aircraft. This case represents the low speed limit of the analysis.

We can observe that this aircraft meets the requirements for the deregulated regime.

**☑ Note: The yellow cases are all the parameters that have to be entered by the user.**

## B.2. FAST AIRCRAFT

### B.2.1. Matching diagram



### B.2.2. Input parameters

|                  |                                   |        |        |         |
|------------------|-----------------------------------|--------|--------|---------|
| Input parameters | V max (mph)                       | 100    | 87     | (kt)    |
|                  | V stall (mph)                     | 40     | 35     | (kt)    |
|                  | TO run (ft)                       | 180    | 55     | (m)     |
|                  | C LT                              | 1.67   | 1.67   |         |
|                  | Climb Rate (ft/min)               | 1900   | 579    | (m/min) |
|                  | Aspect Ratio                      | 10.00  | 10.00  |         |
|                  | Propulsive efficiency (av = 0,85) | 0.85   | 0.85   |         |
|                  | Aircraft efficiency               | 0.70   | 0.70   |         |
|                  | CD0                               | 0.097  | 0.097  |         |
|                  | MAX Fuel consumption (L/h)        | 25.00  | 6.60   | gal/h   |
|                  | CI <sup>3/2</sup> /Cd max         | 10.372 | 10.372 |         |

Fast aircraft input parameters table

### B.2.3. Output results

| Output Results | MATCHING DIAGRAM                        |                   |                    |
|----------------|---|-------------------|--------------------|
|                | W/P                                     | kg/hp             | lb/hp              |
|                |   | 4.28              | 9.44               |
|                | W/S                                     | kg/m <sup>2</sup> | lb/ft <sup>2</sup> |
|                |   | 40.43             | 8.28               |
|                |   |                   |                    |
|                | IP                                      | 0.96              |                    |
|                | Useful Load Fraction                    | 0.51              |                    |
|                | Engine Power (hp)                       | 54                |                    |
|                | Range at max speed (km)                 | 155               |                    |
|                | Wing Area (m <sup>2</sup> )             | 5.76              |                    |
|                | Empty Wing Loading (kg/m <sup>2</sup> ) | 19.98             |                    |
|                | Clmax                                   | 2.02              |                    |

| MASS BREAK DOWN        |    |                   |     |     |
|------------------------|----|-------------------|-----|-----|
|                        |    |                   | kg  | lb  |
| WE                     | WG | S tructure Weight | 55  | 122 |
|                        |    | Engine Weight     | 60  | 132 |
| Payload Weight (Input) |    | 100               | 220 |     |
| Fuel Weight            |    | 18                | 39  |     |
| Empty Weight (Input)   |    |                   | 115 | 254 |
| Gross Weight           |    |                   | 233 | 513 |

| Check | Cl t         | 1,67 |
|-------|--------------|------|
|       | Engine power | 53   |

Fast aircraft output results table

### B.2.4. Interpretation

This aircraft is opposite the one we studied before: the maximum speed is twice higher and the stall speed goes from 23 to 40 mph. This induces a much bigger engine: 54 hp instead of 20, the wing area is also very small, 5.76 m<sup>2</sup> compared to 16.73 m<sup>2</sup> and for the same payload the empty weight is now 115 kg instead of 90 kg, with a lower fuel mass. This explains that the range has been reduced by almost half, compared to the slow aircraft design. The engine weight is a real penalty since it represents half of the total weight. The empty wing loading is now 20.0 kg/m<sup>2</sup> instead of 5.4 kg/m<sup>2</sup>. The take-off field length does not change a lot since there is compensation between the fact that the fast aircraft accelerates very fast because of its powerful engine and the fact that the slow aircraft has very high lift because of the large wing area. On the contrary, the fast aircraft has a climb rate almost 3 times higher than the slow aircraft: the fast aircraft flies 2 times faster and so climbs two times faster, but it also has a very high engine power over weight ratio which makes it very efficient in climb. As we said for the previous case, this configuration is extreme and it is at the limit of the model given by the parametric analysis.